RRP
3-11-83

NASA CR-167890
TRW 37243

3/83

SOLAR ARRAY SWITCHING

POWER MANAGEMENT TECHNOLOGY

FOR

SPACE POWER SYSTEMS

FINAL REPORT

Prepared for

National Aeronautics and Space Administration

Lewis Research Center
21000 Brookpark Road
Cleveland, Ohio 44135

Contract NAS3-22656

NASA CR-167890
TRW 37243

SOLAR ARRAY SWITCHING

POWER MANAGEMENT TECHNOLOGY

FOR

SPACE POWER SYSTEMS

FINAL REPORT

Prepared for

National Aeronautics and Space Administration

Lewis Research Center
21000 Brookpark Road
Cleveland, Ohio 44135

Contract NAS3-22656

1. Report No.	2. Government Accession No.	3. Recipient's Catalog No.
NASA CR-167890		

4. Title and Subtitle	5. Report Date
Study of Solar Array Switching Power Management Technology for Space Power System	September 1982
	6. Performing Organization Code
7. Author(s)	8. Performing Organization Report No.
John E. Cassinelli	
	10. Work Unit No.
9. Performing Organization Name and Address	
TRW Space and Technology Group One Space Park R5/B121 Redondo Beach, CA 90278	11. Contract or Grant No. NAS3-22656
	13. Type of Report and Period Covered Final Report Oct 1980 - Sept 1981
12. Sponsoring Agency Name and Address NASA Lewis Research Center 21000 Brookpark Road Cleveland, Ohio, 44135	14. Sponsoring Agency Code

15. Supplementary Notes

NASA Technical Office: Martin Valgora

16. Abstract

This report documents work performed on the Solar Array Switching Power Management Study.
Mission charactertics for three missions were defined to the depth necessary to determine their power management requirements. Solar array switching concepts were identified that could satisfy the mission requirements. These switching concepts were compared with a conventional buck regulator system on the basis of cost, weight and volume, reliability, efficiency and thermal control. For the missions reviewed, solar array switching provided significant advantages in all areas of comparison.

ORIGINAL PAGE IS
OF POOR QUALITY

17. Key Words (Suggested by Author(s))	18. Distribution Statement
Solar Array Switching, Array Switching, Solar Array Control	Unlimited

19. Security Classif. (of this report)	20. Security Classif. (of this page)	21. No. of Pages	22. Price*
unclassified	unclassified	240	

*For sale by the Clearinghouse for Federal Scientific and Technical Information
Springfield, Virginia 22151

TABLE OF CONTENTS

Illustrations

Appendix B

Appendix C

Data Tables

Final Report

Solar Array Switching Power Management Study

1.0 Introduction

Solar Array Switching Power Management (SASPM) is an approach to power management that employs switches to directly connect groups of solar cells in such a way as to provide system voltage regulation, electrical power distribution, and the ability to reconfigure the solar array for changing load requirements.

The objective of this study is to identify SASPM concepts and technology advancements which have the capability of increasing power systems efficiency and reducing costs. A comparison to conventional power management approaches has been made, and the potential benefits of the SASPM technique in the areas of cost and weight reduction, reliability enhancement, heat rejection requirements, reconfiguration flexibility, and ease of growth demonstrated.

A complete statement of work for this study is presented in Appendix D, and a set of acronyms employed in Appendix E.

1.1 Summary of Study Results

1.1.1 Mission Characteristics

A set of mission characteristics were defined for three following selected typical missions, utilizing projected 1990's technology.

- Manned Low Earth Orbiting (LEO) platform - 250 kw average load
- Unmanned geosynchronous equatorial orbit (GEO) platform - 50 kw average load.
- Unmanned ion propulsion orbit transfer vehicle (IPOTV) - 50 kw to 250 kw load.

For each mission, an electrical power system (EPS) and power management system (PMS) was characterized. Characteristics of these designs are presented in Table 1-1.

1.1.2 Identification of SASPM Concepts

Four basic switching configurations which are capable of controlling solar array segments were defined and compared, and five sequencing concepts for controlling the switch configurations were developed. A system concept was derived for each typical mission. The LEO mission concept is shown in

Table 1-1

Design Mission EPS Characteristics

Mission	System Voltage*	No. Power Channels	Solar Array Type	Solar Array BOL-W (KW)	Solar Array Mass (Kg)	Battery Type	Battery A-hr	Battery No.	Battery DOD	ASU Type	ASU Mass (Kg)	[illegible]	Parts
● LEO	200-240V	11	Conc.	687	15,276	N_i-H_2	250	11	30%	2 bit bin.ct.	293	98.6%	6898
● GEO	200-260V	4	Planar	96	478	Ag-H_2	120	4	75%	4 bit bin.ct.	92	98.6%	1164
● IPOTV	200-260V	3	Planar	250	1,250	N_i-H_2	50	3	75"	2 bit bin.ct.	69	98.6%	5814

*Ion propulsion high voltage is nominally 860 volts.

Note: The major EPS characteristics for the above missions were derived from two studies completed at TRW:

1. Space Power Distribution System Technology Study (NAS8-33198)
2. Multikilowatt Solary Array Study (NAS 32986)

ORIGINAL PAGE IS
OF POOR QUALITY

Figure 3.3-1. Since power must be supplied to both the spacecraft and the ion propulsion system simultaneously, reconfiguration of the solar array is not needed for mission requirements. Each of the power busses has its own feedback control system. The spacecraft bus feedback control measures bus voltage and battery current and controls the solar array switching unit accordingly through the SASU control logic. A microprocessor controller measures battery state-of-health and provides battery charge control by varying the references of the voltage and current error amplifiers. The ion propulsion bus feedback loop measures the bus voltage and controls its SASU through control logic. Inputs from the ion propulsion system can modify the bus voltage and provide for arc protection.

The GEO mission concept is shown in Figure 3.3-2. Solar array reconfiguration is accommodated by a six pole-double throw switch. Four parallel solar array segments are reconfigured into four series segments in this arrangement. The SASU control logic must also be reconfigured to transfer control to the desired power bus and to accommodate the new switching arrangement. The battery and bus control methods are the same as described in the LEO mission except that the battery charge control algorithms are tailored for GEO. Reconfiguration and ion propulsion system modifications are accommodated through spacecraft level commands.

The switching concept for the IPOTV mission is shown in Figure 3.3-3. Since the major portion of the power is for the ion propulsion system, a small portion of the solar array is tapped for the spacecraft. A reconfiguration concept is shown that allows for a 33% increase in the ion propulsion bus voltage. This compensates for voltage degradation accumulated by repeated trips through the Van Allen Belts. Initially four equal solar array segments are utilized with the fourth segment divided into three equal subsegments. The subsegments are switched in series with the remaining segments to attain the voltage increase. The monitoring and control methods are much the same as for the LEO mission.

.1.3 Baseline Conventional Power Processing

Four basic power processing concepts (other than SASPM) were identified and compared for application to each of the typical missions. These concepts are:

- Transformer coupled converter
- Buck regulator/charger
- Boost regulator/charger
- Shunt regulator/charger

Because of excessive dissipation requirements in large systems, the shunt regulator was eliminated from consideration.

Each of the remaining three concepts was extracted from prior work for the three missions, and the optimum conventional system selected for comparison to the SASPM system. The optimum conventional system for all three missions was the buck regulator/charger, because it was the lowest cost and mass system.

1.1.4 Comparison of SASPM to Conventional Power Systems

The comparisons made are summarized in Table 1-2.

1.2 Conclusions

The following benefits were obtained by using SASPM rather than conventional techniques:

- Projected reduction in the cost of power processing: 25% - 67%.
- Projected reduction in the mass of power processing equipment: 17% - 64%.
- Cost and mass of the solar array was reduced 2% for the LEO and GEO missions. At today's cost, this range of savings would be 2 - 16 M$. (Projected 1990s: .1-1 M$). *
- Projected reduction in the mass of the active radiator: 6 - 12%. (eliminates active radiator requirements for power processing)
- Projected reduction in the cost of the active radiator is 10% - 20%.

1.2.1 Areas of Concern

Certain areas of concern became apparent during the conduct of this study:

- High voltage operation in the space plasma environment is a major concern for LEO applications. Recent information from Lewis Research Center indicates that solar array voltage above 500 volts may not be achievable on planar arrays. The concentrator array may offer a solution. It may be possible to bias the reflector cones to keep the plasma away.
- Operation through Van Allen belt region dictates radiation resistant cell.

1.2.2 The Next Step

The SASPM concept can be implemented now on low voltage systems. No advancements in technology are required. However for higher voltage systems some advances in technology are required:

- Development of space qualified high voltage/high current power switchgear

* Based on the Multikilowatt Solar Array Study (reference 2-20, page 2-49)

Table 1-2

Comparison of SASPM and Conventional Systems for Selected Missions

A. Mission: LEO Platform

Conventional System: Buck Regulator/Charger Comparison:

	Buck Regulator	SASPM	Δ
Power Processing Mass (KG)	662	241	-64%
Power Processing Cost ($M)	4.0	2.3	-43%

B. Mission: GEO Platform

Conventional System: Buck Regulator/Charger Comparison:

	Buck Regulator	SASPM	Δ
Power Processing Mass (Kg)	109	91	-17%
Power Processing Cost ($M)	1.2	0.9	-25%

C. Mission: Ion Propulsion Orbit Transfer Vehicle

Conventional System: Buck Regulator/Charger Comparison:

	Buck Regulator	SASPM	Δ
Power Processing Mass (Kg)	116	69	-41%
Power Processing Cost ($M)	1.9	0.6	-67%

The following advancements would enhance solar array switching:

- Development of space qualified, low on-state resistance MOSFETs.
- Development of space qualified CMOS microprocessors.
- Development of a LSI chip incorporating the entire microprocessor controller circuitry.

A suggested SASPM development plan is as follows:

Phase I: 1) Low voltage solar array switching unit (voltage controlled)

- Develop basic power stage configuration.
- Develop control electronics and analyses.
- Demonstrate transient behavior of unit with solar array simulator.
- Explore fiber optics options.

Phase II:

- Demonstrate reconfiguration capability
- Install fiber optics control circuits.
- Develop analytical model.

Phase III:

- Develop high voltage SASU
- Performance testing of SASU and solar array simulator.

Phase IV:

- Integ·ation of SASU and solar array simulator with an argon thruster.
- Performance verification tests.
- System demonstration

2.0 TASK I

MISSION REQUIREMENTS AND DEFINITION

Define a set of mission characterisitics to the depth required to determine their power management requirements. Estimate the power management requirements and constraints. Task I is to be performed for three missions:

1) Manned Low Earth Orbit (LEO) Platform - 250 KWe average load

2) Unmanned Geosynchronous Equatorial Orbit (GEO) Platform - 50 KWe average load.

3) Ion Propulsion Orbit Transfer Vehicle (IPOTV) - 50 - 250 KWe

2.1 LEO Platform

2.1.1 LEO Mission Requirements and Payload Selection

Reference 2-1 through 2-11 were surveyed for load and user requirements applicable to the LEO mission. The survey shows that there is an important trend toward platforms and carriers that do not have their own power sources in order to provide cost effective accomodations for payloads. These platforms and carriers will dock to power platforms for their source of housekeeping functions including power, energy storage, and possibly power conversion and/or regulation. This means that the power module interface may become remote from the individual payload. The interface requirements will be as defined at the docking port between the power module and the experiment platform or carrier for many applications, but directly at the self-contained docking port for other payloads.

One such platform is the Science and Applications Space Platform (SASP) (Reference 2-1). The SASP is intended to be a long lived platform in LEO which receives power from a space power system. The interface requirements are for 30 Vdc and 120 Vdc power. The 30 Vdc requirement is driven by Space Transporation System compatibility requirements. A list of the identified SASP experiment power requirements is given in Table 1 of Appendix A, although in many cases the data is not yet available, as indicated by the letters NA in the table. Since most power systems are 28VDC, that is the voltage that equipment designers use. Of the 70 experiments listed, one requires 400 Hz, three-phase ac at 115 volts (4.16 KW average), and three require 60 Hz, 120 Vac power. The SASP, as presently conceived, provides the necessary power inversion to supply these alternating current requirements.

Another example of an experiment carrier is the Materials Experiments Carrier (MEC), which accommodates the materials processing experiments (Table 2 of Appendix A). The MEC experiments all require 120 Vdc. This requirement is somewhat artificial in that it may have been derived from the fact that 120 volts is the highest voltage projected to be available from the 25 KW Space Platform (SP). It is possible that higher voltages could be used directly, especially for heaters (furnaces) with variable duty cycle capabilities.

The Multi-100 KW Space Platform concept of Reference 2-5 was reviewed for power and voltage requirements. This platform is made up of several modules, and the individual load requirements inside each carrier are given in kilowatts only, without reference to ac or dc, or voltage level. Each carrier's electrical distribution capability (voltage, regulation, frequency, etc.) is identified in Table 3 of Appendix A.

Space construction base power requirements have been tabulated in Table 4 of Appendix A. Overall bus requirements of regulated 26 and 112 Vdc, and unregulated 76 Vdc are given, but individual payload voltage requirements are not known (Reference 2-6).

Orbiter (STS) power requirements were reviewed because the STS will dock to the platform when delivering payloads and/or refurbishing the platform. The requirements (Table 5 of Appendix A) are presented as they would be supplied, i.e., as power bus requirements. The alternating current is supplied by internal inverters on the aft flight deck of the Orbiter, and are not available in the cargo bay without special Orbiter scar. (Weight associated with mounting provisions)

The STS sortie payloads (Table 6 of Appendix A) are candidates for the LEO platform. The loads are designed to operate from the STS 28 Vdc bus, but an inverter is required to supply alternating current loads in the cargo bay. Reference 2-9 contains power requirements for public service payloads, many of which are compatible with both the LEO and GEO platforms. Voltage requirements were not given in the Reference 2-9 study (see Table 7 of Appendix A).

The loads survey indicates that actual voltage levels and regulation requirements are not known at this time for the majority of experiments and equipment. However, the trend toward carriers and modules (even the STS can be considered a module with power requirements given at the cargo bay interface) suggests that power modules should provide relatively gross power at the docking interface, and the carrier would then tailor this power to the specific payload needs.

The selected LEO platform will be capable of supporting payloads in the range of 100 kw to 250 kw, average load. This gives a capture rate for all SASP, MEC, multi-100 kw platform, space construction base, sortie payload and public service payloads of greater than 97%.

The 250 KWe LEO platform power control and distribution system will be capable of providing a shirtsleeve environment at all times for the manned modules. The station will be modular and will contain a docking module which will also serve as a power control and distribution center. The system will be designed to be self dependent during operation, with a man interface capability. The launch vehicle will be the shuttle orbiter, and drag makeup will be provided by ion propulsion. The LEO platform must support a diversity of payloads; therefore a utility approach to electrical power generation, distribution and cost is indicated. For example, the load scenario presented in Reference 2-5 shows a daily average load of 142 KWe, with peaks to 174 KWe. These totals are combined loads from 10 separate modules. Other modules such as the Materials Experiments Carrier (Reference 2-2), and the Science and Applications Space platform (Reference 2-19) add their own multiple loads. This complexity points to the need for a Power Management System (PMS), not only to manage the multiple channel platform with its many subsystems, but to manage the loads themselves. The PMS will be discussed later in this report.

Alternate configurations for a 250 KWe LEO Platform were investigated under Contract NAS8-33198 (Reference 2-17). The trade studies indicated a dc distribution system was superior for this application. The Reference 2-5 study (ac distribution concept) has been reviewed; however, the ac system has not been analyzed and developed to the same degree as the more mature dc system concept.

2.1.1.1 LEO Spacecraft (Housekeeping) Requirements

In addition to supporting a variety of payloads in low earth orbit, the LEO platform must be capable of maintaining its own functions. The energy required for this maintenance is separable into two parts, orbital maintenance power and housekeeping power.

Orbital maintenance is defined as the propulsive functions required to maintain an orbit within prescribed tolerances during satellite operations. Satellites drift from their desired orbit due to nonspherical earth gravitational effects, aerodynamic drag, solar and lunar gravitational effects, and special orbital demands (such as maintenance of an orbit about the noninertially fixed earth's equator). The degree of drift due to the various effects depends on the satellite mission parameters, especially altitude.

The primary orbital disturbance at altitudes below 500 km is aerodynamic drag; therefore, drag makeup will determine the ion propulsion requirements for the LEO platform. An analysis of the orbital maintenance requirements for the LEO platform is presented in Appendix B.

Housekeeping includes all power required by the spacecraft (other than payload support) to perform its mission. Indications are that approximately ten percent of the payload power requirement is a conservative estimate for this function.

2.1.1.2 LEO Mission EPS Operational Requirements

The EPS operational requirements are outlined below:

a) Purpose. To provide utility type electrical power (up to 250 KWe) to a variety of undefined payloads.

b) Mission. Power platform will operate in LEO, 90-minute orbit, 36-minute eclipse maximum. Specific missions will be determined by the payload requirements.

c) Manned Operation.

d) Orbit Maintenance. Ion propulsion engines will be powered separately from the 250 KWe payload requirements.

e) Control. The EPS will be controlled by the PMS, with optional onboard command or external command override.

f) Reliability

- The power system will be reliable to the point that life support requirements are met, including two failure tolerance criteria for crew safety items per NHB 1700.7A (Reference 2-18).
- No single point failure will fail the mission; however, partial power outages will be allowed and be accommodated by redundant power buses.
- Proper component derating and high reliability parts will be incorporated. Failed equipment will be replaced via space shuttle refurbishment. Nominal design life will be 20 years, with a goal of 30 years.

g) Environment

- Space shuttle launch requirements, as reflected at the Orbiter/EPS interface.
- Normal LEO spacecraft design temperatures.

h) Output Capacity

- Provide continuous 250 KWe (maximum) to an undefined number of payloads.
- Be flexible in nature and capable of expansion.
- Provide up to an additional 23 KWe during daylight periods for ion propulsion engines.
- Provide up to an additional 25 KWe continuously for spacecraft housekeeping loads.

2.1.2 Baseline LEO Platform Electrical Power System (EPS)

The baseline EPS which meets the above requirements is as follows. A block diagram of the system is shown in Figure 2.1-1. In addition to the above requirements, other assumptions are:

- The platform will be STS launched and serviced. The design will include on orbit maintenance and repair capability.
- The platform will employ a photovoltaic solar cell array power source.
- The platform will employ SASPM.
- The platform will employ 1990s technology.

2.1.2.1 System Voltage

A 250 KW system occupies an extensive area, and power must be transmitted over relatively long distances. As indicated in Figure 2.1-2, it is costly to transmit large amounts of power over long distances, especially at low voltages.

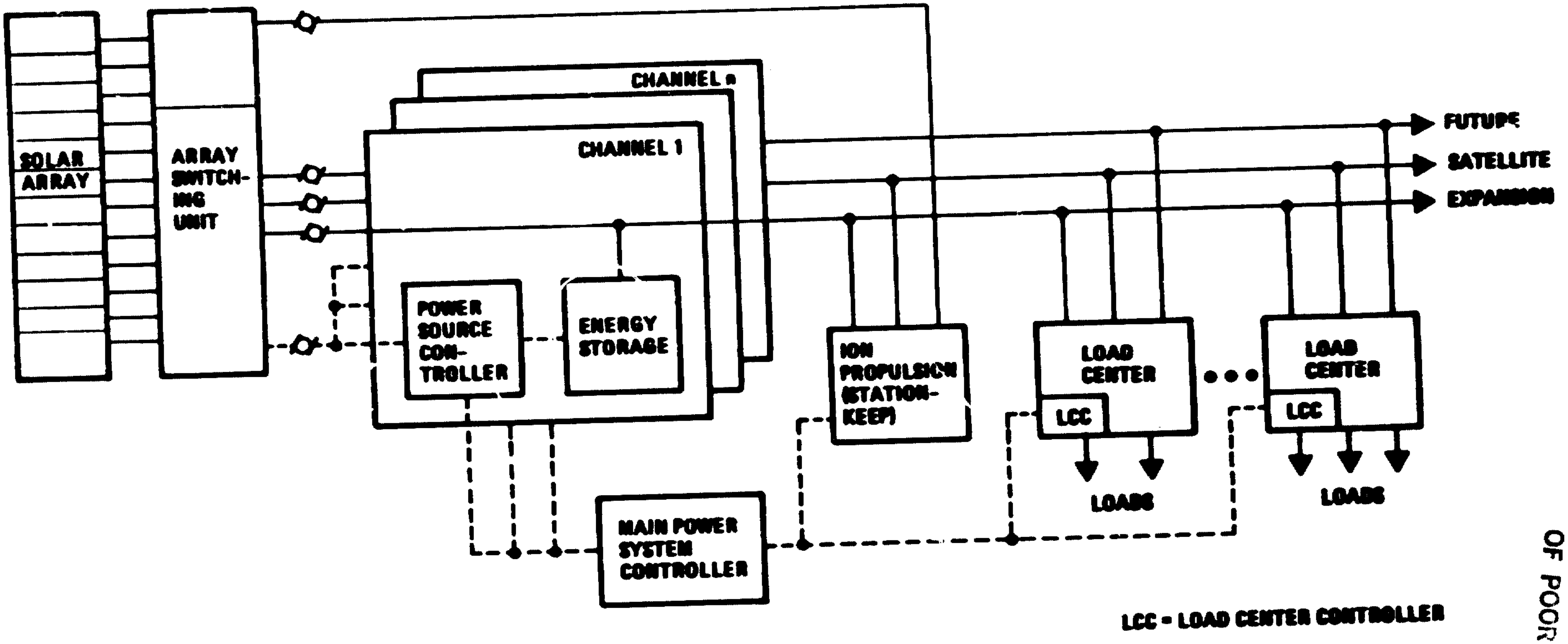

GENERATION – CASSEGRANIAN CONCENTRATOR SOLAR ARRAY
ENERGY STORAGE – NICKEL-HYDROGEN BATTERY
BATTERY CHARGER – SOLAR ARRAY REGULATION
POWER DISTRIBUTION – DIRECT CURRENT AT SOURCE VOLTAGE, 200 TO 240 VDC*
POWER PROCESSING – AS NEEDED WITHIN EACH PAYLOAD OR LOAD CENTER
CHANNEL QUANTITY – DEFINED BY BATTERY CAPACITY (11)
RELIABILITY – FAIL OPERATIONAL, FAIL SAFE
GRACEFUL CAPACITY DEGRADATION WITH FAILURES
LIFE – INDEFINITE; REPLACE FAILED UNIT AT NEXT SERVICE OPPORTUNITY (30 YEAR GOAL)

*ION ENGINE BEAM CURRENT SUPPLIED AT 850 VDC DURING SUNLIGHT ONLY

Figure 2.1-1 LEO Baseline Electrical Power System Design

The curve of Figure 2.1-2 (Reference 2-17) indicates that most of the payoff for higher transmission voltages has occurred at 200 volts. It is felt that for voltages up to 400 Vdc, there will be a minimum effect on 1990s switchgear technology, therefore, a voltage of 200-240 Vdc, allowing for derating, was selected as the EPS main power bus voltage.

The SASPM for the LEO Platform must supply solar electric propulsion at approximately 860 Vdc, and power to the load centers at 200-240 volts. During the sunlit period, the battery will be charged at 240 Vdc, and during eclipse the battery will supply the load centers with the power at the battery discharge voltage (200 Vdc). Power conversion as required will be accomplished within the load centers.

2.1.2.2 Energy Storage

A system efficiency diagram is shown in Figure 2.1-7. The total load in sunlight is 298 kw. In eclipse the load is 276 kw, allowing 1 kw for SEP system standby. The load requirement on the energy storage subsystem during eclipse is:

$$\frac{276\ \text{kw}}{(.995)(.995)} = 278.8\ \text{kw}$$

and, the total energy:

$$278.8\ \text{kw} \times 0.6\ \text{hrs} = 167.3\ \text{kw-hrs}$$

A trade study was conducted comparing Ni-Cd and Ni-H_2 batteries and fuel cells. The fuel cell was a close competitor of Ni-H_2 batteries on a mass basis, but did have several disadvantages (Figure 2.1-3).

- The failure of a single cell results in the total loss of a power module.
- The low electrochemical efficiency of the regenerative fuel cell requires a much larger solar array than that required for charging batteries (Ref 2-17). The result is an increase in aerodynamic drag with an attendant increase in propulsion fuel requirements for orbital altitude maintenance.

ORIGINAL PAGE IS
OF POOR QUALITY

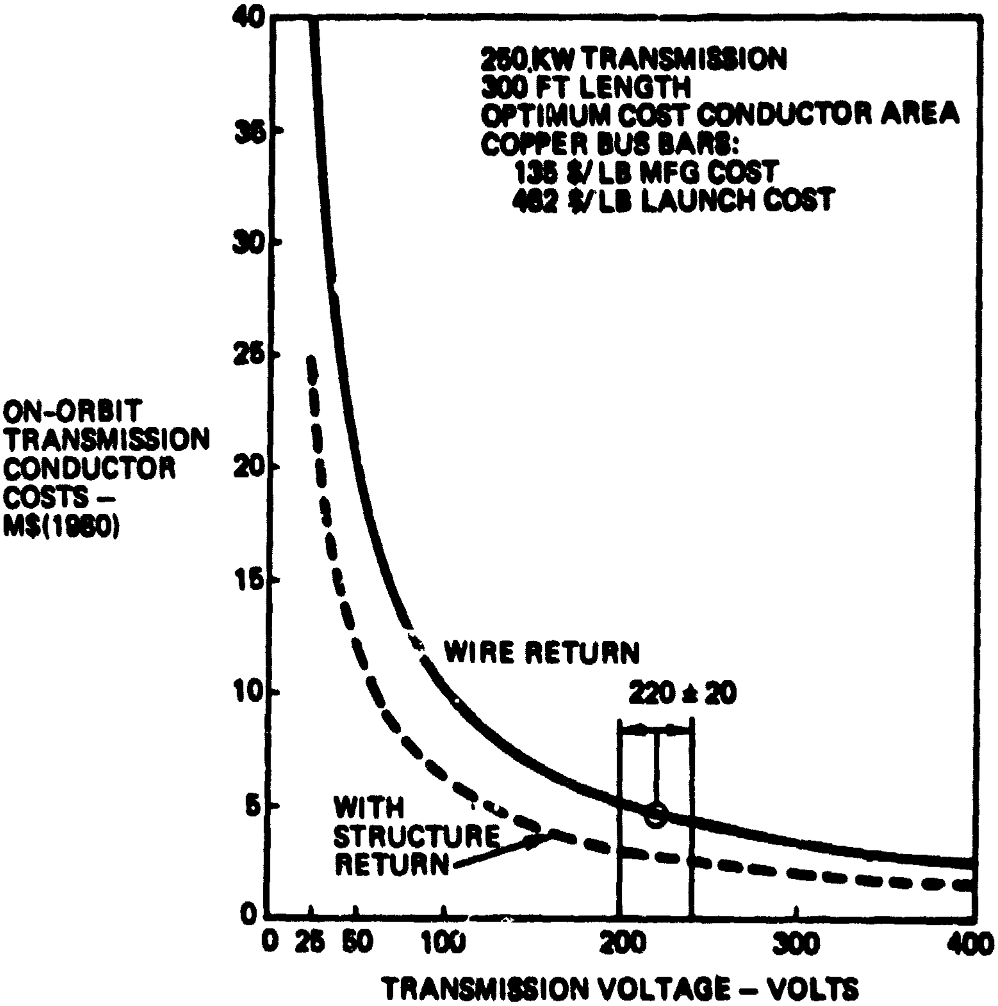

Figure 2.1-2 **Transmission Costs Low Above 200 Volts**

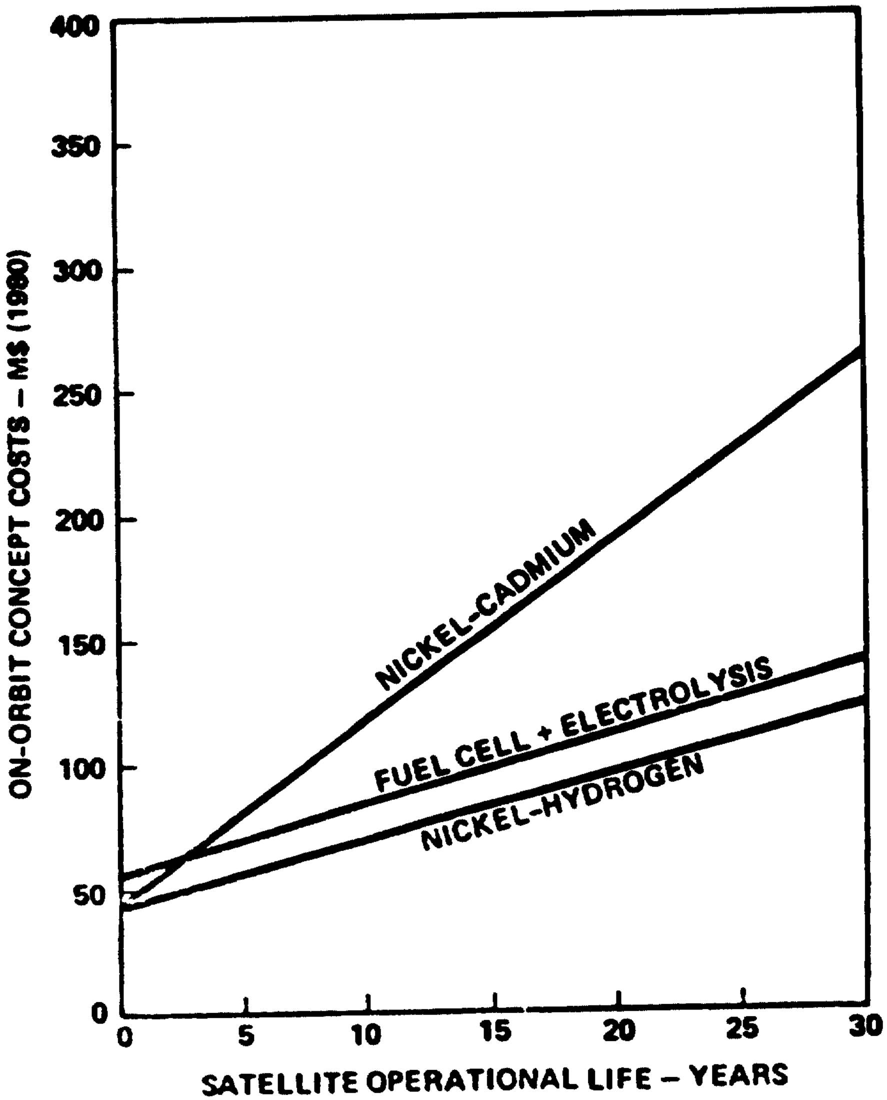

250 KW SYSTEM

ENERGY STORAGE COST PLUS SUPPORT:
- **SOLAR ARRAY**
- **HEAT EXCHANGERS**
- **RADIATORS**

NOTE: These curves do not include orbital altitude maintenance costs, but do include replacement costs as required to replace failed units.

Figure 2.1-3 Comparison of Energy Storage Devices

- The plumbing system required for fuel cells is extremely complex. (Figure 2.1-4)

The results of this analysis (Ref 2-17) indicates a 250 A-hr, Ni-H_2 cell to be the optimum choice for this application. A desired bus voltage of 200 volts dictates a 160 cell battery baseline. At a depth of discharge of 30%, each such battery would have a capability of

$$160 \text{ cells} \times 1.25 \text{ V/cell} \times 250 \text{ A-hr} \times .30 = 15 \text{ kw-hrs}$$

The number of power channels is

$$\frac{167.3 \text{ kw-hr}}{15 \text{ kw-hrs}} = 11 \text{ channels}$$

2.1.2.3 Power Generation

Two solar array concepts were considered for the LEO application. Particulars for the planar array are presented in Figure 2.1-5, and for the cassegranian concentrator solar array in Figure 2.1-6. The concentrator array was selected over the planar array for two reasons.

- The area of the concentrator array is 10% less for a given power output. This reduces aerodynamic drag make-up requirements, which are significant in LEO.
- The cost projection for the concentrator array is 35 percent less than the cost of a comparable planar array in terms of dollars per watt.

ORIGINAL PAGE IS
OF POOR QUALITY

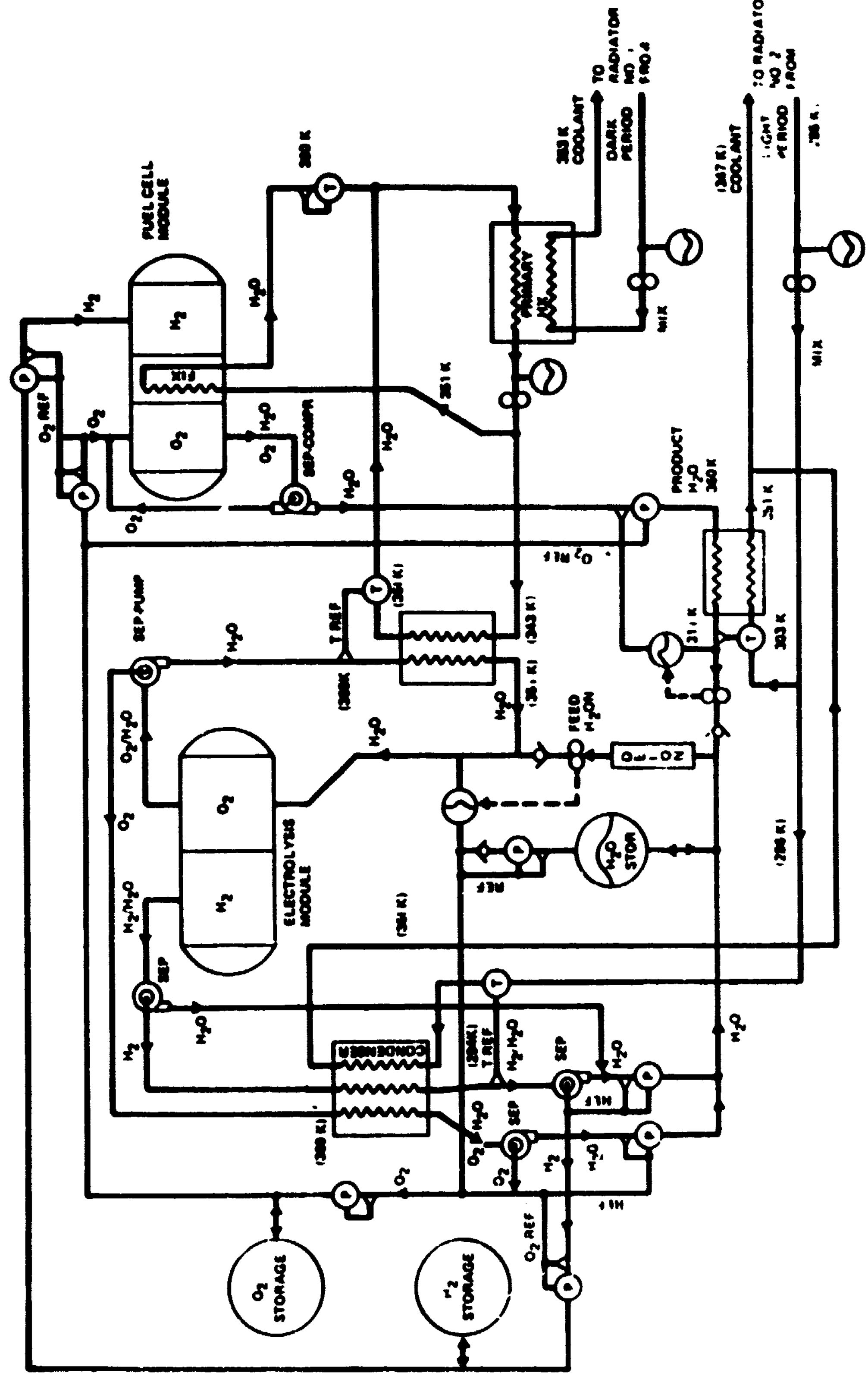

Figure 2.1-4 Fuel Cell Complex Plumbing

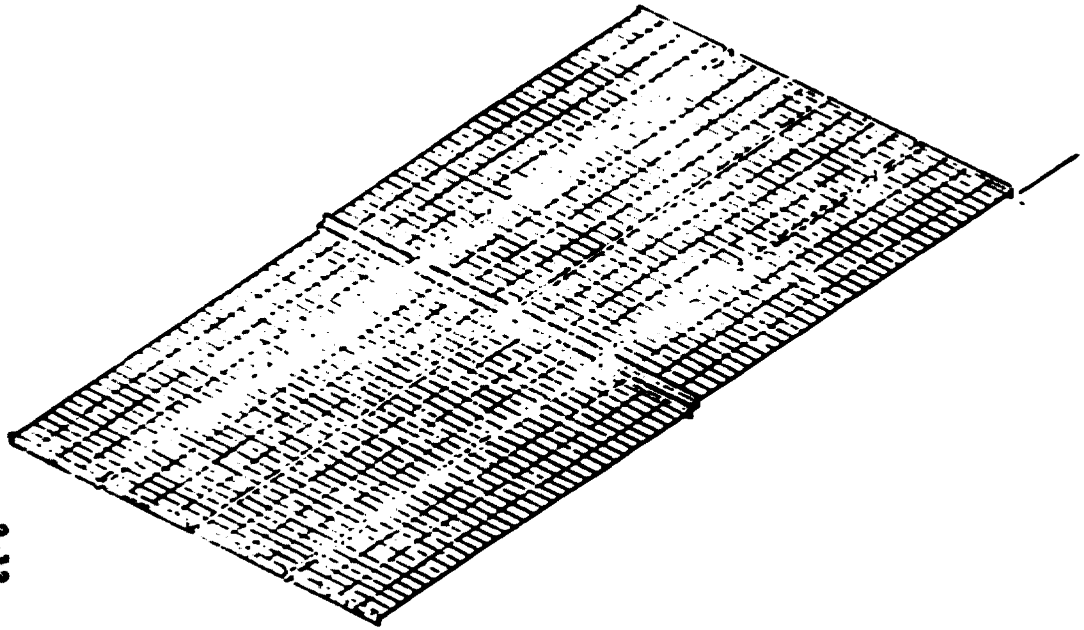

Figure 2.1-5 Planar Solar Array Concept

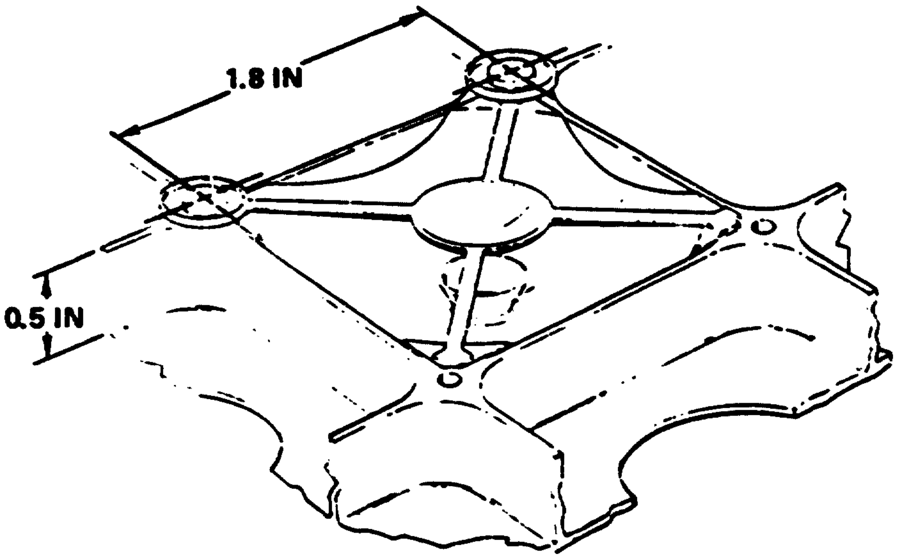

FEATURES

- MINIATURIZED ELEMENTS
- SQUARE RADIATOR APPROX. SAME SIZE AS APERTURE
- LIGHT CATCHER CONE
- SMALL (4 X 4 MM), HIGH EFFICIENCY (30%) SOLAR CELLS
- 12 MM THICK STRUCTURE

ADVANTAGES

- OFF-POINTABLE UP TO 3 DEGREES
- PASSIVE COOLING FOR CR = 100-200
- FAIL-SAFE
- MASS PRODUCIBLE
- LOW-COST COMPONENTS
- DEPLOYS AND STOWS LIKE PLANAR ARRAY

PERFORMANCE (1986) *

- 30 $/W
- 150 W/M^2, 45 W/KG

* Multikilowatt Solar Array Study, reference 2-20.

ORIGINAL PAGE IS OF POOR QUALITY

Figure 2.1-6 Cassegranian Concentrator Solar Array Concept

ORIGINAL PAGE IS
OF POOR QUALITY

2.1.2.4 LEO Mission Baseline Sizing

The LEO Mission SASPM sizing model is shown in Figure 2.1-3

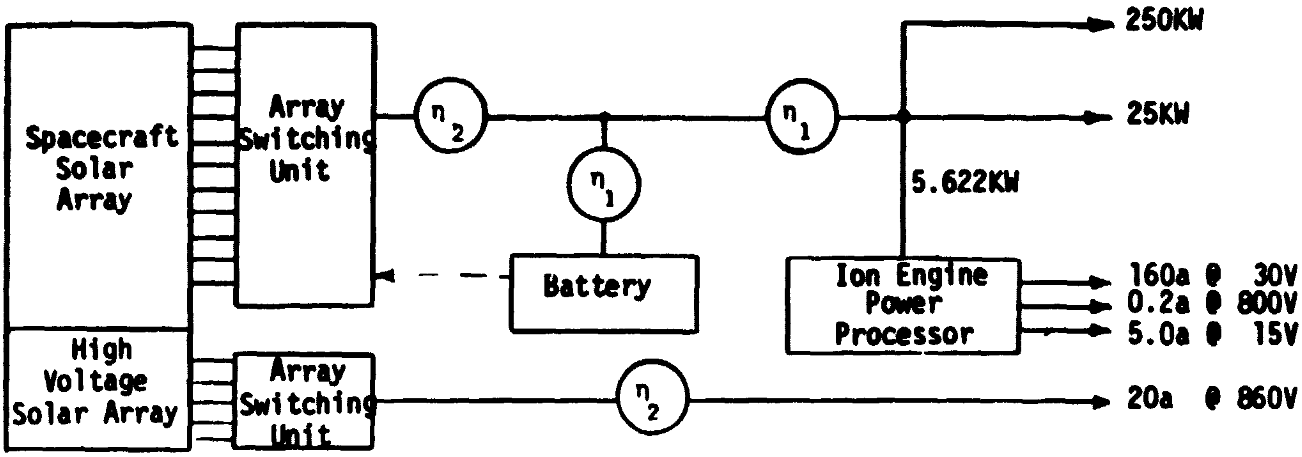

Figure 2.1-7 LEO Solar Array Switching Power Management EPS Sizing Model

Note: Ion engine data was derived from NASA Technical Memorandum 79141 (reference 2-24)

$$\text{Solar array output power} = \frac{P_L + P_H + P_C}{\eta_2 \cdot \eta_1 \cdot d \cdot \varepsilon_p} + \frac{P_I}{\eta_2 \cdot d \cdot \varepsilon_p} \quad (2.1\text{-}1)$$

P_L = Load Power

P_H = Housekeeping power + low voltage ion engine power

P_C = Battery charging power

P_I = Ion propulsion high voltage power

η_1 = Wiring and connector efficiency=(.995)

η_2 = Wiring and connector efficiency=(.99)

d = Solar array end of life efficiency=(.8)

ε_p = Array processor efficiency=(.986)

ORIGINAL PAGE IS
OF POOR QUALITY

Degradation of the concentrator solar array as a function of time in LEO is presented in Figure 2.1-8. For the nominal design life of 20 years, the array will degrade by 15%, and for the design goal of 30 years, by 20%.

From equation (2.1-1) we have

$$\text{Array Power (BOL)} = \frac{P_L + P_H + P_C}{\eta_2 \cdot \eta_1 \cdot d \cdot \varepsilon_p} + \frac{P_I}{\eta_2 \cdot d \cdot \varepsilon_p}$$

All the terms are known except P_C, the battery charging power.

2.1.2.4.1 <u>Battery Charge Requirements</u>

Eclipse requirements: 250 KW to payloads
25 KW to housekeeping loads
1 KW to ion engine standby power

276 KW

$$\text{Batteries supply } \frac{276 \text{ watts}}{(.995)^2} = 278.78 \text{ KW}$$

$$\frac{278.78 \text{ KW}}{200 \text{ volts}} :: 1394 \text{ amperes}$$

$$\text{Charging requirements} = (1394 \text{ amperes})\left(\frac{36 \text{ minute eclipse}}{54 \text{ minute sunlight}}\right)(\text{Recharge ratio})$$

$$= (1394)\left(\frac{36}{54}\right)(1.06) = 985 \text{ amperes}$$

$$(985 \text{ amperes})(240 \text{ volts}) = 236.4 \text{ KW}$$

$$\text{Array Power (BOL)} = \frac{250{,}000W + 30622W + 236{,}400W}{(.99)(.995)(.8)(.986)} + \frac{17{,}200}{(.99)(.8)(.986)}$$

$$= 665402W + 22025W$$

$$= \underline{687{,}427 \text{ watts}}$$

$$\text{Array size} = \frac{687{,}427 \text{ watts}}{150W/M^2} = 4583 \ M^2$$

$$\text{Array mass} = \frac{687{,}427}{45W/Kg} = 15276 \text{ Kg}$$

The data for the solar arrays was taken from Reference 2.1-17.

2.1.2.4.2 Ion Propulsion Beam Power - Array Sizing

Screen power = = 17,200 watts

Line losses $= 17{,}200 \left(\frac{1-.99}{.99}\right) =$ 174 watts

ASU losses $= 17{,}374 \left(\frac{1-.986}{.986}\right) =$ 246 watts

Total = 17,620 watts

The end of life solar array power requirement is 17,620 watts.

BOL requirement $= \frac{17{,}621 \text{ watts}}{0.8} = \underline{22{,}025 \text{ watts}}$

This sizing assumes sunlight only operation of the ion engines.

The ion engine also requires 5788 watts of array power for the lower voltage requirements, including distribution losses.

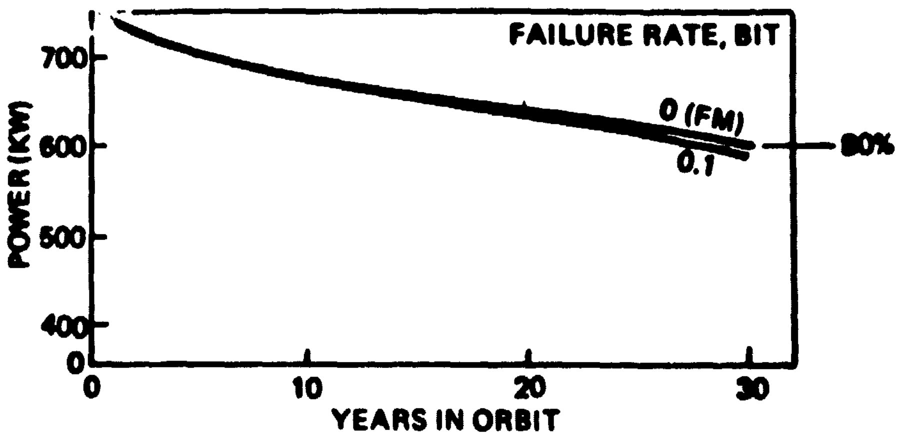

Figure 2.1-8 Concentrator Array Degradation as a Function of Years in LEO

2.1.2.5 Solar Array Output Control

Sequentially-switched solar array segments, controlled by the power source controller and the main power system controller accomplish simultaneous control of both array power and battery charging while supplying load power.

2.1.2.6 Power Transmission and Distribution

In the Reference 2-17 study, the power conditioning for the loads is accomplished in the individual load centers. Each load center receives power with regulation determined by the charge and discharge voltage of the battery. If a user has other requirements, special purpose inverters, converters or regulators can be utilized without penalizing power delivery to other payloads. In addition:

- The eleven payload power buses will have cross tie capability in case of a channel failure. The bus can be isolated from the failed channel and tied to an operable channel until a repair is made.
- Power buses cannot be paralleled without isolation. This is to prevent individual failures or faults from affecting other buses and to insure proportional discharge of the batteries.
- A circuit breaker arrangement will control power delivered to payloads. The main power system controller will monitor the loads so that any one channel will not be overloaded.

2.1.3 Power Management System (PMS) Requirements

The PMS controls all functions associated with transmission, distribution, processing, and conditioning of electrical power between the source, energy storage, and the loads. PMS requirements were derived from References 2-5 and 2-17.

The Electrical Power System (EPS) and PMS designs are interactive, each being reflected in the design of the other. Figure 2.1-1 (page 2-7) depicts the major elements and the associated power management elements. Power management control is indicated by dotted lines. The PMS (and EPS) designs accommodate modular expansion as the loads and/or channels grow in power/quantity. The primary function of the PMS is to maintain a positive energy balance; to ensure that either the energy storage system is completely recharged during each charge/discharge cycle (when eclipse is involved), or that over any group of cycles, on a recurring basis, as long as battery depth of discharge criteria is not exceeded, the energy storage system will be completely recharged. The EPS and PMS are designed to supply unregulated peak power of up to twice the average load during daylight.

PMS reliability criteria are as follows:

- No single failure or credible combination of failures will prevent the system from operating in an acceptable degraded mode of operation.
- The system will employ redundant controls, power conditioning equipment and load paths.
- Control and monitoring circuits will employ independent, redundant power sources.
- In case of module/component failures, the system will commence load shedding according to a predetermined hierarchy determined by a loads analysis and the establishment of criticalities.
- All components of the PMS that are subject to degradation, failure, or wearout during the operational lifetime will be designed for orbital replacement.

The PMS incorporates built-in test capabilities for fault diagnosis that will identify failed or degraded power system elements. The testing system maintains records of the system "health," identifies trends as well as out-of-limit conditions, and provides test data that will make possible the prediction of the remaining life of system elements and forecasting of the required schedule for repairs and replacements.

PMS design will observe the following maintainability criteria:

- The system will be designed for on-orbit maintenance by replacement of failed modules/components.
- The system will use computer-controlled power management techniques with the following capabilities:
  - Continuous monitoring of system health and performance
  - Detection and isolation of faults
  - Shifting loads around failed equipment
  - Prediction of incipient failures and isolation of equipment
  - Shutdown and isolation of failed equipment to prevent damage to other equipment.
- The system will be designed to selectively shut down sections for replacement of failed modules/components.
- Modules/components will be designed for ease of removal and replacement with appropriate mechanical latches, electrical connectors, fluid connectors, etc. Maintenance operations will not require more than two crewmen to accomplish any physical removal/replacement or repair task.
- <u>Environmental</u> - The PMS shall be designed to operate in low earth orbit (400 km) at an inclination of 28.5 degrees.

PMS elements that normally operate in a pressurized environment will continue to perform their intended function without overheating, malfunction, or electrical breakdown in the event that the surrounding pressure is reduced to near vacuum (external conditions at the specified altitude). All PMS components and assemblies when packaged or otherwise configured for delivery to orbit will be designed to withstand the Orbiter flight loads and environments defined in JSD 07700, Vol XIV, Section 4.2 (Ref. 2-23).

Safety. Specific safety design criteria that have been established for the PMS are:

- Safety is a nontradeable consideration in PMS design. No single failure or credible combination of failures will result in injury to crew or damage to other equipment.
- The system shall incorporate redundant control and monitoring circuits. These will employ independent, redundant power sources.
- System design shall provide positive power removal capability before disconnecting and reconnecting modules/components (dead facing).

2.1.4 ASU Projected Design Parameters

Assumptions

a) The parts count associated with the circuit details reflects a nonredundant configuration.

b) The solar array switches and the SASU control logic circuits are packaged in hybrid units to reduce parts count.

c) The μP controller and its associated logic circuits are packaged in LSI chips.

d) The weight estimate is derived from the actual weight of similar circuits employed on existing spacecraft designs.

e) The selected sequencing configuration for the LEO mission is a 2 bit binary count/sequenced arrangement which minimizes parts count.

f) To reduce solar array switch dissipation, four MOSFETS are parallel connected in each hybrid.

Size: The ASU is packaged along the edge of the array closest to the rotary transfer joint. It will be attached to the array stowage container.

Mass:	21.4 Kg (47.1 lb) per channel 5.2 Kg (11.4 lb) total for ion propulsion
Efficiency:	98.6%
*Parts Count:	625 for 10 channels 648 for channel controlling ion propulsion. Total = 6898 Parts

*Includes current, voltage and temperature sensing circuits.

2.2 GEO Platform

2.2.1 GEO Mission Requirements and Payload Selection

References 2-10 through 2-15 were reviewed to obtain suitable mission requirements to allow formulation of the SASPM requirements for a GEO platform. Table 7 of Appendix A summarizes the GEO payload requirements obtained. The Geostationary Platform demonstration was selected as an application for this study because the 25 to 50 KWe load requirement most nearly matched the SASPM study requirements.

2.2.1.1 GEO Spacecraft (Housekeeping) Requirements

In addition to supporting a variety of payloads in geosynchronous earth orbit, the GEO platform must be capable of maintaining its own functions. The energy required for this maintenance is separable into two parts, station keeping and housekeeping power.

In geosynchronous orbit, beyond the first order earth gravitational effect, the second order forces acting on a satellite are the asphericity of the earth, including oblateness and triaxiality, the gravitational attraction of the moon and the sun, and solar radiation pressure. In order to maintain station, a means of overcoming these effects must be supplied in GEO. In this case, ion propulsion is selected as the solution. Power for the ion thrusters is supplied by diverting payload power during those relatively small periods of time when orbit correction is required.

Housekeeping includes all power required by the spacecraft (other than payload support) to perform its mission. The 25 kw SP was taken as a model to determine these requirements; therefore, housekeeping loads of 5 kw are assumed.

2.2.1.2 GEO Mission EPS Operational Requirements

The EPS operational requirements are outlined below:

a) Purpose. To provide electrical power continuously (25 KWe to 50 KWe) to a mix of communications and scientific payloads.

b) Mission. The power platform will operate in GEO, 24 hour orbit, 1.2 hours eclipse maximum. Specific missions will be determined by the payload requirements.

c) Unmanned Operation.

d) Orbit Transfer. The GEO platform will be STS launched into LEO. Orbit transfer to GEO will be accomplished by ion propulsion.

e) Control. The platform will be modular and will be independent in operation. It will be controlled by the PMS, with optional external command override. Station keeping and position transfer will be accomplished by the auxiliary and primary ion propulsion systems.

f) Reliability

- The power system will be reliable to two failure tolerance criteria for crew safety items per NHB 1700.7 (Reference 2-18).
- Standard component derating and high reliability parts will be incorporated. Nominal design life will be eight years in orbit, with a goal of 10 years.

g) Environment

- Space shuttle launch requirements, as reflected at the Orbiter/EPS interface. (Reference 2-23, Appendix 10.1)
- Normal GEO spacecraft design parameters while in orbit.

h) Output Capacity

- Provide continuous 25 KWe to 50 KWe to a combination of communications and scientific payloads.

- Be flexible in nature and capable of expansion.
- Provide up to an additional 5 KWe continuously for spacecraft housekeeping loads.

2.2.2 Baseline GEO Platform Electrical Power System

The baseline EPS which meets the above requirements is as follows. A block diagram of the system is shown in Figure 2.2-1. In addition to the above requirements, other assumptions are:

- The platform will be STS launched into LEO, and transferred to GEO by ion propulsion.
- The platform will employ a photovoltaic solar cell array power source.
- The platform will employ SASPM.
- The platform will employ 1990s technology.

2.2.2.1 System Voltage

The argument of Section 2.1.2.1 for the LEO system voltage applies equally to the GEO platform system voltage.

To minimize the mass of the solar array harness and the distribution system, the highest practical voltage should be used for power transmission. For the beam supply in the ion propulsion subsystem this would be ~860 volts.

Present solar arrays (SEPS, 25 kw SP, PEP) are designed for a maximum power point voltage of approximately 200 volts, at the array average sunlight temperature. Array maximum (cold) voltage is therefore in the neighborhood of 400 volts. This voltage is presently driving the design of high voltage (and high current) switches for space application to about 500 volts, and as much as 500 amps. Therefore, a 200-260 volt system will be baseline for the GEO mission.

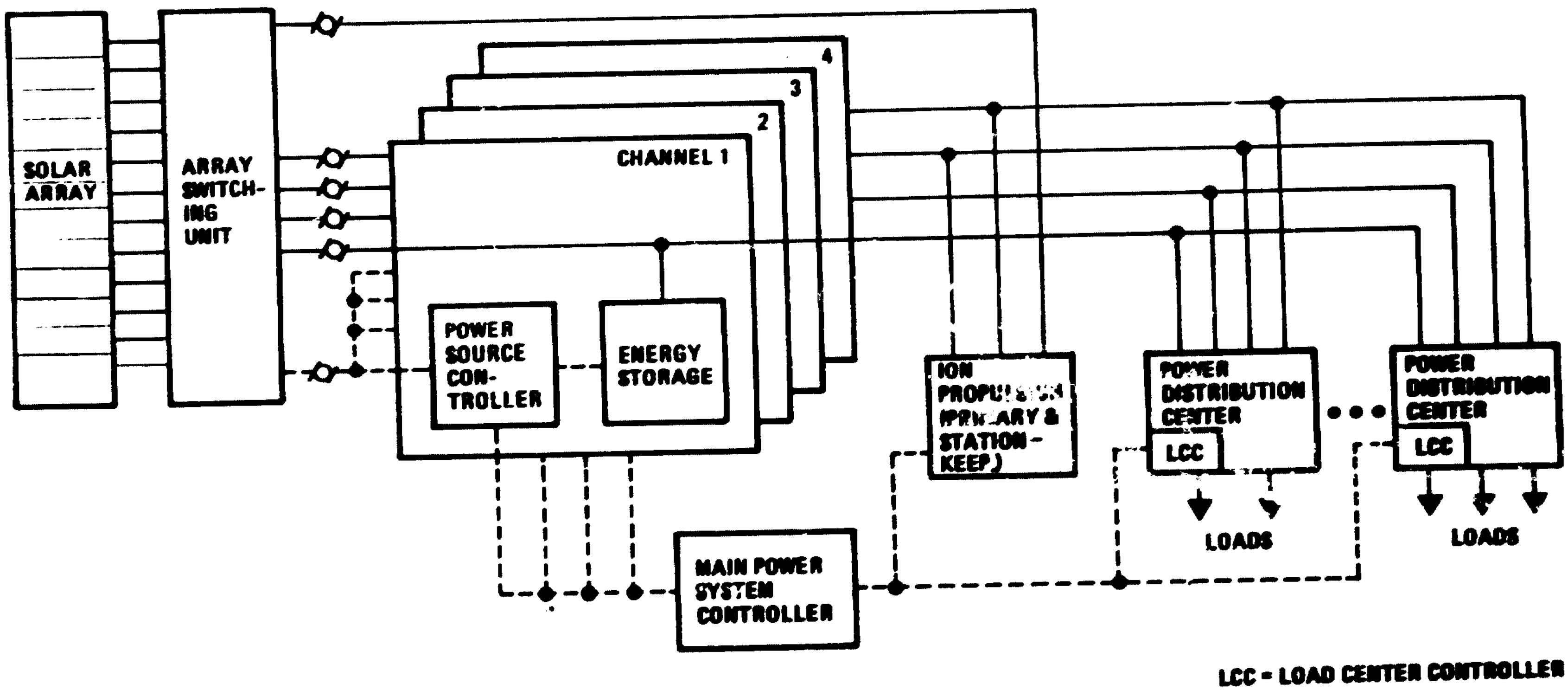

GENERATION – SILICON PLANAR SOLAR ARRAY
ENERGY STORAGE – SILVER-HYDROGEN BATTERY
BATTERY CHARGER – SOLAR ARRAY REGULATION
POWER DISTRIBUTION – DIRECT CURRENT AT SOURCE VOLTAGE, 200 - 260 VDC *
POWER PROCESSING – AS NEEDED WITHIN EACH PAYLOAD OR LOAD CENTER
CHANNEL QUANTITY – DEFINED BY BATTERY CAPACITY (4)
RELIABILITY – FAIL OPERATIONAL, FAIL SAFE
LIFE – 10 TO 15 YEARS
– SLIP RINGS
*ION ENGINE BEAM CURRENT SUPPLIED AT 860 VDC DURING SUNLIGHT ONLY

Figure 2.2-1 GEO Baseline Electrical Power System Design

2.2.2.2 Energy Storage

Mass is critical for GEO applications. Because of their higher specific energy (as projected for the 1990s), silver-hydrogen batteries were selected. A_g-H_2 cells are projected to have a specific energy of 81 Wh/kg by the 1990s, as compared to a projection of 55 Wh/kg for Ni-H_2 cells in the same time frame. The current problem of silver solubility/migration is expected to be controlled and a ten year cycle life (GEO) @ 75% DOD is projected (Reference 2-21). The weight savings on a 150 AH Ag-H_2 battery over a 150 AH Ni-H_2 battery is estimated to be 10kg. This is primarily due to the higher specific energy of the silver electrode over the sintered nickel electrode (a factor of 2.7) and the reduced weight of the cell container.

It is projected that high voltage batteries (120V-250Vdc) will be in use in the 1990s. On-going studies such as the 25 kw Space Platform, (NAS8-33956) the 250 kw Platform study (Reference 2-17) and the Solar Electric Propulsion System have identified the need for this technology.

A system efficiency diagram is shown in Figure 2.2-2. The total load in sunlight is 55kw. It will be the same in eclipse. The ion propulsion system will be used only in sunlight, and therefore no energy storage for this purpose is required. The load requirements on the energy storage device in eclipse are:

$$\frac{55\ \text{kw}}{(.995)^2} = 55554 \text{ watts}$$

The total energy is 55554 watts x 1.2 hours = 66665 watt hours

2.2.2.2.1 Battery Sizing

Assumptions:

- Number of charge/discharge cycles in 10 years: ~1000
- Maximum eclipse duration: 1.2 hrs.
- Minimum sunlight duration: 22.8 hrs.
- Allowable battery depth of discharge: 75%
- Number of series cells: 168 (6 packs of 28 cells each)

- Cell size: 120 ampere-hours
- *Average discharge voltage: 1.2 volts/cell
- Maximum charge voltage: 1.55 volts/cell
- The overall EPS efficiency is defined in Figure 2.2-2

Each battery would have a capability of

168 cells x 1.2 volts/cell x 120 A-hr x .75 = 18,144 watt hrs

The number of channels is

$$\frac{66665 \text{ watt hours}}{18144 \text{ watt hours}} = 4 \text{ channels}$$

*It is recognized that the silver hydrogen battery has multiple plateaus in output voltage, however, for purposes of this study an average of 1.2 volts per cell is assumed.

2.2.2.3 Power Generation

The solar array design characteristics given in Reference 2-20 are shown below: (1990's projected capabilities)

Configuration	Planar	Concentrator
Solar Cell Type	Silicon	Gallium Arsenide
Cell Efficiency, n_c	18%	30%
Cell Cost	Moderate	High
Specific Area	200 w/m^2	150 w/m^2
Specific Mass (no degradation)	(75 w/kg)	(45 w/kg)

It is projected that radiation resistant solar cells will be developed in the 1990s. Radiation damage to silicon cells after ten years in synchronous earth orbit could be less than 15%, (Reference 2-21), which is approximately half of the degradation predicted for today's technology.

Because of the severe mass constraints on a GEO mission, the planar array concept will be baseline. The projection of 18% efficient silicon solar cells increases the planar array specific area to 135 watts/m^2.

2.2.2.4 GEO Mission Solar Array Switching Power Processing

The GEO Mission has two power system configurations; One when orbit transfer or orbit maneuvering is taking place, and one when payloads are being supplied the bulk of the power. The high voltage array is reconfigurable to supply payloads. The SASPM system sizing model is shown in Figure 2.2-2

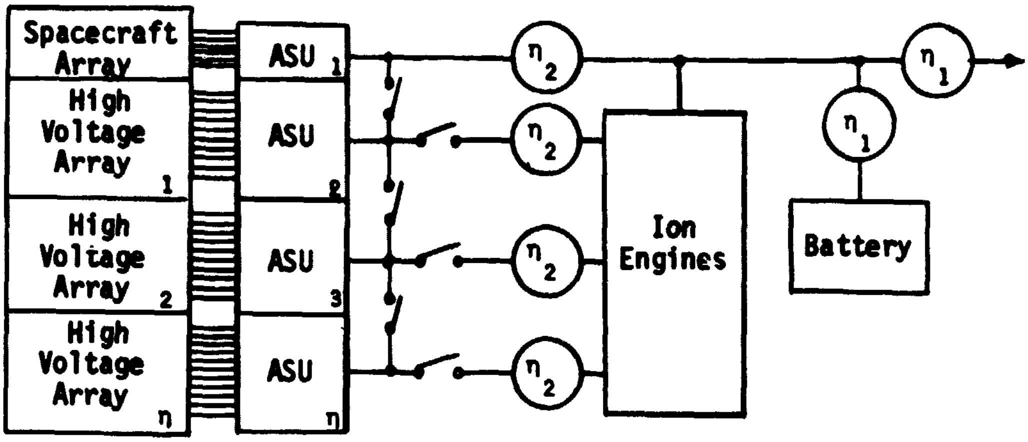

Figure 2.2-2 GEO Solar Array Switching Power Management Sizing Model

$$\text{*Solar array output power} = \frac{P_L + P_H + P_C}{\eta_2 \cdot \eta_1 \cdot d_1 \cdot d_2 \cdot \epsilon_p} \quad (2.2\text{-}1)$$

ORIGINAL PAGE IS OF POOR QUALITY

P_L = Payload power

P_H = Housekeeping power

P_C = Battery charging power

η_1 = Wiring and connector efficiency = (.995)

η_2 = Wiring and connector efficiency = (.99)

d_1 = Solar array end of life efficiency in GEO = (.85)

d_2 = Solar array degradation through Van Allen region = (.75)

ϵ_p = Array processor efficiency = (.986)

*Sizing based on payload operations mode.

In addition to the 15% degradation in GEO, the solar array is projected to degrade 25% as it travels through the Van Allen region (Figure 2.2-3). From equation (2.2-1) we have

$$\text{Array Power (BOL)} = \frac{P_L + P_H + P_C}{\eta_1 \cdot \eta_2 \cdot d_1 \cdot d_2 \cdot \varepsilon_p}$$

ORIGINAL PAGE IS
OF POOR QUALITY

All the terms are known except the battery charging power.

2.2.2.4.1 Battery Charging Requirements

Eclipse requirement: Up to 50Kw for payloads
5Kw for housekeeping loads
55Kw Total

Batteries supply $\frac{55000 \text{ watts}}{(.995)^2} = 55554$ watts

$$\frac{55554 \text{ watts}}{200 \text{ volts average}} = 277.8 \text{ amperes}$$

Charging requirements = (277.8 amps)(recharge ratio)(discharge/charge ratio)

$$= (277.8)(1.1)\left(\frac{1.2 \text{ hours}}{22.8 \text{ hours}}\right)$$

= 16.1 amperes

(16.1 amps)(260 volts) = 4186 watts

$$\text{Array Power (BOL)} = \frac{50{,}000W + 5000W + 4186W}{(.995)(.99)(.85)(.75)(.986)}$$

= <u>95,588 watts</u>

$$\text{Array size} = \frac{95588W}{135W/m^2} = 708 \text{ m}^2$$

$$\text{Array mass} = \frac{95588W}{200W/Kg} = 478 \text{ Kg}$$

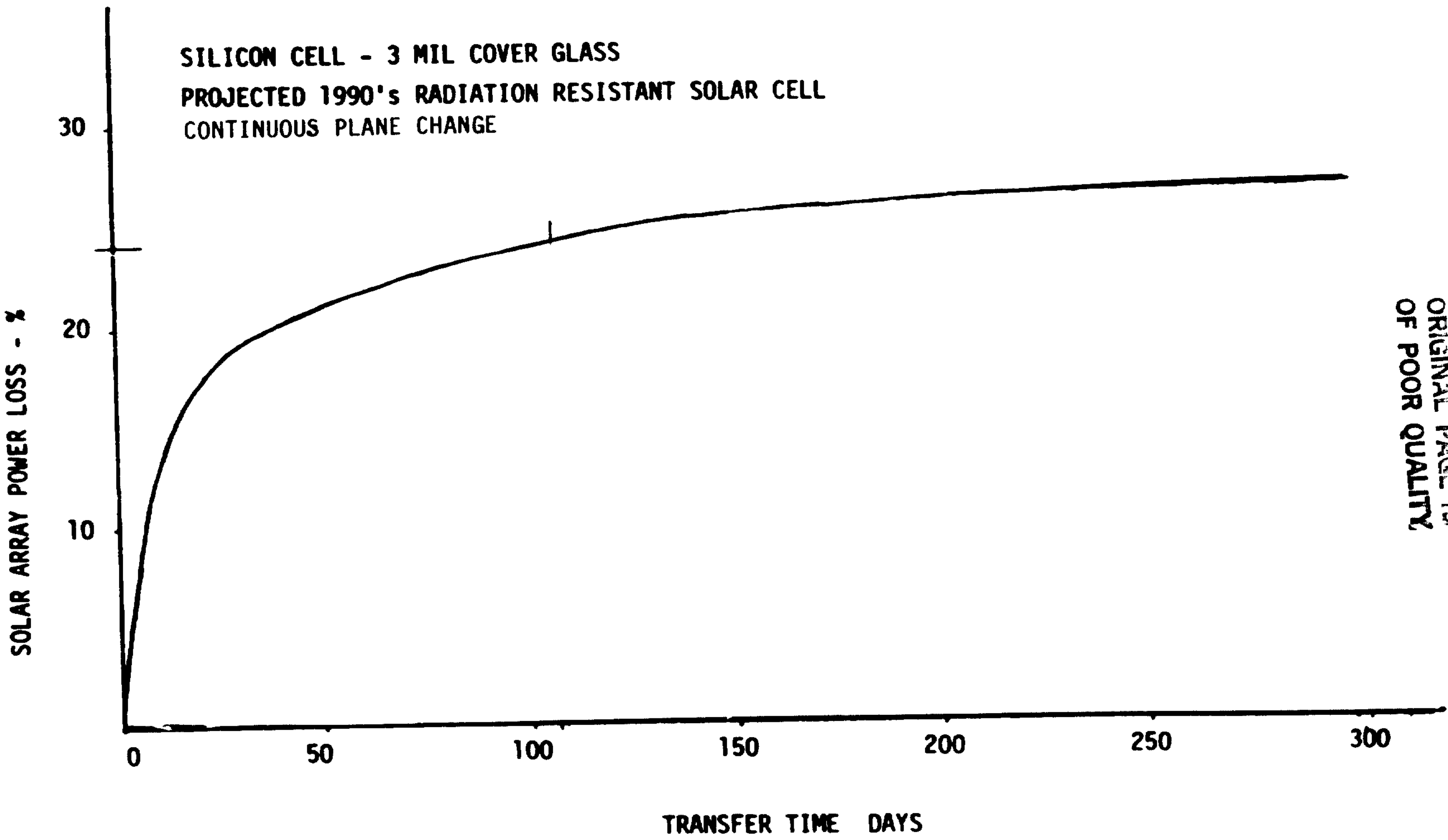

Figure 2.2-3: Silicon Solar Cell Degradation for Spiral Trajectories from LEO to GEO

2.2.2.5 Solar Array Output Control

Sequentially-switched solar array segments, controlled by the power source controller and the main power system controller accomplish simultaneous control of both array power and battery charging while supplying load power. The need for a battery charger and line regulator can be eliminated if no more than one battery per channel is utilized. The configuration of the array switching unit is the subject of Task 2.

2.2.2.6 Power Transmission and Distribution

In the Reference 2-17 study, power conditioning for the loads is accomplished in the individual load centers. Each load center receives power with regulation determined by the charge and discharge voltage of the battery. If a user has other requirements, special purpose inverters, converters or regulators can be utilized without penalizing power delivery to other payloads. In addition:

- The four payload power buses will have cross tie capability in case of a channel failure. The bus can be isolated from the failed channel and tied to an operable channel until a redundant unit is commanded in.
- Power buses cannot be paralleled without isolation. (current limited) This is to prevent individual failures or faults from affecting other buses and to insure proportional discharge of the batteries.
- A circuit breaker arrangement will control power delivered to payloads. The main power system controller will monitor the loads so that any one channel will not be overloaded.

2.2.3 GEO Power Management System (PMS) Requirements

The GEO PMS includes all functions associated with the transmission, distribution, processing, and conditioning of electrical power from the source to the load, including the energy storage subsystem control. The design of the EPS and PMS are interactive, each having an effect on the configuration of the other. The PMS requirements are derived from References 2-17 and 2-18.

Figure 2.2-1 depicts the major EPS elements, with the PMS Control indicated by dotted lines. Both the EPS and the PMS are designed on a modular basis in order to provide a flexible response to demands for load expansion or power increases.

For a 25 KWe to 55 KWe EPS, a transmission (main power bus) voltage of 200 to 240 will be baseline (see Figure 2.1-2). High voltage for the ion propulsion engines (860v) will be supplied directly from the solar array switching unit. Lower voltages, tight regulation, or AC power will be supplied by local converters in the individual payloads. Critical loads will be powered from more than one bus. The EPS will be designed to supply an average continuous load in the range of 25 KWe to 55 KWe. In addition, during daylight, peak loads of approximately twice the average load can be supported by the power system (to an unregulated bus).

PMS reliability criteria for the GEO application are as follows:

- The system failure mode will be a graceful degradation. No single failure or credible combination of failures will prevent the system from operating in an acceptable degraded mode of operation.
- Redundant controls, power conditioning equipment and load paths shall be employed.
- Control and monitoring circuits shall employ independent, redundant power sources.
- In the event of module/component failure of such a magnitude as to degrade system capability, the system will shed loads according to a predetermined heirarchy, based on a load analysis and an established order of criticality.

The PMS incorporates a built in test capability for fault diagnosis that identifies failures and incipient failures (degraded performance). The testing system will maintain records of out of limit conditions, and identify trends. These data will aid in the prediction of incipient failures, and make possible the graceful degradation of the system capability while minimizing the effect on payload operation.

The PMS will observe the following maintainability critera:

- The system will be unmanned. To the degree possible within cost constraints, all components of the PMS that are subject to degradation, failure, or wearout during the 10 year operational lifetime shall be designed so as not to preclude orbital replacement.
- The system will employ computer controlled power management techniques with the following capabilities.
  - Continuous monitoring of system health and performance.
  - Detection and isolation of faults.
  - Shifting loads around failed equipment, or conversely, substituting redundant units for failed equipment.
  - Prediction of incipient failures.
  - Capability to shut down and isolate failed equipment in order to prevent damage to other equipment.

The PMS is designed to operate in a geosynchronous earth orbit. PMS elements will perform their intended function without overheating, malfunction or electrical breakdown while operating in near vacuum conditions. All PMS components and assemblies will be subjected to two flight load and environmental profiles.

- Initial delivery to LEO will be Orbiter. The PMS must withstand the criteria of JSC 07700, Vol. XIV, Section 4.2 (Ref 2-23).
- Orbit transfer from LEO to GEO will be via ion propulsion.

When the platform is in contact with or in the vicinity of the Orbiter, the following safety criteria apply. The basis for these rules is NHB 1700.7, STS Safety Manual (Reference 2-18).

- Safety is a non-tradeable consideration, no single failure or credible combination of failures shall result in crew injury or damage to other equipment.
- On those functions identified as safety critical, two failure tolerant design criteria shall apply.
- On these same functions, the system shall incorporate redundant control and monitoring circuits, with independent, redundant power sources.
- System design shall provide deadfacing of power connectors whereever feasible for maintenance operations.

2.2.4 Ion Engine Power Analysis

The initial solar array power available to the ion engines is computed as the array BOL capability minus the 25% loss in the Van Allen region and the array BOL requirement for housekeeping loads.

$$(95{,}588)(.75) - \frac{5{,}076 \text{ watts}}{(.75)(.85)} = \underline{63{,}729 \text{ watts}}$$

The solar array size required for 0.5 Newton thrust is 17,620 watts of high voltage and 5622 watts of lower voltage power plus distribution losses of 166 watts.

Total solar array requirements for 1/2 Newton thrust ion propulsion = 23,409 watts. Scaling this to the available solar array power

$$\frac{63{,}729 \text{ watts}}{23{,}409 \text{ watts}} \times 0.5 \text{ Newton}$$

results in a thrust capability of 1.361 Newtons. (ISP = 5600 seconds)

2.2.5 ASU Projected Design Parameters (4 channels)

Assumptions

a) The parts count associated with the circuit details reflects a non-redundant configuration.

b) The solar array switches and the SASU control logic circuits are packaged in hybrid units to reduce parts count.

c) The sequencing approach was selected on the basis of minimizing the number of parts.

d) The μP controller and its associated logic circuits are packaged in LSI chips.

e) The weight estimate is derived from the actual weight of similar circuits of existing spacecraft designs.

f) The selected sequencing configuration for the GEO mission is the 4 bit binary count/sequenced arrangement.

g) To reduce solar array switch dissipation, four MOSFETS are parallel connected in each hybrid.

Size: The unit is packaged along the edge of the array closest to the transfer joint. It will be attached to the array stowage container.

Weight: 22.9 Kg (50.3 lb) each of 4 channels, 91.6 Kg total

Efficiency: 98.6%

*Parts count: 291 (each of 4 channels) 1164 total

*Includes current, voltage and temperature sensing circuitry.

2.3 Ion Propulsion Orbit Transfer Vehicle (IPOTV)

2.3.1 IPOTV Mission Requirements

The 250 KWe IPOTV will be capable of providing a means of lifting payloads from LEO to GEO and back. While in GEO, the IPOTV will be capable of supplying any combination of housekeeping and payload support requirements continuously of up to 5 KWe.

The IPOTV will be modular and will contain a docking module which will serve as a power control and distribution center. The system will be designed to be independent during operation. The launch vehicle into LEO will be the Shuttle Orbiter.

An operational scenario for the IPOTV is as follows. The stowed IPOTV would be lifted into LEO by the orbiter where it would be docked with the 250 KWe LEO Platform until required. The platform would supply housekeeping facilities in order to preclude the necessity for extending the IPOTV solar array and therefore increasing drag. When desired, a payload would be docked with the IPOTV, and lifted into any desired orbit from LEO to GEO. If the payload power requirements are within the capability of the IPOTV, the IPOTV could be used as a power platform to support the payload. At termination of the need for the IPOTV during a given mission, the IPOTV could:

a. Remain in GEO until required to return a payload.

b. Return to LEO to repeat the scenario.

A prime consideration is minimization of the trips through the Van Allen belt because of radiation degradation considerations.

The IPOTV, under the above scenario, must be capable of supporting a diversity of payloads, therefore, a utility approach similar to that employed on the LEO Platform is indicated. This approach points to the requirement for a Power Management System (PMS), both to manage loads and to control operation of a highly complex, independent, unmanned system.

2.3.1.1 IPOTV Life Estimation

Life of the IPOTV is based on the number of trips through the Van Allen belt, and the dwell time there. This subject is addressed in Appendix B.

2.3.1.2 IPOTV Mission EPS Operational Requirements

The EPS operational requirements are outlined below:

a) Purpose. To provide electrical power of 5 KWe continuously to a mix of housekeeping loads and payloads in GEO, and to supply an initial 250 KWe (minus housekeeping loads) of power to an ion propulsion system for lifting the payload between LEO and GEO

b) Mission. The IPOTV lifting from LEO to GEO, and dwelling at GEO in a 24 hour orbit, with 1.2 hours eclipse maximum.

c) Unmanned Operation

d) Orbit Transfer. The IPOTV will be STS launched into LEO. Orbit transfer to GEO will be accomplished by ion propulsion.

e) Control. The IPOTV will be modular and will be completely independent in operation. It will be controlled by the PMS, with external command override.

Station keeping and position transfer, orbit transfer and drag makeup will be accomplished by ion propulsion.

f) Reliability. The EPS will be reliable to the point that life support requirements are met, including the two failure tolerant criteria for crew safety items in Reference 2-18 when the IPOTV is attached to or within the vicinity of the orbiter or the 250 KWe manned platform. Proper component derating and high reliability parts will be incorporated. Nominal design life will be 8 to 10 years in orbit excluding the solar array, which is considered replaceable.

g) Environment

- Space shuttle launch requirements, as reflected in Reference 2-23.
- Normal LEO and GEO spacecraft design requirements while in orbit.

h) Output Capacity

- Provide continuous 5 KWe to housekeeping (and possibly payloads).
- Provide up to 250 KWe (minus housekeeping loads) (BOL) during daylight hours for ion propulsion.

2.3.2 Baseline IPOTV Electrical Power System

The baseline EPS which meets the aforementioned requirements is as follows. A block diagram of the system is shown in Figure 2.3-1. In addition to the above requirements, other assumptions are:

- The IPOTV will employ a photovoltaic solar cell array power source.
- The IPOTV will employ SASPM.
- The IPOTV will employ 1990s technology.

2.3.2.1 System Voltage

Ongoing studies (SEPS, 25KW SP, PEP) are looking at solar arrays designed for a maximum power point voltage of approximately 200 volts for a warm array. The 25KW SP has a 120 volt dc bus for payloads and housekeeping. The design is directly applicable to the spacecraft bus on the IPOTV.

The desired voltage (860V) for ion propulsion offers some problems of implementation. For example, in LEO, plasma interaction starts at approximately 200 volts, with arcing and corona occurring somewhere above 500 volts. Environmental interactions are discussed in more detail later in this report.

2.3.2.2 Energy Storage

A system efficiency diagram is shown in Figure 2.3-2. The total (maximum) load in sunlight is 250 KW.

The requirement for standby power for advanced argon engines has not been studied. For this analysis 5 KW maximum has been estimated.

Eclipse requirements

a) 5 KW to housekeeping loads

b) 5 KW ion engine standby power

$$\text{Batteries supply} = \frac{10{,}000 \text{ watts}}{(.995)^2} = 10{,}100 \text{ watts}$$

$$\frac{10{,}100 \text{ watts}}{100 \text{ volts}} = 101 \text{ amperes}$$

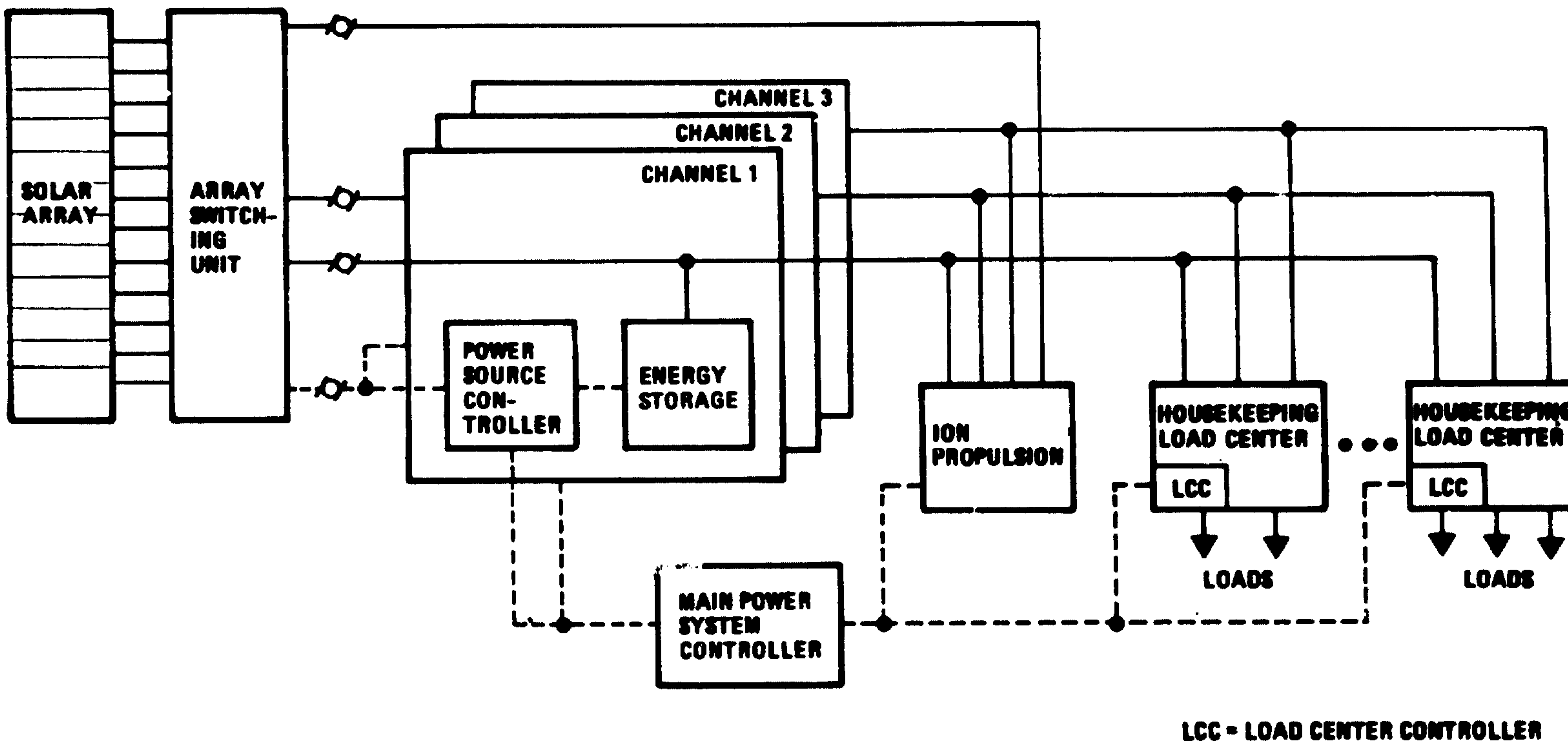

GENERATION – SILICON PLANAR SOLAR ARRAY
ENERGY STORAGE – NICKEL-HYDROGEN BATTERY FOR HOUSEKEEPING
BATTERY CHARGER – SOLAR ARRAY REGULATION
POWER DISTRIBUTION – DIRECT CURRENT AT SOURCE VOLTAGE, 100 TO 120 VDC*
POWER PROCESSING – AS NEEDED WITHIN EACH LOAD CENTER
CHANNEL QUANTITY – DEFINED BY BATTERY CAPACITY (3)
RELIABILITY – FAIL OPERATIONAL, FAIL SAFE
LIFE – FUNCTION OF USAGE, REPLACE FAILED UNIT AT NEXT SERVICE OPPORTUNITY
– SLIP RING
*ION ENGINE BEAM CURRENT SUPPLIED AT 860 VDC DURING SUNLIGHT ONLY

Figure 2.3-1 IPOTV Baseline Electrical Power System Design

ORIGINAL PAGE IS
OF POOR QUALITY

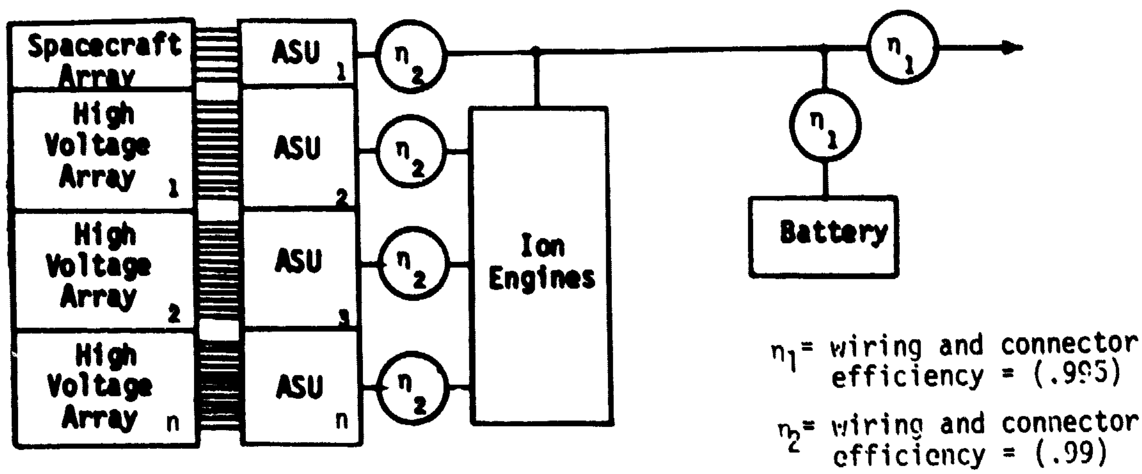

Figure 2.3-2 IPOTV Solar Array Switching Power Management Sizing Model

The total energy = 10,100 watts x 1.2 hrs = 12,120 watt-hrs.

This is the maximum discharge case (GEO).

A 50 amp-hour, $Ni\text{-}H_2$ cell was selected for this application. Eighty cells in series constitute a single battery. At a depth of discharge of 75% each such battery will have a capacity of

80 cells x 1.25 v/cell x 50 A-hrs x .75 = 3750 watt-hrs

The number of power channels is

$$\frac{12120 \text{ watt-hrs}}{3750 \text{ watt hrs/channel}} \approx 3 \text{ channels}$$

2.3.2.3 Power Generation

Design characteristics for planar and concentrator arrays were presented in Section 2.2.2.3. Because of the severe mass constraints (transition time in the Van Allen belt region is inversely proportional to total mass) on the IPOTV, the planar array will be baseline. (minimum mass)

2.3.2.3.1 Battery Charging Requirements

The maximum battery charging requirement occurs in LEO.

$$\text{Maximum battery charge} = (101 \text{ amperes})\left(\frac{36 \text{ minute eclipse}}{54 \text{ minute sunlight}}\right)(\text{recharge ratio})$$

$$= (101)\left(\frac{36}{54}\right)(1.06)$$

$$= 71.4 \text{ amperes}$$

(71.4 amps)(120 volts) = 8,568 watts

2.3.2.3.2 ASU Output Requirements

1. Housekeeping: 5000 watts/(.995)(.99) = 5,076 watts
2. Battery Charging: 8568 watts/(.995)(.99) = 8,698 watts

Total: 13,774 watts

Losses in the ASU:

$$13,774\left(\frac{1-.986}{.986}\right) = 196 \text{ watts}$$

The concept of the IPOTV power system is to start with a 250 KW array and use it until it degrades to 55 KW, at which time it is to be replaced.

The degradation factor is $\frac{55}{250} = 0.22$

$$\text{Array Power} = 13{,}774 + 196 = 13{,}970 \text{ watts, (EOL)}$$

$$\text{Array BOL requirement} = \frac{13970}{.22} = \underline{63{,}500 \text{ watts}}$$

Housekeeping loads and battery charging require 63,500 watts of array power (BOL). An array reconfiguration schedule based on the percent reduction of output power can be implemented so that initially 15 KW would be allocated to the spacecraft bus. As the array degrades, array increments of 1 KW capability would be switched in. This would allow the maximum power to be supplied to the ion engines. <u>This flexibility is not available with conventional power processing techniques.</u>

$$\text{Array size} = \frac{250{,}000 \text{ watts}}{135\text{W/m}^2} = 1852\text{m}^2$$

$$\text{Array mass} = \frac{250{,}000 \text{ watts}}{200\text{W/Kg}} = 1250\text{Kg}$$

2.3.2.3.3 <u>High Voltage Array Output</u>

Initial output power of the high voltage array would be 250KW-15KW = 235KW.

Each 0.5 Newton ion engine requires 23,409 watts (Section 2.2.4).

The projected initial thrust capability $= \frac{235{,}000}{23{,}409}$ (.5 Newton)= 5.019 Newtons

2.3.2.4 <u>Solar Array Output Control</u>

Control will be similar in design to the LEO system.

2.3.2.5 <u>Power Transmission and Distribution</u>

For the spacecraft bus, the regulation will be determined by the battery charge and discharge voltage. The high voltage bus will initially be controlled at 960 volts. After the solar array degrades to 720 volts, the array will be reconfigured back to 960 volts. Reconfiguration is covered in Section 3.

- The three spacecraft power busses will have cross-tie capability in case of a channel failure.

- Power busses cannot be paralled without isolation. This is to prevent individual failures or faults from affecting other busses, and to insure proportional discharge of the batteries.
- A circuit breaker arrangement will control power delivered to payloads. The main power system controller will monitor the loads so that any one channel will not be overloaded.

2.3.3 IPOTV Power Management System (PMS)

The PMS includes all functions associated with the transmission, distribution, processing and conditioning of electrical power from the source to the load, including the energy storage subsystem control. The design of the EPS and PMS are interactive, each having an effect on the configuration of the other.

Figure 2.3-1 depicts the major elements of the EPS, with the PMS control indicated by dotted lines. Both the EPS and the PMS are designed on a modular basis in order to provide a flexible response to varying demands.

A transmission (main power bus) voltage of 100-120 volts for the spacecraft housekeeping loads is baseline. High voltage for the ion propulsion (860V) will be supplied directly from the solar array switching unit. Lower voltages, tight regulation, or AC power will be supplied by local conversion in the individual loads. Critical loads will be powered from more than one bus. During daylight only, peak power of 235 kw will be available to the ion propulsion system, at the beginning of life.

PMS reliability criteria for the IPOTV application are as follows:

- The system failure mode will be a graceful degradation. No single failure or credible combination of failures will prevent the system from operating in an acceptable degraded mode of operation.
- Redundant controls, power conditioning equipment and load paths shall be employed.
- Control and monitoring circuits shall employ independent, redundant power sources.

- In the event of module/component failure of such a magnitude as to degrade system capability, the system will shed loads according to a predetermined heirarchy, based on a load analysis and an established order of criticality.

The PMS incorporates a built-in test capability for fault diagnosis that identifies failures and incipient failures (degraded performance). The testing system will maintain records of out of limit conditions, and identify trends. These data will aid in the prediction of incipient failures, and make possible the graceful degradation of the system capability while minimizing the effect on system operation.

The PMS will observe the following maintainability criteria:

- The system will be unmanned. To the degree possible within cost constraints, all components of the PMS that are subject to degradation, failure, or wearout during the 10 year operational lifetime shall be designed so as not to preclude orbital replacement in LEO.

- The system will employ computer controlled power management techniques with the following capabilities.

  -Continuous monitoring of system health and performance.

  -Detection and isolation of faults.

  -Shifting loads around failed equipment, or conversely, substituting redundant units for failed equipment.

  -Capability to shut down and isolate failed equipment in order to prevent damage to other equipment.

The PMS is designed to operate in transition orbits from LEO to GEO. PMS elements will perform their intended function without overheating, malfunction or electrical breakdown while operating in near vacuum conditions. All PMS components and assemblies will be subjected to two flight load and environmental profiles.

- Initial delivery to LEO will be by Orbiter to a manned LEO platform. The PMS must withstand the criteria of JSC 07700, Vol. XIV, Section 4.2 (Ref. 2-23) while in these modes.
- Orbit transfer from LEO to GEO will be via ion propulsion. When the platform is in contact with or in the vicinity of the Orbiter or the LEO platform the following safety criteria apply. The basis for these rules is NHB 1700.7, STS Safety Manual (Ref. 2-18).
- Safety is a non-tradeable consideration; no single failure or credible combination of failures shall result in crew injury or damage to other equipment.
- On those functions identified as safety critical, two failure tolerant design criteria shall apply.
- On these same functions, the system shall incorporate redundant control and monitoring circuits, with independent, redundant power sources.
- System design shall provide deadfacing of power connectors for maintenance operations.

2.3.4 ASU Projected Design Parameters (3 channels)

A conceptual design was not completed for the IPOTV mission. Data was extrapolated from the LEO mission, which has similar design requirements.

Size: The ASU is packaged along the edge of the solar array closest to the rotary transfer joint. It will be attached to the array stowage container.

Weight: Approximately 23 kg (51 lb), each of three channels

Efficiency: Approximately 98.6%

*Parts count: Estimate 1938 total parts (each of 3 channels)

*Includes current, voltage and temperature sensing circuitry.

REFERENCES

2-1. "Final Report for Payloads Requirements/Accommodations Assessment Study for Science and Applications Space Platforms (Volume II)," Report No. 86254-6001-UE-00, dated 26 November 1980. (MDAC)

2-2. "Materials Experiment Carrier Payload Requirements Review," Report No. MPS.6-80-081, dated 1 April 1980. (TRW)

2-3. "Materials Experiment Carrier Concepts Definition Study (Volume IV)," Report No. MPS.6-80-288, dated 20 October 1980. (TRW)

2-4. "Materials Experiment Carrier Concepts Definition Study (Volume V)," Report No. MPS.6-80-289, dated 12 November 1980. (TRW)

2-5. "Study of Power Management Technology for Orbital Multi-100 KW Applications (Volume III)," Report No. NASA-CR 159834, dated 15 July 1980. (GDC)

2-6. "Space Station Systems Analysis Study," Report No. DPD 524-MA-04, dated 28 February 1977. (MDAC)

2-7. "Space Transportation System User Handbook," dated June 1977.

2-8. "Summarized NASA Payload Descriptions - Sortie Payloads," July 1975.

2-9. "Integrated Planning Support Functions (Study 2.7)," Volume II, Aerospace Report No. ATR-77(7378)-1, Vol. II, dated June 1977.

2-10. "NASA Space System Technology Model (Volume I)," dated May 1980.

2-11. "NASA Space Systems Technology Model (Volume II)," dated May 1980.

2-12. "NASA Space Systems Technology Model (Volume III)," dated May 1980.

2-13. "Systems Studies for a Land Mobile Satellite Service," JPL Report No. 15-86, dated 15 September 1980.

2-14. "Space Stations Systems Analysis Study," McDonnell-Douglas Report No. MDS-G6715-Pt-2-Vol-3, dated 28 February 1977.

2-15 "Space Stations Systems Analysis Study," McDonnell-Douglas Report No. MDC-G6508-Pt-1-Vol-2, dated 1 September 1976.

2-16. Raymond W. Wolverton, Flight Performance Handbook for Orbital Operations, John Wiley and Sons, Inc., New York 1963.

2-17. "Space Power Distribution System Technology Study," NAS8-33198, Phase 1 Oral Review dated 8 December 1980. (TRW)

2-18. "STS Safety Manual," NHB 1700.7A.

2-19. Science and Applications Space Platform Study, MDC G8294. (MDAC)

2-20. Multi-Kilowatt Solar Array Study, Contract NAS8-32986. (TRW)

2-21. AIAA Presentation, "Future Space Power - The NASA Research Perspective," J. P. Mullin, L. P. Randolf, and W. R. Hudson, May 6-11, 1980.

2-22. AIAA Presentation, "Investigation of High Voltage Spacecraft System Interactions With Plasma Environments," N. J. Stevens, F. D. Berkopec, C. K. Purvis, N. Grier, J. Stakins, April 25-27, 1978.

2-23. JSC 07700, Volume XIV, ICD2-19001, Shuttle Orbiter, Cargo Standard Interfaces.

2-24 AIAA Presentation, "Primary Electric Propulsion for Future Space Missions," D.C. Byers, F. F. Terdan, and I. T. Myers, May 8-11, 1979.

3.0 TASK II

CANDIDATE CONCEPTS ANALYSIS AND SELECTION

> "Identify SASPM concepts that could satisfy the requirements defined in Task I. Compare the SASPM concepts according to cost, weight and volume, reliability, efficiency, and thermal control. Determine the concept impacts on mission characteristics and hardware. Establish conventional power processing baseline data."

3.1 Identification of Candidate Concepts

Four basic switching configurations which are capable of controlling solar array segments have been defined. These four candidate concepts are shown in Figure 3.1-1. From these basic configurations, or some conbination thereof, the SASPM implementation scheme will be derived.

3.1.1 Series Switching, Series Array Configuration

This configuration is presented in block diagram form in Figure 3.1-1 (A). Primary features of this concept are:

- The unused solar array sections are bypassed, with each bypassed section being open circuited.
- The bypass switches are effectively in series with the solar array sections.
- The open circuit voltage is controlled by control switch status (open-close).
- The solar array voltage is the control parameter. The individual section (and therefore solar array) current is not directly controlled.

Advantages of the series switched, series array configuration are:

- The bypassed solar array sections are open-circuited. There is no power generated by the open section, and therefore no need to dissipate such power elsewhere.
- Because of the open circuit condition, shadowed cell stress (hot spots) and reverse voltage stress may be circumvented by proper selection of generating solar array sections under varying spacecraft attitudes and shadow patterns.
- This configuration provides the capability of extinguishing arcs in the ion propulsion system, in case the arc is not automatically extinguished by array voltage collapse.

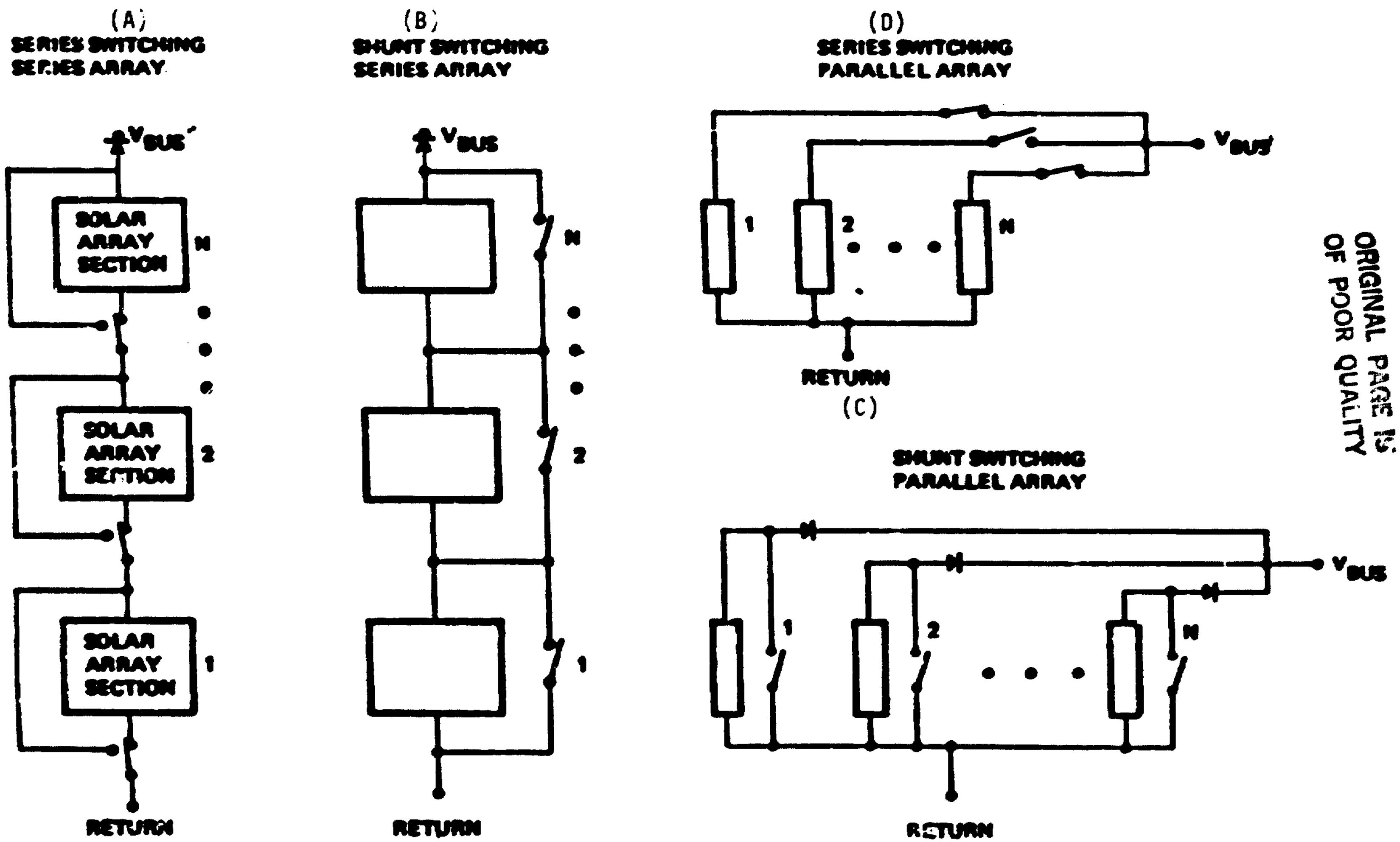

Figure 3.1-1. Basic Solar Array Switching Configuration

There are some inherent disadvantages in this type of solar array switching:

- The switchgear tends toward complexity, with each switch being a "double-throw" device, (two separate on positions), rather than an on-off function.
- The wiring can be complex if the switches are not directly on the solar array, but are located in a central location.
- The switches are in series, therefore each switch must be rated to conduct the full string current (but only a fraction of the voltage).
- In order to prevent reverse current flow during eclipse periods, a blocking diode is required between the solar array and battery buses. In order to provide isolation of solar array sections for hot spot control, it may be necessary to install a blocking diode in each section.
- The series connected switches result in higher losses when array power is needed.
- The switches are not referenced to ground which requires a more complex drive circuit.

3.1.2 Shunt Switching, Series Array Configuration

The block diagram for this system is shown in Figure 3.1-1 (B). Primary features for this concept are:

- Solar array sections whose output is not required are shorted by switches.
- These switches control solar array open circuit voltage rather than the short circuit current of the array sections.
- The section (and therefore solar array) current is not directly controlled.

Advantages of the shunt switched, series array configuration are:

- Dissipation occurs in the switches only when they are closed; only when excess (to the load requirements) solar array power is available.

There are some disadvantages to this type of solar array switching arrangement:

- The number of solar cells that can be shorted is limited. In the shorted condition, a weak cell can be driven in the reverse direction, which creates a hot spot and/or reverse voltage stress.

- Each solar array section requires a series blocking diode in order to prevent current flow into a dark (or shorted to ground) solar array from the remainder of the system.
- Because of the string length per switch element, and the difficulty involved in isolating individual sections, cell shadowing stress may be a problem.
- The individual switches are floating (not referenced to ground) with the exception of the bottom switch in each string.
- If the switches are centrally located, the wiring can be complex.

3.1.3 Shunt Switching, Parallel Array Configuration

The block diagram for this version is shown in Figure 3.1-1(C). Salient features of this type of arrangement are:

- The solar array sections that are not required for load support are shorted by switches.
- The technique is to employ the switches to control short circuit current of the solar array strings instead of the open circuit voltage as was the case for the series array configurations.

The advantages of the technique are:

- The switch drive electronics are referenced to ground in all cases, and are therefore comparatively simple, adding no additional wiring complexity to the existing design.
- Maximum switch dissipation occurs only when excess solar array power is available and the switch is closed.

Disadvantages of the shunt switched configuration are:

- In order to protect against reverse current flow in eclipse or during ground fault conditions on the solar array, series blocking diodes are required.
- Cell stress during shadowing (or cracked cells) is a problem which must be overcome by cell paralleling or shunting techniques.
- The switch gear must withstand the high voltage of a cold array. This may be in the neighborhood of 800 volts with a nominally operating 400 volt solar array if the batteries are not clamping the bus.

3.1.4 Series Switching, Parallel Array Configuration

This system is presented in block diagram form in Figure 3.1-1 (D). Primary features are:

- Solar array sections not required for load support are open circuited by switches.
- As in the previous parallel connected configuration, the switches are employed to control current rather than voltage.

Advantages of series switching are:

- Of all configurations considered, the series switching, parallel array one offers the best opportunity for centralized switching, and therefore minimizes wiring complexity.
- By placing the switches between the main power bus and the solar array, an opportunity is offered to provide the blocking diode function in the SASU.
- The switch drive is comparatively simpler than that used for either of the series solar array segment configurations.
- This configuration provides the capability of extinguishing arcs in the ion propulsion system.

Disadvantages are:

- Maximum power dissipation in the switches occurs when the switches are closed, which occurs at maximum system load.

3.1.5 Cost Comparison of Switch Configurations

Concept B costs are higher than those for the concept A because:

- The switchgear must withstand the full range of the solar array voltage, and therefore higher voltage switchgear is required.
- Techniques for overcoming cell stress during shadowing must be implemented (probably shunt diodes).
- Series blocking diodes are required. In concept A this feature may be incorporated into the switch.

The costs of concept C are driven above Concept B by requiring more complex switchgear, each switch being a "double-throw" device, (two separate on positions), rather than an on-off function. The wiring will be more complex if the switches are not directly on the solar array, but are located in a central location. Concepts A and B offer a high probability of centralizing switching, while the other two concepts probably demand on array switching. A further cost driver is that the switches are in series, and therefore each switch must be rated to conduct the full string current.

Concept D has more severe cell stress due to shadowing, and therefore the cost of implementing this concept will be higher than concept C.

3.1.6 Switch Configuration Weight and Volume

The requirement for series blocking diodes increases the weight and volume of concept B over concept A, assuming this function can be incorporated into the switch in concept A. concept C requires a larger and heavier switch, and more extensive wiring if the switching function is not directly on the solar array as is highly likely with a lightweight array.

3.1.7 Switch Configuration Reliability

The reliability of all four concepts can be enhanced by redundancy. There appears to be no inherent advantage in any of the concepts.

The preferred failure modes will be "switch closed" in concepts A and C, and "switch open" in concepts B and D. Each of such failed sections would then become part of the always on portion of the array. The reliability of the switches themselves will be addressed in section 4.

3.1.8 Switch Configuration Efficiency

Switch dissipation losses are the least at full load for the shunt switching concepts. The highest efficiency can be obtained in the shunt switching of parallel array segments (concept B). The shunt switching of series array segments does, however, have losses associated with the increased wiring complexity.

3.1.9 Thermal Aspects

For a lightly loaded system, the shunt switching concepts shunt the excess array current through the switches, with concept B switching the most current (full string output) and concept D a less amount. The series switched elements dissipate less, with concept C dissipating only a portion of its normal current losses, and concept A (open) being required to dissipate no power. There will be marginally more thermal losses in the systems requiring longer wire runs.

3.1.10 Recommendations

The foregoing cursory look at cost, weight and volume, reliability, efficiency, and thermal control was undertaken to determine if any of the switching configuration concepts should be eliminated from further consideration. The concepts and criteria are compared in Table 3-1.

TABLE 3-1

Comparison of Concepts

Concept	Criteria*				
	Cost	Weight	Reliability	Efficiency	Thermal
A	1	1	1	1	1
B	2	2	1	1	3
C	3	3	1	2	2
D	4	3	1	2	3

*Note: 1 is best.

3.2 Solar Array Switching Unit (SASU) Functions

The analysis of the three proposed missions shows that the SASU must accomplish several functions. First, it must provide voltage regulation for both the 100 - 260 volt spacecraft busses and the 860 volt ion propulsion busses. The SASU must also provide the charge control mechanism for the spacecraft batteries which (mechanism) requires additional control circuitry that can be modified based on the battery state-of-health. For the ion propulsion application, arcing conditions can occur within the ion engines which result in a short on the ion propulsion power bus. Although the solar array is in itself current limiting, a required function of the SASU is to ensure that the solar array voltage can be diminished to the point that the arc is extinguished. For the GEO and IPOTV applications, solar array reconfiguration is advantageous and can be performed by the SASU. Finally, there are times when the solar array must be deactivated for maintenance and refurbishment. This function can easily be accomplished by the SASU.

The critical parameter specifications for the functions to be performed by the SASU are listed in Table 3-2. These parameters can be broken into two general categories of dc or steady state conditions and ac or time variant conditions. The dc conditions require a monitoring and control mechanism that can control related system parameters within a certain accuracy or resolution. This requirement has a direct effect on the size of the array segments that must be switched. For example, a voltage regulation specification of 5% requires that the incremental change in array output capability must be small enough to maintain the 5% accuracy for all bus loading conditions. The ac conditions set the requirements for the SASU to respond to perturbations in the power system. The ability of the SASU to respond to perturbations is a function of the frequency at which the sections are switched and the size of the array segment that is switched. For example, the designer must decide whether to switch four 1 KW sections at a fixed frequency or eight 500 watt sections at twice the frequency for a four KW load change on the bus. A review of Table 3-2 shows that the array sections size and the switching frequency are the two principal design variables that must be determined in the design of an SASU.

ORIGINAL PAGE IS
OF POOR QUALITY

Table 3-2 SASPM Critical Parameter Specifications

Specification	Specified In	Affects SAS Design Parameter
Voltage Regulation Specification		
DC Voltage Limit	Percent	Array section size
Transient response • Turn on/off • Load/source	Percent Overshoot Time Period	Array section size Switching Frequency
Output impedance	Ohms Frequency Range	Array section size Switching frequency
Stability	Phase/Gain Margin	Switching frequency
Load Variations/ Characteristics	Watts/Time	Array section size Switching frequency
EMI Susceptibility	Vp-p/Frequency	Array section size Switching frequency
Battery Charging/State-of-Health Specifications		
DC Current Limit • Full charge • Trickle charge	Amperes	Array section size
Voltage Limit • Temperature compensated • Programmable	Volts, °F	Array section size
Ampere-Hour Integration	Ampere-Hours/ SOC/DOD	Switching frequency
Cell Voltage Monitoring	Volts	Array section size
Overtemperature Protection	°F	Array section size
ARC Protection Specifications (SEPs)		
DC Current Limit	Amperes	Array section size
Transient Response	Time Period	Switching frequency
Stored Energy	Joules	Array section size Switching frequency
Solar Array Reconfiguration Specifications		
SEPS and S/C Bus Voltages	Volts	Array section size
Power Requirements	Watts	Array section size
Reconfiguration Time	Seconds	Switching frequency

3.2.1 SASU Sequencing Approaches

Once the switch configuration has been selected, then the manner in which the switches are sequenced must be investigated. Five basic sequencing concepts were derived for the study and are shown in Figure 3.2-1 The advantages and disadvantages of each concept are discussed below.

3.2.1.1 Series Sequenced

The series sequenced approach uses a shift register to sequentially switch each array segment. Each array segment is equal in size. The advantages of this approach are that the control method is straightforward, the stability of the feedback loop is easily determined, and a minimum number of control lines is required to the shift register. The disadvantages of this approach are that a large number of switches are required for fine control of the power bus, and a high switching frequency is required for a fast transient response.

3.2.1.2 Binary Count

The binary count approach uses a binary counter as the sequencing device. The solar array segment sizes are binary weighted for this approach. The advantage of this approach over the series sequenced approach is that the required number of switches is reduced. This approach, like the series sequenced approach, uses a minimum number of control lines and the control method is straightforward. The feedback loop stability is also easily determined. A disadvantage of this approach is that the last segment requires a very large switch. Also, a very high switch frequency is required for fast response.

3.2.1.3 Binary Count/Sequenced

This approach combines the advantages of the shift register and the binary counter. The binary counter is used for fine control and the shift register is used to switch large segments. In this manner, the number of switches are reduced over the series-sequenced approach and the requirement to switch large power in the final section is eliminated. Like the first two approaches, this approach uses a minimum number of control lines, the control method is straightforward, and the feedback loop stability is easily determined. This approach also has the same disadvantage as the first two in that a high switching frequency is required for fast response.

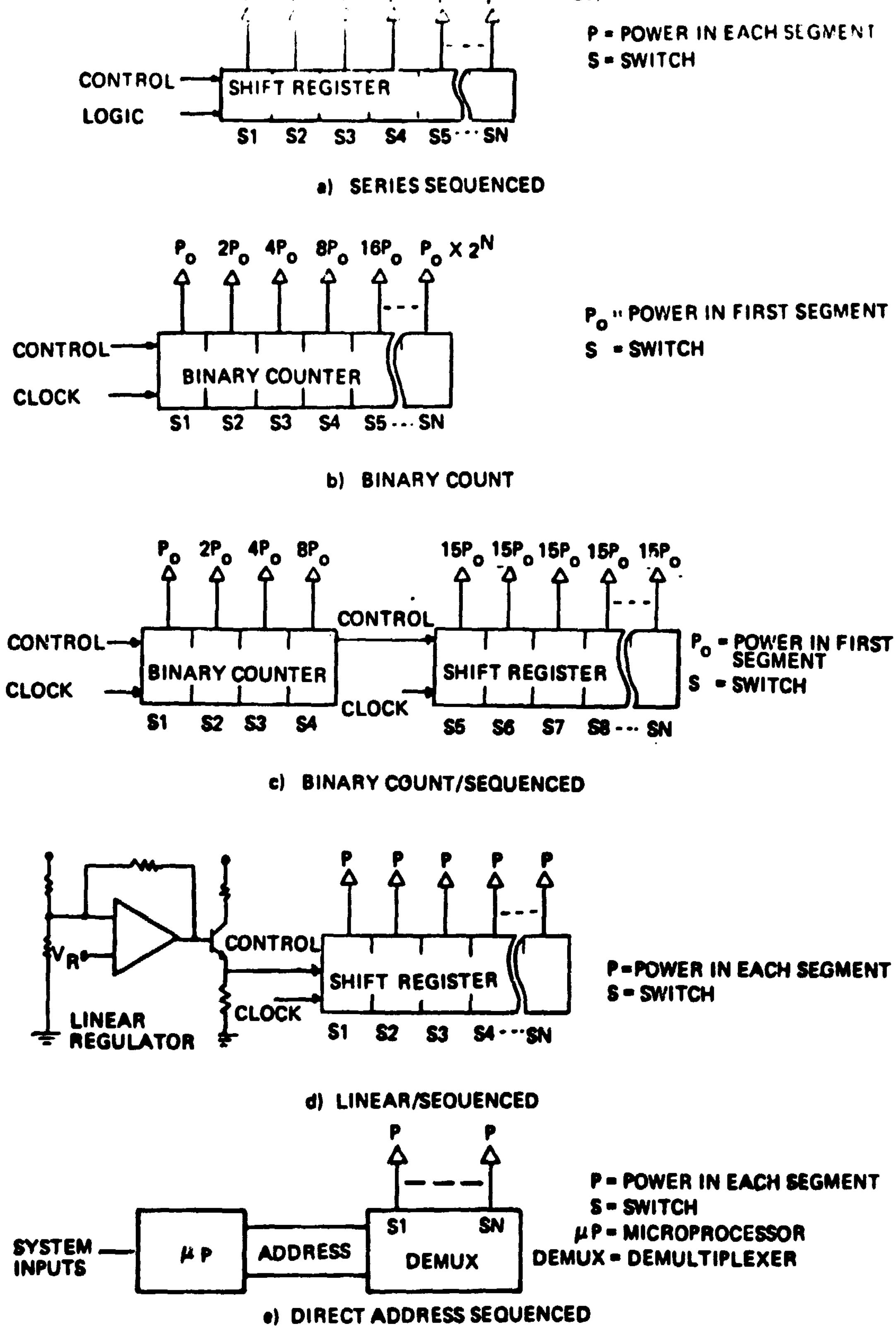

FIGURE 3.2-1 BASIC SEQUENCING CONCEPTS

3.2.1.4 Linear/Sequenced

The linear sequenced approach uses a small linear shunt regulator in conjunction with a shift register. The linear regulator provides the fine control up to the power level in each array segment. An advantage of this approach is that fine control can be provided by the linear regulator with a relatively lower switching frequency in the shift register. This approach also has increased design flexibility when considering the linear and digital design trade-offs. The disadvantages of this approach are that higher power is dissipated in the linear regulator as compared to the digital approaches and the stability of the feedback loop is more complex with the combination of linear and digital elements.

3.2.1.5 Direct Address

The direct address approach uses a microprocessor in conjunction with a demultiplexer to provide the switching control. An advantage of this approach is that several switches could be addressed simultaneously and thereby reduce the transient response time. This approach also provides the maximum flexibility in adapting to varying spacecraft conditions over the life of the mission. The disadvantage of this approach is that it is the most complex control scheme, and the stability of the feedback loop would be difficult to determine if multiple array segments were switched at varying frequencies. The speed of the microprocessor could be a limiting factor if a fast transient response is required.

3.2.1.6 Summary

Five sequencing approaches have been presented that illustrate the parameters that must be considered during the design of the sequencing circuitry. Many other approaches could be devised based on other schemes. Each approach must be evaluated towards any specific application in order to determine the optimum system. A further discussion of sequencing approaches is given in section 4.2.

3.3 SASPM System Concepts

System concepts were derived for each of the three missions. The LEO mission concept is shown in Figure 3.3-1. Since power must be supplied to both the spacecraft and the ion propulsion system simultaneously, reconfiguration of the solar array is not desirable. Each of the power busses has its own feedback control system. The spacecraft bus feedback control measures bus voltage and battery current and controls the solar array switching unit accordingly through the SASU control logic. A microprocessor controller measures battery state-of-health and provides battery charge control by varying the references of the voltage and current error amplifiers. The ion propulsion bus feedback loop measures the bus voltage and controls its SASU through control logic. Inputs from the ion propulsion system can modify the bus voltage and provide for arc protection.

The GEO mission concept is shown in Figure 3.3-2. Solar array reconfiguration is accommodated by a six pole-double throw switch. Four parallel solar array segments are reconfigured into four series segments in this arrangement. The SASU control logic must also be reconfigured to transfer control to the desired power bus and to accommodate the new switching arrangement. The battery and bus control methods are the same as described in the LEO mission except that the battery charge control algorithms are tailored for GEO. Reconfiguration and ion propulsion system modifications are accommodated through spacecraft level commands.

The switching concept for the IPOTV mission is shown in Figure 3.3-3. Since the major portion of the power is for the ion propulsion system, only a small portion of the solar array is tapped for the spacecraft. A reconfiguration concept is shown that allows for a 33% increase in the ion propulsion bus voltage to account for degradation. Initially four equal solar array segments are utilized with the fourth segment divided into three equal subsegments. The subsegments are switched in series with the remaining segments to attain the voltage increase. The monitoring and control methods are much the same as for the LEO mission.

3.4 Array Switchgear Location Options

There are four candidate locations for mounting the solar array switchgear.

3.4.1 Inboard of Rotating Joint

In this configuration each array section is hardwired through individual current transfer (slip) rings or a wrap-up device. The ON-OFF command

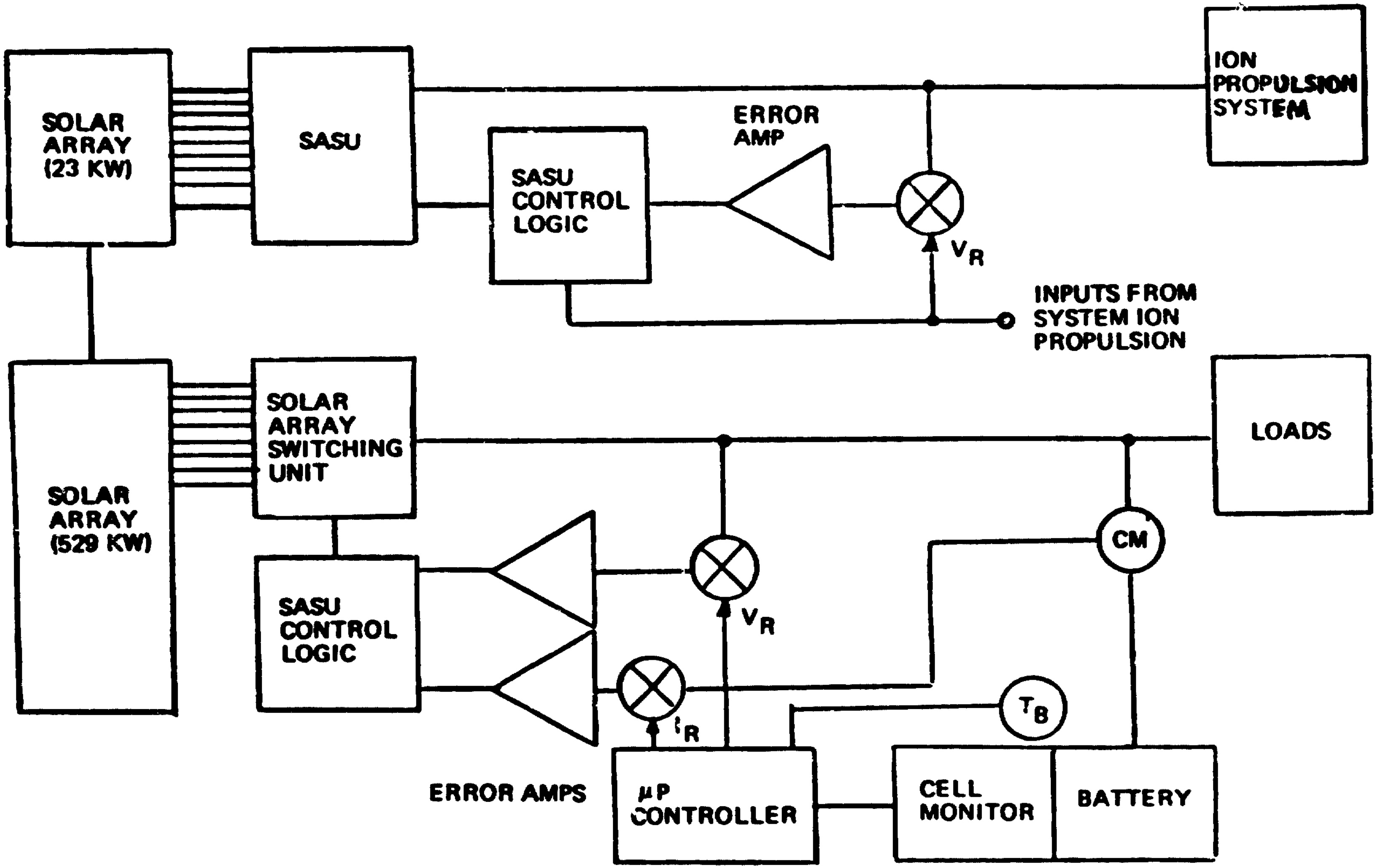

FIGURE 3.3-1 LEO SOLAR ARRAY SWITCHING CONCEPT

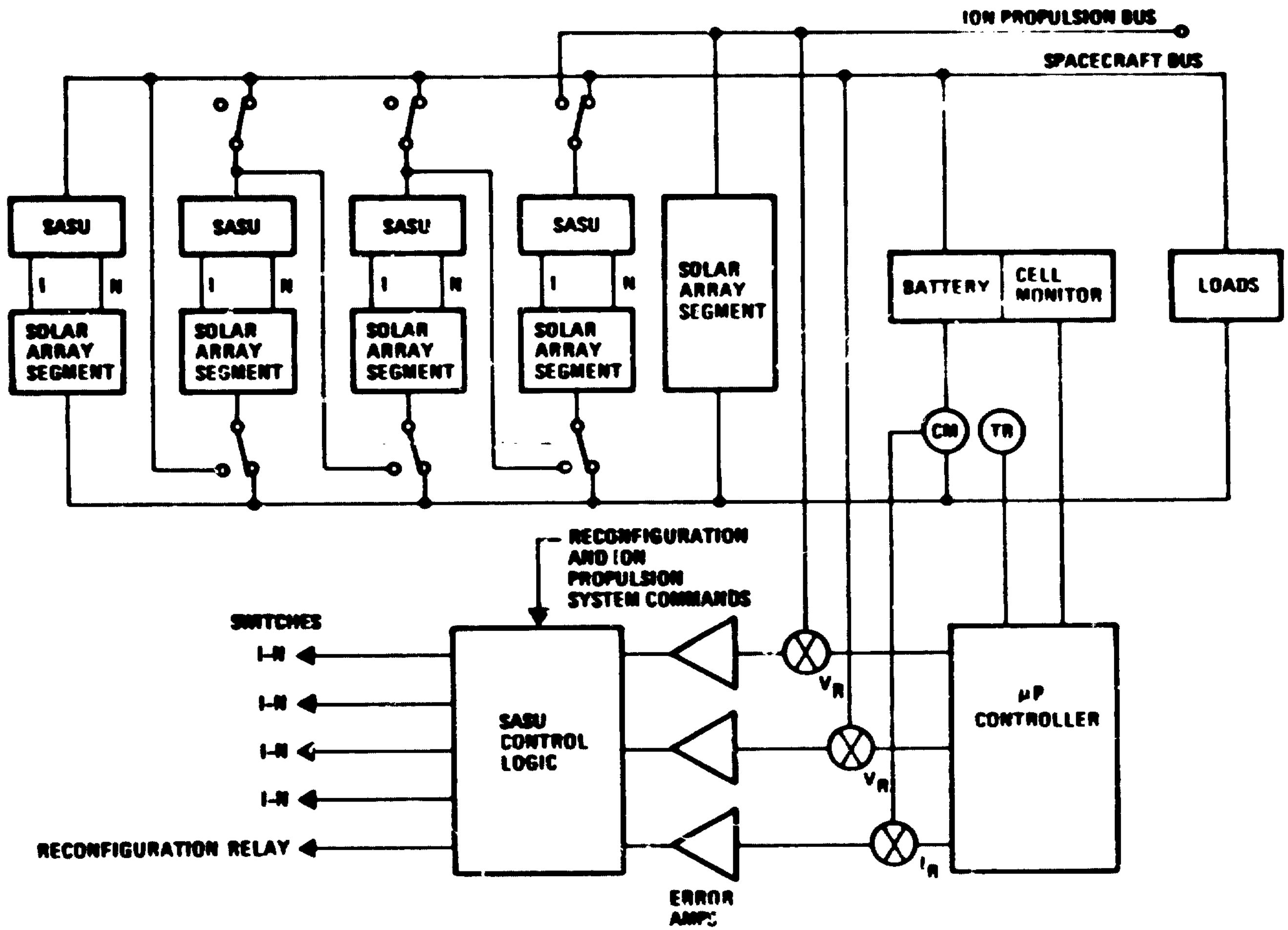

FIGURE 3,3.2 GEO SOLAR ARRAY RECONFIGURATION

ORIGINAL PAGE IS
OF POOR QUALITY

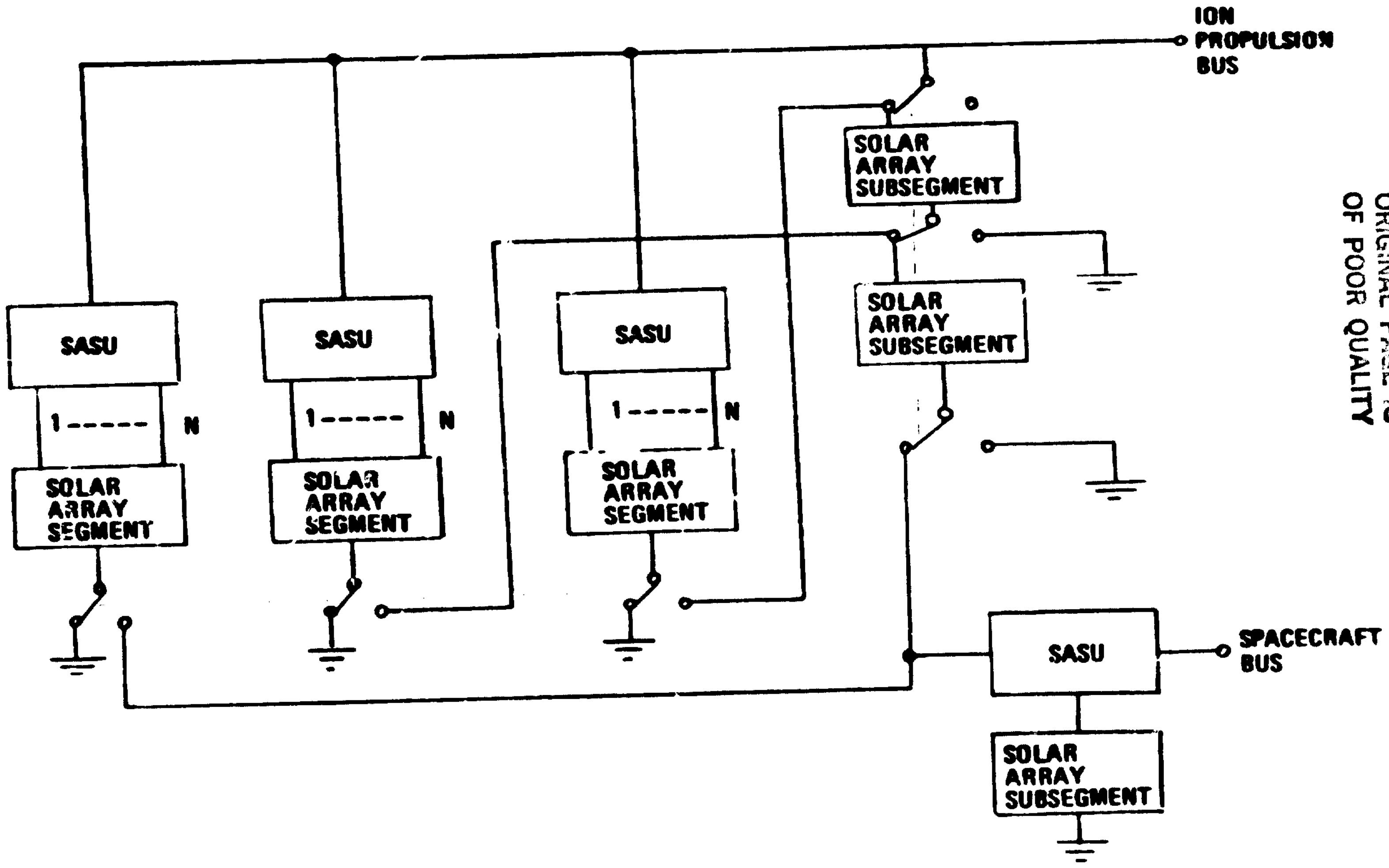

FIGURE 3.3-3 IPOTV Solar Array Switching Concept

data link does not have to cross the rotary joint. The electronics and switches may be more easily be packaged to provide thermal control and protection from the radiation environment. The disadvantage is proliferation of power transfer rings and/or associated wiring. A power ring would be required for each array section.

3.4.2 On Array Panel Stowage Box

Mount the switchgear and controls in or on the array panel stowage box. This location provides some radiation shielding, and a base for passive thermal control. The temperature swings of the solar array in geosynchronous orbit range from - 180°C to 60°C, so it is possible that a small heater will be required during eclipses. This location also allows paralleling the power strings on the array side of the rotary joint, thereby permitting the use of fewer and larger slip rings. This approach would facilitate on-orbit replacement of the array and switchgear. The array could be folded in the stowage box and the entire wing plus electronics could be replaced. An alternate location between the stowage box and the rotary joint has similar characteristics, and the switchgear could be replaced on orbit separately from the array.

In order to avoid having a large number of control wires cross the rotary joint, a data bus and a remote integration unit (command decoding and telemetry encoding) might be mounted on the solar array. The coupling device across the rotating joint might be an optical device.

3.4.3 Edge of Cell Blankets

Mount the switches along the edge of the solar array on the blanket frames. This approach has the same transfer ring advantage as candidate number 2, and a similar wiring advantage. The switchgear will have to be mounted on a fold out structure, a data bus along the array would minimize the number of control wires, but the switch electronics will be exposed to the radiation environment. If heaters are required they would be distributed along the array.

3.4.4 On Solar Array Blanket

Mount switchgear on the solar array blanket. This is not considered feasible for the lightweight planar arrays because the blanket is very lightweight and flexible. Thermal dissipation might be a problem. The concentrator arrays, if chosen may have room to mount the switches on the array, between the solar cells and below the optics. This approach would require either a data bus throughout the array, or a large number of command lines. The switch electronics would receive some radiation protection from the array structure and optics, however, if thermal cycling is a problem, it would be difficult to provide heating for the switch electronics.

3.5 Candidate Concepts Analysis and Selection

Candidate concepts were identified in Section 3.1. A further requirement of Task II is to evaluate the capability to accommodate the following mission related situations:

3.5.1 Differing Load Requirements Of New Users

Within the capability of the power sources, the expansion or reconfiguration of the payloads is readily achievable. The flexibility of expanding or restructuring payloads is actually inherent in the multichannel approach of the power system. The system utilizes multiple high voltage batteries and distribution buses to deliver power to a variety of loads.

The block diagram of a power distribution concept is shown in Figure 3.5-1. It can be seen in the block diagram that each power bus operates independently of the others to avoid battery paralleling. Load buses in each of the external load center modules are formed by tying into two or more of the power buses via circuit controllers to provide power source redundancy and a means of load balancing on the channels. The simultaneous connection of a load bus to more than one power bus is avoided by the "exclusive or" function of the circuit controllers.

The possibility of a single load bus tying two or more batteries together is prevented by the operation of the circuit controllers.

Deadfacing on each power bus is provided. This enables the users to replace existing load centers or add on new ones. The configuration of a new load center must be selected on the basis of the load power requirements. If one channel cannot provide the required load, power processors (not shown) will be utilized to tap power from several buses. This technique assures user isolation and prevents paralleling channels. Individual load buses in the load centers are formed in the same manner as before to provide power bus redundancy and capability of balancing

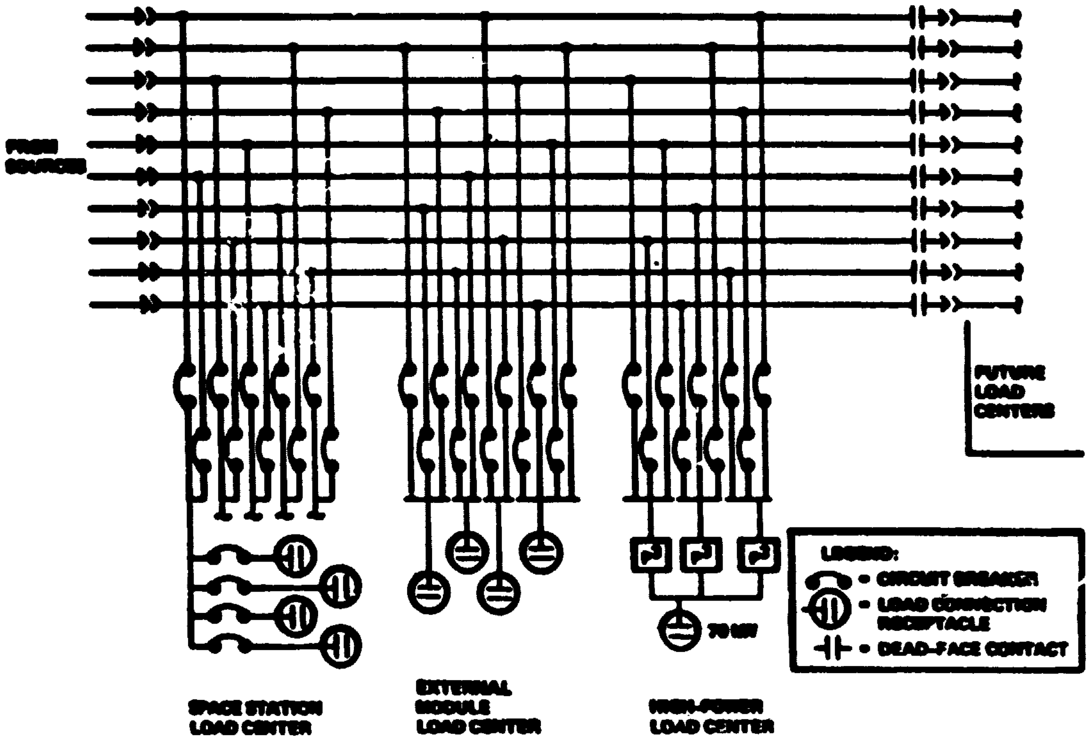

Figure 3.5-1 Recommended Power Distribution Network Concept

3.5.2 Load Changes Due to Changing Mission Phases

This includes situations such as shifting from primary electric propulsion loads to "on-station" loads and back to ion propulsion for return or relocation of station keeping.

For the GEO mission, it is necessary to reconfigure the solar array for either the primary ion propulsion or the "on station" payload which is accomplished by SASPM.

The block diagram of the GEO mission concept is shown in Figure 3.3-2. Solar array reconfiguration is accommodated by a six-pole,double-throw switch. Four parallel solar array sections(normally utilized for the on-station payloads)are reconfigured into four series connected sections for the ion propulsion loads. The reconfiguration and the ion propulsion modifications are accomplished through spacecraft level commands. In the ion propulsion operating mode during orbital transfer from LEO to GEO, the solar array is configured to supply a high voltage and, at the same time, the low voltage housekeeping loads for the spacecraft. After transfer to GEO, the major part of the array will be reconfigured to supply payloads at 260 volts. A small section of the solar array will remain connected to the ion propulsion bus to supply high voltage for stationkeeping thrusters which will be operated only during sunlight periods. The SASU control logic must also be reconfigured to transfer control to the desired power bus and to accommodate the new switching arrangement.

The configuration change of the system is not autonomous, as mentioned before; it is accomplished by spacecraft level commands. To modify the system for the ion propulsion loads, first the payloads (with the exception of necessary loads) are sequentially turned off. Then, the individual solar array sections in each channel are converted from a parallel to a series connected arrangement by the ground command operated transfer switches. The control logic of each SASU is also reconfigured to operate in conjunction with the modified system arrangement. To establish a normal GEO operation for the spacecraft, the above process is carried out in reverse. Once the desired system configuration is obtained, the load balancing on the channels and the power bus regulation is autonomously achieved.

3.5.3 Failure of Components

The electrical power system for all three missions will be designed to meet the stated requirement of the reliability criteria that no single failure or credible combination of failures will prevent the system from operating in an acceptable degraded mode of operation. The system design will employ both component and unit level redundancies in all power and control logic circuits.

The potential failure modes of the system are discussed below. The discussion is limited in scope to an overview of the circuit redundancy types to be employed.

The failure modes of the solar array switches in the SASU are either open or short. Dependent upon the sequencing configuration, switch redundancy against an open or short failure may be required. For the series sequenced or the linear/sequenced approach where shift registers are utilized, protection against an open failure is supplied either by parallel redundant switches or by the inclusion of an extra array segment. Redundancy to protect against shorted switches in the above configurations is not required because each power bus is loaded with at least a minimum load which can be supplied by several array segments. The other sequencing approaches which are implemented by binary counters or demultiplexers will need quad redundancy for protecting the switches against open or short failures. In a combinational arrangement such as the binary count/sequenced configuration, only the binary counter operated switches will require quad redundancy.

The control logic, the microprocessor (μP) controllers and the associated sensor will require redundancy. There are three types or redundancy configurations to be considered and evaluated: the quad, the majority voting and the standby arrangements. Between the three approaches the reliability, the complexity, and the circuit parts count must be traded off to gain a fair comparison. The quad and majority voting arrangements yield a higher figure for probability of success than the standby one at the cost of higher parts count. The disadvantage of requiring a higher number of circuit components, however, can be minimized by the packaging concept of incorporating the majority of the discrete parts into hybrid units. The standby redundant configuration is less complex but it requires additional circuitry for failure detection, and an autonomous transfer of operation to the standby channel.

The individual transfer switches used to reconfigure the system in GEO or IPOTV missions will need protection against short and open failures in the form of a quad redundancy.

3.5.4 Deactivation of a Section For Maintainance (at LEO).

The system is designed to accomplish easy maintainance in low earth orbit by replacing failed or degraded modules and components.

The state-of-health and the performance for the power subsystem is continuously monitored by the PMS which includes capabilities for fault diagnosis that will identify trends as well as out-of-limit conditions. The PMS design will utilize computer controlled power management techniques to shut down and isolate failed equipment, to shift loads between power buses, to predict incipient failures and remaining life for the degraded elements, and to forecast the required schedule for repairs and replacements.

Before the maintainance work at low earth orbit can be started, for safety it is necessary to deactivate the power bus channel that supplies power to the failed or degraded equipment the maintainance crew is scheduled to replace. The deactivation of the power section is accomplished by spacecraft level commands which first shut down or transfer all the loads that are connected to the affected power bus, then disconnects the associated battery from the line, and finally opens all the switches in the SASU to remove solar array power. The crewmen can then proceed to carry out the maintainance operation.

3.5.5 Hybrid of SASPM plus Conventional Processing

The hybrid approach to SASPM is comprised of a small linear shunt regulator operating in conjunction with sequentially switched solar array segments to maintain bus voltage regulation. The linear regulator provides the fine control up to the power level in a given array segment.

One of the advantages of this approach is that fine control of the bus voltage can be provided with a relatively lower switching frequency for the sequentially operated solar array segments. To achieve a fast transient response, the linear shunt can be designed to handle larger transient currents for a short duration of time. The other advantage of the linear shunt is that the designer has a greater flexibility when considering the sizing of the solar array segments.

The hybrid approach increases cost and complexity.

3.6 Baseline Conventional Power Processing

Four basic conventional power processing concepts have been identified:

1. Transformer Coupled Converter (TCC) system
2. Buck Regulator/Charger system
3. Boost Regulator/Charger
4. Shunt Regulator/Charger

Block diagrams of these systems, along with a list of comparative advantages, disadvantages, are shown in figures 3.6-1 through 3.6-4. Dotted lines indicate areas of comparison with SASPM.

3.6.1 Ion Propulsion Conventional Power Processing Baseline

An argon thruster was selected. The argon thruster requires eight less power supplies than the mercury ion bombardment type thruster. Power processors are required for the following functions:

- Screen
- Accelerator
- Discharge
- Neutralizer keeper

The discharge supply will power the cathode heater and start a cathode heater discharge. This supply is then switched to the anode via a relay for the main discharge (Reference 3-3).

3.6.1.1 Thruster Requirements:

- Thruster range (T), 0.25 to 0.5 Newton for LEO and GEO platforms.
  0.5 to 1.0 Newton for the Orbit Transfer Vehicle.
- Specific impulse (I_{sp}) 5600 seconds
- Propellant type, Argon (M) = 39.9
- Thr[illegible]er size, 50 centimeters
- Propellant utilization (N_u) = 0.9
- Ion generation loss, 250 ev/ion
- Thrust loss factor = 0.95
- 1985 to 1990 technology

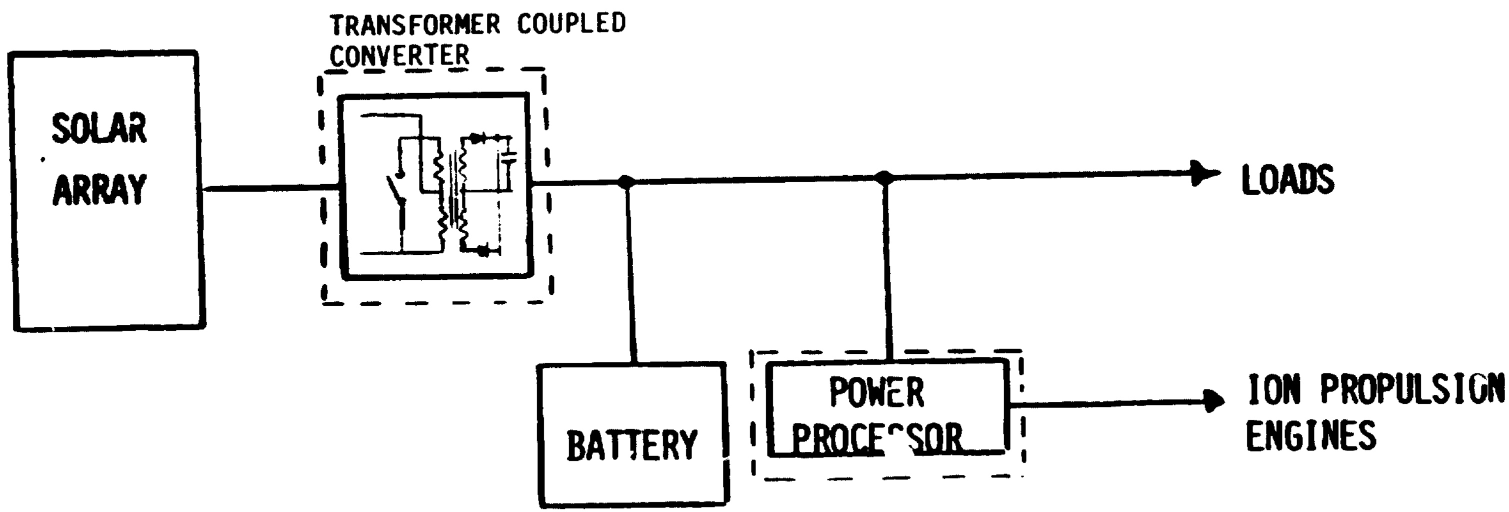

Advantages	Disadvantages
• Maximum flexibility in matching solar array and load voltages. • Battery and solar array isolated even with TCC failure. • Higher efficiency than buck approach when load voltage is much lower than solar array voltage. • Undesirable failure modes are relatively easy to avoid.	• More complex circuitry compared to buck or boost circuits. • Generally larger and heavier than either buck or boost when the load voltage is near the solar array voltage.

FIGURE 3.6-1
TRANSFORMER COUPLED CONVERTER

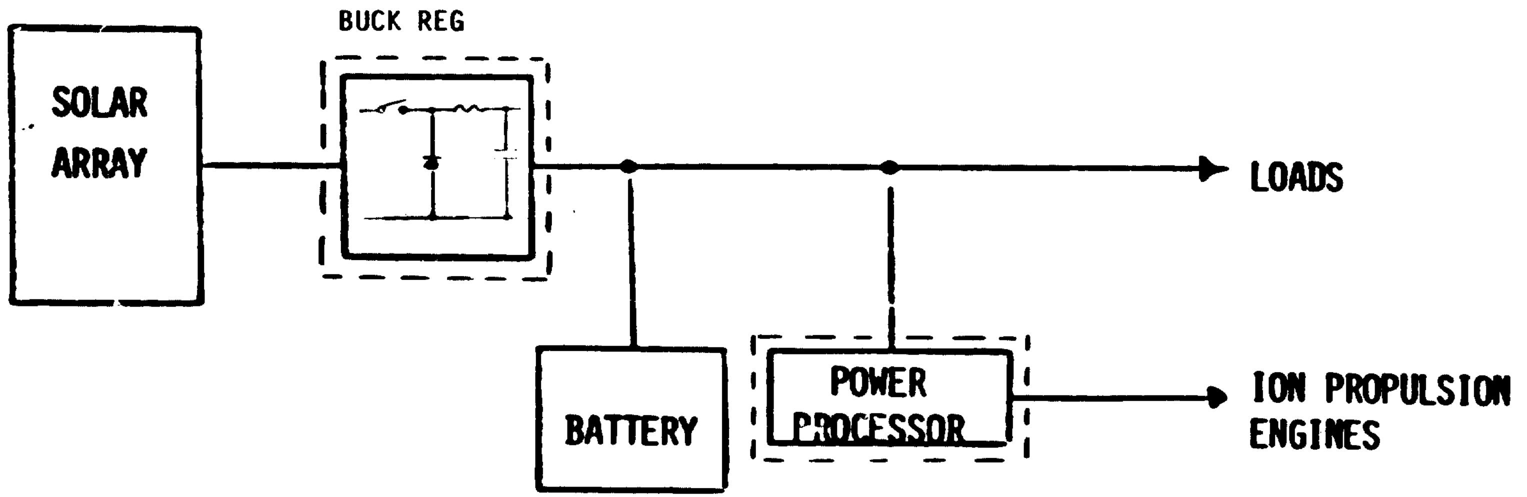

Advantages	Disadvantages
• Matches impedance between solar array and load.	• Minimum solar array voltage must be greater than maximum required load voltage.
• More efficient than TCC when load voltage is close to minimum solar array voltage.	• Failed (shorted) power switch connects solar array directly to battery.
• Maximum efficiency at minimum solar array voltage.	• Relatively low efficiency when load voltage is much lower than solar array voltage.
• Losses decrease as output loads are reduced.	• Size and weight become greater than TCC when solar array voltage is much higher than required load voltage.
• Less complex circuitry compared to TCC and about the same as the boost.	

FIGURE 3.6-2
BUCK REGULATOR/CHARGER

ORIGINAL PAGE IS
OF POOR QUALITY

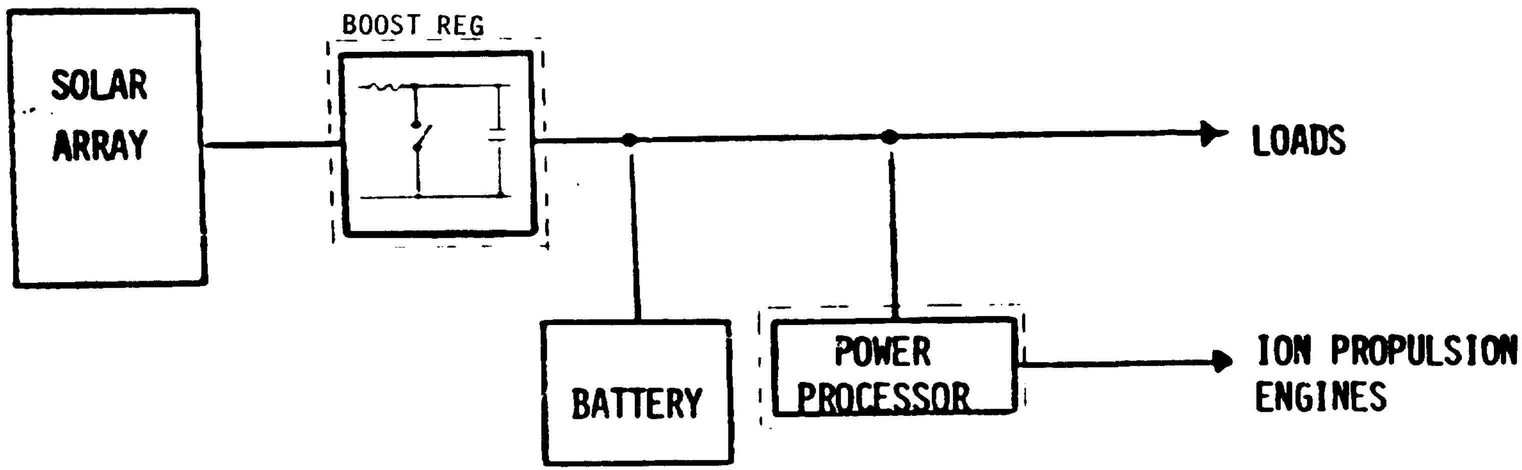

Advantages

- Slightly higher efficiency than buck when load voltage is near the solar array voltage.
- Smallest size and lowest weight when compared to buck or TCC when solar array voltage range is less than 2 to 1.
- Overvoltage failure mode of buck regulator can be easily avoided.
- Circuit complexity about the same as buck regulator and less than TCC.

Disadvantages

- Maximum solar array voltage must be less than required load voltage.
- Battery cannot be disconnected from the solar array by the boost regulator.
- Input voltage transients (> 1 ms) above the load voltage are passed through the boost regulator.
- Efficiency maximum at maximum solar array voltage.
- Size and weight become greater than TCC when solar array voltage is much lower than required load voltage.

FIGURE 3.6-3
BOOST REGULATOR/CHARGER

ORIGINAL PAGE IS
OF POOR QUALITY

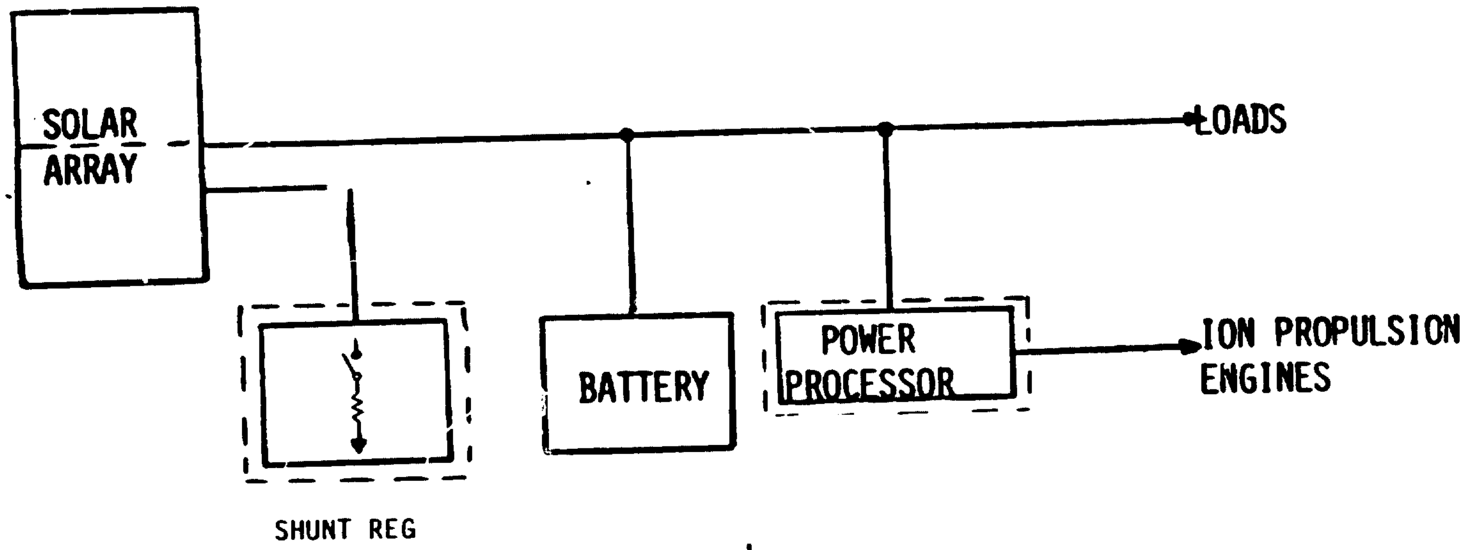

Advantages

- Maximizes efficiency at solar array end-of-life.
- Offers constant array load (full shunt).
- Can operate with failed (disconnected) battery in sunlight.

Disadvantages

- Cold solar array voltage is available to fully charged battery leaving eclipse.
- Maximum array voltage across shunt switch.
- Battery is tied directly to solar array.
- Cannot match load impedance.
- Difficult to dissipate heat.

FIGURE 3.6-4
SHUNT REGULATOR/CHARGER

Estimated power requirements for the thruster are given in Table 3-3. (Data was derived from Reference 2-24)

Function	1/2 Newton	1 Newton	Regulation	Ripple
Screen				
Voltage, V_{DC}	860 nominal	860 nominal	10%	1%
Current, A_{DC}	20	40	-	-
Discharge				
Voltage, V_{DC}	30	30	1%	2%
Current, A_{DC}	160	335	-	-
Accelerator				
Voltage, V_{DC}	800	1400	10%	5%
Current, A_{AC}	0.2	0.4	-	-
Neutralizer Keeper				
Voltage, V_{DC}	$15V_{DC}$ @ 5A to		15%	2%
Current, A_{AC}	$120V_{DC}$ @ 0A		-	-

Table 3-3 Argon Thruster Power Requirements

Estimates of the mass and losses of these supplies and for a main system controller are given below. The mass estimates include structure weight.

3.6.1.1.1 Screen/Accelerator

$$M_S \approx 0.3 P_B^{.75} + 0.6 P_B^{.5} + 0.06 P_B + 2.2$$

$$P_{LS} \approx \frac{5}{95} P_B$$

Where M_S = Mass of power processor, Kg

P_B = Beam power, KW

P_{LS} = Screen/Accelerator losses, KW

3.6.1.1.2 Discharge

$$M_D \approx 1.1 P_D^{.75} + P_D^{.5} + 0.06 P_D + 1.4$$

$$P_{LD} \approx \frac{1}{9} P_D$$

Where M_D = Mass of power processor, Kg

P_D = Discharge power, KW

P_{LD} = Discharge supply losses, KW

3.G.1.1.3 Neutralizer Keeper

$M_K \simeq .7$

$P_{LK} \simeq \frac{2}{5} P_K$

Where M_K = Mass power processor, Kg

P_{LK} = Neutralizer keeper supply losses, KW

P_K = Neutralizer keeper power, KW

3.G.1.1.4 Thruster System Controller

$M_C = 4$

$P_{LC} = 0.15$

Where M_C = Mass of power processor

P_{LC} = Controller supply losses

The ion propulsion power processing described in this section will be used as the basis for comparison to SASPM techniques.

3.6.2 Shuttle Launch Costs

The Shuttle launch costs were given in Reference 3-1. Launch costs will be one of the factors in the Task IV comparison between conventional power processing and SASPM.

NASA's Shuttle launch cost reimbursement policy (Reference 3-2) defines weight* dependent and length dependent user charges, respectively, as

$$C_W = 1.333 \times \frac{\text{Spacecraft total weight}}{\text{Total weight capacity}} \times (\text{Dedicated launch cost})$$

$$C_L = 1.333 \times \frac{\text{Spacecraft total length}}{\text{Total length capacity}} \times (\text{Dedicated launch cost})$$

where dedicated launch cost is given as $30.2 million (1981 dollars). The user will be charged the larger of the two cost figures. The full dedicated launch cost will be charged if either spacecraft weight or length exceed 75 percent of full capacity; i.e., 22,110 kg or 13.72 m.

Figure 3.6-5 illustrates this reimbursement policy in terms of cost contours plotted in a mass vs. length diagram. The graph shows the fixed cost plateau reached when mass or length exceed the 75-percent-of capacity level. The dashed diagonal designates the break even points of weight and length dependent charges. Using the dedicated Shuttle launch cost, the weight and length dependent charges are

$$C_W = \$1.384 \text{ million per 1000 kg}$$

$$C_L = \$2.30 \text{ million per meter}$$

The slope of the breakeven line is defined by

$$\frac{W}{L}_{BE} = \frac{2.30}{1.384} = 1.611 \times 10^3 \text{ kg/m}$$

If launch charges were always weight-dependent and varied linearly, the launch cost savings due to weight reduction would be defined simply by the relation.

$$\Delta\text{cost} = 1.384 \text{ million per 1000 kg}$$

*Note, the terms weight and mass are used interchangeably in this context.

C-2

ORIGINAL PAGE IS
OF POOR QUALITY

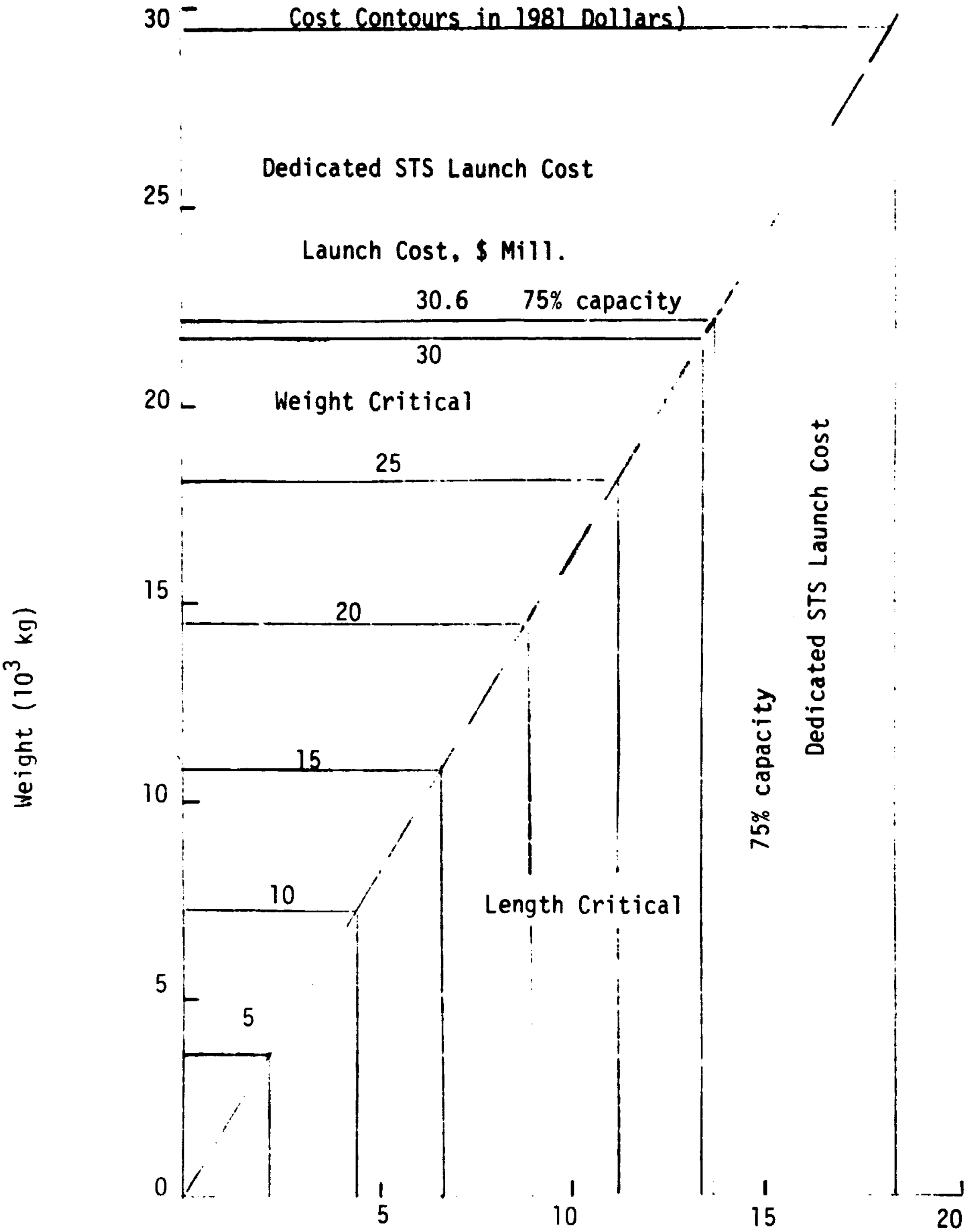

Figure 3.3-5 Shuttle Launch Cost Contours in Terms of Cargo Weight and Length

Actually, under certain conditions these savings will not always be fully realized under the NASA launch cost reimbursement policy; i.e., if spacecraft dimensions make the launch cost length-dependent. Figure 3.6-6 shows bars of weight savings (M) for several values of assumed spacecraft length. In one case, the entire M is in the weight-critical region, in the second case it straddles the cost breakeven line and in the third case it is entirely in the length critical region of the cost contour diagram. Accordingly, the cost savings reflect either all or part of the weight savings; or, in the third case, no cost savings are realized at all in spite of large weight savings. Another effect of NASA's non-proportional cost allocation is the partial loss of potential savings if the gross weight exceeds the 75 percent limit.

The above discussion is based on a literal interpretation of the official NASA Shuttle launch cost reimbursement rules. However, in effect there will be some cost savings achievable even beyond the cutoff defined by the 75-percent-of capacity limit beyond which the user will be charged the full cost of a dedicated Shuttle launch. The approximately 7000 kg of cargo capacity beyond this limit constitute a valuable space capacity for smaller additional cargo, which could be charged up to $9.69 million for transportation. The extra capacity could thus partly defray the launch cost of the primary user, and any weight savings achieved would translate into potential dollar savings to both users. For this study, it is assumed that all the available weight capacity and/or length is utilized.

The following weight and length dependent charges will be the basis for a comparison of SASPM and conventional power processing:

$$C_W = \frac{\$30.2 \text{ million (1981 dollars)}}{65{,}000 \text{ lb.}} = 465 \frac{\text{Dollars}}{\text{Lb}}$$

$$C_L = \frac{\$30.2 \text{ million (1981 dollars)}}{60 \text{ feet}} = 503{,}333 \frac{\text{Dollars}}{\text{Foot}}$$

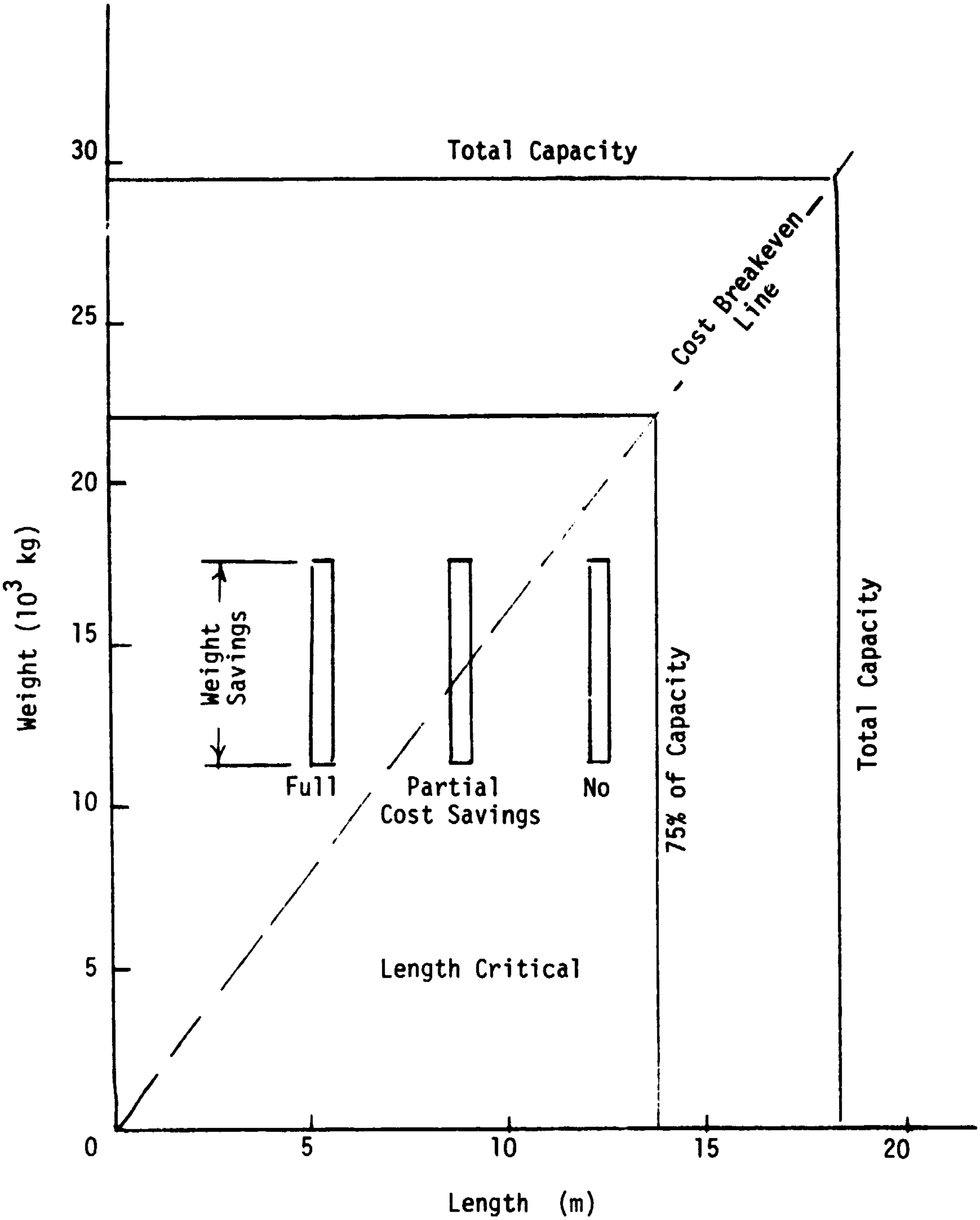

Figure 3.6-G Examples of Launch Cost Savings Variation with Cargo Length

3.7 Power Requirements Specifications

It was determined that if accurate comparisons to conventional power management techniques are to be made, an electrical power subsystem requirements specification was necessary, so that both the SASPM and the conventional subsystem would meet the same requirements; therefore, specifications have been prepared for each of the three missions. These are presented in Appendix C.

In order to define and evaluate the SASPM concepts, it is necessary to understand the load types to be accommodated and the solar array response to these loads. This evaluation is presented in Section 4.0.

REFERENCES

3-1. NAS3-22661, Study of Integrated Propulsion for Near-Earth Space Missions, Technical Progress Report No. 8, dated June 13, 1981.

3-2. "Space Transportation System Reimbursement Guide", NASA, JSC-11802, May 1980.

3-3. NASA TM 81729, "Extended Operating Range of the 30 - cm Ion Thruster With Simplified Power Processor Requirements", V. K. Rawlin, April 1981.

4.0 TASK III

CONCEPTS DEFINITION AND IMPACTS

"Provide further definition of the Task II concepts. Further define and quantify the SASPM concepts."

4.1 Impact of Various System Characteristics on Solar Array Switching

The following list of parameters and the impact on solar array switching were evaluated.

a) Voltage levels.
b) Reconfiguration (as described in Task II).
c) Isolation of user loads.
d) Voltage regulation improvement (if required).
e) Electrical transient performance/short circuit capability.
f) Fault protection (ability to correct for).
g) Control techniques.
h) Eclipse effects (ability to correct for).
i) Conductor/grounding arrangements.
j) EMI/filtering.
k) Modularity/commonality/growth.
l) Applicability to and impact on existing array.
m) Effect on energy storage and user loads.
n) Effect on array-spacecraft dynamics.
o) Impact of shuttle constraints.
p) Stowage/deployment.
q) Interactions with space environment.

Each topic is discussed in the following paragraphs.

4.1.1 Voltage Levels

Solar array systems of more than 50kw occupy extensive areas, and current must be transmitted over relatively long distances. The effect of the longer line length is to induce large losses in the distribution system. These losses are directly proportional to the square of the transmission voltage, and inversely proportional to the size of conductor employed.

For any given system, a cost model which weighs system voltage and conductor cost can be generated, and then solved on the basis of minimum cost. Such a model (Figure 4.1-1) was generated for a 250kw model, and this model indicated that large savings accrue up to about 200 volts. Above this point, the sensitivity to cost savings with increasing voltage are not nearly as great.

ORIGINAL PAGE IS
OF POOR QUALITY

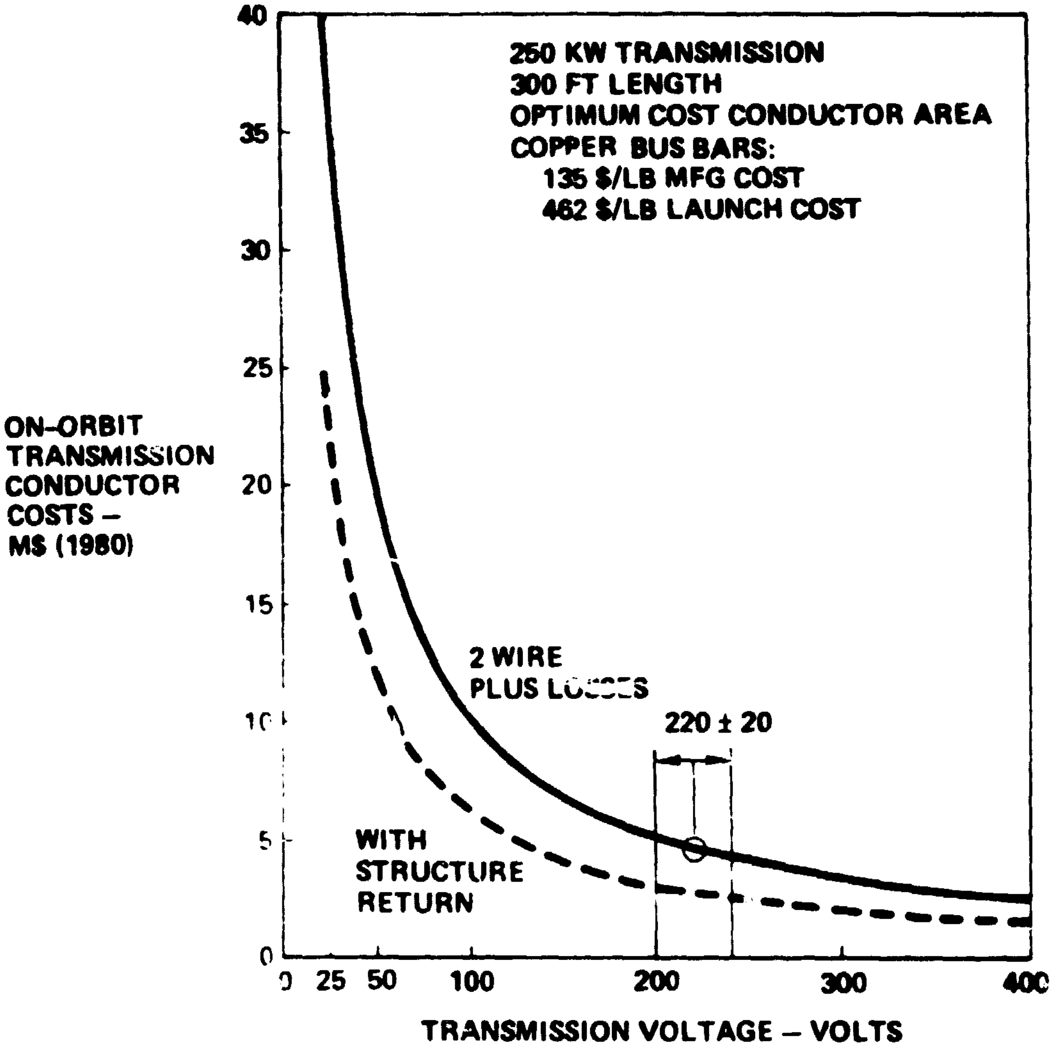

Transmission Costs for
High Voltage Systems
Figure 4.1-1 (Reference 2-17)

As system voltage increases, the availability and cost of other system equipment becomes a problem. For voltages up to 500 Vdc, there will be little effect on switchgear technology in the 1990s. Above this level, switchgear voltage may be a problem.

In addition, in the 200 to 500 volt range of solar array voltage, interaction of the array with the normal ambient space plasma begins to occur. (LEO) Leakage from the array to the plasma has the effect of shunting as much as five percent of the solar array output in LEO

The effect of higher voltage is manifold. In the initial case, costs are reduced by decreasing conductor size and therefore total system cost is less. This is countered by development cost for high voltage components, and increased solar array area (and possibly more expensive array manufacturing techniques) because of the interaction of the solar array with the space plasma. Further discussion of this subject is presented in Section 4.1.17.

4.1.2 Reconfiguration

Flexibility and modularity for expansion of the SASPM controlled system is inherent in the multichannel approach being considered. Individual load buses may be separated and isolated as desired. Within a given bus, the users provide isolation via their own local converter, if necessary. The solar array control switches are configured so that they can remove any desired portion of the array in case of emergency, load failure or to deadface all or portions of the system for maintenance or for load reconfiguration or changeout.

Most missions tend to be multiphase, with a different system configuration being optimum for each phase. The SASPM technique allows reconfiguration to meet optimum requirements. For instance, the GEO mission requires a large amount of high voltage (~800 Vdc) power for the solar electric propulsion system in the initial phase of the mission while transitioning from LEO to GEO. The system shown in Figure 4.1-2 allows this configuration.

After reaching GEO, the bulk of the power is required to supply system loads at 200 - 260 Vdc. With SASPM, this reconfiguration is comparatively simple as the individual segments are switched from a series arrangement for ion propulsion to a parallel configuration for payload support. (Figure 4.1-2).

ORIGINAL PAGE IS
OF POOR QUALITY

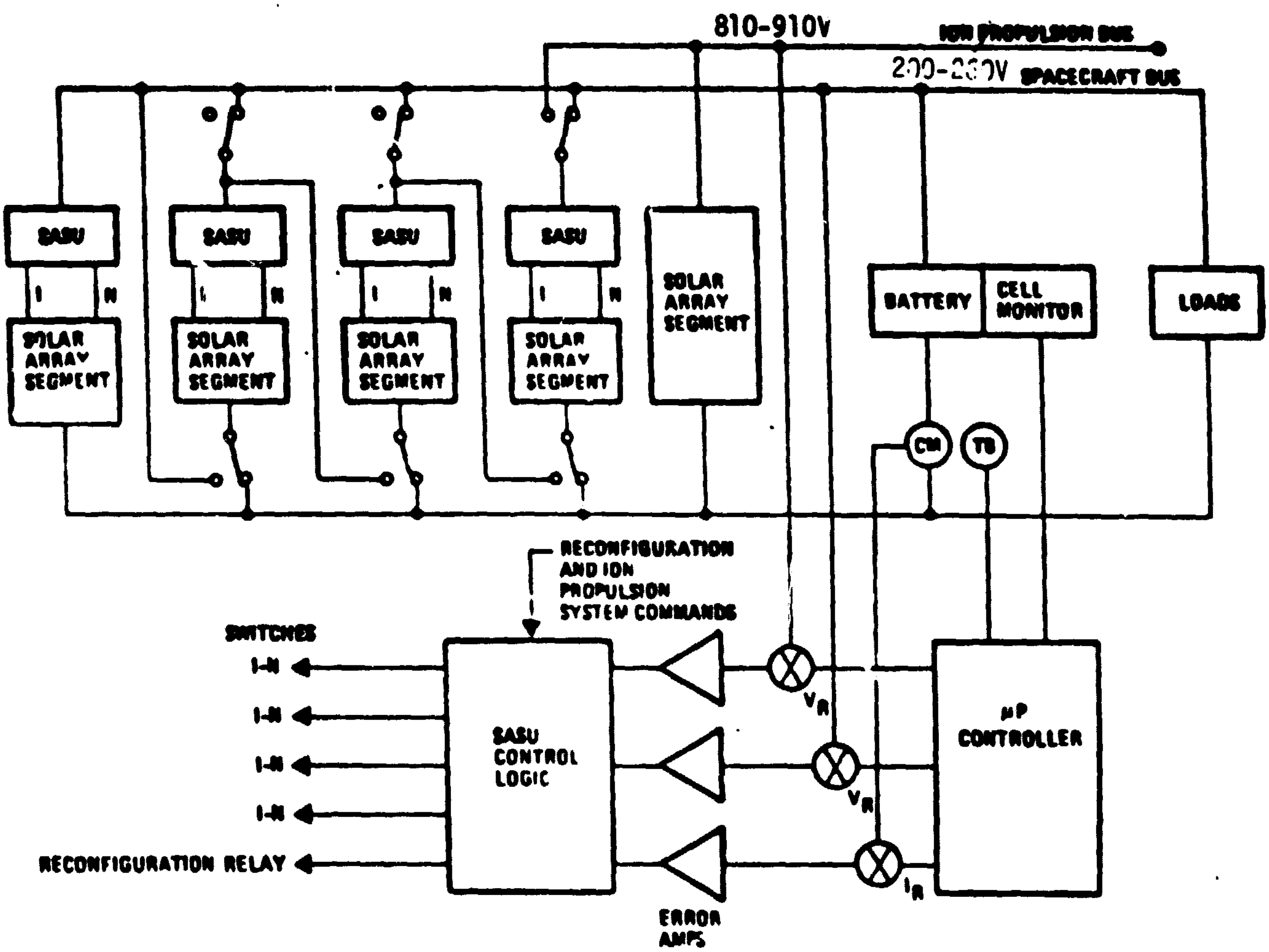

GEO Solar Array Reconfiguration

Figure 4.1-2

The IPOTV system (Figure 4.1-3) has a slightly different problem to solve. Although its primary function is to supply solar electric propulsion and not support payloads, the transition through the Van Allen belt does degrade system voltage (and current). The required voltage can be maintained by adding subsegments to the string as required. This reconfiguration for voltage compensation may be either automatic (PSM control) or be ground controlled. Relatively few switches are required to achieve these benefits.

4.1.3 Isolation of User Loads

Isolation between loads can be achieved by two techniques. Array sections can be dedicated to individual loads, or to groups of loads. This is seen in the GEO vehicle where the solar electric propulsion system is connected to a dedicated bus.

The power busses can be isolated from user loads via converters, either in groups or individually. To maximize flexibility with the variations in payload complement visualized, it is recommended that each payload provide its own isolation, if required (and requirements for peculiar voltage) and fine control by providing its own converter, rather than using central conversion.

4.1.4 Voltage Regulation Requirement

The basic SASPM concept employs batteries as a primary regulating element. During both charge and discharge the battery clamps the primary bus voltage to the battery voltage. It tends to be an infinite current source and sink and therefore acts as a voltage regulator for both load and solar array power variations.

When the system is operated without a battery, regulation is limited by the number of switched solar array segments, the SASPM switching speed, and by the amount of energy stored in the system. Tight regulation can be maintained for <u>steady-state</u> loads (within the limits of one solar array segment step change) by addition of a linear shunt whose capability covers only one segment change of solar array capability. Another technique is to extend the amount of stored energy in the system by adding capacitors. This technique is of value for small transient load changes (or for supplying pulse loads).

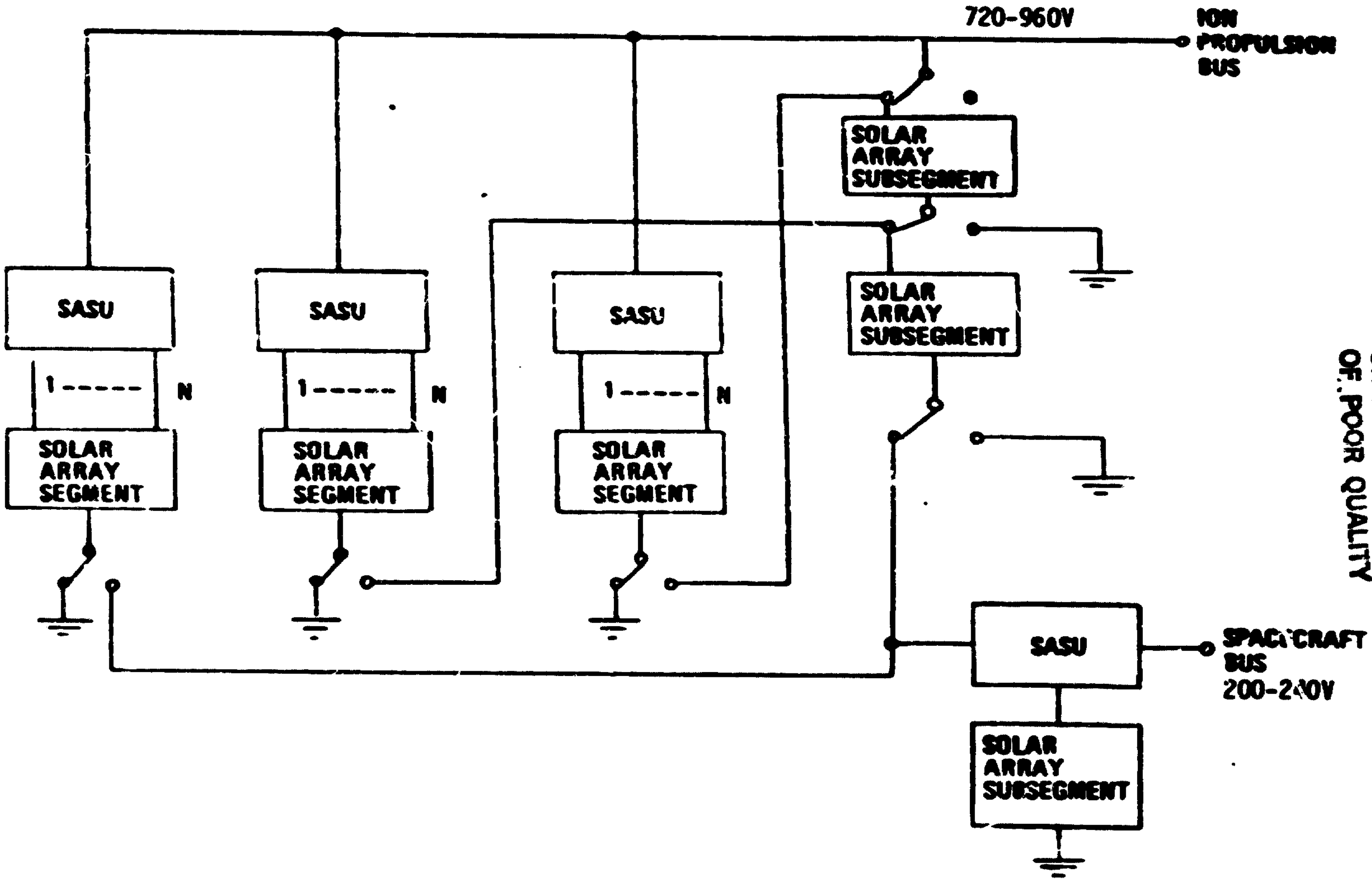

IPOTV Solar Array Reconfiguration

Figure 4.1-3

The recommended regulation method is to use batteries on the main power bus for normal spacecraft housekeeping loads and unpredictably variable payloads.

For other large loads, such as ion propulsion thrusters which are not operated in eclipse, and where load changes are predictable, straight SASPM techniques can be employed. This technique is particularly effective when minor voltage changes are not overly important, for a form of solar array peak power point tracking can be attained by throttling the ion thrusters. SASPM can easily meet voltage regulation requirements of ion thrusters.

4.1.5 Electrical Transient Performance/Short Circuit Capability

The normal SASPM system employs batteries to clamp the main bus and therefore exhibits battery response voltage characteristics for transient performance. The system voltage will not collapse to solar array short circuit voltage under effectively dead short conditions, but will be clamped at battery discharge voltage, therefore supplying sufficient current to clear shorts.

Although the SASPM switches are sized for I_{sc}, they will never see this current in a SASPM system containing a battery.

In the case of a no battery system, system transient response is limited by switching time, and short circuit voltage will tend to collapse to zero unless there is sufficient stored energy in the system. The three mission power systems will contain batteries for eclipse operation of the spacecraft housekeeping loads; this energy source will also supply the SASPM system switch controls.

4.1.6 Ability to Protect Against Faults

The bulk of fault protection must occur on the load side of the main power bus, as in any distribution system. Load circuit breakers, fuses, and current limiting circuitry must be coordinated to isolate faults at the lowest possible level.

If the fault occurs upstream of the load protection devices, such as a hard main bus short, the system response depends upon whether a battery supplies the bus, as described in Section 4.1.5.

In the SASPM system bus with no stored energy, system voltage will collapse toward zero, and array switches will be opened by a separate control system. All solar array (and battery) switches will be designed to open short circuit currents.

4.1.7 Control Techniques

The SASPM control techniques involve combinations of modularized solar arrays and stored system energy, controlled by switches.

For the spacecraft bus on all missions the primary control parameter is battery current. The full charge current, the medium or taper charge current, and the trickle charge current determine the array section size.

A microprocessor provides the following analytical functions:

a. Temperature compensated voltage limits
b. Ampere hour integration
c. Temperature compensated recharge fraction
d. Battery cell analysis
e. Emergency load shedding
f. Load bus assignments

Telemetry and status monitoring provide the following control parameters:

a. Switch status
b. Solar array voltage, current, and temperature
c. Battery, bus, and load currents
d. Bus voltage

For the ion propulsion bus on the LEO platform and the orbit transfer vehicle, the primary control is bus voltage. Because of GEO reconfiguration to a battery clamped bus, current control will be used in this application. (The battery clamped mode dominates the mission).

Bus voltage is programmable from the ion propulsion system, and the thruster controls the beam current.

In addition to the natural arc suppression provided by solar array response, the switches can be opened using spacecraft bus power to isolate the array from the ion engine. The control parameters required are under-voltage sensing, a time delay to avoid false triggering, and an override feature for restart when the engines are off.

Telemetry and status monitoring provide the following control parameters:

a. Solar array maximum power point current and voltage projections

b. Switch status

c. Solar array current, voltage and temperature

d. Bus voltage

e. Ion engine currents

4.1.8 Ability to Correct for Eclipse Effects

In order to define and evaluate the SASPM concepts it is necessary to understand the load types to be accommodated and the solar array response to these loads. There are four load types that the SASPM system is required to accommodate.

1. Resistive loads
2. Constant current loads
3. Constant power loads
4. Battery loads (charging)

Each load type presents a different demand on the SASPM system. These will be addressed separately, recognizing that the actual delivered power will most likely be to a combination of several load types.

The solar array output varies with temperature, and the temperature variation for LEO is -80^{o}C at eclipse exit to 80^{o}C in sunlight. The variation in GEO is more pronounced: -180^{o}C at eclipse exit to 60^{o}C in sunlight.

4.1.8.1 Resistive Loads

Heaters are typical resistive loads. Figure 4.1-4 shows the impact of array temperature on resistive loads in the absence of any regulation scheme. Full system loads (load line A) are designed to operate at, or near the maximum power point of the warm solar array, operating point (1). At eclipse exit, the cold solar array characteristic causes a shift to operating point (2), with a corresponding voltage change (ΔV_1). If the solar array is lightly loaded (load line B), the operating point will be at point (4) at eclipse exit and will move to point (3) as the array temperature stabilizes in sunlight.

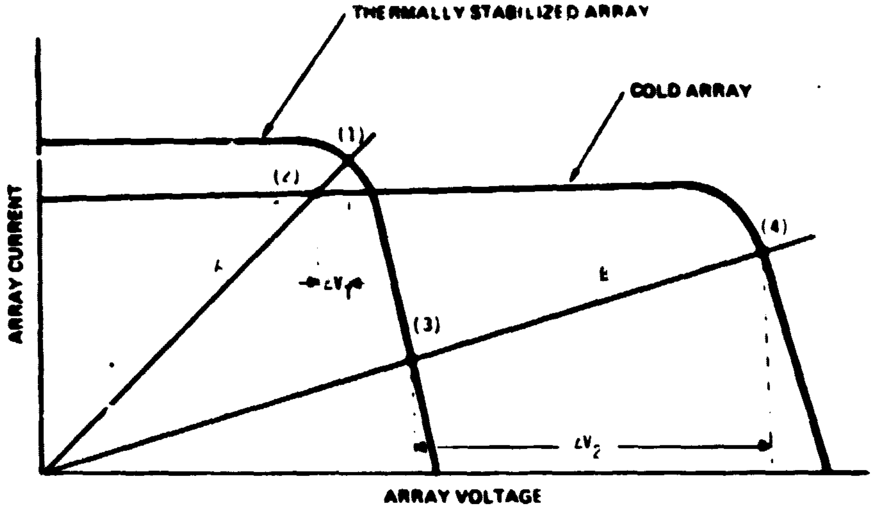

Figure 4.1-4 Impact of Array Temperature on Resistive Loads

In this case there is a wide voltage swing, ΔV_2. The above discussion assumes there is no battery to supplement array power, or to absorb excess array power. Figure 4.1-5 shows how a SASPM system could control the array if the loads were pure resistive, even with a significant reduction in load coinciding with eclipse exit. (Switching parallel array segments).

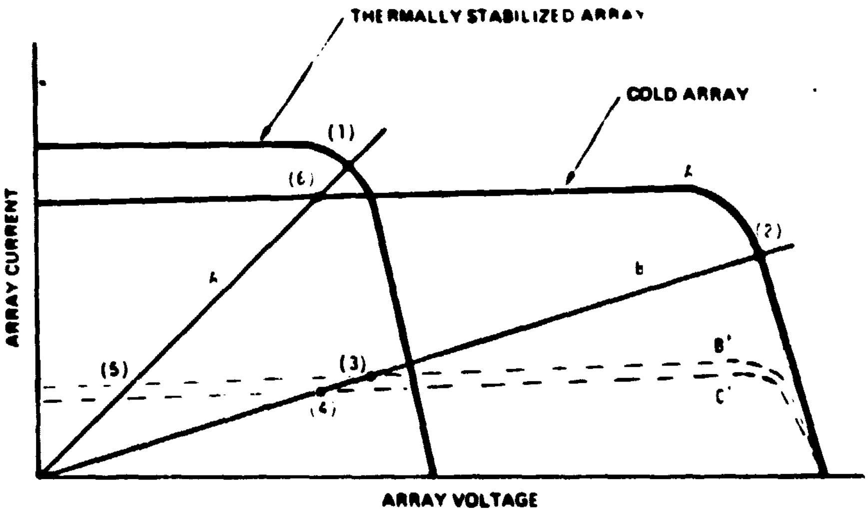

Figure 4.1-5 SASPM Control, Resistive Loads.

In this figure, the array is designed to operate at the maximum power point under full load (load line A), and all SASPM array sections are switched in. If, at eclipse exit the load drops significantly (load line B), the operating point jumps momentarily to (2) with a corresponding large voltage increase. The SASPM switches out array sections until the system reaches equilibrium at (3) or (4). If the total load is restored before the array heats up the system shifts momentarily to operating point (5) until the SASPM controls increase array output to A and operating point (6) (all array sections on). As the array heats up operating point (1) is restored. The voltage transient described above was limited to the difference between a cold and warm array, which could be eliminated by allowing the array to warm up before closing the array switches.

4.1.8.2 Constant Current Loads

This is characteristic of loads with input power regulated by a linear dissipative regulator. The high voltage beam current on ion propulsion engines is also a constant current load. The wide voltage variation from a cold array at eclipse exit to a thermally stabilized array in sunlight cannot be controlled by switching parallel array sections in or out as it was for resistive loads. See Figure 4.1-6.

If voltage regulation is required during the period between eclipse exit and thermal stabilization (≈ 5 minutes), a switching arrangement using series array segments instead of parallel array segments should be used, (assuming no load fluctuations).

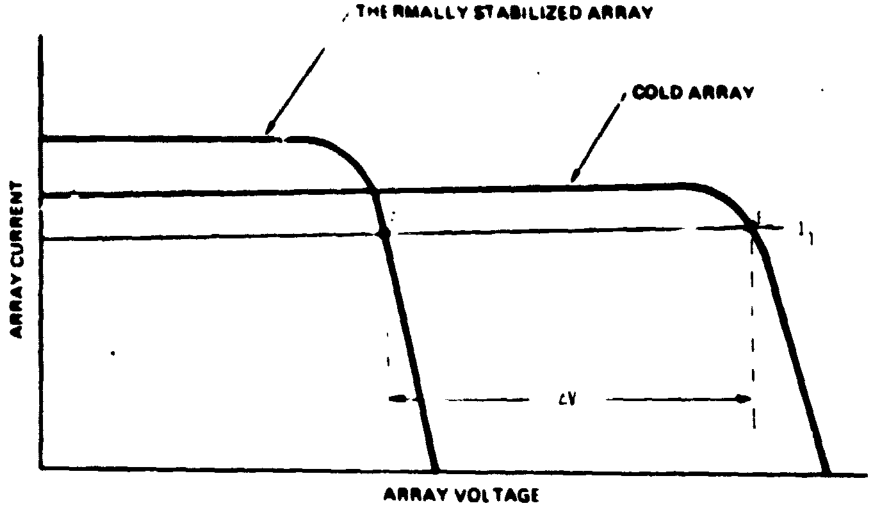

Figure 4.1-6 Impact of Array Temperature on Constant Current Loads

4.1.8.3 <u>Constant Power Loads</u>

Constant power demand is characteristic of loads utilizing a regulated power processor. In Figure 4.1-7, the load line and operating point are shown for a thermally stabilized array, and an array at eclipse exit.

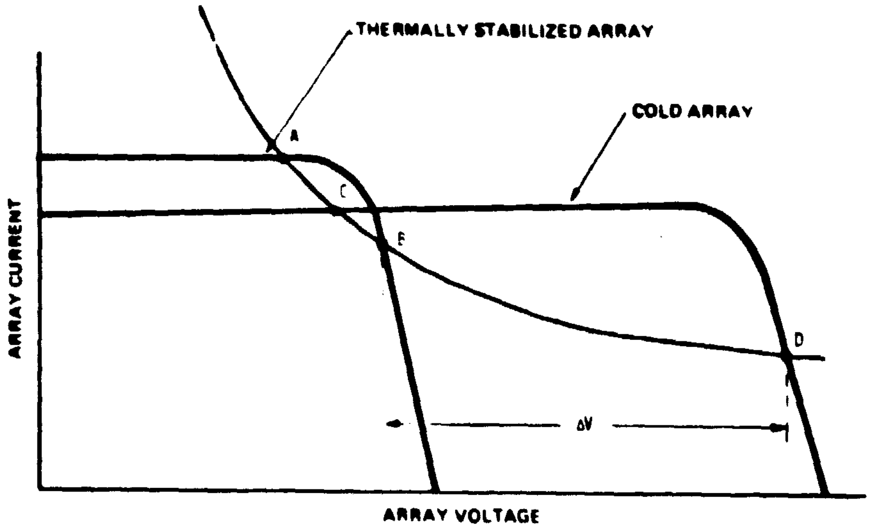

Figure 4.1-7 Impact of Array Temperature on Constant Power Loads

Points B and D are stable operating points and A and C are unstable. For an uncontrolled array, the voltage swing is large (factor greater than 2) between a cold and warm array. Array switching of series voltage sections could control this wide fluctuation, with the degree of control dependent upon array section size.

Figure 4.1-8 characterizes the SASPM technique to control voltage and current to constant power loads. (Thermally stabilized array).

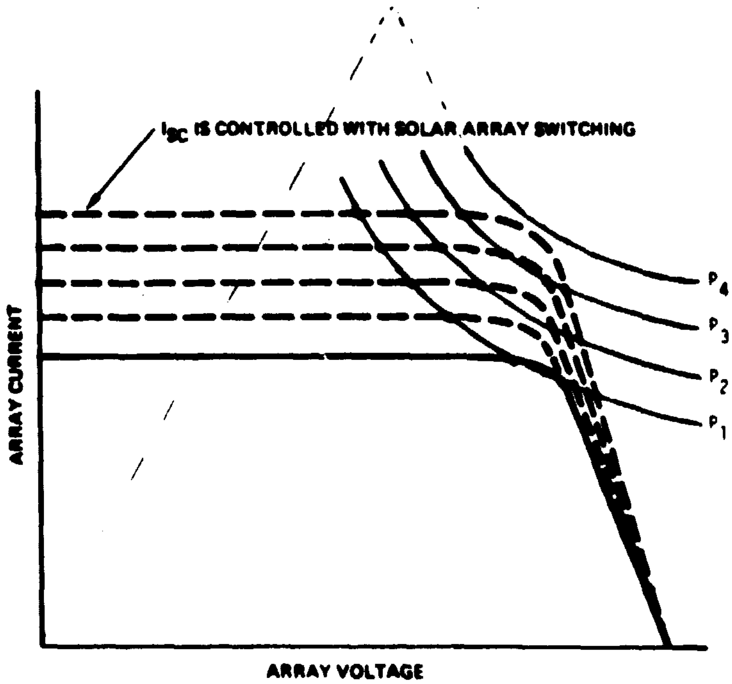

Figure 4.1-8 SASPM Control - Constant Power Loads

As array sections are switched in and out, the voltage varies much like in the constant current case. If a step load above the active array segments occurs (to P_4 in Figure 4.1-8) the array voltage will collapse toward zero. Step load reductions are easily accommodated as they were in the constant current case.

To avoid collapsing the array voltage, load increases must be predetermined and the appropriate number of array sections brought on line in advance. This would not be necessary if energy storage or a dissipative shunt were employed.

4.1.8.4 Battery Loads

If a battery were paralleled with the solar array, the response characteristic would appear as in Figure 4.1-9. Charging the battery would be accomplished by controlling the current by switching array segments in or out, depending on the state of charge and desired charge rate.

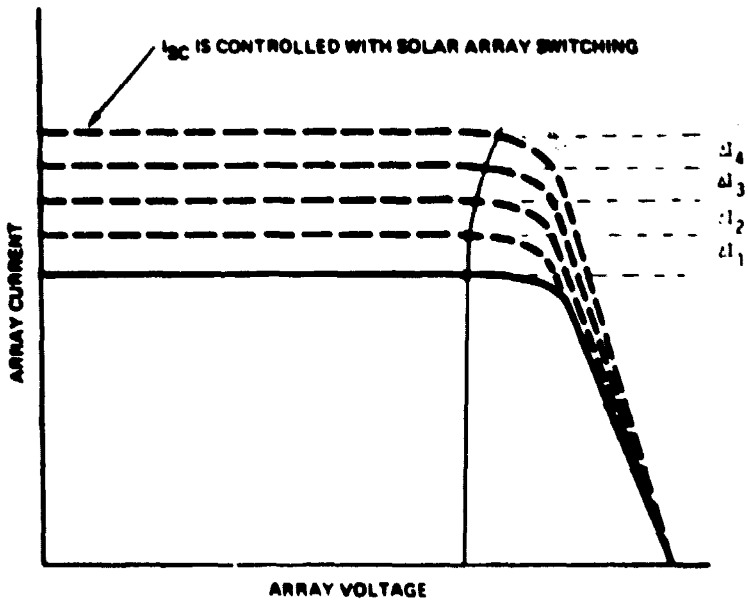

Figure 4.1-9 SASPM Control - Battery on Line

4.1.8.5 Digital Bus Control in the Absence of Energy Storage

Using a SASPM voltage control loop and parallel array segments, the control system will find two levels of solar array output having operating points (1) and (2) (Fig. 4.1-10) such that $V_1 < V_{REG} < V_2$. Since the array is incrementally switched, no operating point can exist between V_1 and V_2.

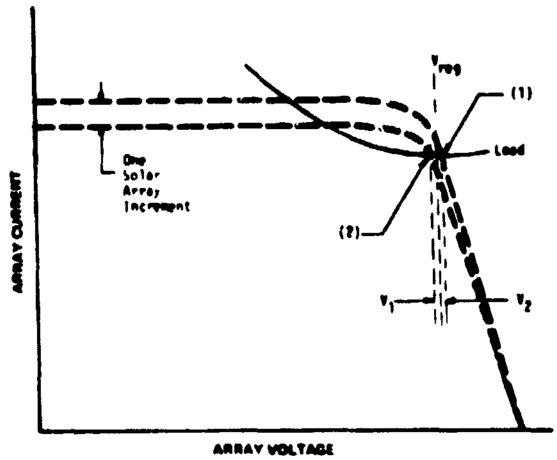

Figure 4.1-10 SASPM Voltage Control

If $(V_1 - V_2) \leq 2\Delta V$, where ΔV is 1/2 the total voltage regulation tolerance, the bus will stabilize at V_1 or V_2, and will remain until a change occurs in solar array output or load.

If $(V_1 - V_2) > 2\Delta V$, then the system will limit cycle between points (1) and (2) causing a ripple current of magnitude $(I_1 - I_2)$ to flow in the main bus. This can be removed from the bus by a filter. A second filter may be required in each switched string to prevent the solar array string from radiating at the switching frequency.

$(V_1 - V_2)$ is a property of the source-load characteristics. Limit-cycling may be avoided:

1) By widening the regulation tolerance band, $\pm\Delta V$.
2) By decreasing the switching increment size.
3) By over designing the solar array. This pushes the operating point toward the more steeply sloped part of the array curve, decreasing $(V_1 - V_2)$.

The above relationships apply to resistive and to mixed loads as well as to constant power loads.

4.1.8.6 Hybrid System

By adding a linear shunt it is possible to increase the frequency response at low impedance beyond that of which the digitally-switched system is capable.

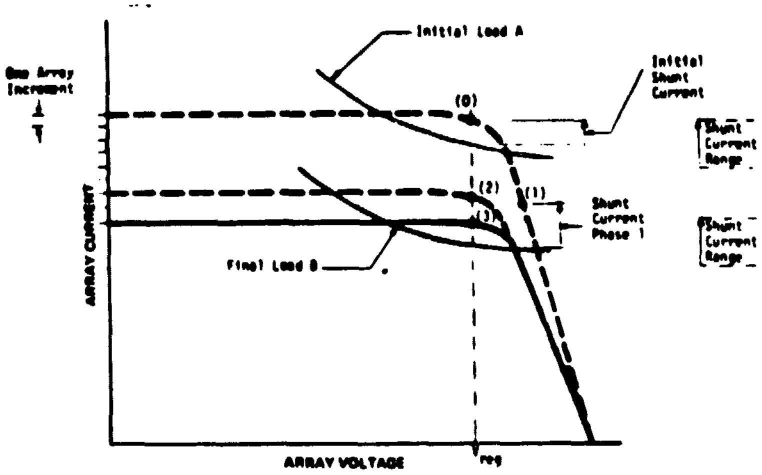

Figure 4.1-11 Response of a limited - capacity shunt/switched solar array system to a large load decrease

In Figure 4.1-11, a sudden load change from Level A to Level B will result in the following sequence of events:

1. The shunt immediately saturates, and the operating point moves from (0) to (1).
2. The digital control turns off solar array sections until the shunt regains control, at which point the operating point moves to (2). During this period, voltage is out of regulation. The worst-case is that of a load disconnect immediately after eclipse exit, when the voltage can double for the period required for the array switch gear to catch up.
3. Switch disconnect continues to occur until the shunt operates near its midpoint, and the load operating point moves to (3).

By using the same analytical method, it is possible to demonstrate that a step increase beyond one half the linear range of the shunt will result in collapse toward zero of the bus voltage for the period required for the digital control to restore operating balance.

ORIGINAL PAGE IS
OF POOR QUALITY

During transient periods, the battery takes up all current surges in either direction while the digital control is acquiring final balance.

Figure 4.1-12 shows the response of a battery-clamped system to large load changes.

The system is shown operating with load line A, array characteristic C. The operating point is (1), with a small battery charge current, I_1. An instantaneous change to load line B causes an immediate shift to operating point 2, and a large transient charge current, I_2. The control system senses the large current and decreases the solar array output in steps until array characteristic D and operating point (3) are reached. When the load is increased to curve A, the system cycles through operating point (4) and back to operating point (1).

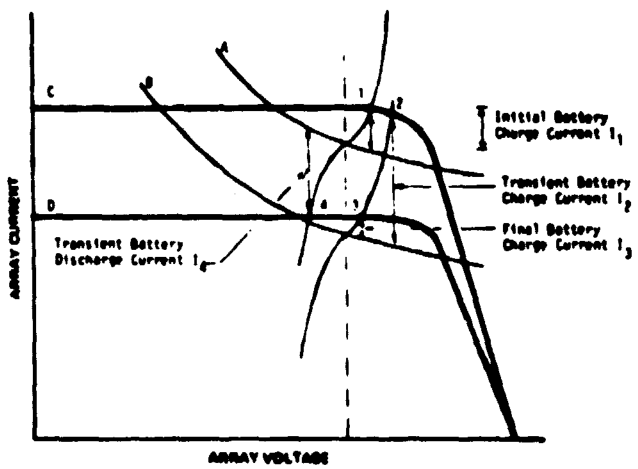

Figure 4.1-12 Battery Clamped System - Large Load Changes

4.1.9 Conductor/Grounding Arrangements

There are no effects in this area of concern which are peculiar to solar array switching techniques. The general problem of spacecraft electrostatic charging and space plasma leakage is discussed in detail in Section 4.1.17.

.1.10 EMI/Filtering

The SASPM equipment for all three missions should be designed to meet the requirements outlined in MIL-STD-1541 and MIL-STD-461. Special attention must be paid to the control of conducted and radiated interference generated by the high voltage and power switching circuits. (Except for the high voltage, the problem is no worse than on many existing spacecraft designs.

The solar array switches configured with either bipolar or MOSFET power transistors will require rise and fall time control circuitry to slow down switching action. While the rise and fall time control for the bipolar transistors is more involved, the control is relatively simple for the MOSFET devices because they inherently exhibit high input impedance and intrinsic gate-to-source and drain-to-source capacitances. The use of the MOSFET power devices provides another advantage over bipolar technology in the implementation of the rise and fall time control of the switches.

The switch gear and relays which are used to accomplish configuration changes such as modification of the system for the ion propulsion loads will require arc suppression networks across the contacts, not only for reducing the possibility of accelerated wear-out and potential welding of contacts, but also for attenuating the high frequency noise spectrum generated by the contact arcing.

The transient response on the spacecraft bus is controlled by the battery characteristics, however, the ion propulsion bus may need a capacitor bank to increase transient response and to reduce the narrow and broadband ripple voltage generated by the system.

For control and logic lines, the use of fiber optics will insure high immunity to EMI.

4.1.11 Modularity/Commonality/Growth

The present solar array concepts for larger power systems (25kw range) and those projected for larger systems are electrically segmented and therefore lend themselves to modularity concepts. Both fine switching resolution and a highly flexible modularity concept can be implemented, with the solar cell strings capable of being grouped and switched in any desired configuration.

As the desire for system growth to satisfy additional load requirements becomes apparent, additional power channels can be added to satisfy these requirements. Open ended algorithms will be programmed in the control system in order to enhance the ability to reprogram for load growth and diversification. This technique will allow for flexible growth at the power system/payload interface so that payload mixes may be diversified as desired.

4.1.12 Impact on Existing Arrays

There are no existing arrays of a size and construction such that they could be considered for power systems of the size examined in this study. The next generation of solar arrays (the PEP array of JSC, and the SP array being developed by TRW and Lockheed under MSFCs common solar array program) are segmented both electrically as described in Section 4.1.11 and mechanically so as to allow for ease of growth. The wiring of these solar arrays is designed to terminate both plus and minus leads for each cell string at the solar cell blanket container. This construction lends itself well to segment switching either on the array, or inboard of the power transfer device, with a minimum amount of solar array redesign. As previously discussed, the natural segmentation of the solar array lends itself ideally to control by SASPM.

4.1.13 Effect on Energy Storage and User Loads

The use of SASPM offers a minimal impact on battery charging. If anything, SASPM offers a more benign battery charge regimen than many other techniques, with both battery full charge and taper charge algorithms being easily modified, either in flight or prior to flight, to meet any desired pattern.

System loads attached directly to the main power bus will see an input voltage swing which is determined on the high side by the battery full charge voltage, and on the low side by the battery discharge voltage. For other than battery determined voltages, the loads must supply their own conditioning.

4.1.14 Effect on Array-Spacecraft Dynamics

There is no impact on spacecraft dynamics peculiar to SASPM other than that there might be some minor reduction of solar array aerodynamic drag because of the smaller solar array required using the SASPM control technique.

4.1.15 Impact on Shuttle Constraints

Structurally, there is no impact on the shuttle peculiar to SASPM. Electrically, the basic SASPM system does not match up well with the orbiter in the sortie mode. The orbiter voltage is regulated in the 24 to 32 volt range. If there is a desire to operate SASPM in parallel with the orbiter fuel cells, the SASPM power will have to add a series regulator in order to match system voltages and dynamic properties. In the area of safety, SASPM allows the array to be open circuited during launch.

4.1.16 Stowage/Deployment

As previously discussed, the SASPM control switching might be mounted in the solar cell blanket stowage container, or a container located close to the array stowage box. Location of the switches so as to maintain proper shielding, EMI, and dynamic environments must be considered. This problem is of no greater magnitude than most control systems will have when they mate with large solar arrays. The array switches will be open during solar array deployment; this provides isolation while the array is partially illuminated.

ORIGINAL PAGE IS
OF POOR QUALITY

4.1.17 Interaction with Space Environment

This section examines the status of our knowledge of how large, high powered solar arrays interact with the space ambient plasma, both that generated by ion engines, and that existing in the natural environment. Of prime concern is the loss of solar array power through plasma leakage and the means whereby this loss may be mitigated. Additional effects of the spacecraft/plasma interaction (i.e., the degradation optical of surface properties by contaminant deposition, and the generation of electromagnetic interference (EMI) in the spacecraft potential equilibration process) are of major concern but are not addressed in this study, but is being addressed on a continuing basis by LeRC. Table 4-1 summarizes the conclusions of this brief survey.

4.1.17.1 Configurations and Orbits

The spacecraft configuration for LEO is shown in Figure 4.1-13. Two arrays, about 300' x 85' with a power conditioning module and an experiment module, each about 60' long attached are shown. Since the self-generated plasma due to the ion engines decreases rapidly with distance, the ion engines have been assumed to be located at the far end of the experiment modules. If this is not possible, the ion engines should be mounted at the farthest end of the power conditioning module away from the solar array. The ion engines being considered are to use argon as the propellant rather than mercury. Most prior ion engine work such as for the SEPS missions considered the use of mercury. All three mission configurations are considered herein.

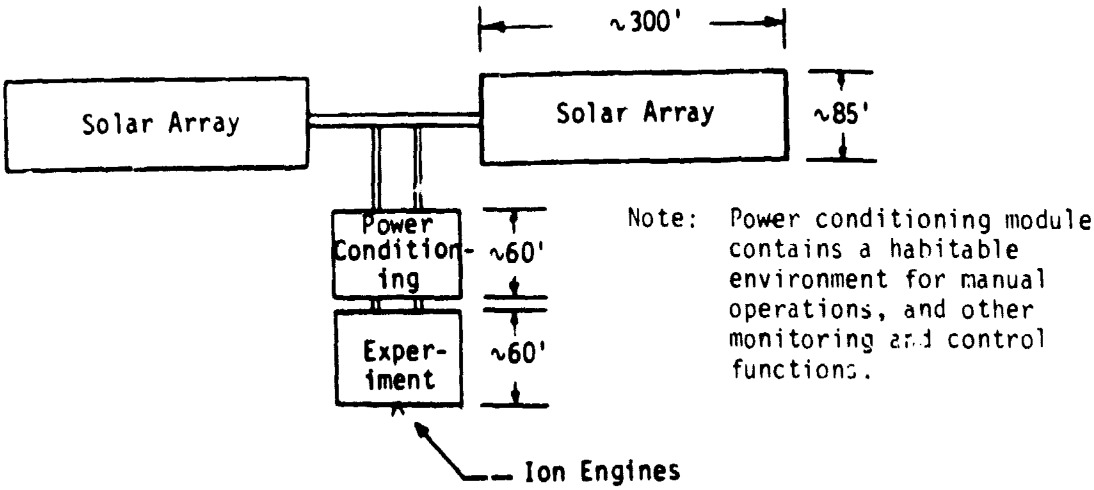

Figure 4.1-13 LEO Spacecraft Configuration

Table 4-1 Plasma Power Loss Summary

- Low Earth Orbit operations with ion thrusters requires that both natural and self-gnerated plasma environments be taken into account.
- Current predictions are that natural environment losses are $\sim$4% of the 860 volt portion of the solar array output and 0.6% to 40% for the self generated environment for the 860 volt supply. (depending on the distance of ion engines from the solar array)
- For the 240 volt portion of the array, the power losses are 0.4% for the natural environment and 0.6% to 40% for the self-generated environment. (Depending on the distance of the ion engines from the solar array.)
- Plasma density, dimensional and power (voltage, current) level extrapolations need to be studied analytically and verified experimentally.
- All of the ongoing physical processes are not understood and must be investigated further.
- Analytical models need to be improved and checked out experimentally.
- Exact flight configurations need to be analyzed and tested
  - Argon vs mercury ions
  - Solar cell layout and array configuration

ORIGINAL PAGE IS
OF POOR QUALITY

4.1.17.2 Overview of the Plasma Power Loss Problem

The loss of power from solar arrays by plasma leakage arises from the collection of the highly mobile plasma electrons by the more positive exposed portions of the array such as the interconnects and exposed sides of the solar cells. The return electrical current path is provided by the collection of the less mobile ambient plasma ions, again by exposed interconnects, but even more so by any exposed metal which is connected to structure. This assumes that the negative end of the array is grounded to structure.

Because of the greater efficiency with which plasma electrons are collected, the total spacecraft system generally equilibrates with the most positive portion, ($\sim$10%) of the solar array at positive potentials relative to the undisturbed plasma, and the remainder ($\sim$90%), negative.

It is at the higher array voltages (>200 volts) that power losses begin to become significant - in a non-linear fashion. Many physical processes are involved, not all of them clearly understood:

- Pinhole effects at positive potentials.
  - Secondary emission
- Sheath processes
  - Non-linear expansion with potentials.
- Magnetic field constraints on particle trajectories.
- High electric field emission of electrons.
- Ultraviolet radiation effects - photoemission.

- **Ram and wake effects due to spacecraft velocity.**
- **Arc and corona breakdown (avalanche) effects.**
  - Plasma generation

The local plasma density, which may be as high as 10^6 particles per cc in the 400 km altitude range applicable to LEO, affects many of the physical processes which must be taken into account. At GEO altitudes, the density is in the order of 1 to 10 particles per cc, and ram and wake effects, for example, are not significant. Plasma power loss is not expected to be a serious problem at GEO altitudes until supply voltages exceed many kilovolts.

For the spacecraft configurations under consideration, the ion engines are expected to create a plasma environment in addition to the natural environment. The fast ions coming out of the engine collide with slow neutrons producing the low energy ions of the charge exchange plasma. The only measurements available on this charge exchange plasma are those by Komatsu and Sellen at TRW (Ref. 4-6). These were made on a SEPS type mercury thruster, and only at relatively short distances from the thruster.

4.1.17.3 Plasma Power Loss in the 400 km Altitude Natural Environment

Predictions of plasma power loss in the 400 kn altitude natural environment have been made by Purvis, Stevens and Berkopec (Ref. 4-1) for a 500 KW array assuming a 2×10^5 particle per cc plasma density (Figure 4.1-14). Presented here is Figure 6 and 7 reproduced from their report, and summarizes their results. Figure 6 depicts the voltage distribution assumed, the plasma sheath configuration and the ram geometry around the orbit. Also shown is the plasma leakage currents for ram and isotropic conditions as functions of the array operating voltage. For the 500 KW array power, a leakage current of one ampere at 1000 volts represents 0.2% of the total power. Note that the maximum ram condition, which occurs at dawn and dusk on each orbit, results in about an order of magnitude greater power loss.

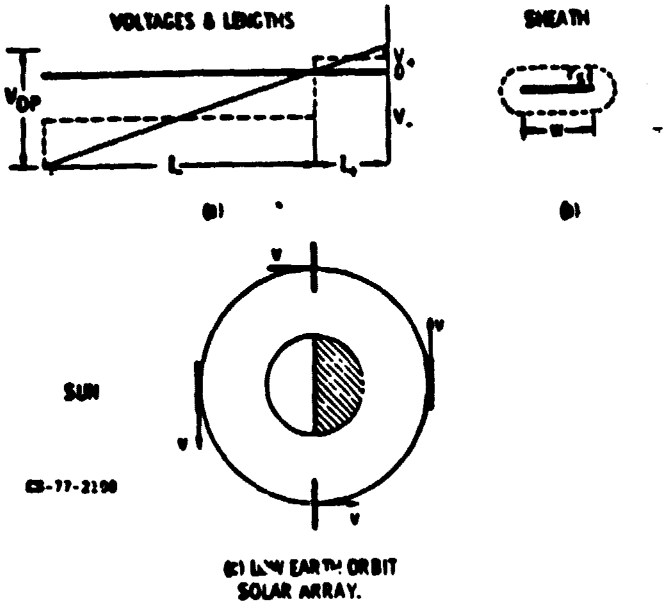

Figure 6. - Interaction computation models.

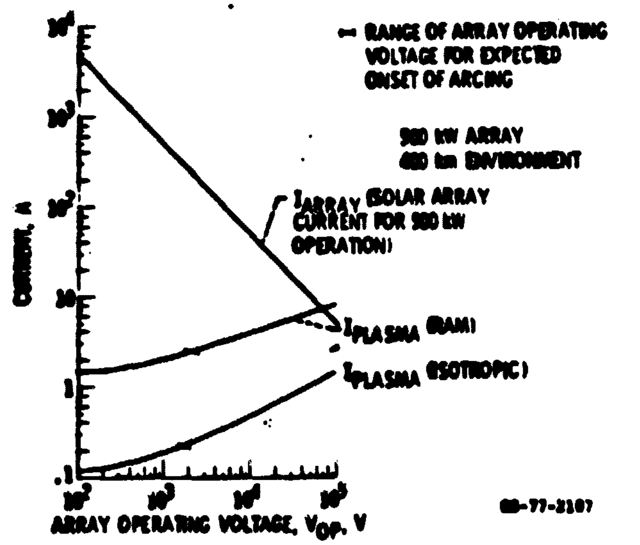

Figure 7. - Plasma/solar array coupling currents vs solar array operating voltage for a 500 kW array, in thermal environments; 400 km environment.

Figure 4.1-14 Plasma Interaction Figures from Purvis, et al (4-1)

ORIGINAL PAGE IS OF POOR QUALITY

Fig. 4.1-15 compares the percentage power loss obtained by Purvis, et. al with experimental data obtained by McCoy and Konradi (Ref. 4-2) in a 90' x 75' chamber using a 1m x 10m conductive plastic panel. If McCoy's density figure of 10^6 particles per cc is assumed to be correct, his data is not inconsistent with the Purvis prediction. Since the data on Fig. 4.1-15 is for the isotropic case, the ram case would give a power loss percentage of about 5% of a 1000 volt array operating voltage. Also shown on Fig. 4.1-15 is a TRW computation, attempting to reproduce Purvis' results, which gives a somewhat lower power loss.

The Purvis computations take into account the pin-hole effect discussed by Stevens, Berkopc and Purvis (Ref. 4-3) and Kaufman and Robinson (Ref 4-4) which increases the effective electron current collection area. The arc or corona-like breakdown effects reported for negative metal-positive dielectric situations by Inouye and Sellen (Ref. 4-5) are not taken into account. Stevens, et. al (Ref. 4-3) also report arcing at negative surface potentials, and McCoy, in a private communication with G. Inouye, reports arcing at both positive and negative potentials greater than 200 volts.

Summarizing this analysis, then, the following points can be made:

- Initial experimental and analytical data indicates plasma power loss to be less than 10% at 860 volts.
- Area (power) extrapolations need more investigation.
- All of the attendant physical processes need to be investigated more thoroughly.
- Exact flight configurations need to be analyzed and tested.

4.1.17.4 Self-Generated Plasma Power Loss

As with the natural environment problem, the self-generated plasma power loss problem suffers from a shortage of experimental data and only preliminary analysis - mainly having to do with mercury ion thrusters. Experimental data are provided by Komatsu and Sellen (Ref. 4-6) and by Kaufman (Ref. 4-7). Analytical models have been presented by Kaufman (Ref. 4-8) and Park and Katz (Ref. 4-9).

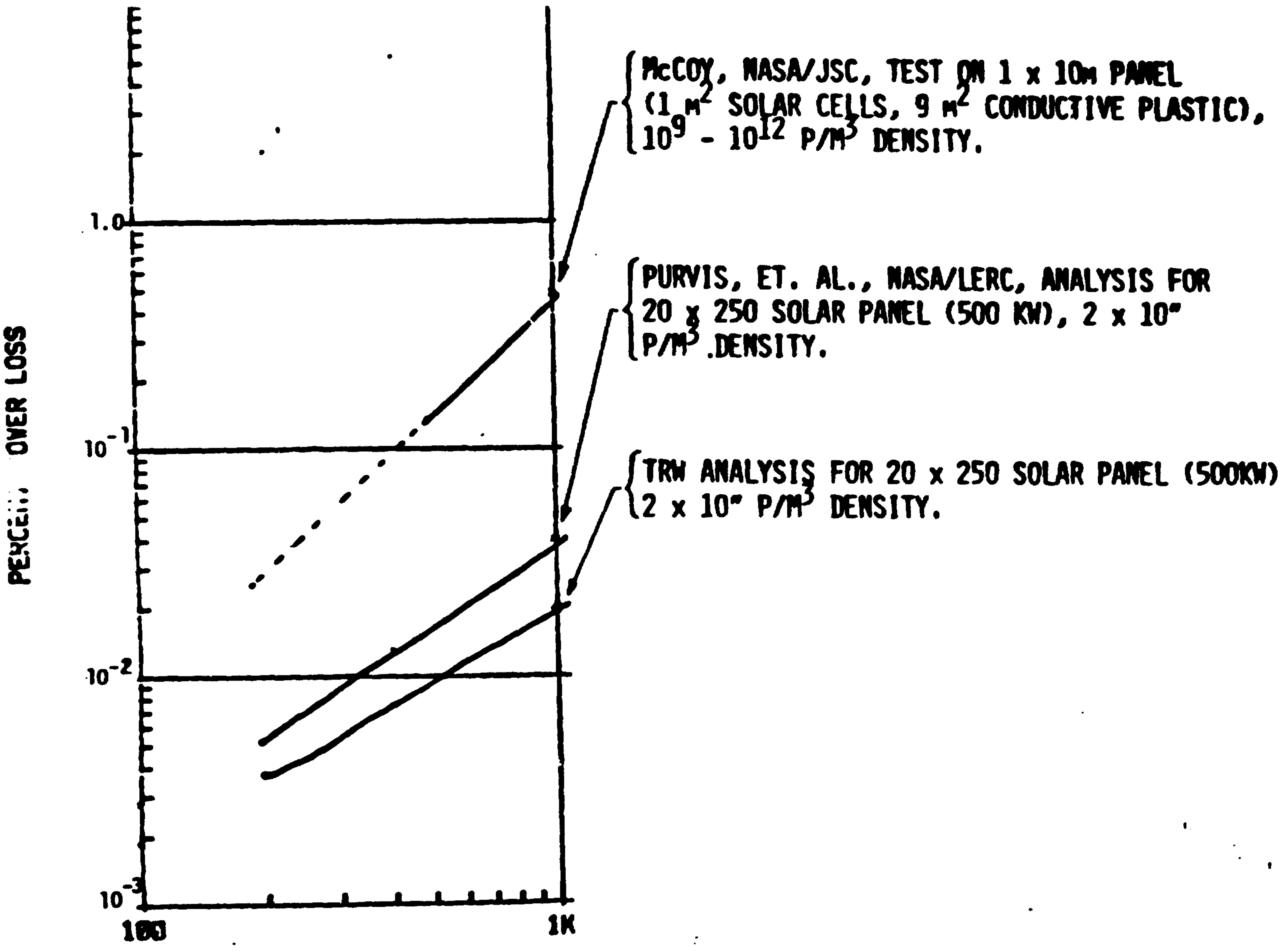

% POWER LOSS vs. OPERATING VOLTAGE

Figure 4.1-15 Isotropic Plasma - No Ram

Figure 4.1-16 is reproduced from the report by Kaufman (Ref. 4-8), and shows electron current densities as a function of distance along the SEPS array. Integrating over the length of the array gives a total current of 0.74 amps assuming a constant (average) array voltage, or a power loss of 148 watts for a 200 volt operating voltage. The percentage power loss, assuming 25 KW total power, is 0.59%.

Kaufman's model assumes that all of the self-generated plasma electrons incident on the solar arrays are collected and, therefore, the power loss current is independent of array voltage. The power loss is, therefore, proportional to the array voltage:

$$\text{Percent Power Loss at 860 v} = \frac{860}{200} = .59\% = 2.54\%$$

$$\text{at 240 v:}\quad \frac{240}{200} = .59\% = 0.71\%$$

Since these power loss calculations are based on the SEPS configuration, (dimensions, voltages, power) they should be redone for the configurations under consideration here. The results do, however, give an indication of the power loss magnitudes. Effects of argon ions rather than mercury ions should be included in the new calculations. The effects of multiple supply voltages (and currents) should also be studied and included in the analysis. For the present purposes, their effects were assumed to be independent. Because of the common structure potential, it is obvious that the two supplies, 240 volts and 860 volts are not independent.

The results of the computations presented by Park and Katz (Ref. 4-9) predict that nearly 40% of the total ion thruster beam current is collected. Insulating the low voltage (<500 volt) sections of the array reduces this loss to 4.7%, assuming that the insulation is so effective that the pinhole effect is not operating. It should be noted in this connection that McCoy (private communication with G. Inouye)

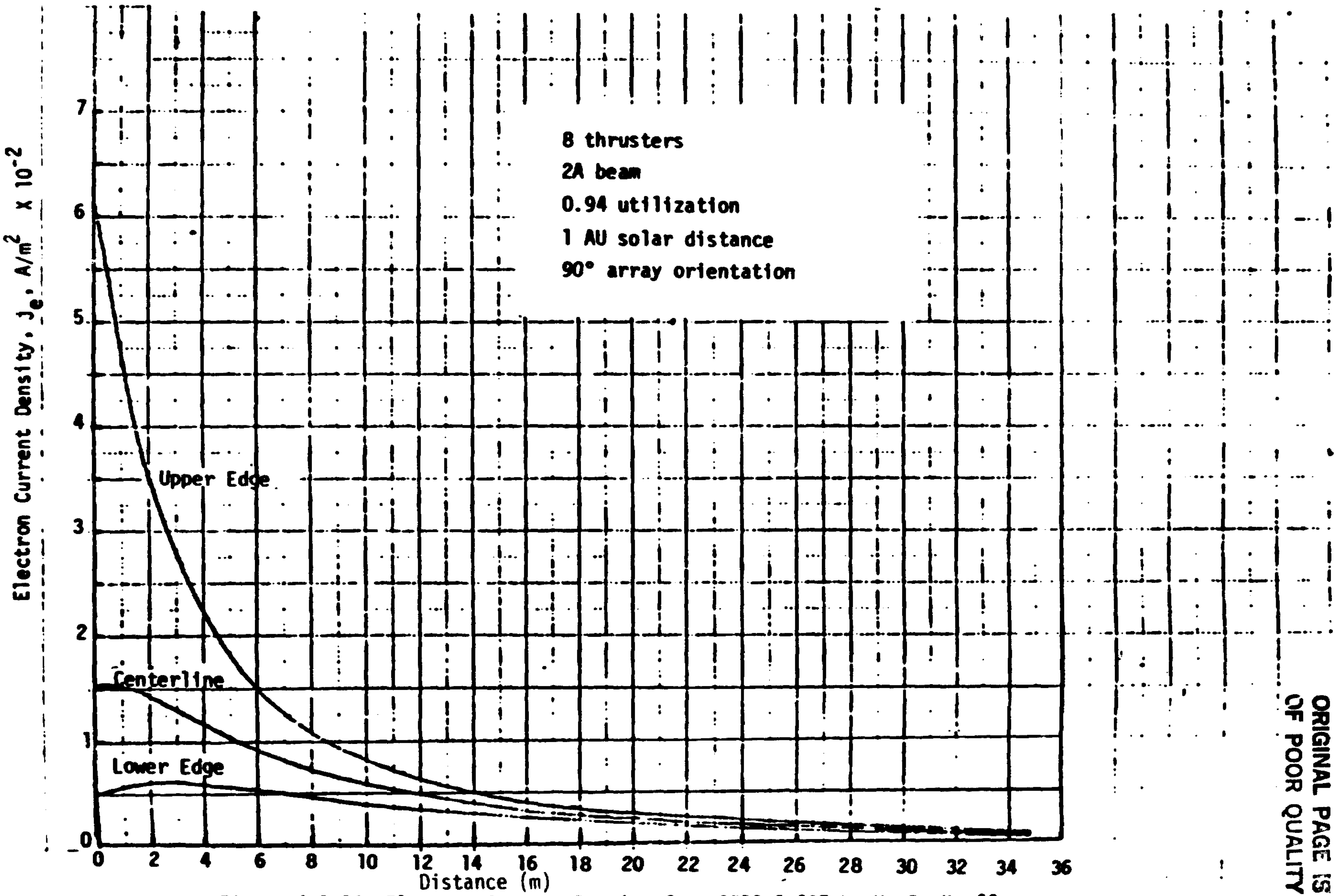

Figure 4.1-16 Electron Current Density from SEPS-I-207 by H. R. Kauffman

has stated that he attempted to cover interconnects with kapton tape to reduce power losses in a solar array test and found that it was completely ineffective.

Park and Katz' computations were based on a particular distribution of solar array voltages up to 2800 volts. As with the Kaufman analysis, the extrapolation to other voltages and dimensional configurations is not simple or even possible to perform here. Also, the data used were applicable to mercury ions rather than argon ions.

Summarizing the status of self-generated plasma power loss, the following points are made:

- Current predictions range from 0.6% to 40% plasma power loss.
- More experimental data is needed.
  - Argon rather than mercury ions.
  - Size and voltage scaling.
- All of the physical processes need to be investigated more thoroughly.
  - Secondary emission, photoemission, high field emission, surface potential effects, avalanche breakdown.
- Analytical plasma interaction models need to be developed further and checked out experimentally.
- Exact flight configurations need to be analyzed and tested.
- Plasma power loss minimization techniques need to be developed.
  - Electric and magnetic "shielding" techniques.
  - Material development to minimize and withstand interaction processes.
- Keep ion engines as far away from the array as possible.

4.2 Solar Array Switching (SAS) Sequencing Approaches

SAS sequencing approaches were described in Section 3.2.

The various approaches were comparatively evaluated for the LEO mission utilizing either bipolar or MOSFET transistors for the switches. The number of required solar array segments were calculated as a function of percentage resolution on the basis of the following equations:

1) Series sequenced approach: $N = \frac{100}{R}$

   where N = Number of segments, and R = % resolution

2) 2 bit binary count/sequenced: $N = \frac{1}{3} \cdot \frac{100}{R} + 1$

3) 4 bit binary count/sequenced: $N = \frac{1}{15} \cdot \frac{100}{R} + 3$

4) Binary count $R = \frac{100}{2^N - 1}$

The number of required solar array segments versus resolution plot is shown in Figure 4.2-1. It can be seen that the series sequenced approach requires the highest and the binary count approach requires the lowest number of segments for a given percentage resolution. The curves of the combinational arrangements such as the 2 and 4 bit binary count/sequenced approaches fall between the above extremes.

The maximum segment current of each approach for the LEO spacecraft bus was also calculated from the equations:

1) Series Sequenced Approach

$$I_M = \frac{191.5}{N} \text{ Amps}$$

where N = Number of Segments

2) 2 Bit Binary Count/Sequenced

$$I_M = \frac{191.5}{N-1} \text{ Amps}$$

3) 4 Bit Binary Count/Sequenced

$$I_M = \frac{191.5}{N-3} \text{ Amps}$$

4) Binary Count

$$I_M = \frac{191.5}{2} = 95.8\text{A}$$

With the aid of the curves in Figure 4.2-1, the maximum segment current for each approach was plotted (Figure 4.2-2) as a function of percentage resolution for the LEO spacecraft bus. It can be observed from the curves that the binary count approach requires the highest (whereas the series sequenced approach requires the lowest) segment current for a given percentage resolution. The curves of the 2 and 4 bit binary count/sequenced arrangements fall between the plots of binary count and series sequenced approaches.

Parametric studies were conducted to determine the number of power stages required utilizing either bipolar or MOSFET transistors for the solar array switches in each of the sequencing approaches. The results were plotted and are shown in Figure 4.2-3 through Figure 4.2-7.

The number of bipolar stages (including subdrivers) is determined by the segment current of the switches, the redundancy approach, the gain of the transistors (forced beta of 10 was assumed for each) and the input current from the majority voting logic circuitry (10mA).

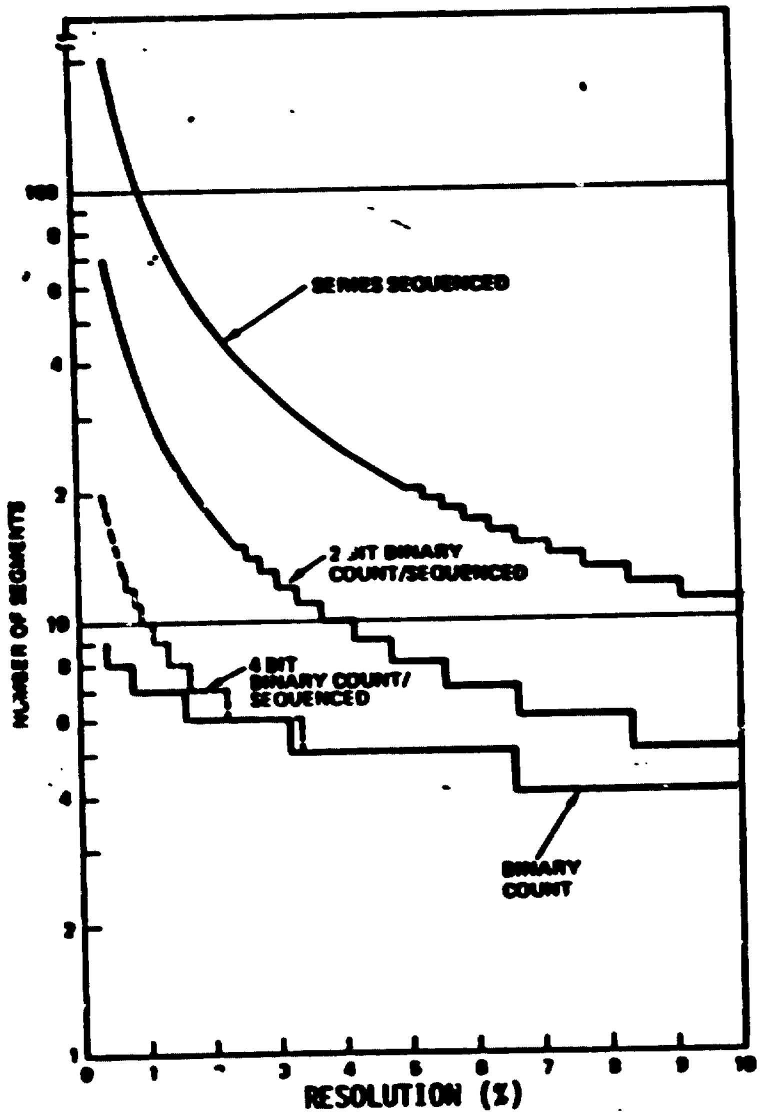

Figure 4.2-1
Number of Required Solar Array Segments vs. Resolution

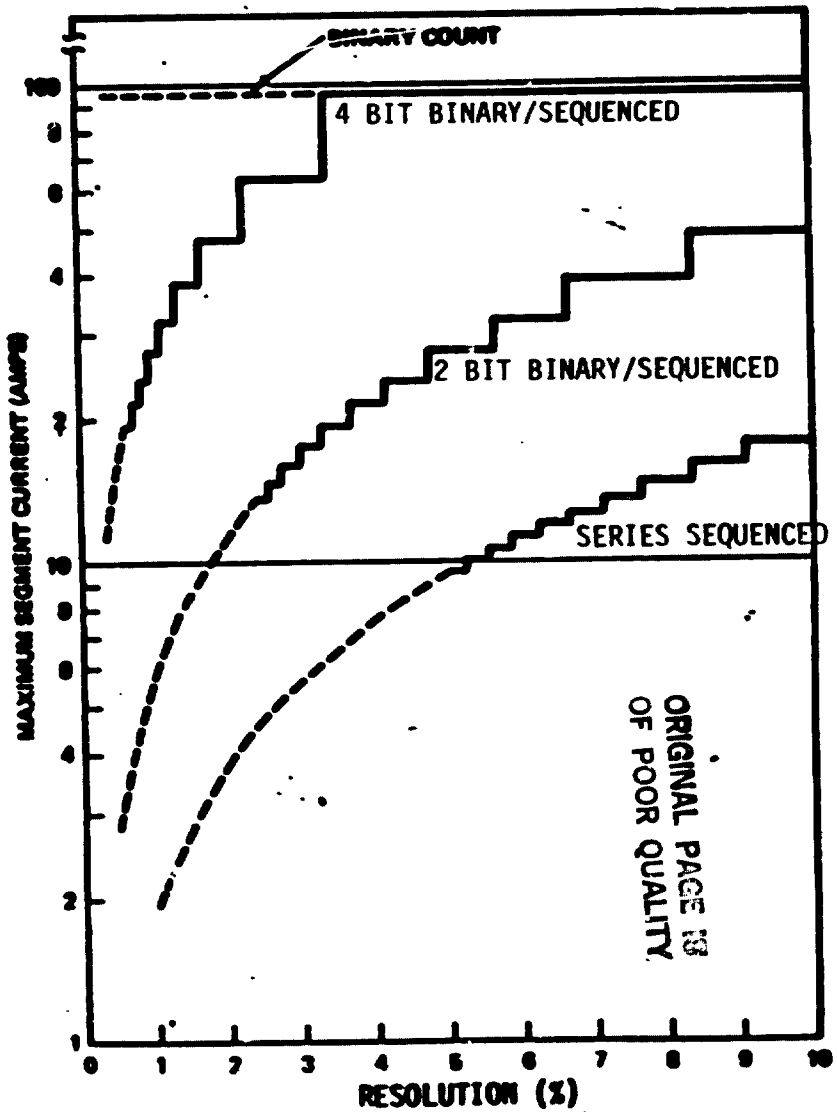

ORIGINAL PAGE IS OF POOR QUALITY

Figure 4.2-2
Maximum Segment Current vs. Resolution for LEO Spacecraft Bus

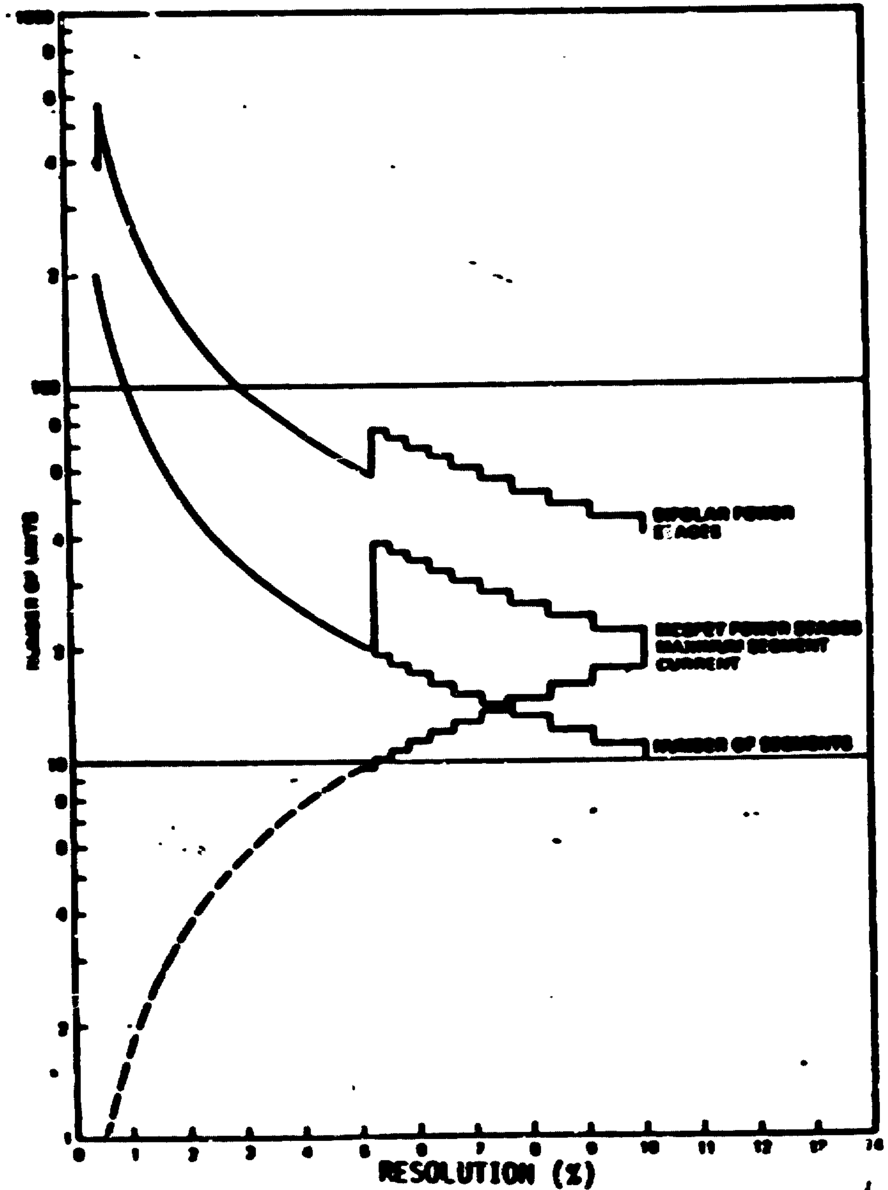

Figure 4.2-3
Series Sequenced LEO Spacecraft Bus

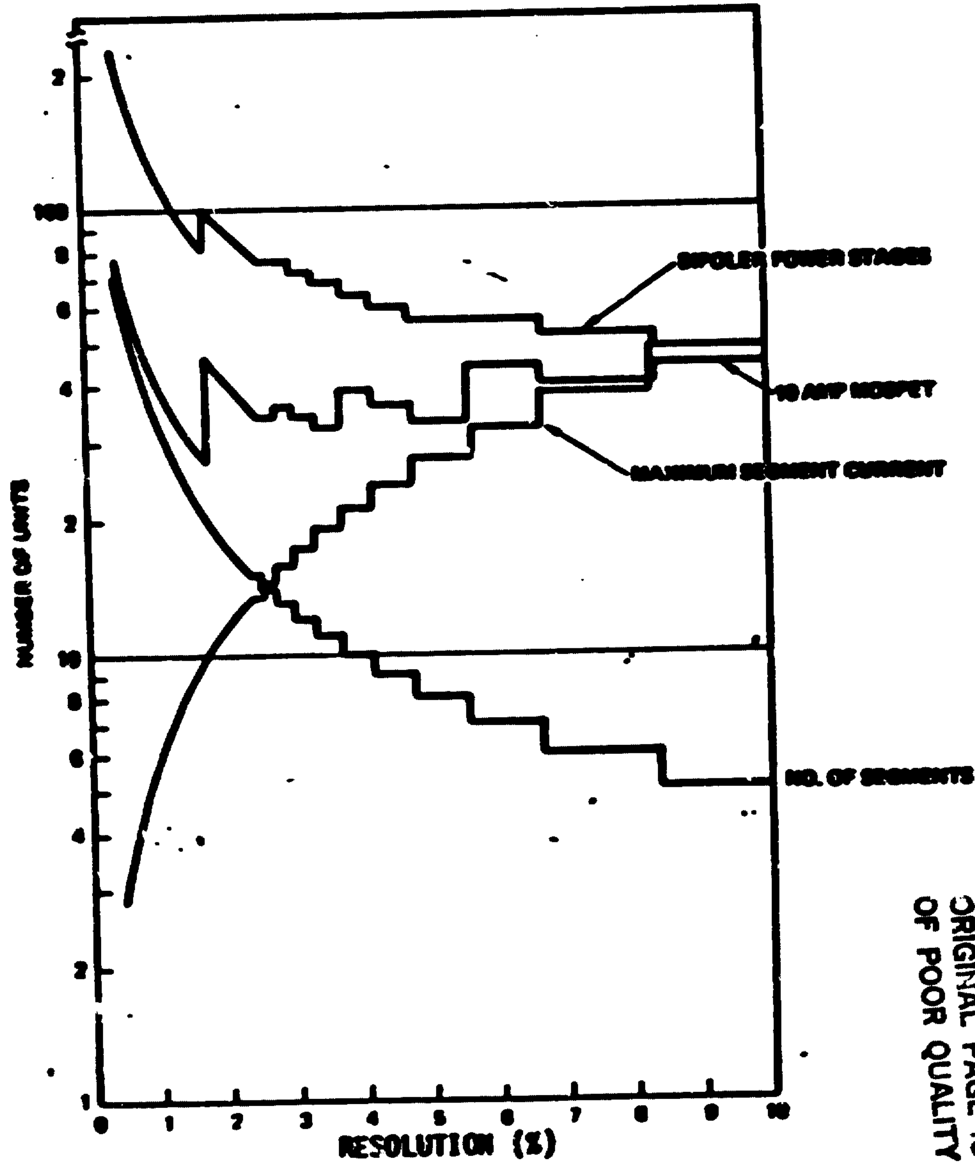

Figure 4.2-4
2 Bit Binary Sequenced LEO
Spacecraft Bus

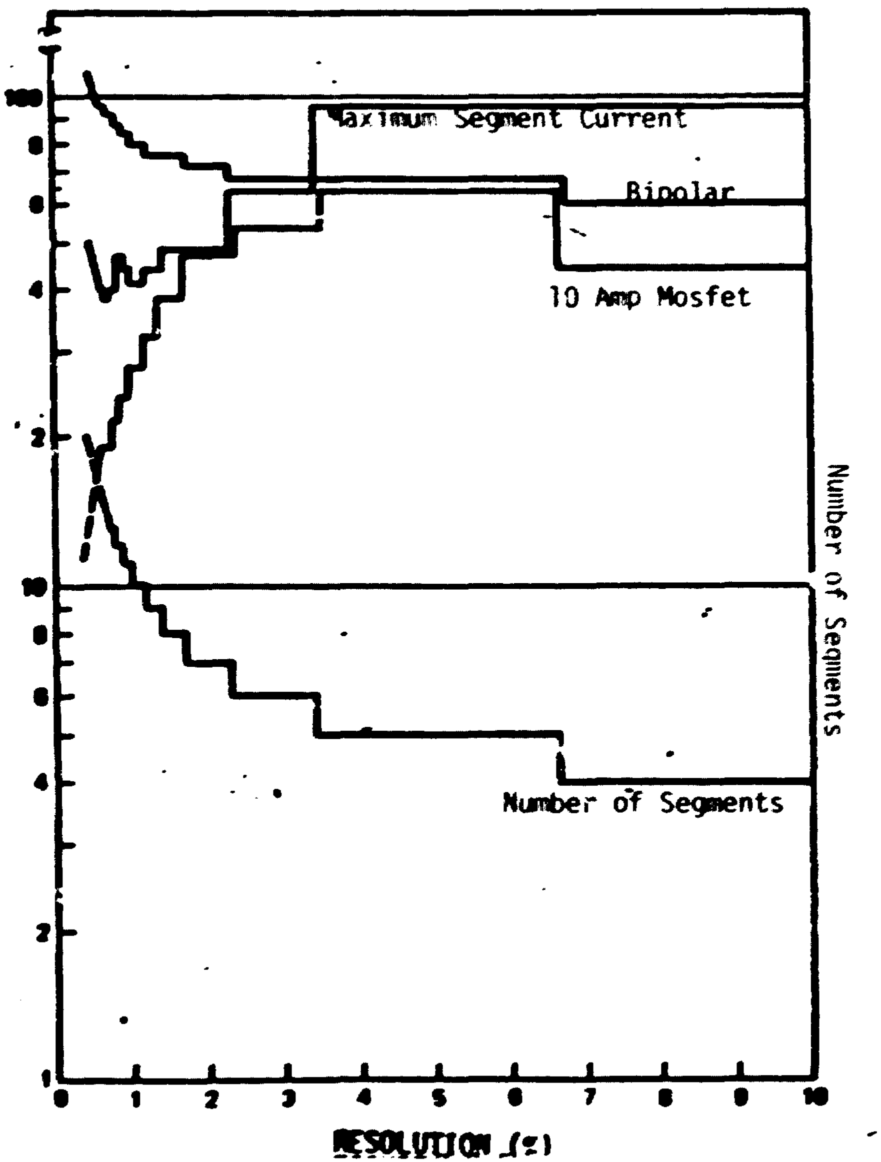

Figure 4.2-5
4 Bit Binary/Sequenced LEO
Spacecraft Bus

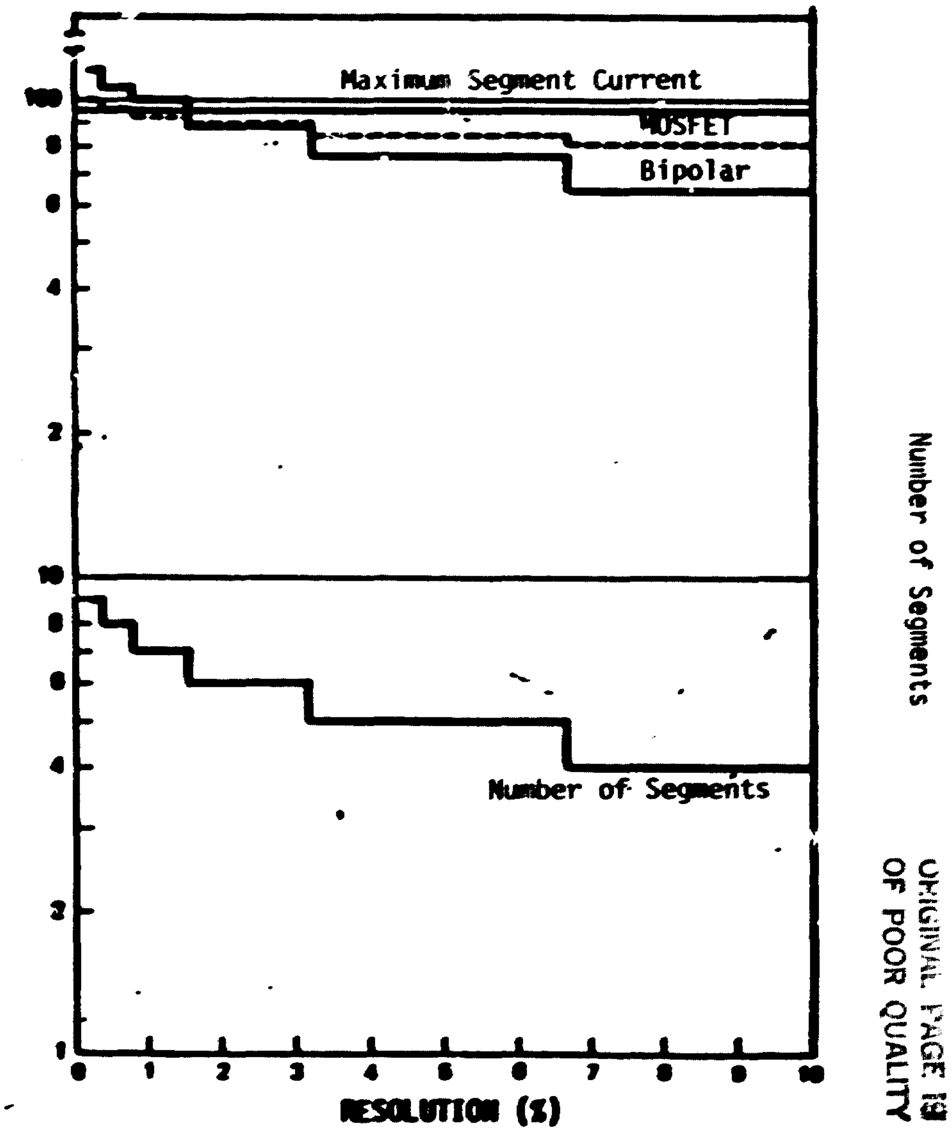

Figure 4.2-6
Binary Count

ORIGINAL PAGE IS
OF POOR QUALITY

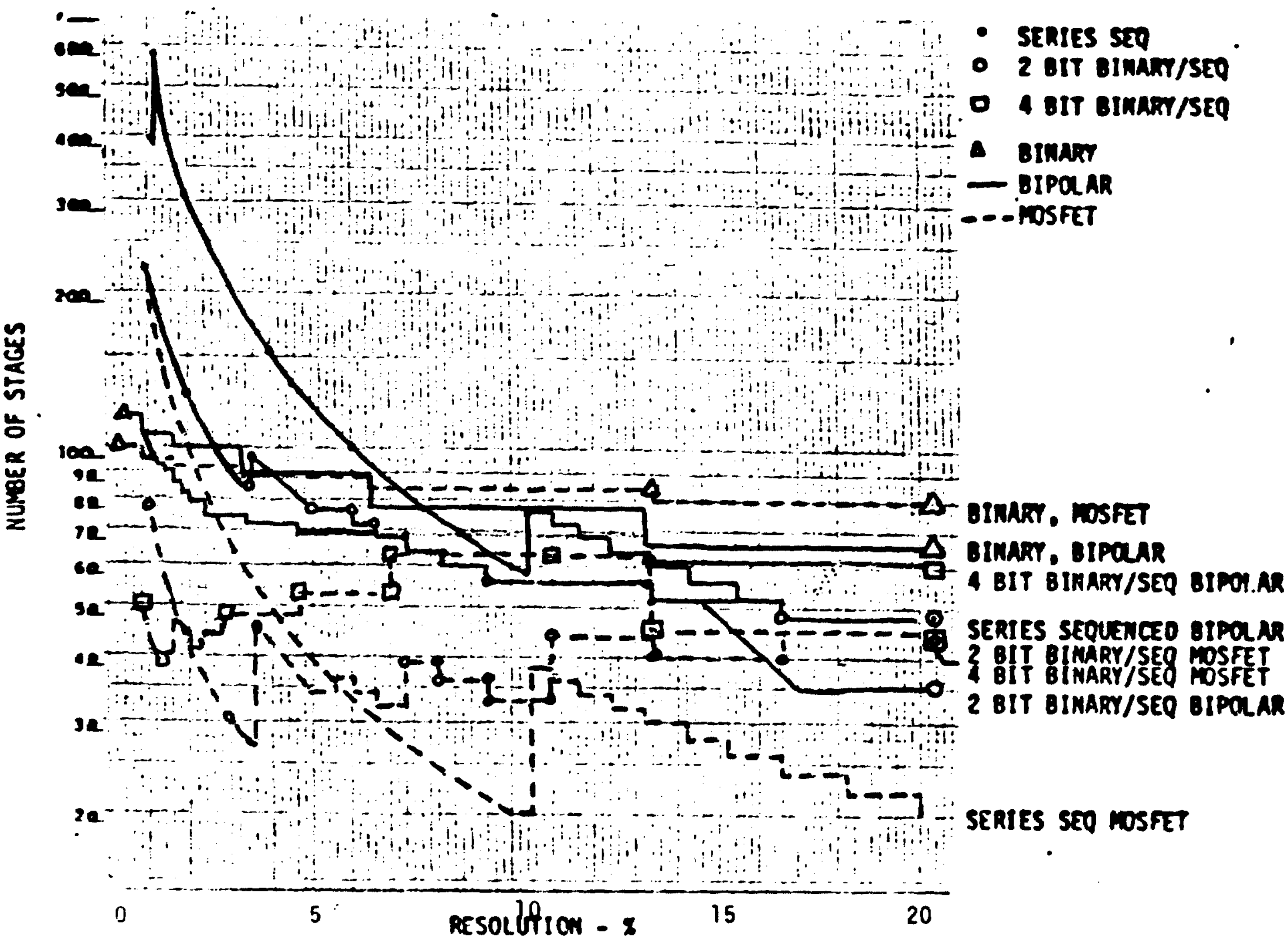

Figure 4.2-7

Number of Power Stages Per Channel vs. Resolution

LEO Spacecraft Bus

On the basis of this, if the segment current is between

10 mA and 100 mA:	1 stage
100 mA and 1A:	2 stages (one power and one driver stage)
1A and 10A:	3 stages (one power and two driver stages)
10A and 100A:	4 stages (one power and three driver stages)

are required.

The number of parallel MOSFET power transistors is determined by the maximum MOSFET current. Since the MOSFET transistor is a voltage controlled device, there is no change in subdriver configuration as a function of segment current.

If the segment current is between

10 mA and 10A:	1 single
10 A and 20 A:	2 parallel
|	|
90 A and 100 A:	10 parallel

MOSFETS are required.

In Figure 4.2-3 through 4.2-6, the number of segments, the segment current, and the number of bipolar and MOSFET power stages are plotted as a function of percentage resolution.

The advantage of utilizing MOSFET transistors over the bipolar ones is evident from the plots of the series sequenced or the binary count/sequenced combinational arrangements to achieve reduction in the number of power stages. However, in case of the binary count approach (Figure 4.2-6), the usage of MOSFET power transistors does not yield an advantage over the bipolar ones above 3% resolution.

It should be noted that the abrupt increases shown on the curves for the number of power stages are due to exceeding the maximum current capability of either the bipolar transistor stages or the MOSFET devices. A typical example can be seen in the series sequenced plot (Figure 4.2-3) at the 5% resolution point where the segment current is over 10 A and the number of segments are 20. Since between 10 A and 20 A it is required to parallel 2 MOSFET transistors, the total number of the MOSFET power stages increases from 20 to 40. Similarly, between 10 A and 100 A, 4 bipolar stages are required per segment and the total number of stages changes from 60 to 80.

Figure 4.2-7 combines the power stage curves generated in the previous plots to gain a direct comparison.

The results of the parametric study for the linear sequenced approach are tabulated in Tables 4-2 through Table 4-4 . The linear sequenced arrangements in Table 4-2 and 4-3 are configured with 400 W and 200 W bipolar linear power strings, respectively.

The linear sequenced arrangement in Table 4-4 , on the other hand, employs 100 W MOSFET linear power strings.

Column 1 of the tables shows the number of prime and redundant linear strings. In all cases it is assumed that one extra string is required for redundancy to protect against an open failure.

Column 2 contains the number of linear stages. The numbers given in the column include the count for the subdriver stages and the switches in which two devices are series connected to provide protection against a short failure. To illustrate the count of linear stages for example, in row 1 of Table 4-2 , it is shown that there are 1 prime and 1 redundant linear strings with a current carrying capability of 2A each (column 3). For both the prime and redundant strings, there are two devices series connected, each of which requires 3 bipolar stages. Therefore, the total number of linear stages is 12.

Column 4 contains the percentage resolution of the digital segments.

Under column 5, the codes for the type of digital segments are given.

Columns 6 and 7 contain the number of digital stages and total stages (including the linear and digital ones), respectively.

The percent resolution for the digital segments was determined with the aid of the previously developed plots of the sequencing approaches.

The comparison of the tables clearly indicates that the usage of MOSFET devices in the linear sequenced approach provides a significant advantage over the bipolar counterparts.

Table 4-2

Linear Sequenced Approach for LEO Spacecraft

Bus 400 Watt Bipolar Linear Power String

NO. OF LINEAR STRINGS		NO. OF LINEAR STAGES	I_L P_L = 400W	% RES. DIG.	TYPE OF DIGITAL SEGMENT	NO. OF DIGITAL STAGES	TOTAL STAGES
PRIME	RED						
1	1	12	2.0	1.04	$4B^2S$	78	90
2	1	18	4.0	2.1	$4B^2S$	72	90
3	1	24	6.0	3.1	$4B^2S$	68	92
4	1	30	8.0	4.2	$2B^2S$	60	90
5	1	36	10.0	5.2	$2B^2S$	56	92
6	1	42	12.0	6.2	$2B^2S$	56	98
7	1	48	14.0	7.3	$2B^2S$	52	100
8	1	54	16.0	8.3	S^2 OR $2B^2S$	48	102
9	1	60	18.0	9.4	S^2 OR $2B^2S$	48	108

Notes: $4B^25$ - 4 Bit Binary Count/Sequenced

$2B^25$ - 2 Bit Binary Count/Sequenced

S^2 - Series Sequenced

ORIGINAL PAGE IS
OF POOR QUALITY

Table 4-3

Linear Sequenced Approach for LEO Spacecraft Bus

200 Watt Bipolar Linear Power String

NO. OF LINEAR STRINGS PRIME	RED	NO. OF LINEAR STAGES	I_L (A) P_L = 200W	% RES. DIG.	TYPE OF DIGITAL SEGMENT	NO. OF DIGITAL STAGES	TOTAL STAGES
1	1	12	1.0	.52	$4B^2S$	96	108
2	1	18	2.0	1.04	$4B^2S$	78	96
3	1	24	3.0	1.6	$4B^2S$	74	98
4	1	30	4.0	2.1	$4B^2S$	72	102
5	1	36	5.0	2.6	$4B^2S$	68	104
6	1	42	6.0	3.1	$4B^2S$	68	110
7	1	48	7.0	3.6	$2B^2S$ OR $4B^2S$	68	116
8	1	54	8.0	4.2	$2B^2S$	60	114
9	1	60	9.0	4.1	$2B^2S$	56	116
10	1	66	10.0	5.2	$2B^2S$	56	122
11	1	72	11.0	5.7	$2B^2S$	56	128
12	1	78	12.0	6.2	$2B^2S$	56	134
14	1	84	14.0	7.3	$2B^2S$	52	136
16	1	90	16.0	8.3	S^2OR $2B^2S$	48	138
18	1	96	18.0	9.4	S^2OR $2B^2S$	48	144

ORIGINAL PAGE IS
OF POOR QUALITY

ORIGINAL PAGE IS
OF POOR QUALITY

Table 4-4

Linear Sequenced Approach for LEO Spacecraft Bus

100 Watt MOSFET Linear Power String

NO. OF LINEAR STRINGS		NO. OF LINEAR STAGES	I_L P_L = 100W	% RES. DIG.	TYPE OF DIGITAL SEGMENT	NO. OF DIGITAL STAGES	TOTAL STAGES
PRIME	RED						
1	1	12	0.5	.26	$4B^2S$	66	78
2	1	18	1.0	.52	$4B^2S$	38	56
3	1	24	1.5	.78	$4B^2S$	40	64
4	1	30	2.0	1.04	$2B^2S$	38	68
5	1	36	2.5	1.3	$2B^2S$	32	68
6	1	42	3.0	1.6	$2B^2S$	28	70
7	1	48	3.5	1.9	$2B^2S$	44	92
8	1	54	4.0	2.1	$2B^2S$	40	94
10	1	60	5.0	2.6	$2B^2S$	34	94
12	1	66	6.0	3.1	S^2	32	98
14	1	72	7.0	3.6	S^2	28	100
16	1	78	8.0	4.1	S^2	24	102
18	1	84	9.0	4.6	S^2	22	106
20	1	90	10.0	5.2	S^2	20	110
22	1	96	11.0	5.7	S^2	36	132
24	1	102	12.0	6.2	S^2	32	134
28	1	108	14.0	7.3	S^2	28	136
32	1	114	16.0	8.3	S^2	24	138
36	1	120	18.0	9.4	S^2	22	142

4.2.1 Redundancy Approaches

The failure modes of the solar switches in the SAS are either open or short. Dependent upon the sequencing configuration, switch redundancy against an open or short failure may be required. For the series sequenced or the linear/sequenced approach where shift registers are utilized, protection against an open failure is needed either by parallel redundant switches or by the inclusion of an extra array segment. Redundancy to protect against shorted switches in the above configurations is not required because each power bus is loaded with at least a minimum load which will be supplied by several array segments. The other sequencing approaches which are implemented by binary counters or demultiplexers will need quad redundancy (for the switches) against open or short failures. In a combinational arrangement such as the binary count/sequenced configuration, only the binary counter operated switches will require quad redundancy.

The control logic, the μP controllers and the associated sensor will require redundancy. There are three types of redundancy configurations to be considered and evaluated for possible candidates: the quad, the majority voting and the standby arrangements. Between the three approaches, the reliability, the complexity and the circuit parts count must be traded off to gain a fair comparison. The quad and majority voting arrangements yield a higher figure for probability of success than the standby one at the cost of higher parts count. The disadvantage of requiring a higher number of circuit components, however, can be minimized by the packaging concept of incorporating the majority of the discrete parts into hybrid units. The standby redundant configuration is less complex but it requires additional circuitry for failure detection and an autonomous transfer of operation to the standby channel.

4.2.2 Sequencing Approaches Conclusions

- The SASPM complexity is dependent on the required redundancy and the power handling capability of the switching devices.

- The optimum sequencing method is unique for each application and set of requirements.

- The MOSFET technology is more cost effective than bipolar for the LEO spacecraft bus.

- Good regulation ($\approx$5%) does not sacrifice cost for the LEO spacecraft bus application.

REFERENCES

4-1. "Interaction of Large, High Power Systems with Operational Orbit Charged Particle Environments", by C. K. Purvis, N. J. Stevens and F. D. Berkopec; NASA/LeRC TM-73867, dated October 1977.

4-2. "Sheath Effects Observed in a 10 Meter High Voltage Panel in Simulated Low Earth Orbit Plasma", by J. E. McCoy and A. Konradi; Spacecraft Charging Technology Conference - 1978 Proceedings NASA Conf. Pub. 2071, AFGL-TR-79-0082, November 1978.

4-3. "Investigation of High Voltage Spacecraft System Interactactions with Plasma Environments", by N. J. Stevens, F. D. Berkopec and C. K. Purvis; NASA/LeRC TM-78831, April 1978.

4-4. "Interaction of High Voltage Surfaces with the Space Plasma", by H. R. Kaufman and R. S. Robinson, NASA/LeRC CR-165131, dated May 1980.

4-5. "TDRSS Solar Array Arc Discharge Tests", by G. T. Inouye and J. M. Sellen, Jr.; Spacecraft Charging Technology Conference - 1978 Proceedings, NASA Conf. Pub. 2071, AFGL-TR-79-0082, November 1978.

4-6. "Beam Efflux Measurements", by G. K. Komatsu and J. M. Sellen, Jr.; NASA/LeRC CR-135038, 1976.

4-7. "Charge-Exchange Plasma Generated by an Ion Thruster", by H. R. Kaufman, NASA/LeRC CR-134844, dated June, 1975.

4-8. "SEPS Solar Array Interaction with an Ion Thruster Generated Charge Exchange Plasma", by H. R. Kauffman; SEPS-I-297 eport.

4-9. "Spacecraft-Generated Plasma Interaction with High Voltage Solar Array", by D. E. Parks and I. Katz, AIAA/DGLR 13th International Electric Propulsion Conference, April 1978.

5.0 TASK IV
COMPARISONS

TRW shall compare the definition and mission impacts obtained from Task III with the use of conventional power processing techniques for each mission. For each technique, TRW shall estimate the benefits or penalties (such as cost, performance, characteristics, electric propulsion payload improvement, electric propulsion trip time improvement, and flexibility) of SASPM over conventional techniques. TRW shall identify any new capability resulting from SASPM and examine its worth. The penalties of providing any improvement in voltage regulation (if needed) shall be quantified in terms of characteristics such as complexity, reliability, weight and cost, and shall be displayed on curves.

TRW shall examine the desirability of certain user loads having their own dedicated section of array isolated and separately managed from other user loads and estimate any penalty for providing this feature.

5.1 Study Costing Parameters

Shuttle transportation costs are derived assuming a dedicated launch with full capability utilized.

- Dedicated Launch - 30.2M$
- 29,484 Kg - $1024/Kg
- 65,000 Lb - $465/Lb

The costs for the solar arrays, and pumped fluid radiators was taken from reference 5-1.

- Cassegranian Concentrator Solar Array
  - Projected manufacturing cost - $30/watt
  - Projected mass - 45w/kg
- Planar Solar Array
  - Projected manufacturing cost - $46/watt
  - Projected mass - 200w/kg
- Pumped fluid radiator
  - Projected manufacturing cost - $33/watt
  - Projected mass - 12.4Kg/Kw
  - Heat exchangers - $40,000 each
  - Projected mass of heat x chargers - 10 kg each
  - Plumbing/engineering - $20,000/Heat exchanger
- Power Processors
  - Estimated manufacturing cost - $300/Part
  - Projected mass - based on projections from existing designs.

5.2 Conventional Processing Models

It has been determined that the fourth candidate of Section 3.6 (a linear shunt approach) is not viable for the high power systems being considered, because of excessive thermal dissipation requirements. This analysis will be limited to the other three candidates plus ion propulsion processing.

5.2.1 Ion Propulsion Conventional Power Processing

Ion engine power processing requirement is assumed to be the same, regardless of which power processing system is used for spacecraft power. Power processing for the ion engine was discussed in Section 3.6.1.

The power requirements for an 0.5 newton engine are listed below:

Screen: (860V)	17,200 watts
Discharge: (30V)	4,800 watts
Accelerator: (800V)	160 watts
Neutralizer keeper:(15V)	75 watts

Because of the long transmission distances required (> 300 feet) it is not cost effective to transmit power at low voltages such as 30 volts. This power will be drawn from the spacecraft bus. The high voltage power required by the screen will be drawn from a high voltage solar array.

The spacecraft bus will be required to supply the following power to the ion engine:

Discharge power	4800 watts
Discharge processor losses = .11 (4800)	533 watts
Accelerator power	160 watts
Accelerator processor losses = .15 (160)	24 watts
Neutralizer keeper power	75 watts
Neutralizer keeper losses = .4 (75)	30 watts
TOTAL =	5622 watts

5.2.1.1 High Voltage Array Requirement

$$\text{Solar Array Requirement} = \frac{P_I}{(E_p)(\eta_2)(d)}$$

P_I = Ion engine high voltage power (0.5 newton argon engine) = 17,200 watts

E_p = Power processor efficiency = 0.95

η_2 = Wiring and cabling efficiency = 0.99

d = Solar array degradation factor = 0.8

The beginning of life array requirement is:

$$\text{S/A Requirement} = \frac{17{,}200 \text{ watts}}{(.95)(.99)(0.8)}$$

$$= \underline{\underline{22{,}860}} \text{ watts}$$

The end of life array requirement is:

$$(22{,}860)(.8) = \underline{\underline{18{,}288}} \text{ watts}$$

This array sizing assumes sunlight only operation of ion engines.

5.2.1.2 Power Processing Mass Estimates

The mass of the screen/accelerator power processor is estimated from the following formula: (Reference 2-24)

$$\text{Mass (kg)} \simeq 0.8\, P_B^{3/4} + 0.6\, P_B^{1/2} + 0.06\, P_B + 2.2$$

Where P_B = beam power in KW (17.2)

$$\text{Mass} \sim 0.8\ (8.44) + 0.6\ (4.15) + 0.06\ (17.2) + 2.2$$
$$\simeq 12.47\text{kg or } 27.4\ \text{lb}$$

The mass of the discharge power processor is estimated to be:

$$\text{Mass, kg} \simeq 1.1\, P_D^{3/4} + P_D^{1/2} + 0.06\, P_D + 1.4$$

Where P_D = discharge power in KW (4.8)

$$\text{Mass} = (1.1)\ (3.24) + 2.19 + 0.06\ (4.8) + 1.4$$
$$= 7.44\text{kg or } 16.4\ \text{lb}$$

The mass of the neutralizer keeper is estimated to be 0.7 kg and the mass of the thrust system controller is estimated to be 4.0 kg. The total power processing mass for an 0.5 newton thruster is estimated to be 24.6 kg (54.1 lb).

5.3 LEO Platform

The LEO Platform requirements are described in Section 2.1.

5.3.1 Transformer Coupled Converter (TCC) System

The LEO Mission TCC sizing model is shown in Figure 5.3-1

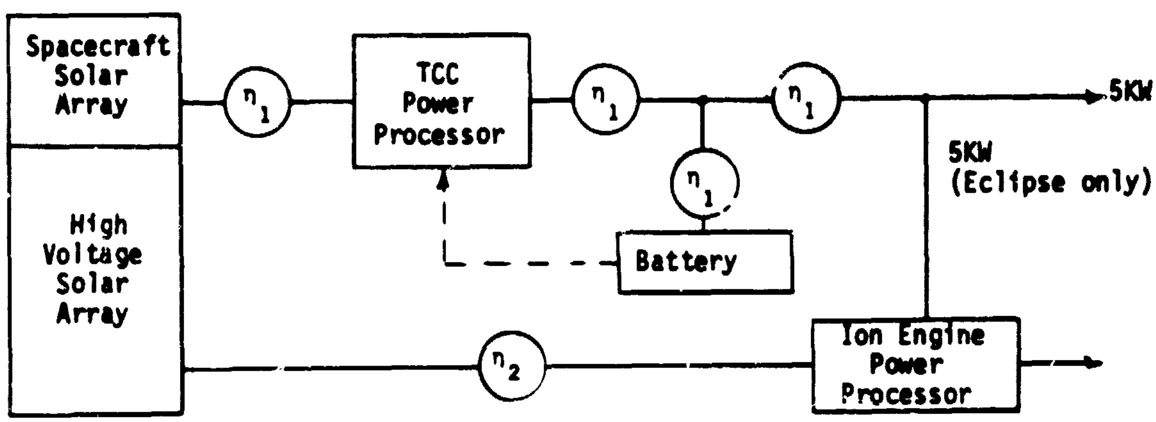

Figure 5.3-1 LEO Mission TCC Sizing Model

ORIGINAL PAGE IS OF POOR QUALITY

$$\text{Solar array output power} = \frac{P_L + P_H + P_C}{(n_1)^3\ (d)(\varepsilon_T)} + \frac{P_I}{n_2\ (d)\ (\varepsilon_p)} \qquad (5.3\text{-}1)$$

P_L = Load Power

P_H = Housekeeping power + low voltage ion engine power

P_C = Battery charging power

P_I = Ion propulsion high voltage power

n_1 = Wiring and connector efficiency (99.5%)

n_2 = Wiring and connector efficiency (99%)

d = Solar array end of life efficiency (80%)

ε_T = TCC efficiency (95%)

ε_p = High voltage processor efficiency

5.3.1.1 Power Generation - Solar Array Sizing

From equation(5.3-1)we have, with

P_L = 250,000 watts

P_H = 30,622 watts

P_C = 236,400 watts (Section 2.1.2.4)

P_I = 17,200 watts

n_2 = 0.99

n_1 = 0.995

d = 0.8

ε_T = 0.95

$$\text{Array Power (BOL)} = \frac{250{,}000w+30{,}622w+236{,}400w}{(.995)(.995)(0.995)(0.8)(.95)} + \frac{17{,}200w}{(0.99)(.8)(.95)}$$

$$= 690{,}600 + 22{,}860w$$

$$= \underline{\underline{713{,}460 \text{ watts}}}$$

5.3.1.2 TCC Projected Design Parameters

5.3.1.2.1 Assumptions

- The parts count associated with the circuit reflects a non-redundant configuration.
- The weight estimate was derived based on TRW designs extrapolated to the 1990's. plus a reduction factor assuming a switching frequency between 20 and 30 KHz.
- Each power stage is fused to protect against internal TCC faults.
- Overload and overvoltage protection has not been implemented.
- Conversion efficiency of 95% is based on projected improvements in existing designs.

5.3.1.2.2 Projected Parameters

- Size: Each of the 11 TCC power processors will occupy approximately 0.085 M^3 (3 FT^3) and will contain four power stages.
- Mass: Each of the 11 TCC power processors has a mass of approximately 75 Kg (165 lb). The ion propulsion high voltage power processor is estimated to be 12.5 Kg (27.5 lb).
- Efficiency of TCC: 95%
- Efficiency of high voltage power processor: 95%
- Parts count: 1326 parts for each of the TCC powerprocessors including parts for current, voltage, and temperature sensing. (Represents 4 power stages per channel).
- The parts count for ion propulsion power processing is estimated to be 567, representing 2 high voltage power stages plus 17 parts for sensing circuits. The parts count for the low voltage supplies were not included here or in the SASPM System because they are identical.
- The total mass of the power processing system is 839 Kg, and the total parts count is 15,153.

5.3.1.2.3 Power Processing Cost

Manufacturing cost = ($300/part) (15,153 parts) = $4,545,900

Transportation cost = ($1024/Kg) (839 Kg) = $ 359,136

5.3.1.2.4 Cooling System Parameters

TCC output requirements:

Payload power =	$250{,}000w/(\eta_1)^2$	= 252,519w
Housekeeping power =	$25{,}000w/(\eta_1)^2$	= 25,252w
Low voltage ion engine power =	$5{,}622w/(\eta_1)^2$	= 5,679w
Battery charging power =	$236{,}400w/(\kappa_1)^2$	= 238,782w
	TOTAL	= 522,232w

Losses in TCC = $522{,}232w \left(\frac{1 - .95}{.95}\right)$

= 27,486 watts

Losses in high voltage power processor

= $17{,}200w \left(\frac{1 - .95}{.95}\right)$

= 905 watts

The radiator mass required to dissipate this heat is:

(12.4 Kg/Kw) (28.391 Kw) = 352 Kg

Mass of heat exchangers = (12) (10 Kg) = 120 Kg

Δ radiator cost:

Manufacturing cost =	(\$33/watt)(28,391 watts)	= \$936,903
Transportation cost =	(\$1024/Kg) (472 Kg)	= \$483,328
Heat exchangers =	(12) (\$40,000)	= \$480,000
Plumbing/engineering =	(12) (\$20,000)	= \$240,000

5.3.2 Boost Regulator System

The LEO Platform sizing model utilizing the buck regulator is the same as the model shown in Figure 5-1, except that the boost regulator is projected to have a conversion efficiency of 95.5%.

5.3.2.1 Power Generation - Solar Array Sizing

From equation 5.2-1 we have

$$\text{Array Power (BOL)} = \frac{250{,}000w + 30{,}622w + 236{,}400w}{(.995)\,(.995)\,(.995)\,(.8)\,(.955)} + \frac{17{,}200w}{(.99)(.8)(.95)}$$

$$= 686{,}984\ w + 22{,}860w$$

$$= \underline{\underline{709{,}844\ \text{watts}}}$$

5.3.2.2 Boost Regulator Projected Design Parameters

5.3.2.2.1 Assumptions

The assumptions are identical to the assumptions for the TCC (section 5.2.1.2) except that the projected efficiency is 95.5%.

5.3.2.2.2 **Projected Parameters**

- **Size:** Each of the 11 boost regulators will occupy approximately 0.08 M^3 (2.5 Ft^3)
- **Mass:** The boost regulators have a mass of approximately 54.5kg each (120 lbs.)

  The mass of the ion propulsion power processor is 12.5kg (27.5 lbs.)
- Efficiency of boost regulator: 95.5%
- Efficiency of high voltage power processor: 95%
- Parts count: 926 parts for each of the boost regulators, including current, voltage, and temperature sensing.

  The parts count for high voltage power processing for the ion engine is 567.
- The total mass of the power processing system is 612 kg, and the total parts count is 10,753.

5.3.2.2.3 Power Processing Cost

Manufacturing cost = ($300/part)(10,753 parts) = $3,225,900

Transportation cost = (612 Kg)($1024/kg) = $626,688

5.3.2.2.4 Cooling System Parameters

The 95.5% efficiency of the boost regulator results in 24,608 watts lost in heat, and there is a 905 watt loss in the ion propulsion high voltage power processor. The radiator mass required to dissipate this heat is

(12.4 kg/Kw)(25.513Kw) = 316 Kg

Mass of heat exchangers = (12)(10Kg) = 120 Kg

Δ Radiator cost:

Manufacturing cost = ($33/watt)(25,513 watts) = $841,929

Transportation cost = (436Kg)($1024/Kg) = $446,464

Heat exchangers = (12) ($40,000) = $480,000

Plumbing/engineering = (12) ($20,000) = $240,000

ORIGINAL PAGE IS
OF POOR QUALITY

5.3.3 Buck Regulator System

The LEO Platform sizing model utilizing the buck regulator is the same as the model shown in Figure 5.3-1, except that the boost regulator is projected to have a conversion efficiency of 96.5%.

5.3.3.1 Power Generator - Solar Array Sizing

From equation (5.3-1) we have

$$\text{Array Power (BOL)} = \frac{250{,}000w+30{,}622w+236{,}400w}{(.995)(.995)(.995)(.8)(.965)} + \frac{17{,}200}{(.99)(.8)(.95)}$$
$$= 679{,}865w + 22{,}860w$$
$$= \underline{\underline{702{,}725 \text{ watts}}}$$

5.3.3.2 Buck Regulator Projected Design Parameters

5.3.3.2.1 Assumptions

The assumptions are identical to the assumptions for the TCC (section 5.3.1.2.1) except that the projected efficiency is 96.5%.

5.3.3.2.2 Projected Parameters

- Size: Each of the 11 buck regulators will occupy approximately $0.08M^3$ ($2.5\ Ft^3$).
- Mass: The buck regulators have a mass of approximately 59 Kg (130 lb.) The mass of the ion propulsion power processor is 12.5Kg (27.5 lb.)
- Efficiency of buck regulator: 96.5%
- Efficiency of high voltage power processor: 95%
- Parts count: 966 parts for each of the buck regulators, including current, voltage, and temperature sensing.
  The parts count for high voltage power processing for the ion engine is 567.
- The total mass of the power processing system is 662Kg, and the total parts count is 11,193.

5.3.3.2.3 Power Processing Cost

Manufacturing cost	= ($300/part) (11,193 parts)	= $3,357,900
Transportation cost	= (662 Kg) ($1024/Kg)	= $ 677,888

5.3.3.2.4 Cooling System Parameters

The 96.5% efficiency of the buck regulator results in 18,991 watts lost in heat, and there is a 905 watt loss in the ion propulsion high voltage power processor. The radiator mass required to dissipate this heat is

ORIGINAL PAGE IS
OF POOR QUALITY

(12.4Kg/KW) (19.846kw) = 246Kg

Mass of Heat exchangers = (12) (10Kg) = 120 kg

ΔRadiator Cost:

Manufacturing	= ($33/watt) (19,846 watts)	= $654,918
Transportation	= (366 kg) ($1024/kg)	= $314,784
Heat exchangers	= (12) ($40,000)	= $480,000
Plumbing/engineering	= (12) ($20,000)	= $240,000

Table 5-1

LEO Platform Sizing Summary

	TCC	Boost Regulator	Buck Regulator
Mass of processors, Kg	838	612	662
Mass of solar array, Kg	15,832	15,774	15,616
Mass of radiator (power processing), Kg	472	436	366
Cost of processors, M$	4.55	3.23	3.36
Cost of solar array, M$	21.40	21.30	21.08
Cost of radiator (power processing), M$	1.66	1.56	1.37
Cost of transportation, M$	17.55	17.35	17.04
Parts count, electrical	15,193	10,753	11,193
Total mass =	17,142kg	16,822kg	16,664kg
Total cost =	45.2M$	43.4M$	42.9M$

5.3.4 LEO Platform Sizing Conclusion

The buck regulator system is the optimum conventional power system for the LEO platform.

ORIGINAL PAGE IS
OF POOR QUALITY

5.4 GEO Platform

The GEO Platform requirements are described in Section 2.2.

5.4.1 Transformer Coupled Converter (TCC) System

The GEO Mission has two power system configurations; one when orbit transfer or orbit maneuvering is taking place and one when payloads are being supplied the bulk of the power. The TCC system sizing model is shown in Figure 5.4-1.

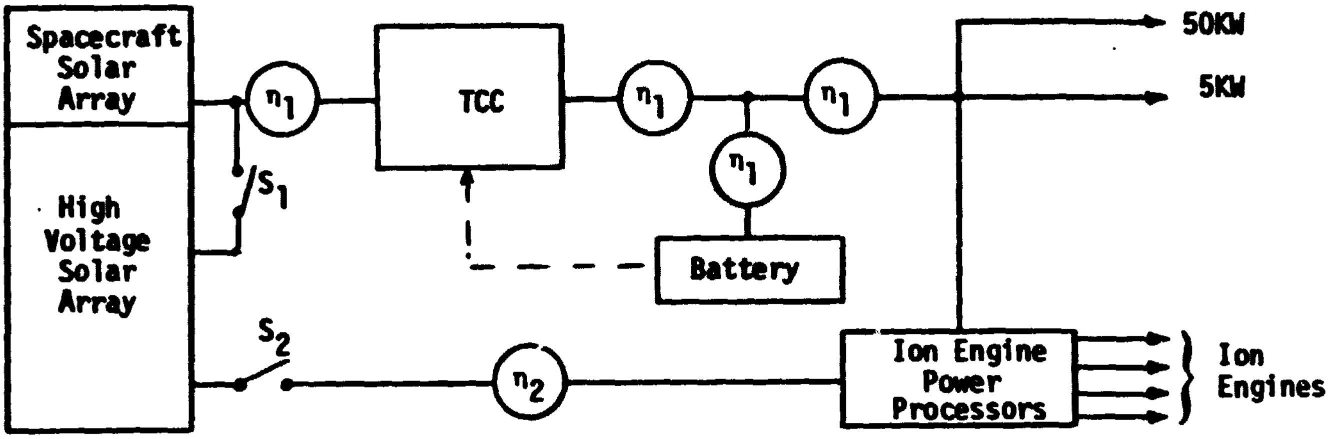

Figure 5.4-1 GEO Mission TCC Sizing Model

$$\text{Solar Array output power} = \frac{P_L+P_H+P_C}{(\eta_1)^3(d_1)(d_2)(\xi_T)} \qquad (5.4\text{-}1)$$

P_L = Load Power

P_H = Housekeeping power

P_C = Battery charging power

$\eta 1$ = Wiring and connector efficiency (99.5%)

$\eta 2$ = Wiring and connector efficiency (99%)

d_1 = Solar array end of life efficiency (on orbit degradation)

d_2 = Solar array degradation factor (Van Allen transition)

ξ_T = TCC efficiency (95%)

The on orbit case, where payloads are being supplied, sizes the solar array requirement.

5.4.1.1 Power Generation - Solar Array Sizing

The beginning of life solar array requirements account for two degradation factors. The first accounts for the degradation through the Van Allen region and the second accounts for ten years in GEO. The factors are 25% and 15% respectively.

From equation (5.4-1) we have

P_L = 50,000 watts

ORIGINAL PAGE IS OF POOR QUALITY

P_H = 5,000 watts

P_C = 4,186 watts (Section 2.2.2.4.1)

η_1 = .995

d_1 = .85

d_2 = .75

ξ_1 = .95

$$\text{Array Power} = \frac{50{,}000w + 5{,}000w + 4{,}186w}{(.995)^3(.85)(.75)(.95)}$$

$$= \underline{\underline{99{,}208 \text{ watts}}}$$

5.4.1.2 Ion Engine Power Analysis

The solar array power available to the ion engines is assumed to be the BOL capability minus the 25% loss in the Van Allen region, and less the 5kw housekeeping array requirement.

$$99{,}208 \text{ watts } (.75) - \frac{5{,}000 \text{ watts}}{(.95)(.995)^3}$$

$$\underline{74{,}406w} - 5{,}343 \text{ watts} = 69{,}063 \text{ watts}$$

accounting for line losses

$$(69{,}063 \text{ watts})\ (.99) = \underline{68{,}372 \text{ watts}}$$

The solar array size required for 0.5 newton thrust is 18,288 watts for high voltage (Section 5.2.1).

The ion engine also requires 5,622 watts (plus distribution losses) at a lower voltage.

$$18{,}288 + \frac{5622}{(\eta_1)^3(.95)} = \underline{24{,}296 \text{ watts}}$$

Scaling this to the available solar array power

$$\frac{\underline{68{,}372 \text{ watts}}}{24{,}296 \text{ watts}} \ (0.5 \text{ Newton})$$

results in a thrust capability of 1.407 Newtons

5.4.1.3 TCC Projected Design Parameters

5.4.1.3.1 Assumptions

The assumptions are identical to those stated in section 5.3.1.2.1.

5.4.1.3.2 Projected Parameters

- Size: Each of the four TCC power processors will occupy approximately $0.028M^3$ (1 Ft^3) and will consist of one power stage.
- Mass: Each of the four TCC power processors has a mass of approximately 23kg (50.5 lb.). The three power processors for ion engine control have an estimated total mass of 37 kg (81.4 lb.).
- Efficiency of TCC: 95%
- Efficiency of high voltage power processor: 95%
- Parts count: 563 parts for each of the TCC power processors, including parts count for current, voltage, and temperature sensing. The parts count for each of the three high voltage power processors is estimated to be 584.
- The total mass of the power processing system is 129kg and the total parts count is 4004.

5.4.1.3.3 Power Processing Cost:

Manufacturing:	(\$300/part) (4004 parts)	= \$1,201,200
Transportation:	(\$1024/kg) (129kg)	= \$ 132,096

5.4.1.3.4 Cooling System Parameters

The power system has two modes, the on orbit payload mode, and the ion engine operating mode. First the on orbit payload mode will be analyzed.

TCC requirements: Payload: $50kw/(\eta_1)^2$ = 50,504 watts

Housekeeping: $5kw/(\eta_1)^2$ = 5,050 watts

Battery charging: $4.228kw/(\eta_1)^2$ = 4,228 watts

Total 59,782 watts

Losses in TCC = 59,872 $\left(\frac{1-.95}{.95}\right)$ = 3146 watts

The initial transition to GEO will require cooling for the ion engine power processors as well as for housekeeping and battery charging power processing.

Ion engine power requirements

68,372w $\left(\frac{1-.95}{.95}\right)$ = 3599 watts

TCC regulator requirements

Housekeeping	5,050 watts
Battery charging	4,228 watts
total	9,278 watts
Losses = 9,278 $\left(\frac{1-.95}{.95}\right)$ =	488 watts
Total radiator requirement =	4,087 watts

Since this requirement is greater than the on orbit payload case, the radiator will be sized to meet this requirement.

Δ Radiator mass = (12.4Kg/Kw) (4.087Kw) = 50.7 Kg

Mass of heat exchangers = 7 (10Kg) = 70 Kg

Δ Radiator Cost:

Manufacturing	= ($33/watt) (4087 watts)	= $139,841
Transportation	= ($1024/kg)(120.7 Kg)	= $123,597
Heat exchangers	= 7 ($40,000)	= $280,000
Plumbing/engineering	= 7 ($20,000)	= $140,000

5.4.2 Boost Regulator System

The GEO Platform sizing model utilizing the boost regulator is the same as the model shown in Figure 5.4-1, except that the boost regulator is substituted for the TCC, and the boost regulator is projected to have a conversion efficiency of 95.5%.

5.4.2.1 Power Generation - Solar Array Sizing

From equation (5.4-1) we have:

$$\text{Array Power} = \frac{50{,}000w+5{,}000w+4{,}186w}{(.995)^3(.85)(.75)(.955)}$$

$$= \underline{98{,}688 \text{ watts}}$$

5.4.2.2 Ion Engine Power Analysis

Power available to ion engines

98,688 watts (.75) - 5343 watts = 68,673 watts

Accounting for line losses

68,673 watts (.99) = 67,986 watts

Thrust capability:

$$\frac{67{,}986 \text{ watts}}{24{,}296 \text{ watts}} (.5 \text{ Newton}) = \underline{1.399 \text{ Newtons}}$$

5.4.2.3 Boost Regulator Projected Design Parameters

5.4.2.3.1 Assumptions

The assumptions are identical to those stated in Section 5.3.1.2.

5.4.2.3.2 Projected Parameters

- Size: Each of the four boost regulators will occupy approximately $0.022M^3$ ($.75 Ft^3$) and will consist of one power stage.
- Mass: Each of the four boost regulators have a mass of approximately 17kg (37.9 lb). The three power processors for ion engine control have an estimated total mass of 37 kg (81.4 lb.)
- Efficiency of boost regulator: 95.5%
- Efficiency of high voltage power processors: 95%
- Parts count: 440 parts for each of the boost regulators, including parts count for current, voltage, and temperature sensing. The parts count for each of the three high voltage power processors is estimated to be 584.

The total mass of the power processing system is 105kg and the total parts count is 3412.

5.4.2.3.3 Power Processing Cost

Manufacturing cost = ($300/part) (3412 parts) = $1,023,600

Transportation cost - (105kg) ($1024/kg) = 107,520

5.4.2.3.4 Cooling System Parameters

Ion engine processor requirements

$67{,}986 \text{ watts } \left(\frac{1-.955}{.955}\right) = 3{,}578 \text{ watts}$

Boost regulator requirements

Housekeeping	5,050 watts
Battery Charging	4,228 watts
Total	9,278 watts

$\text{Losses} = (9{,}278 \text{ watts})\left(\frac{1-.955}{.955}\right) = 437 \text{ watts}$

Total radiation requirement = 4,015 watts

The radiator mass required to dissipate this heat is

(12.4Kg/Kw)(4.015 Kw) = 49.8 Kg

Mass of heat exchangers = 7 (10 Kg) = 70 Kg

Δ Radiator Cost:

Manufacturing cost	= ($33/watt)(4,015 watts)	= $132,495
Transportation cost	= ($1,024/Kg)(119.8Kg)	= $125,675
Heat exchangers	= 7 ($40,000)	= $280,000
Plumbing/engineering	= 7 ($20,000)	= $140,000

5.4.3 Buck Regulator System

The GEO Platform sizing model utilizing the buck regulator is the same as the model shown in Figure (5.4-1), except that the buck regulator is substituted for the TCC, and the buck regulator is projected to have a conversion efficiency of 96.5%.

5.4.3.1 Power Generation - Solar Array Sizing

Utilizing equation 5.4-1:

$$\text{Array power} = \frac{50{,}000w+5{,}000w+4{,}186w}{(.995)^3\ (.85)(.75)\ (.965)}$$

$$= 97{,}666 \text{ watts}$$

5.4.3.2 Ion Engine Power Analysis

Power available to ion engines:

(97,666 watts) (.75) - 5,343 watts = 67,907 watts

Accounting for line losses

(67,907w) (.99) = 67,228 watts

Thrust capability:

$$\frac{67{,}228 \text{ watts}}{24{,}296 \text{ watts}} (.5 \text{ Newton}) = 1.384 \text{ Newtons}$$

5.4.3.3 Buck Regulator Projected Design Parameters

5.4.3.3.1 Assumptions

The assumptions are identical to those stated in Section 5.3.1.2.

5.4.3.3.2 Projected Parameters

- Size: Each of the four buck regulators will occupy approximately $0.023M^3$ ($.08\ Ft^3$), and will consist of one power stage.
- Mass: Each of the four buck regulators has a mass of approximately 18Kg (39.8 lb). The three power processors for ion engine control have an estimated total mass of 37 Kg (81.4 lb).
- Efficiency of buck regulator: 96.5%
- Efficiency of high voltage power processors: 95%
- Parts count: 453 parts for each of the buck regulators, including parts count for current, voltage, and temperature sensing. The parts count for each of the three high voltage power processors is estimated to be 584.
- The total mass of the power processing system is 109kg and the total parts count is 3564.

5.4.3.3.3 Power Processing Cost

Manufacturing cost	= (\$300/part)(3564 parts)	= \$1,069,200
Transportation cost	= (109Kg) (\$1024/Kg)	= \$ 111,616

5.4.3.3.4 Cooling System Parameters

Ion engine processor requirements

$$67{,}228 \text{ watts } \left(\frac{1-.95}{.95}\right) = 3{,}538 \text{ watts}$$

Buck regulator requirements:

Housekeeping	5,050 watts
Battery charging	4,228 watts
Total	9,278 watts

$$\text{Losses} = 9{,}278 \text{ watts } \left(\frac{1-.965}{.965}\right) = 367 \text{ watts}$$

Total radiator requirement = 3905 watts

This requirement will drive the radiator size. The radiator mass required to dissipate this heat is

(12.4Kg/Kw)(3.905 Kw) = 48.4 Kg

Mass of heat exchangers - / (10Kg) = 70 Kg

Δ radiator cost:

Manufacturing cost	= $33/watt) (3905 watts)	= $128,865
Transportation cost	= (118.4kg) ($1024/Kg)	= $121,242
Heat exchangers	= 7 ($40,000)	= $280,000
Plumbing/engineering	= 7 ($20,000)	= $140,000

Table 5-2: GEO Mission Sizing Summary

	TCC	Boost Regulator	Buck Regulator
Mass of processors, Kg	129	105	109
Mass of solar array, Kg	496	493	488
Mass of radiator (power processing) Kg	121	120	118
Cost of processors, M$	1.20	1.02	1.07
Cost of solar array, M$	4.56	4.54	4.49
Cost of radiator (power processing) M$	0.52	0.51	0.67
Cost of transportation, M$	0.76	0.74	0.73
Parts count, electrical	4004	3412	3564
Total mass =	746 Kg	718 Kg	715 Kg
Total cost =	7.0 M$	6.8 M$	6.7 M$

The buck regulator system is the optimum conventional power system for the GEO platform.

5.5 Ion Propulsion Orbit Transfer Vehicle (IPOTV)

The IPOTV requirements are described in Section 2.3.

5.5.1 Buck Regulator System

Because of the similarity in design to the LEO Platform, the buck regulator system is assumed to be optimum, and will be the only conventional system analyzed. The IPOTV Mission sizing model is shown in Figure 5.5-1.

ORIGINAL PAGE IS
OF POOR QUALITY

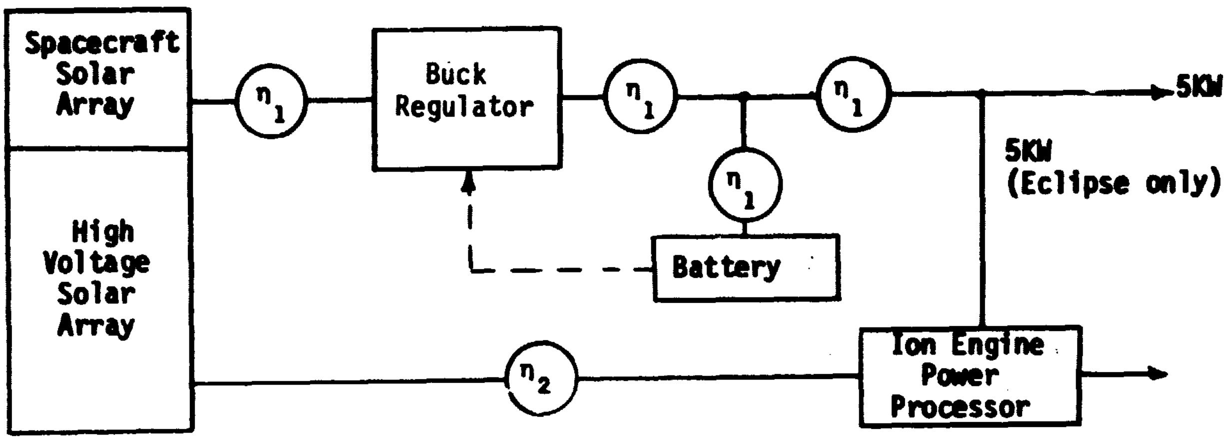

Figure 5.5-1 IPOTV Mission Sizing Model

$$\text{Low voltage solar array output power} = \frac{P_H + P_C}{(\eta_1)^3(d)(\xi_B)} \tag{5.5-1}$$

P_H = Housekeeping power

P_C = Battery charging power

η_1 = Wiring and connector efficiency (99.5%)

d = Solar array end of life efficiency (22%)

ξ_B = Buck regulator efficiency (96.5%)

5.5.1.1 Power Generation - Solar Array Sizing

The concept of the IPOTV power system is to start with a 250 KW array and use it until it degrades to 55 KW before replacing it.

From equation (5.5-1) we have

P_H = 5,000 watts

P_C = 8,568 watts (Section 2.3.2.3)

η_1 = .995

$d = \dfrac{55\ \text{KW}}{250\ \text{KW}} = .22$

ξ_B = .965

$$\text{Low voltage array power (BOL)} = \frac{5{,}000w+8{,}568w}{(.995)^3(.22)(.965)}$$

ORIGINAL PAGE IS OF POOR QUALITY

$$= \underline{\underline{64{,}878 \text{ watts}}}$$

High voltage solar array:

Total array output at BOL = 250 KW

High voltage array = 250,000 w - 64,878 w

= 185,122 watts

Each 0.5 newton ion engine requires 24,296 watts of array power (Section 5.4.1.2)

$$\text{Projected initial thrust capability} = \frac{185{,}122w}{24{,}296w} \text{ (0.5 Newton)}$$

$$= \underline{\underline{3.810 \text{ Newtons}}}$$

5.5.1.2 Buck Regulator Projected Design Parameters

5.5.1.2.1 Assumptions

The assumptions are identical to the assumptions for the TCC (Section 5.2.1.2) except that the projected efficiency is 96.5%.

5.5.1.2.2 Projected Parameters

- Size: Each of the three buck regulators will occupy approximately $0.01M^3$ ($.31 \; Ft^3$) and will consist of one power stage.
- Mass: The buck regulators have a mass of approximately 14.8 Kg (36.6 Lbs) each. The mass of the ion propulsion power processors is estimated to be 95 Kg (209 lb).
- Efficiency of buck regulator: 96.5%
- Efficiency of high voltage power processor: 95%
- Parts count: 522 parts for each of the buck regulators, including current, voltage and temperature sensing, The parts count for the high voltage power processing is estimated to be 4321.
- The total mass of the power processing system is 139 Kg and the total parts count is 5887.

5.5.1.2.3 <u>Power Processing Cost</u>

Manufacturing cost	= (\$300/part) (5887 parts)	= \$1,766,100
Transportation cost	= (\$1024/kg) (139 kg)	= \$ 146,336

5.5.1.2.4 <u>Cooling System Parameters</u>

Buck regulator output requirements.

- Housekeeping 5000 watts/η_1^2 = 5,050 watts
- Battery charging 8568 watts/η_1^2 = 8,654 watts

Total =13,704 watts

Buck regulator losses:

$$13{,}704\ \left(\frac{1-.965}{.965}\right) = 497 \text{ watts}$$

High voltage power processor losses

$$185{,}122\text{w}\ \left(\frac{1-.95}{.95}\right) = 9743 \text{ watts}$$

The radiator mass required to dissipate this heat is

(12.4 Kg/Kw) (10.24 KW) = <u>127 Kg</u>

Mass of heat exchangers (assuming 5 ion engines)

8 (10 Kg) = 80 Kg

Δ radiator cost:

Manufacturing	= (\$33/watt)(10,240 watts)	= \$337,920
Transportation	= (\$1024/Kg)(207 Kg)	= \$211,968
Heat exchangers	= 8 (\$40,000)	= \$320,000
Plumbing/engineering	= 8 (\$20,000)	= \$160,000

Table 5-3: IPOTV Mission Sizing Summary

Mass of processors, Kg	139
Mass of solar array, Kg	1250
Mass of radiator (power processing), Kg	207
Cost of processors, M\$	1.8
Cost of solar array, M\$	11.5
Cost of radiator (power processing), M\$	0.8
Cost of transportation, M\$	0.3
Parts count, electrical	5887
Total mass =	1596
Total cost =	14.1 M\$

5.6 SASPM/Conventional System Comparison Summary

Since the buck regulator was the best of the three conventional systems analyzed, a comparison of the buck regulator system and SASPM will be made.

The comparison parameters for the three missions are listed in Tables 5-4, 5-5 and 5-6. The efficiency of the buck regulator is 96.5% and the solar array switching unit is 98.6% efficient.

TABLE 5-4 LEO MISSION SIZING COMPARISON

	Buck Regulator	SASU	Delta	%
• Mass of Processors, Kg	662	241	421	(64%)
Parts Count (Electrical)	11,193	6,898	4,295	(38%)
Cost @ $300/Part, M$	4.0	2.3	1.7	(43%)
• Solar Array Requirement, watts	702,725	687,427	15,302	(2%)
Area, square meters	4,685	4,583	102	(2%)
Mass, Kg	15,616	15,276	340	(2%)
*Cost (incl. transportation) M$	37.2	36.4	0.8	(2%)
• ** Active Radiator Requirement, watts	19,846	None	19,846	-
Area, square meters	44	--	44	-
Mass, Kg (incl. heat exchanger)	366	--	366	-
Cost (incl. transportation)M$	1.7	--	1.7	-
• Total Mass, Kg	16,664	15,517	1147	6.8%
• Total Cost, M$	42.9	38.7	4.2	9.8%

* This cost is based on projected 1990's cost which is more than an order of magnitude lower than today's cost.

** Every effort is made to use existing structure for a passive radiator, however, there may be a requirement for a small amount of added mass for passive thermal control.

TABLE 5-5 GEO MISSION SIZING COMPARISON

Power Processor	Buck Regulator	SASPM	Delta	%
• Mass of Processors, Kg	109	91	18	(17%)
Parts Count (Electrical)	3,564	2,508	1,056	(30%)
Cost @$300/Part, M$ + Transportation	1.2	0.9	0.3	(25%)
• Solar Array Requirement, watts	97,666	95,588	2,078	(2%)
Area, square meters	723	708	15	(2%)
Mass, Kg	488	478	10	(2%)
*Cost, incl transportation, M$	5.0	4.9	0.1	(2%)
• Active Radiator Requirement, watts	3,905	None	3,905	-
Area, square meters	8.6	-	8.6	-
Mass, Kg (incl. heat exchangers)	118	-	118	-
Cost (incl. transporation) M$	0.7	-	0.7	
• Total Mass, Kg	715	569	146	(20%)
• Total Cost, M$	6.9	5.8	1.1	(16%)

* This cost is based on projected 1990's cost which is more than an order of magnitude lower than today's cost.

TABLE 5-6 IPOTV MISSION SIZING SUMMARY

Power Processor	Buck Regulator	SASU	Delta	%
• Mass of Processors, Kg	116	69	47	(41%)
Parts Count (Electrical)	5,887	1,938	3,949	(67%)
Cost @ $300/Part, M$ + Transportation	1.9	0.6	1.3	(67%)
*• Solar Array Requirement, Kw	250	250	0	--
Area, Square Meters	1,852	1,852	0	--
Mass, Kg	1,250	1,250	0	--
Cost, incl. transportation, M$	12.8	12.8	0	--
• Active Radiator Requirement, watts	10,240	None	10,240	--
Area, square meters	23	--	23	--
Mass, Kg	207	--	207	--
Cost, incl. transporation, M$	1.0	--	1.0	--
• Ion Engine Initial Thrust Capability, N	3.810	5.019	1.209	(32%)
• Trip Time - First Round Trip LEO to GEO and back, days	399	312	87	(22%)
• Total Mass, Kg	1,573	1,319	254	(16%)
• Total Cost, M$	15.7	13.4	2.3	(15%)

* Solar array beginning of life capability is fixed at 250 Kw by design.

5.7 Dedicated Array Sections

For a large utility type spacecraft, no advantage was found for dedicating array sections for individual loads. However, there are no unusual penalties associated with this concept. There is reduced flexibility, and increased complexity across the rotary joint.

5.8 Conclusions

Benefits were obtained in all objectives:

- Projected reduction in the cost of power processing: 25% - 67%
- Projected reduction in the mass of power processing equipment: 17% - 64%
- Cost and mass of the solar array was reduced 2% for the LEO and GEO missions. At today's cost, this range of savings would be 2 - 16 M$. (Projected 1990s: 0.1 - 1M$) *
- Projected reduction in the mass of the total spacecraft active radiator: 6 - 12%. (Eliminate active radiator for power processing)
- Projected reduction in the cost of the total spacecraft active radiator is 10% - 20%.
- SASPM has inherent "redundancy" in the number of switches used to control small parts of the array. A failure results in a reduction of the maximium power available. A failure in a series regulator could be catastrophic forcing redundancy which would increase mass and cost.
- The SASPM concept lends itself to solar array reconfiguration for various series/parallel combinations of array strings.
- It was determined that for the missions analyzed, SASPM supplied adequate voltage regulation and there was no need to provide a means of tighter control.

5.8.1 Areas of Concern:

- High voltage operation in the space plasma environment is a major concern.
- Operation through Van Allen belt region dictates radiation resistant cell.

* Based on $30/watt, 1981 dollars. This is optimistic, and may not be achievable. Todays costs are around 700-800 dollars/watt.

References

5-1. "Space Power Distribution System Technology Study", NAS8-33198, Phase I Oral Review dated 8 December 1980. (TRW)

6.0 Task V

TECHNOLOGY RECOMMENDATIONS

Technology advancements required to implement SASPM will be identified. Approximate development costs and schedule estimates will be provided for those advancements that require additional technology support.

A major goal in the SASPM design effort was to utilize existing space qualified components wherever possible and to identify required technology advances for components which are unique to the high voltage and power application of the SASPM and not readily available. The category of components which necessitate future technology advances is discussed below.

6.1 Power FET Devices

The advantage of utilizing MOSFET power devices over bipolar ones for the solar array switches to achieve a significant reduction in parts count is evident from the previously conducted parametric trade study which was covered in Section 3. However, the high voltage MOSFET power devices are not space qualified and exhibit an unacceptably high on-state resistance (0.3 ohms) that causes high solar array switch dissipation.

One solution to this problem within the present technology is to parallel several well-matched MOSFETs within a hybrid package to reduce the on resistance to a value comparable to that of the bipolar devices. As an example, in the baseline design, four MOSFETs were paralleled to achieve 0.075 ohm on resistance. The development work to hybridize the parallel connected MOSFET devices (including the associated drive circuit components) will require a concerted and coordinated effort between the contractor and a selected hybrid vendor. The development plan presently envisioned entails an estimated timespan for the overall effort of approximately 12 months.

Extensive review of the future trends in the development of high voltage and low on-resistance silicon MOSFET power devices reveals little expectation for a major breakthrough within the next few years. However, research work has begun in the semiconductor industry to utilize material other than silicon for high voltage field effect transistors. GaAs, in particular, offers a realistic possibility that the on-resistance and, therefore, the power dissipation of the power FETs will be appreciably reduced at all frequencies. It is predicted that the on-resistance of the GaAs FETs will be less than one-twelfth of the present silicon MOSFET devices. It is also expected that the GaAs FETs will have even lower conduction losses than the silicon bipolar devices. The estimated time period for the development work of the GaAs FETs is several years.

6.2 Microprocessor Controller

The baseline design of SASPM utilizes a space qualified microprocessor employing TTL logic elements. The power consumption of a microprocessor with TTL devices is a magnitude greater than that of one configured with CMOS. At the present time, space qualified CMOS microprocessors are not commercially available, but efforts in the industry are underway to qualify them.

ORIGINAL PAGE IS
OF POOR QUALITY

To reduce parts count, it is planned that the entire circuitry of the microprocessor controller will be incorporated in a LSI chip. This will necessitate an undertaking and schedule similar to that employed for the process of hybridizing the solar array switches. The proposed task is within the capability of existing LSI technology.

6.3 High Voltage/Power Switchgear

On the GEO mission, switchgear is utilized to reconfigure and modify the SASPM to power either the spacecraft or the ion propulsion loads. For the IPOTV, the switchgear is incorporated in the SASU to increase ion propulsion bus voltage by 33% to compensate for the graceful degradation of the solar array voltage. Comparable switchgear has been used in utility systems for carrying relatively high current and interrupting DC voltages below approximately 30V for some time. Latching versions of electromechanical devices show good reliability, high efficiency, wide variety and acceptable cost.

At higher voltages internal arcing tends to cause significant deterioration in the switching contacts, adversely effecting reliability operation. A survey was made of conventional relay and semiconductor manufacturers to determine the availability of high voltage/power switchgear devices. Assistance in this survey was given by the personnel of several NASA centers who are experts in this field. LeRC has been funding some switchgear development work and was able to direct the study team to a few corporate centers where this technology is being pursued.

The findings of the survey indicate that numerous vendors make high power switchgear as shown in Table 6-1, but most products will require major development in order to become qualified for the proposed application.

One of the most promising candidate devices is the Teledyne-Kinetics 1320 (2PDT) motor driven switch which has been used in the space shuttle equipment. This device is rated for 100A at 400V and employs an external transistor bypass

Table 6-1
HIGH POWER RELAYS

28V coils, latching, SPDT

	Contacts	Size	Wt	Price	Delivery	Notes
Westinghouse AVC - 41 (NBB)	80A 400V	5.5"x3.5"x6.0"	3.5 lb or less	2 un. $5K ea 50 un. $3K ea + $30K non recurring	6 mo. ARO 12 mo. ARO	- Not space qualified. - Pull-in/Release <25 ms @ 19V, 25°C.
ITT Jennings RT16	100A 15KV continuous	16" 13"	6 - 7 lbs.	$1000 ea in Low Quan.	16 wks ARO	
ITT Jennings RF10BL-26N1009	75A 15KV continuous	1.6" diam x 4.6"ht	16 oz (more for latch version)	$644 ea 5 pcs $601 ea 10 pcs	14 wks ARO	- No arc suppression (provide externally). - May need 200-300µF Cap across contacts for 100 Adc break. - Tested by ARCO to break. 50 Adc/200V into resistive load.
Teledyne Kinetics 1320 (2PDT) (motor driven) (xstr bypass)	100A 400V	3.8"x3.6"x3.2"	2.8 lb			- 12A max peak current surge into motor. Transistor bypass is mounted external to switch. - Used on shuttle.
Hartman A-751 (modified to house latch coil & herm. sealed)	250A 135V (See notes)	6.8"x9.1"x5.4"	12 lb	31K ea @ 100 pc level $1.5K ea @ 10 pc. level	Proto 6 mo. ARO Del. 12 mo ARO	- Tested to 650V, 600A not break at failure. - Can be rated to 400V.
Hartman A-754 (similar to A-751)	100A	2.9"4.1"x5.6"	5 lb.	$850 ea 10 pcs $700 ea 100 pcs	12 mo ARO	- Not space qual, but can be. - Can be rated to 400V. - Can be made latching.
Kilovac Corp. KE-22 (See Notes)	C5A 25KV	2" diam x 3 3/4"ht	10 oz	$330 ea £10 units	6 - 8 wks. ARO	- Non Latch - Norm closed - SPST
Hartman AH-1120A AH-1102B	250A 400V	9.0"x6.0"x5.4"	12 lb.	10 pc $900/B 10 pc $690/A	6 mos prot. 12 mos del.	- SPST (can be made into SPDT). - B includes current sensing coil.
Hartman AH-1102C	100A 400V	5.5"x4.5"x5.0"	4 lb	$775 ea 10 pcs $600 ea 100 pcs	6 mos proto 12 mos del.	- SPST (can be made into SPDT). - Includes current sensing coil.
Hartman Z-200-5	50A, 28V	1.1"x1.8"x2.6"	0.3 lb	Currently being used. PCU, EBU	12 mo ARO	- Space qual. - Interrupts 500Adc.

across the switch contacts. Hybrid components which combine semiconductors with electromechanical devices (such as the above Teledyne-Kinetics 1320) are being pursued by a number of manufacturers; and significant progress is being made to fill the switchgear needs of future high power systems.

Semiconductor devices are expected to increase their applicability as the primary power switch in solid state switchgear. In particular, there are two devices that should prove useful in higher voltage switchgear products. One is the D60T bipolar transistor made by Westinghouse; the other is the IRF 350 power HEXFET manufactured by International Rectifier. It was found that the D60T device has been applied to a hybrid switch made by Westinghouse.

To reduce power loss and circuit complexity, the use of MOSFET devices in the high voltage solid state switch application appears to be advantageous. To evaluate the relative merits of the MOSFET approach, technology support is required.

6.4 Fiber Optics

The use of fiber optics technology for data transmission between the solar array switches and the control logic offers the following advantages over a conventional wiring or RF transmission approach:

- Immunity to voltage transients and electromagnetic interference.
- High voltage isolation.
- Elimination of signal crosstalk.
- Reduction of sliprings/wrap-ups for data.
- Small size and reduced weight.

Over the past few years, several organizations (TRW, JPL, SFC, Wright-Patterson AFB and Kennedy Space Center) have been involved in the development of fiber optics technology. TRW participation in the fiber optics field began with the ESSEX study contract sponsored by Wright-Patterson AFB. The

ESSEX concepts were further developed in a follow-on Goddard SFC project called the Fiber Optics Data Bus Systems Study.

Presently, a multi-year IRAD Project (Fiber Optics Data Link) is in work. In 1981 this study accomplished a major milestone by testing commercially packaged XMTR/RCVR link and interface circuitry to 50 MBS. This progress is hindered by the components tested to date not being space qualified. There are only limited sources of components and materials available which are useful in the 50 to 100 MBS frequency range.

The Fiber Optics Data Link study is scheduled to continue until the end of 1983, and additional technology support will be required to complete the development work.

6.5 High Voltage Solar Arrays

The technology of high voltage solar arrays appears to be a major technology driver involving direct energy transfer to the ion engines. Plasma interaction and arcing in LEO appears to be a problem "somewhere" above 500 volts, with the effects beginning to become apparent as low as 200 volts.

In order to fully understand the phenomena, space testing is probably required. Recent evidence suggests that the effects of plasma may be cell size dependent. This is being looked at as part of an on going study at NASA Lewis Research Center. With the Shuttle becoming operational and higher voltage space platforms being considered, there will be greater opportunity for space testing of plasma mitigation techniques.

The plasma interaction is greatest for the LEO platform; which employs a concentrator solar array. It may be possible to bias the focusing cones in such a way as to keep the plasma away from the array. The trade off would be one of comparing the power required for biasing to the losses associated with the plasma.

It is reasonable to expect, with continued investigation by NASA Lewis, that a thousand volt operational array could be demonstrated in the 1990's.

6.6 Technology Development Plan

The conceptual design of the SASPM shows the requirement for high voltage solid state array switches and high voltage, high power switchgear to be used for power transfer and control.

An industry survey reveals that MOSFET technology is progressing at a rate that will most likely produce the required solid state array switches without additional technology support. Todays microprocessor technology will support the array switching concept with power requirements dropping to one tenth of todays requirements within the next several years. Fiber optics technology is projected to be ready well ahead of the 1990's technology readiness for all three missions. The real development need does not involve solar array switching per se, but is centered on the requirement for high voltage and high power switchgear to be used for reconfiguration, power transfer and/or control. An industry assessment has shown the need for development of such devices to acquire technology readiness by FY 1990. A plan for achieving this development has been prepared and is presented herein. The proposed plan also includes the development of a resettable solid state circuit breaker which has also been established as a requirement for a high voltage, high power circuit protection device.

Some development is underway for the 25 KW Space Platform which is planned for the mid-eighties. This switchgear would be applicable for the IPOTV spacecraft bus power distribution. Other on going studies such as the Space Power Distribution Technology Study (NAS8-33198) out of MSFC show that development is required to accommodate a 200 - 260 volt power bus.

6.6.1 Hybrid Devices

One possible approach to produce usable switchgear devices for Space Platform application is to combine the high voltage fast speed characteristics of semiconductor devices with the low contact losses of electromechanical devices in order to produce high voltage, high current, efficient hybrids. This approach does not optimize response time, but concentrates instead on achieving low "on" losses and simple control interfaces for use in high voltage applications where cycle life is not extremely important, e.g., for reconfiguration of arrays.

Voltage capability will be determined primarily by the solid state device voltage rating since the electromechanical devices generally have very high ratings in their normally open state, and have high voltage isolation capabilities between their contact and control elements.

The combination of electromechanical devices (solenoid or motor driven) and solid state switching devices overcomes the disadvantages of each and tends to meet the greater demands being imposed on switchgear. As stated previously, these configurations have combined high current, low voltage electromechanical devices with high voltage and medium to high current semiconductor devices to produce low "on" losses and arc suppression capabilities.

6.6.2 Resettable Solid State Circuit Breaker (RSSCB)

This development effort is required to avoid the use of fuses in applications where fuse replacement is not practical. The RSSCB is basically a fast acting solid state switch that is capable of significant overload stresses, and is able to sense its own current and place itself into the open configuration automatically. An external command would then be required to reset the RSSCB into the closed position for resumption of power flow.

Solid state switch technology is being studied at Lewis Research Center as part of an on going program by Ira Meyers.

6.6.3 Development Task Statements

A development plan has been catergorized into two basic tasks, A and B. Task A is concerned with the development of a hybrid switch configuration (which consists of electromechanical devices which are motor or solenoid driven) and solid state switching devices. This task qualifies the unit for space application. Task B consists of the development of the resettable solid state circuit breaker through space qualification. Presented herein are brief descriptions of each sub task within each of the above main tasks.

6.6.4 Hybrid Switch Development

6.6.4.1 Task A1 Requirement Definition

This task is concerned primarily with the definition of requirements for the hybrid configuration. Technical/design objectives, reliability, efficiency, availability and allowable mass are some of the parameters that require definition.

6.6.4.2 Task A2 Survey

Based upon the requirements defined in Task A1, an updated industry wide survey of hardware is to be performed to determine what is needed to meet these requirements.

6.6.4.3 Task A3 Preliminary Design

The preliminary design of the hybrid switch configuration with solid state devices will be performed. The information used in performing this task will be based on that derived from Task A2. Long lead time components will be identified and procured for eventual feasibility testing.

6.6.4.4 Task A4 Detail Design

Detail design will be performed. Consideration will be given to the use of MOSFET, high voltage and high current transistors (D70T, D60T), and other components derived from the industry wide survey. Circuit schematics and drawings will be prepared.

6.6.4.5 Task A5 Breadboard and Test

To prove the feasibility of the selected configurations a breadboard will be developed and testing will be conducted. System and performance characteristics of individual components will be acquired. Recommendations leading toward design improvement will also be identified.

6.6.4.6 Task A6 Report and Specifications

Specifications of selected components used for the hybrid switching concept will be prepared and documented.

6.6.4.7 Task A7 Packaging and Test

The design of the packaging of the flight configured hybrid system with solid state devices will be accomplished. Detail design drawings will be developed. Testing of the final configuration will be performed. Modifications and revisions of the packing design will be made if required as a result of testing.

6.6.4.8 Task 8 Qualification

Qualification of the hybrid unit will be performed using the appropriate tests as outlined in MIL-STD-1540A for electrical and electronic equipment. Functional, thermal vacuum and cycling, random vibration, leak, and burn in are some of the key tests to be performed.

ORIGINAL PAGE IS
OF POOR QUALITY

6.6.4.9 Task 9 Final Report and Specification

A final report consisting of the flight configuration and associated salient features, performance characteristics and/or specifications will be prepared.

6.6.5 Resettable Solid State Circuit Breaker

6.6.5.1 Task B1 Requirements Definition

This task is concerned primarily with establishing or defining the requirements for circuit protection, using such devices as fuses, circuit breakers or any other available techniques. Technical design objectives, availability and cost are some of the parameters that will be defined.

6.6.5.2 Task B2 Survey

An industry wide survey will be performed to determine the hardware that satisfies the requirements that are established in Task B1.

6.6.5.3 Task B3 Preliminary Design

An assessment of circuit protection techniques required for the LEO and GEO space platform systems showed the need for a large variety of circuit protection devices. In particular, the resettable solid state circuit breaker appears to be a strong candidate for high voltage, high power system circuit protection. A preliminary design of this approach making use of the hybrid switching concept will be performed. Long lead time components will be procured for feasibility testing of the preferred approach.

6.6.5.4 Task B4 Detail Design

The detail design of the resettable solid state switch circuit breaker will be performed under this task. Circuit schematics, including component identifications, and associated drawings will be prepared.

6.6.5.5 Task B5 Breadboard and Test

A breadboard of the resettable solid state circuit breaker configuration will be developed to determine the feasibility of this approach. System and performance characteristics of individual components will be acquired and documented.

6.6.5.6 Task B6 Report and Specifications

The design of the resettable solid state circuit breaker and feasibility test results will be documented including recommendations for further improvement in components and circuitry. Specifications of selected components will also be prepared.

6.6.5.7 Task B7 Packaging and Test

The design of the packaging of the flight configured resettable solid state circuit breaker will be accomplished. Detail design drawings will be developed. Testing of the final configuration will be performed. Modifications and revisions to the packaging design will be made, if required as a result of testing.

6.6.5.8 Task B8 Qualification

Qualification of the resettable solid state circuit breaker unit will be performed using the appropriate tests as outlined in MIL-STD-1540A for electrical and elec' onics equipment. Functional, thermal vacuum and cycling, random vibration, leak and burn in are some of the key tests to be performed.

6.6.5.9 Task B9 Final Report and Specifications

This task involves writing a final report on the resettable solid state circuit breaker design study. It will include the flight configuration, including salient features, performance characteristics and/or specifications.

ORIGINAL PAGE IS
OF POOR QUALITY

6.6.6 Schedule of Performance

Figure 6.6-1 shows a proposed schedule for development of the hybrid switch and resettable solid state circuit breakers. The schedule shows the time phasing of Tasks A1 thru B9, which are defined in the preceding sections.

6.6.7 Cost Estimate

A summary of estimated costs required to accomplish each subtask of Tasks A and B is shown on Table 6-2 Costs shown are based on manhours for assigned TRW labor categories and associated tasks for fiscal year 1982 through fiscal year 1985 based on TRWs burdened bidding rates which have been established for the identified fiscal year. Total costs include materials and parts for feasibility tests (breadboard) and packaging for qualification testing, publication, travel and other direct costs.

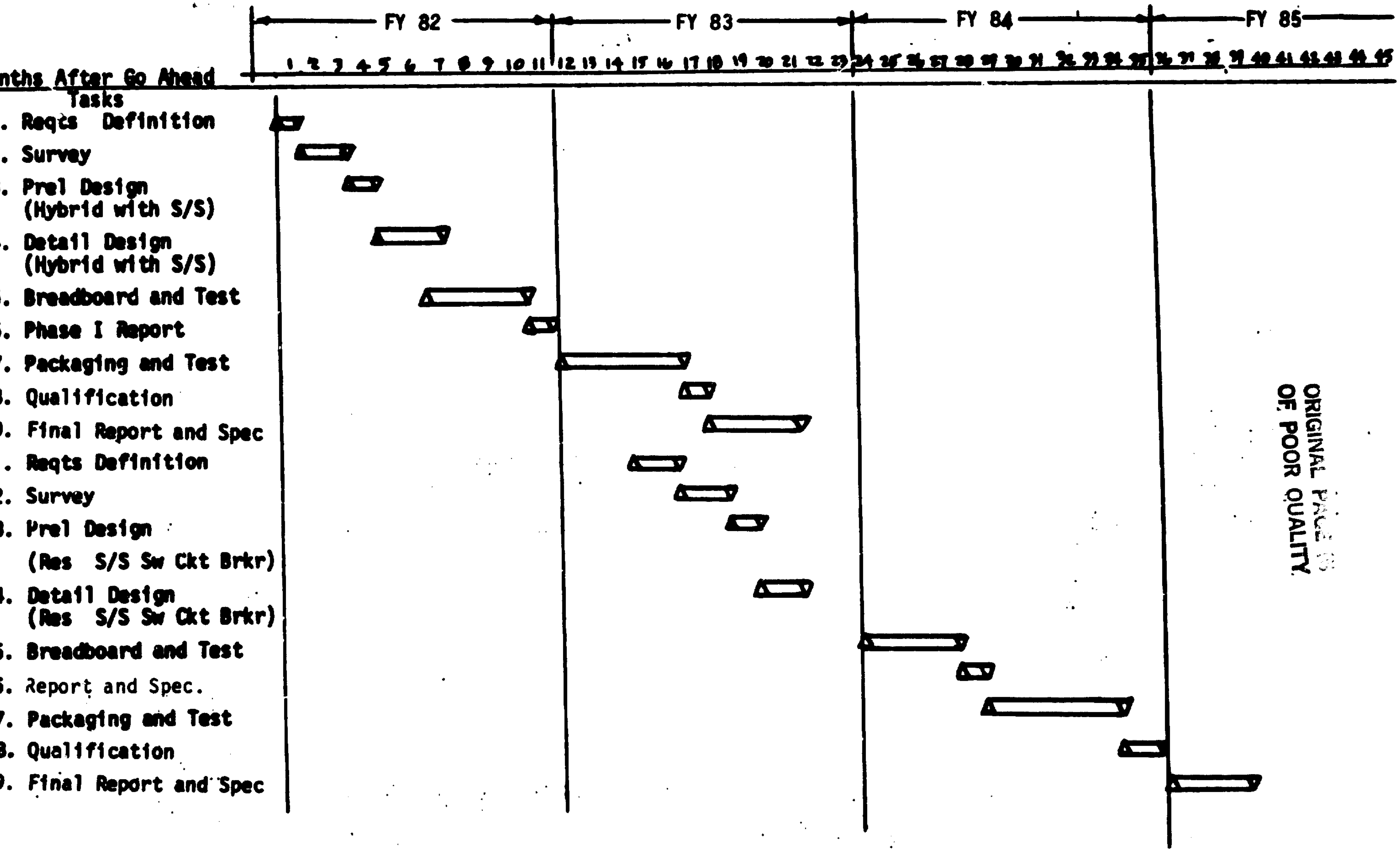

Figure 6.6-2 Schedule of Performance for Switchgear Development

ORIGINAL PAGE IS OF POOR QUALITY

Table 6-2

Cost Summary/Task
Development of Switchgear and Resettable Circuit Breakers

	FY'82	FY'83	FY'84	FY'85	Remarks Parts & Matl.
A1. Requirements Definition	$12,000				
A2. Survey	24,000				
A3. Prel Design (Hybrid with S/S)	12,000				
A4. Detail Design	24,500				
A5. Breadboard and Test	93,000				$20,000
A6. Phase I Report and Spec.	23,000				
A7. Packaging and Test		$100,000*			$15,000
A8. Final Report and Spec.		26,500			
A9. Qualification		56,200			
B1. Requirements Definition		26,500			
B2. Survey		26,500			
B3. Prel Design (Res S/S Sw Ckt Brkr)		3,200			
B4. Detail Design (Res S/S Sw Ckt Brkr)		27,100			
B5. Breadboard and Test			$104,100		$15,000
B6. Phase III Report			28,000		
B7. Packaging and Test			104,000		$10,000
B8. Qualification				$59,000	
B9. Final Report and Spec.			34,500	34,500	
Travel	$ 5,000	$ 5,000	$ 5,000	$ 1,000	
Publication	8,500	13,000	12,000	3,500	
CADM	1,700	2,600	2,400	700	
Total/FY	$203,700	$296,600	$285,000	$74,200	

Total Program Cost $859,500

- Burdened labor shown
- G&A fee not shown

* Includes matls. and parts. Costs shown are for reference only. This is not a firm proposal to accomplish these referenced tasks.

6.6.8 Fiber Optics Control Circuitry

There are advantages in using fiber optics (EMI, mass, and parts reduction). The following items need further analysis and development in order to enhance the fiber optics option.

- Light activated power switches
- Multiplexing techniques
- Light weight, accurate transducers
- Rotary joints
- High density fiber bundles

6.6.9 Strawman SASPM Development Program

A suggested SASPM development program in four phases is as follows:

Phase I: 1) Low voltage solar array switching unit (Voltage controlled)

- Develop basic power stage configuration
- Develop control electronics and analyses
- Demonstrate transient behavior of unit with solar array simulator, or a solar array
- Explore fiber optics options

Phase II:

- Demonstrate reconfiguration capability
- Install fiber optics control circuits
- Develop analytical model

Phase III:

- Develop high voltage SASU (≈ 200 volts)
- Performance testing of SASU and solar array simulator, or solar array

Phase IV:

- Integration of SASU and solar array or simulator with an argon thruster
- Performance verification tests
- System demonstration

6.7 Technology Summary

- SASPM can be utilized now on present low voltage systems, however the system has not been demonstrated with hardware.

- High voltage systems for ion propulsion require development of high voltage switches.

- MOSFET technology provides significant parts reduction.

- SASPM eliminates concentrated heat loads in power processing, and reduces parts count and cost.

6.7.1 Demonstration Required for Technology Readiness

- Verify high voltage operation in space plasma environment (LEO) this is required for ion engine control. High voltage operations in LEO may drive the solar array design to the concentrator concept. It may be possible to bias the reflector cones on the array to keep the plasma away.

- Demonstrate acceptable solar array degradation through Van Allen Belts, i.e., radiation resistant cell, or annealing. Ground testing would be acceptable.

6.7.2 Microprocessor Technology

- Space qualified TTL devices are available now and 8 bit CMOS devices will be available in the near term.

APPENDIX A

Mission Requirements

Tables

ORIGINAL PAGE IS
OF POOR QUALITY

Table 1. Power Requirements of SASP Experiments

Item	P_{avg}	P_{peak}	V	P_{stby}
IR[1] Astrophysics No. 1	130 W	310 W	28 Vdc	60 W
IR Astrophysics No. 2	3.78 kW	3.78 kW	28 Vdc	500 W
HE[2] Astrophysics No. 1	1.39 kW	NA[3]	NA	NA
HE Astrophysics No. 2	2.33 kW	NA	NA	NA
HE Astrophysics No. 3	1.36 kW	NA	NA	NA
HE Astrophysics No. 4	2.08 kW	NA	28 Vdc	NA
HE Astrophysics No. 5	1.9 kW	1.9 kW	28 Vdc	1.9 kW
HE Astrophysics No. 6	1.88 kW	NA	28 Vdc	1.88 kW
HE Astrophysics No. 7	1.9 kW	NA	NA	NA
HE Astrophysics No. 8	300 W	NA	28 Vdc	50 W
HE Astrophysics No. 9	1.88 kW	NA	NA	NA
HE Astrophysics No. 10/11	1.93 kW	1.93 kW	28 Vdc	1.93 kW
Large Area Modular Array Reflector	2.33 kW	NA	NA	NA
Additional Cosmic Ray Installation	5.74 kW	NA	NA	NA
Additional X-Ray Installation	2.28 kW	NA	NA	1.88 kW
Solar Physics No. 1[4]	2.7 kW	NA	28 Vdc	NA
Solar Physics No. 2[4]	2.35 kW.	NA	28 Vdc	NA
100-m Pinhole Camera	2.28 kW	NA	28 Vdc	NA
Solar Gamma-Ray Spectrometer	2.28 kW	NA	28 Vdc	NA
Solar Optical Telescope	3.78 kW	NA	NA	NA
Soft X-Ray Facility	2.13 kW	NA	28 Vdc	NA
1-km Pinhole Camera	2.28 kW	NA	28 Vdc	NA
Space Plasma Physics No. 1[4]	3.08 kW	NA	28 Vdc	NA
Space Plasma Physics No. 2	3.77 kW	NA	NA	NA
Space Plasma Physics No. 3	9.16-25 kW	NA	NA	NA
Space Plasma Physics No. 4	2.03 kW	NA	28 Vdc	NA
Space Plasma Physics No. 5	2.08 kW	NA	NA	NA
Chemical Release Module	500 kW	NA	NA	NA
Tether Facility	1.29 kW	NA	NA	NA
Particle Beam Injector	1.88-400 kW	NA	NA	NA
Atmospheric Gravity Wave Antenna	7.56-250 kW	NA	NA	NA
Magnetic Pulsations Experiment	25 kW	NA	NA	NA
Astronomy No. 1	1.91 kW	2.09 kW	28 Vdc	1.84 kW
Astronomy No. 2	5.78 kW	NA	NA	NA
Astronomy No. 3	2.38 kW	2.43 kW	28 Vdc	NA

*Notes are given at end of table.

ORIGINAL PAGE IS
OF POOR QUALITY

Table 1. Power Requirements of SASP Experiments (Continued)

Item	P_{avg}	P_{peak}	V	P_{stby}
Astronomy No. 4	2.78 kW	2.78 kW	NA	NA
Astronomy No. 5	2.78 kW	5.78 kW	NA	NA
Astronomy No. 6	3.28 kW	5.78 kW	28 Vdc	NA
UV and Planetary Telescope	2.78 kW	3.08 kW	NA	2.08 kW
Planet Detection Telescope	2.78 kW	2.78 kW	28 Vdc	NA
IR Telescope	2.78 kW	NA	NA	NA
Resource Observatory No. 1[5]	2.37 kW	NA	28 Vdc	NA
Resource Observatory No. 2[6]	2.64 kW	NA	28 Vdc	228 W
Soil Moisture No. 1	1.66 kW	NA	28 Vdc	1.17 kW
Soil Moisture No. 2	1.83 kW	[illegible]	28 Vdc	NA
Tethered Magnetometer	1.28 kW	2.29 kW	28 Vdc	0
Laser Fluorescence Spectrometer	4.78 kW	NA	NA	NA
Gravity Gradiometer	<1 W	1 W	NA	NA
Earth Resource Synthetic Aperture Radar	4.16 kW	NA	28 Vdc	1.26 kW
Thermal IR Imager	2.08 kW	NA	28 Vdc	NA
Multispectral IR Imager	2.08 kW	NA	28 Vdc	NA
Material Processor No. 1	1.16 kW	NA	28 Vdc	NA
Material Processor No. 2	4.16 kW	5.86 kW	400 Hz 3ϕ 115 V	1.86 kW
Material Processor No. 3	25 kW	60 kW	28 Vdc and 120 Vdc	NA
Life Science Lab Module	9.16-26.16 kW	NA	28 Vdc and 120 V 60 Hz	
Long Habitability Module	6.16-11.16 kW	NA	28 Vdc and 120 V 60 Hz	NA
Logistics Module	3.16 kW	NA	28 Vdc and 120 V 60 Hz	NA
Environment Observation No. 1[5]	1.55 kW	1.85 kW	28 Vdc	NA
Environment Observation No. 2[5]	2.66 kW	NA	28 Vdc	NA
Environment Observation No. 3[5]	1.67 kW	NA	28 Vdc	NA
Environment Observation No. 4	2.25 kW	NA	28 Vdc	NA
Light Detection/Ranging Facility	3.79 kW	3.88 kW	28 Vdc	NA
Cryogenic Limb-Scan Interfer/Radiometer	2.38 kW	2.86 kW	28 Vdc	NA
Dual Antenna Altimeter	2.21 kW	NA	28 Vdc	NA
Large Antenna Multifrequency Microwave Radiometer	2.25 kW	NA	28 Vdc	NA

C-3

Table 1. Power Requirements of SASP Experiments (Continued)

Item	P_{avg}	P_{peak}	V	P_{stby}
Dual Frequency Scatterometer	200 kW	NA	28 Vdc	100 W
National Oceanic Satellite System	2.58 kW	3.02 kW	28 Vdc	NA
Ocean Topography Experiment	1.97 kW	NA	NA	NA
Advanced Operational Meteorological	2.5 kW	NA	28 Vdc	NA
Ocean Synthetic Aperture Radar	2.08 kW	NA	28 Vdc	1.81 kW

(1) IR = Infrared

(2) HE = High-Energy

(3) NA = Not Available

(4) Three Separate Experiments

(5) Four Separate Experiments

(6) Five Separate Experiments

ORIGINAL PAGE IS
OF POOR QUALITY

Table 2. Power Requirements of MEC Experiments

Item	Pmin (kW)	Ppeak (kW)	V (Vdc)
Float Zone Processing System	4	40	120
Advanced Solidification Experiment System	1.5	22	120
High Gradient Directional Solidification System	2.5	40	120
Acoustic Containerless Processing System	1.5	26	120
Electromagnetic Containerless Processing System	2	12	120
Electrostatic Containerless Processing System	1.5	26	120
Solution Crystal Growth System	1	14	120
Vapor Crystal Growth System	2.5	30	120
Bioprocessing System	2.5	11	120

ORIGINAL PAGE IS
OF POOR QUALITY

Table 3. Voltage Types and Maximum Power Levels (in kW) for Multi-100 kW Space Platform*

Load Location	High Voltage			
	Regulated 115 +5 Vdc	Unregulated (TBD)	Low Voltage Regulated 28 ±4 Vdc	400 +1 Hz 3-Phase 115/200 Vac
Multidiscipline Lab	20	(500)**	15	20
Materials/ Processing Lab	20	60	10	20
Construction Module	20	(75)***	10	20
Crane	5	-	2	5
Control Center	20	-	10	20
Crew Habitat No. 1	3	-	4	2
Crew Habitat No. 2	3	-	4	2
Berthing Module	15	50†	20††	5
Logistics Module	-	-	2	-
Power Management	5	-	10	5

*Not all connected simultaneously.

**Intermittent 500 kW for plasma physics experiment

***Intermittent 75 kW for microwave power transmission antenna test

†Continuous 50 kW for O_2/H_2 reliquefaction equipment

††Includes 14 kW for Orbiter support

Table 4. Power Requirements for Space Construction Base Payloads

Item	P_{avg} (kW)	P_{max} (kW)
TA-1* Antenna	NA**	75
TA-2 Antenna	NA	455
Construction Lighting	6	NA
Construction Fabrication	2	9
Construction General Support	2	NA
Space Processing (Crystals)	12	18.5
Space Processing (Glass)	20	30
Space Processing (Bioprocessing)	4	8
Life Support	1	NA
Multi-Discipline Lab	12	16
Sensor Development	10	12

Bus voltages: 26 Vdc (Reg), 76 Vdc (Unreg), 112 Vdc (Reg)

Power requirements of each item from each bus are not available.

Housekeeping Power = 6.93 kW

*TA = Test Article
**NA = Not Available

ORIGINAL PAGE IS
OF POOR QUALITY

Table 5. STS Orbiter Power Requirements

Item	P_{avg}	P_{peak}*	V
Primary Payload Bus	7 kW	12 kW	27-32 Vdc
Auxiliary Payload Bus	800 kW	1.6 kW	25.7-32 Vdc
Aft Payload Bus	3 kW	4 kW	28-32 Vdc
AC No. 2 or AC No. 3	690 VA**	1 KVA	115 +5 Vac

Requirements for ripple:

(1)	Narrowband	<0.9 volt p-p (30 Hz to 7 kHz) falling 10 dB/decade to <0.28 volt p-p at 70 kHz, constant to 400 MHz.
(2)	Broadband	<1.6 volts p-p (30 Hz to 7 kHz) falling 10 dB/decade to <0.5 volt p-p at 70 kHz, constant to 400 MHz.
(3)	Resistive Load	<0.8 volt p-p (dc to 50 MHz). For broadband cases, no component should exceed 0.4 volt p-p.
(4)	Dedicated Fuel Cell	<0.1 volt p-p (30 Hz to 10 MHz). (Orbiter Bus C.)

*15 minutes, once in any 3-hour period.

**3-phase.

Table 6. Power Requirements for Certain Sortie Payloads

Item	DC Power P_{avg}	DC Power P_{max}	DC Power V	AC Power P_{avg}	AC Power P_{max}	AC Power V
I-M Shuttle IR* Telescope Facility	750 W	1.2 kW	28 $\pm$4			
Deep Sky UV** Survey Telescope	992 W	1.38 kW	28 $\pm$4			
I-M Diffration Limited UV Optical Telescope	400 W	722 W	28 $\pm$4			
Very Wide Field Galactic Camera	28 W	80 W	28 $\pm$4			
Cometary Simulation	1.14 kW	1.77 kW	28 $\pm$4			
30m IR Interferometer	1 kW	1.5 kW	28 $\pm$4			
Advanced XUV Telescope	400 W	450 W	28 $\pm$4			
Meteoroid Simulation	1.35 kW	1.88 kW	28 $\pm$4			
Solar Variation Photometer	20 W	NA††	28 $\pm$4			
1m Uncooled IR Telescope	500 W	1 kW	28 $\pm$4			
3m Ambient Temperature IR Telescope	944 W	1.16 kW	28 $\pm$4			
1.5m IR Interferometer	1.5 kW	1.78 kW	28 $\pm$4			
Selected Area Deep Sky Survey Telescope	400 W	500 W	28 $\pm$4			
2.5m Cryogenically Cooled IR Telescope	944 W	1.26 kW	N/A			
IR UV Optical Telescopes	2.43 kW	3.59 kW	28 $\pm$4			
IR UV Telescopes	1.18 kW	2 kW	28 $\pm$4			
Schwarzchild Camera	80 W	100 W	28 $\pm$4			
Far UV Electronographic Schmidt Camera/ Spectrograph	30 W	44 W	28 $\pm$4			
UC Berkeley Black Brant Payload	140 W	280 W	28 $\pm$4			
XUV Concentrator/ Detector Array	150 W	200 W	28 $\pm$4			

*IR = Infrared

**UV = Ultraviolet

†XUV =

††NA = Not Available

ORIGINAL PAGE IS
OF POOR QUALITY

Table 6. Power Requirements for Certain Sortie Payloads

Item	DC Power			AC Power		
	P_{avg}	P_{max}	V	P_{avg}	P_{max}	V
Proportional Counter Array	30 W	NA	28 ±4			
Attached Far IR Spectrometer	10 W	30 W	28 ±4			
Aries/Shuttle UV Telescope	250 W	300 W	28 ±4			
UC Berkeley Black Brant Payload No. 1	140 W	280 W	28 ±4			
Combined UV/XUV Measurements	800 W	1.17 kW	28 ±4			
Combined IR Payload	1.94 kW	2.66 kW	28 ±4			
Combined UV Payload	1.39 kW	1.88 kW	28 ±4			
Attached Far IR Photometer	5 W	10 W	28 ±4			
Cosmic Background Anisotropy	20 W	50 W	28 ±4			
Sortie Medium Aperture Optical Telescope	320 W	480 W	28 ±4			
UV Photometer and Spectrograph	230 W	280 W	28 ±4			
Faint Surface Phenomena	10 W	20 W	28 ±4			
Lyman B Imaging	9 W	15 W	28 ±4			
X-Ray Angular Structure	575 W	625 W	28 ±4			
High Inclination Cosmic Ray Survey	300 W	345 W	28 ±4			
X-Ray/Gamma Ray Pallet	725 W	NA	28 ±4			
Gamma Ray Pallet	360 W	NA	28 ±4			
Magnetic Spectrometer	234 W	NA	28 ±4			
High Energy Gamma Ray Survey	285 W	NA	28 ±4			
High Energy Cosmic Ray Study	100 W	NA	28 ±4			
Gamma Ray Photometric Studies	400 W	NA	28 ±4			
Low Energy X-Ray Telescope	360 W	404 W	28 ±4			
High Resolution X-Ray Telescope	625 W	865 W	28 ±4			
Antiproton Measurements	500 W	550 W	28 ±4			
Liquid "X" Detector	500 W	550 W	28 ±4			

ORIGINAL PAGE IS OF POOR QUALITY

Table 6. Power Requirements for Certain Sortie Payloads

Item	DC Power			AC Power		
	P_{avg}	P_{max}	V	P_{avg}	P_{max}	V
High Sensitivity Medium Energy Gamma Ray Survey	180 W	210 W	28 ±4			
Transition Radiation Detector	50 W	NA	28 ±4			
Graded Cerenkov Detector	100 W	115 W	28 ±4			
High Energy Gamma Ray Detector	180 W	NA	28 ±4			
Dedicated Solar Sortie Mission	2.75 kW	3.05 kW	28 ±4			
Solar Fine Pointing Payload	2.6 kW	2.9 kW	28 ±4			
ATM Spacelab	2.25 kW	2.7 kW	28 ±4			
Solar Far IR Telescope, Ambient Temperature	974 W	1.19 kW	28 ±4			
Flare Coarse Monitoring Package	610 W	NA	28 ±4			
Solar Activity Early Payload	2.4 kW	2.8 kW	28 ±4			
Solar Flare Detailed X-Ray Structure	260 W	405 W	28 ±4			
Solar Activity Growth Processes	995 W	1.14 kW	28 ±4			
Solar Atmospheric Wave Propagation	654 W	NA	28 ±4			
Physics of Flaring Bright Points	104 W	NA	28 ±4			
Density from Certain Types of Ions	182 W	327 W	28 ±4			
Coronal Dynamics	613 W	NA	28 ±4			
Solar Flare Plasma Flow	100 W	110 W	28 ±4			
Solar Flare Detailed X-Ray Structure (No. 2)	250 W	375 W	28 ±4			
Atmospheric and Magnetospheric Plasmas in Space	5.77 kW	10 kW	28 ±4			
Lidar System	270 W	NA	28 ±4			
Electron Accelerator	1.28 kW	1.4 kW	28 ±4			
Chemical Release	3 W	106 W	28 ±4			
Diagnostic Payload	120 W	430 W	28 ±4			
Zero G Cloud Physics Laboratory	1 kW	1.9 kW	28 ±4			
Shuttle Imaging Microwave System	-	-	-	1.82 kW at 400 Hz	2.01 kW at 400 Hz	115 ±7

Table 6. Power Requirements for Certain Sortie Payloads

Item	DC Power			AC Power		
	P_{avg}	P_{max}	V	P_{avg}	P_{max}	V
Scanning Spectro-Radiometer	964 W	NA	28 ±4			
Active Optical Scatterometer	264 W	1.08 kW	28 ±4			
High Resolution Mapper of Multiple High-Level Ozone Fields	40 W	150 W	28 ±4			
Space Shuttle Calibration Facility	3.48 kW	NA	28 ±4			
Active and Passive Cloud Radiance Experiment	500 W	NA	28 ±4			
Microwave Limb Sounder	150 W	NA	28 ±4			
Standard Earth Observations Package	1 kW	NA	28 ±4			
Atmospheric X-Ray Emission Experiment	60 W	60 W	28 ±4			
Specialized Multispectral Imaging System	200 W	300 W	28 ±4			
Meteorology Radar Facility	500 W	NA	28 ±4			
Mark II Interferometer Solar	434 W	NA	28 ±4			
Earth Resources Shuttle Imaging Radar	5 kW	7.5 kW	28 ±4	NA	NA	NA
Shuttle Imaging Microwave Systems A	930 W	NA	28 ±4			
Mark II Interferometer Earth	130 W	NA	28 ±4	254 W at 400 Hz	570 W at 400 Hz	115 ±7
Multifrequency Radar Land Imagery	2.19 kW	3.02 kW	28 ±4			
Multifrequency Dual Polarized Microwave Radiometry	350 W	438 W	28 ±4			
Microwave Scatterometer	475 W	559 W	28 ±4			
Multispectral Scanning Imagery	2.19 kW	3.02 kW	28 ±4			
Laser Altimeter/ Profilimeter Experiment	318 W	795 W	28 ±4			
Multifrequency Propagation Experiment	355 W	443 W	28 ±4			

ORIGINAL PAGE IS
OF POOR QUALITY

Table 6. Power Requirements for Certain Sortie Payloads

Item	DC Power			AC Power		
	P_{avg}	P_{max}	V	P_{avg}	P_{max}	V
Ocean Wave Spectrum Analysis	415 W	565 W	28 $\pm$4			
Precision Laser Ranging System	300 W	NA	28 $\pm$4			
Vector Geomagnetic Field Measurement	50 W	NA	28 $\pm$4			
Biological Experiment (SPA No. 1)	NA	NA	-	5.67 kW at 400 Hz	9.3 kW at 400 Hz	115 $\pm$7
Furnace Experiment (SPA No. 2)	-	-	-	6.8 kW at 400 Hz	18.1 kW at 400 Hz	115 $\pm$7
Levitation Experiment (SPA No. 3)	-	-	-	7.8 kW at 400 Hz	2.14 kW at 400 Hz	115 $\pm$7
General Purpose Experiments (SPA No. 4)	-	-	-	3.5 kW at 400 Hz	4.9 kW at 400 Hz	115 $\pm$7
Dedicated Experiments (SPA No. 5)	-	-	-	6.8 kW at 400 Hz	23.8 kW at 400 Hz	115 $\pm$7
Automated Furnace (SPA No. 12)	-	-	-	6.25 kW at 400 Hz	13.3 kW at 400 Hz	115 $\pm$7
Automated Levitation (SPA No. 13)	-	-	-	7.1 kW at 400 Hz	16 kW at 400 Hz	115 $\pm$7
Manned and Automated Experiments (SPA No. 14)	NA	NA	28 $\pm$4	13.6 kW at 400 Hz	22 kW at 400 Hz	115 $\pm$7
Automated Furnace and Levitation (SPA No. 15)	NA	NA	28 $\pm$4	9.9 kW at 400 Hz	21.5 kW at 400 Hz	115 $\pm$7
Biological and General Purpose Experiments (SPA No. 16)	-	-	-	4.6 kW at 400 Hz	9.3 kW at 400 Hz	115 $\pm$7
Biological and Automated Experiments (SPA No. 19)	-	-	-	6.8 kW at 400 Hz	23.8 kW at 400 Hz	115 $\pm$7
Minimum Biological Experiments (SPA No. 21)	-	-	-	3.15 kW at 400 Hz	4.85 kW at 400 Hz	115 $\pm$7

Table 6. Power Requirements for Certain Sortie Payloads

Item	DC Power			AC Power		
	P_{avg}	P_{max}	V	P_{avg}	P_{max}	V
Minimum Furnace Experiment (SPA No. 22)	-	-	-	3.64 kW at 400 Hz	6.3 kW at 400 Hz	115 ±7
Minimum General Purpose Experiments	-	-	-	2.27 kW at 400 Hz	3.6 kW at 400 Hz	115 ±7
First Spacelab Mission	472 W	925 W	28 ±4	140 W at 400 Hz	244 W at 400 Hz	115 ±7
Free Flying Teleoperator	445 W	689 W	28 ±4			
Life Sciences Shuttle Laboratory	2.76 kW	3.7 kW	28 ±4			
Life Sciences Mini-laboratories	284 W	1.1 kW	28 ±4			
First Life Sciences Spacelab Mission	335 W	1.62 W	28 ±4			
Animal Waste Management Demonstration	150 W	NA	28 ±4			
Integrated Real Time Contamination Monitor	392 W	NA	28 ±4			
Drop Dynamics	-	-	-	125 W at 60 Hz	175 W at 60 Hz	115 ±7
Wall-less Chemistry Facility	380 W	NA	28 ±4	800 W at 60 Hz	NA	115 ±7
Thermal Conductivity Measurements	28 W	NA	28 ±4			
Critical Point Phenomena	250 W	NA	28 ±4			
Combustion Experiments	271 W	NA	28 ±4			
Tunable Lasers for Atmospheric Measurements	200 W	1.1 kW	28 ±4			
Autonomous Navigation, Earth Pointing Experiment	150 W	NA	28 ±4			
Microwave Radiometer	50 W	NA	28 ±4			
Meteor Spectroscopy	15 W	NA	28 ±4			
Environmental Effects on Polymeric Materials	150 W	NA	28 ±4			
Zero G Steam Generator	500 W	NA	28 ±4			

ORIGINAL PAGE IS
OF POOR QUALITY

Table 6. Power Requirements for Certain Sortie Payloads

Item	DC Power			AC Power		
	P_{avg}	P_{max}	V	P_{avg}	P_{max}	V
Multispectral Scanner for Coastal Zone Oceanography	170 W	260 W	28 ±4			
Search and Rescue Imaging Radar	900 W	NA	28 ±4			
Hadamard Imaging Spectrometer	122 W	NA	28 ±4			
Colony Growth in Zero G	60 W	90 W	28 ±4			
Interpersonal Transfer of Microorganisms in Zero G	140 W	NA	28 ±4			
Special Properties of Biological Cells	60 W	140 W	28 ±4			
Sampling of Airborne Particles	60 W	560 W	28 ±4			
Advanced Technology Laboratory No. 1	1.3 kW	2.5 kW	28 ±4			
Liquid Helium Research Facility	-	-	-	2 kW at 50 Hz	3 kW at 60 Hz	115 ±7
Electromagnetic Environment Experiment	791 W	1.28 kW	28 ±4			
CO_2 Laser Data Relay Link	131 W	171 W	28 ±4			
Communication Relay Tests	1.01 kW	1.73 kW	28 ±4	452 W at 400 Hz	515 W at 400 Hz	115 ±7
Large Reflector Deployment	177 W	356 W	28 ±4	514 W at 400 Hz	685 W at 400 Hz	115 ±7
TWT Open Envelope Experiments	897 W	917 W	28 ±4			
Millimeter Large Wave Aperture Experiment				1.2 kW at 60 Hz	1.5 kW at 60 Hz	115 ±7
Microwave Interferometer Navigation and Tracking Aid	50 W	85 W	28 ±4	50 W at 400 Hz	125 W at 400 Hz	115 ±7
Shuttle Navigation via Global Positioning Satellite	69 W	103 W	28 ±4	100 W at 400 Hz	150 W at 400 Hz	115 ±7
Adaptive Multibeam Antenna Experiment	300 W	NA	28 ±4			
Video Data Compression	80 W	NA	28 ±4			
High Data Rate Laser Transmitter	5 W	130 W	28 ±4			

Table 6. Power Requirements for Certain Sortie Payloads

Item	DC Power P_{avg}	DC Power P_{max}	DC Power V	AC Power P_{avg}	AC Power P_{max}	AC Power V
High Data Rate Laser Receiver	275 W	350 W	28 ±4			
Bandwidth Compressive Modulation Shuttle Experiment	-	-	-	1.3 kW	NA	115 ±7

ORIGINAL PAGE IS OF POOR QUALITY

Table 7. Transmit Power Requirements for Certain Public Service Payloads

Item	Power	Orbit
Diplomatic/UN Hotlines	200 W	GEO
High Capacity Long Line Telephone Service	25 kW	GEO
Computer Long Line	100K	GEO
Holographic Teleconferencing	75 kW	GEO
National Information Service No. 1	5 kW	GEO
Advanced TV Broadcast	50 kW	GEO
Military Aircraft Communications	20 kW	GEO
Mobile Communication Trunk	200 kW	GEO
Electronic Mail Transmission	100 kW	GEO
Police Wrist Radio Communications No. 1	20 kW	GEO
Voting/Polling Wrist Radio System	25 kW	GEO
Personal Wrist Radio Communications No. 1	6 kW	GEO
Military Wrist Radio Communications No. 1	25 kW	GEO
Energy Use Monitor	6 kW	GEO
Disaster Communications Net	25 kW	GEO
Personal Wrist Radio Communications No. 2	70 kW	GEO
Personal Navigation No. 1	200 W	GEO
Personal Navigation No. 2	8 W	GEO
Radar Ground Mapper	1 kW	LEO
High Resolution Earth Mapping Radar	1 mW	LEO
UN Truce Observation Radar	1 mW	LEO
Advanced Array Radar	1 mW	LEO
Coastal Passive Radar	2 mW	GEO

Appendix B

Ion Propulsion Requirements

General solutions for spacecraft positioning problems are offered by ion propulsion thrusters. Of interest here is the effect on solar array design of using such a propulsion system; solar array sizing being of paramount importance, with array degradation being a subset of this parameter. The positioning problems addressed here are:

- Atmospheric drag make-up at low earth altitudes
- Orbit transfer with and without orbit inclination changes

1.0 Atmospheric Drag at Low Earth Altitudes

The primary orbital disturbance at altitudes below 500 km is aerodynamic drag; therefore, drag make-up will determine the ion propulsion requirements for the LEO platform.

The drag force (F) caused by the earth's atmosphere is dependent upon the following parameters:

- The density of the atmosphere at altitude h(p).
- The square of the orbital velocity (V^2).
- The effective frontal area of the spacecraft (A_{eff}).
- The coefficient of drag, determined by the spacecraft geometry (C_D).

There are many models for the density of the atmosphere in the range of altitudes of interest because of variations such as solar activity and sunlight or eclipse comparative durations. Figure B-1 graphically displays two such models. The upper curve is Wolverton's "standard" density model and the lower curve is based on the 1976 NOAA/NASA standard atmosphere. Computations for this study will be based on the NOAA/NASA standard model. Effects of fluctuations in atmospheric density are expected to average out for the long term mission.

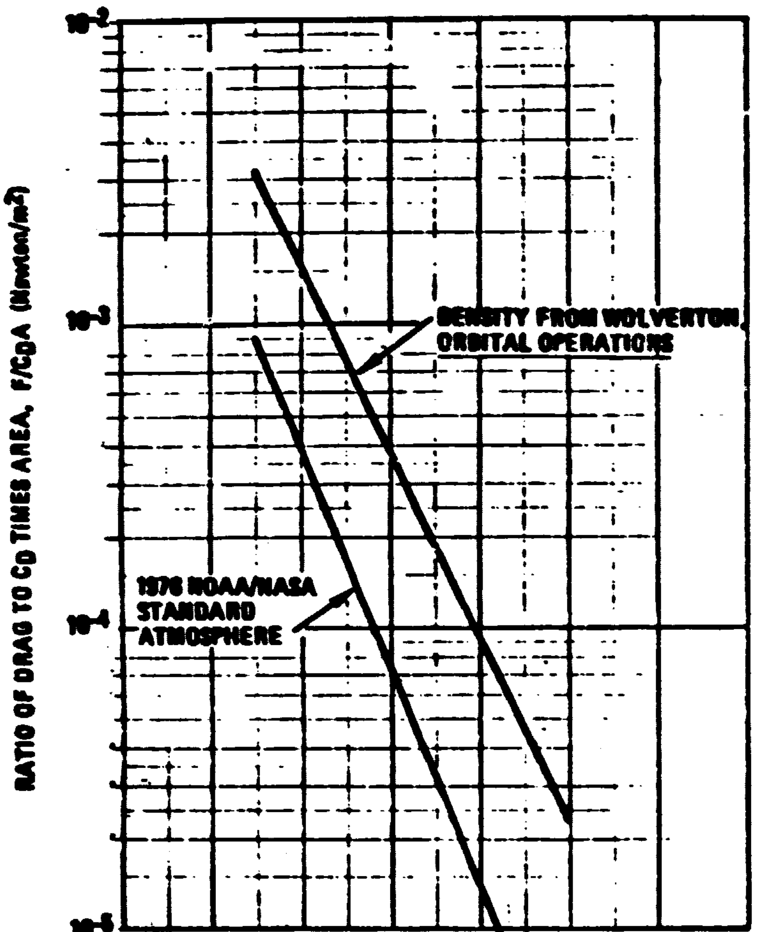

Figure B-1 Drag as a Function of Altitude

The orbital velocity is dependent upon the orbital altitude. V^2 is computed from the following formula:

$$V^2 = \frac{(1.4069 \times 10^{16}\ ft^3/s^2)}{\text{Radius of orbit in feet}}$$

ORIGINAL PAGE IS OF POOR QUALITY

The effective frontal area of the spacecraft is the area as viewed along the negative velocity vector. The frontal area of the solar array varies from full face area to edge area along the velocity vector. An estimate of 0.55 times the full face area has been made for the effective drag area over an orbit $[A_{eff} \approx \frac{1}{\pi} A\ (1 + f)]$,where f is the ratio of array thickness to width. The area of the LEO solar array is 4583 m^2. The effective area computes to 2521 m^2. The coefficient of drag will be taken as 2.3 for this analysis. This value represents a worst case for the geometries to be considered. To counteract drag, the required thrust must be equal but opposite to the drag force. The drag force (F) is as follows:

$$F = (\frac{1}{2} \rho\ V^2) \cdot A \cdot C_D$$

Both ρ and V^2 are functions of the altitude (h), and depend upon the altitude model used. Figure B-2 is a plot of drag force as a function of altitude for a normalized (1 m^2) solar array for both recognized atmospheric models.

The power required from the solar array to supply the thrust required to exactly offset the drag force is:

$$P = \frac{F \cdot I \cdot sp \cdot g_0}{2 \eta_1 \eta_2}$$

where:

P = power required

F = drag force (same as thrust)

Isp = specific impulse of selected thruster

g_0 = acceleration due to gravity

η_1 = power conditioning efficiency

η_2 = thruster efficiency

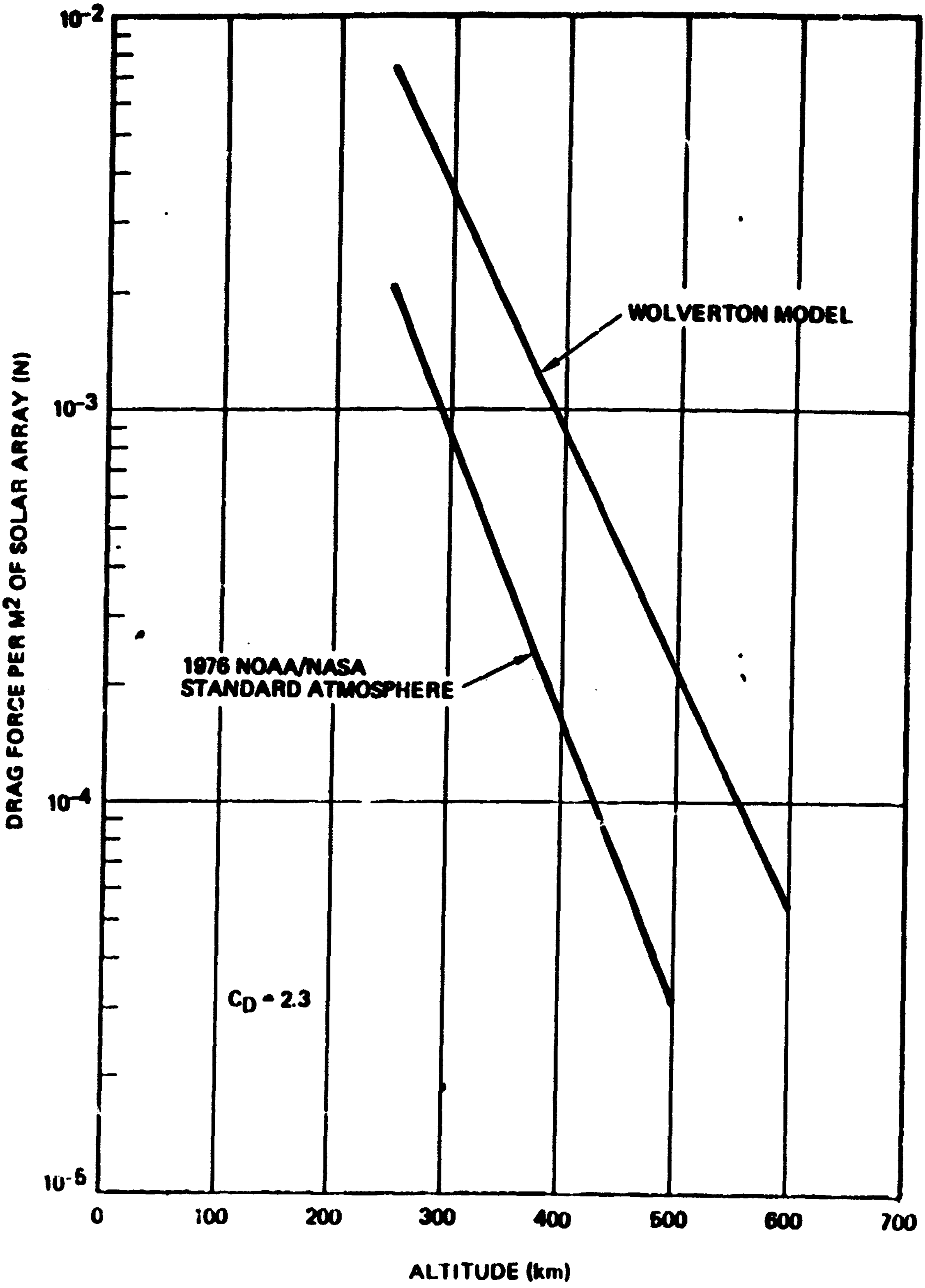

Figure B-2. Normalized Drag Force at given Altitudes (per m^2)

I_{sp} varies as a function of beam voltage. Figure B-3 gives the power required per m^2 of solar array for a range of I_{sp} from 100 to 800 volts, utilizing argon thrusters with a mass utilization efficiency of 88%. The power conditioning efficiency selected is selected as 80% and the thruster efficiency (as a function of I_{sp}) is presented in Figure B-4.
The value of g_0 is assumed constant at 9.8 m/sec^2 over this altitude range, and area is effective area over the orbit.

2.0 Orbit Transfer

The velocity increment requirements for orbit raising with or without orbit inclination changes have been calculated by the Edelbaum approximation which closely approximates the optimum Δv required for a low, continuous thrust spiral maneuver. For a change in altitude corresponding to a change in orbital velocity from vo to v and/or an inclination change of i degrees, the propulsion requirement is

$$\Delta v = (v_0^2 - 2v_0 v \cos(\frac{\pi}{2} \Delta i) + v^2)^{1/2},$$

where the orbital velocity is

$$v = (\mu/a)^{1/2}.$$

For v in meters/sec the gravitational constant, μ, is 3.984×10^{14} $m^3 sec^2$ and a is the radius of the circular orbit in meters.

Figures B-5 and B-6 show the Δv requirements versus final altitude for starting altitudes of 200 and 1000 km for a number of inclination changes. Note that the inclination change is a significant part of the total maneuver, especially for low and intermediate altitudes. The decrease in Δv requirements for a given inclination change toward higher altitudes reflects the proportionality of the inclination change to the square root of the orbit radius.

Using equation (B-1), the total velocity increment required to raise from several starting altitudes to synchronous altitude with an inclination change of 28.5 degees are given in Table 1.

ORIGINAL PAGE IS
OF POOR QUALITY

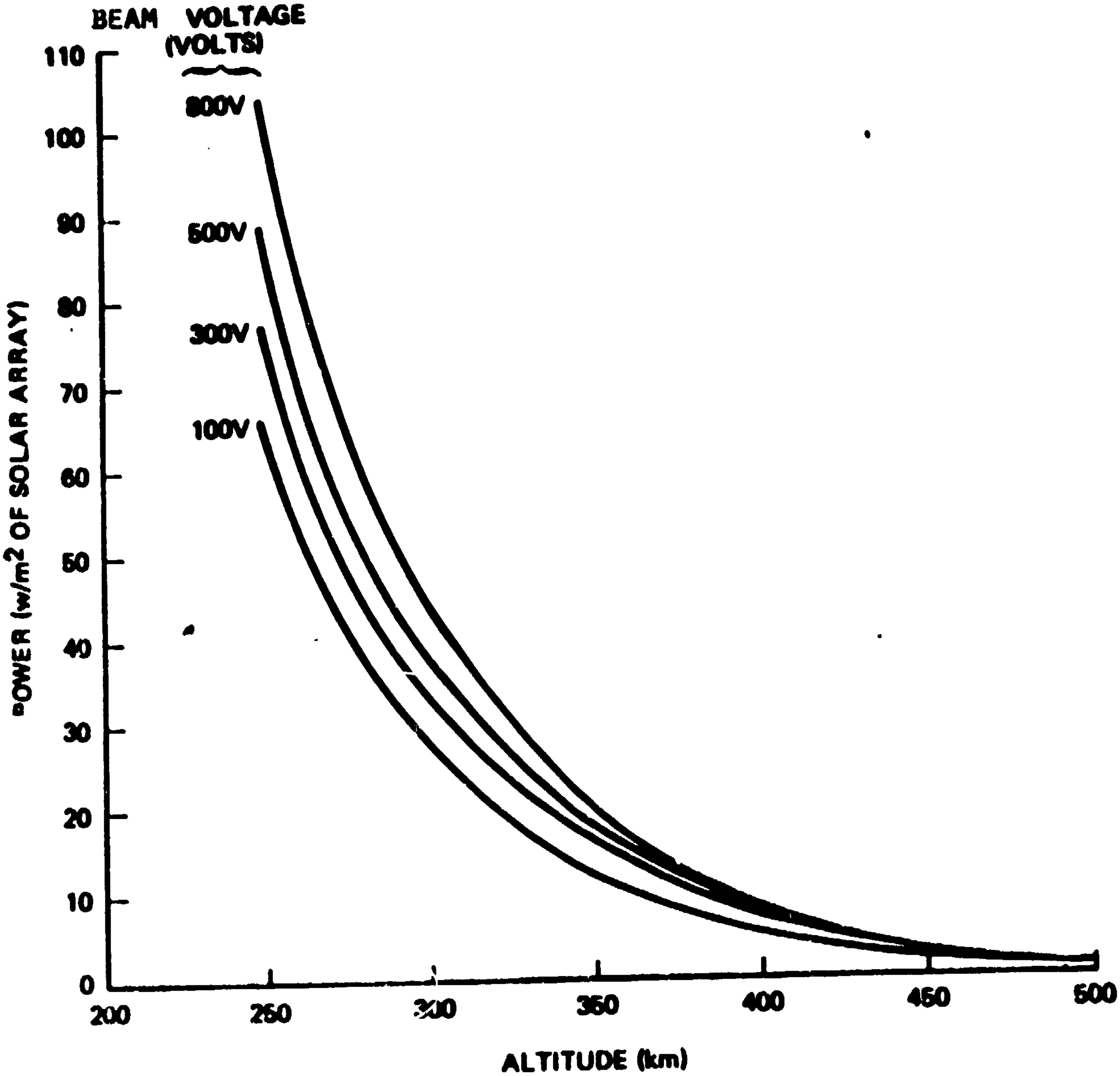

Fibure B-3. Power Required per M^2 of Solar Array

ORIGINAL PAGE IS
OF POOR QUALITY

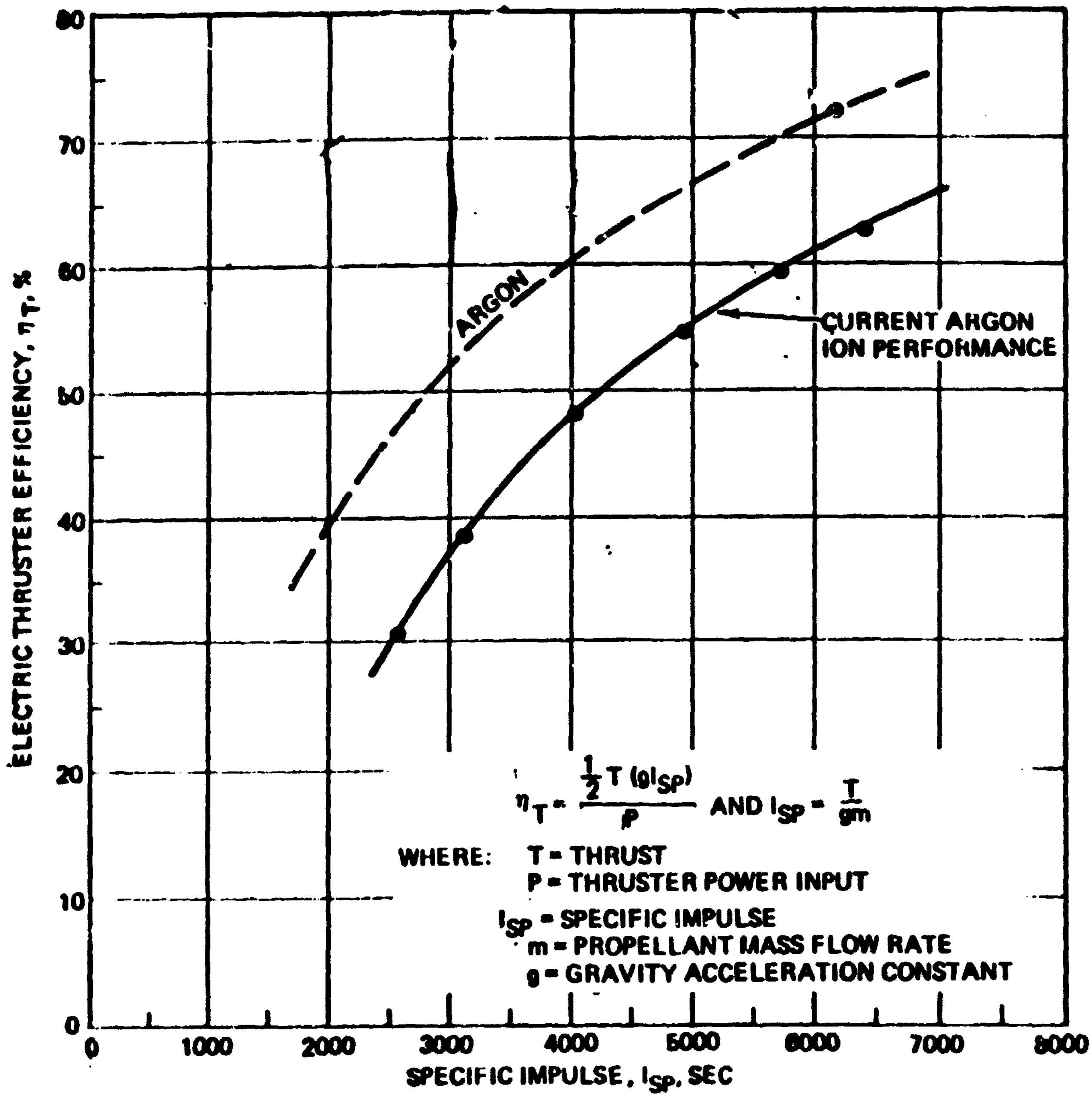

Figure B-4. Electric Thruster Module Efficiency Versus Specific Impulse

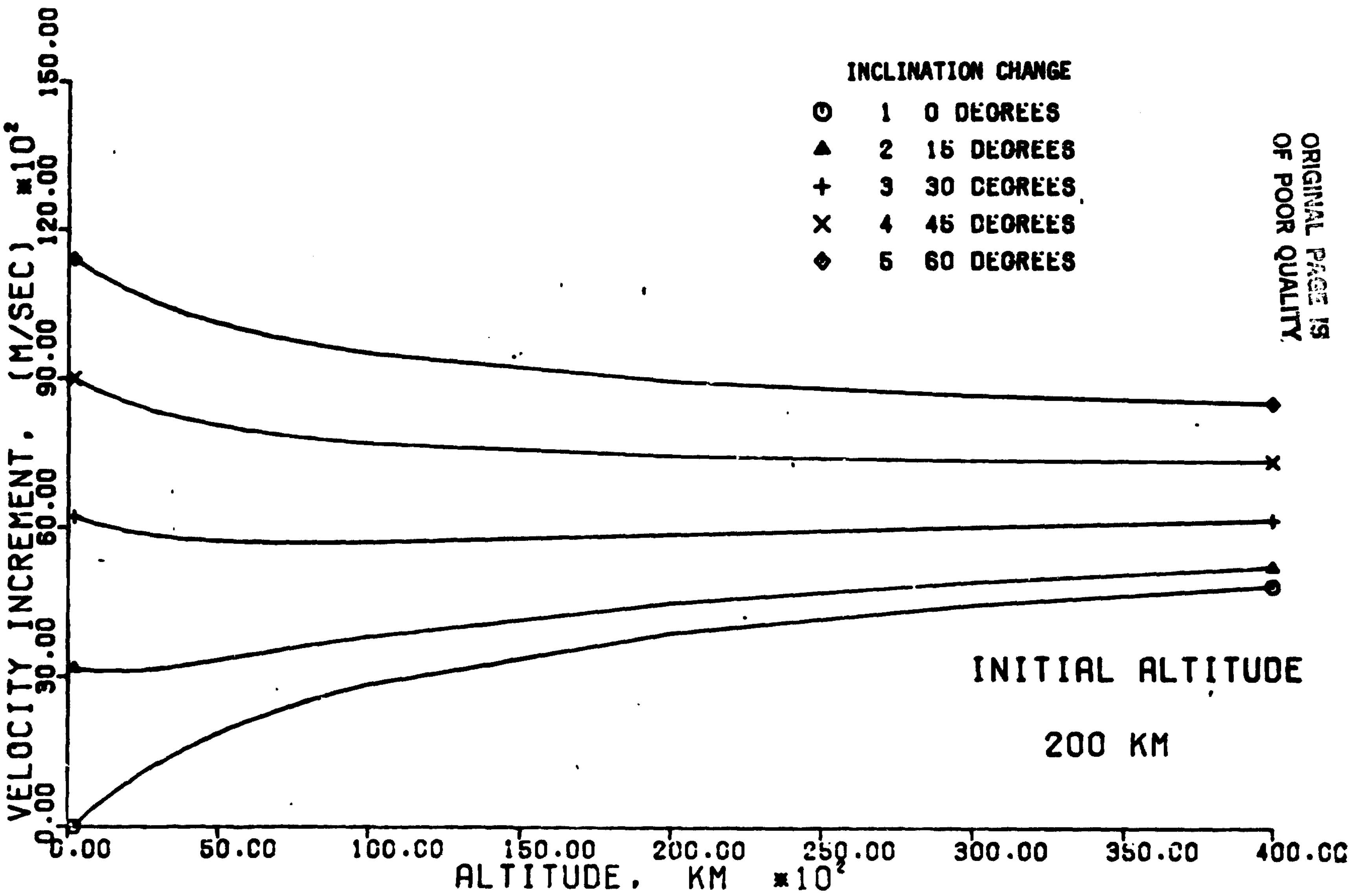

Figure B-5
VELOCITY INCREMENT FOR ORBIT TRANSFER
FROM 200 km INITIAL ALTITUDE

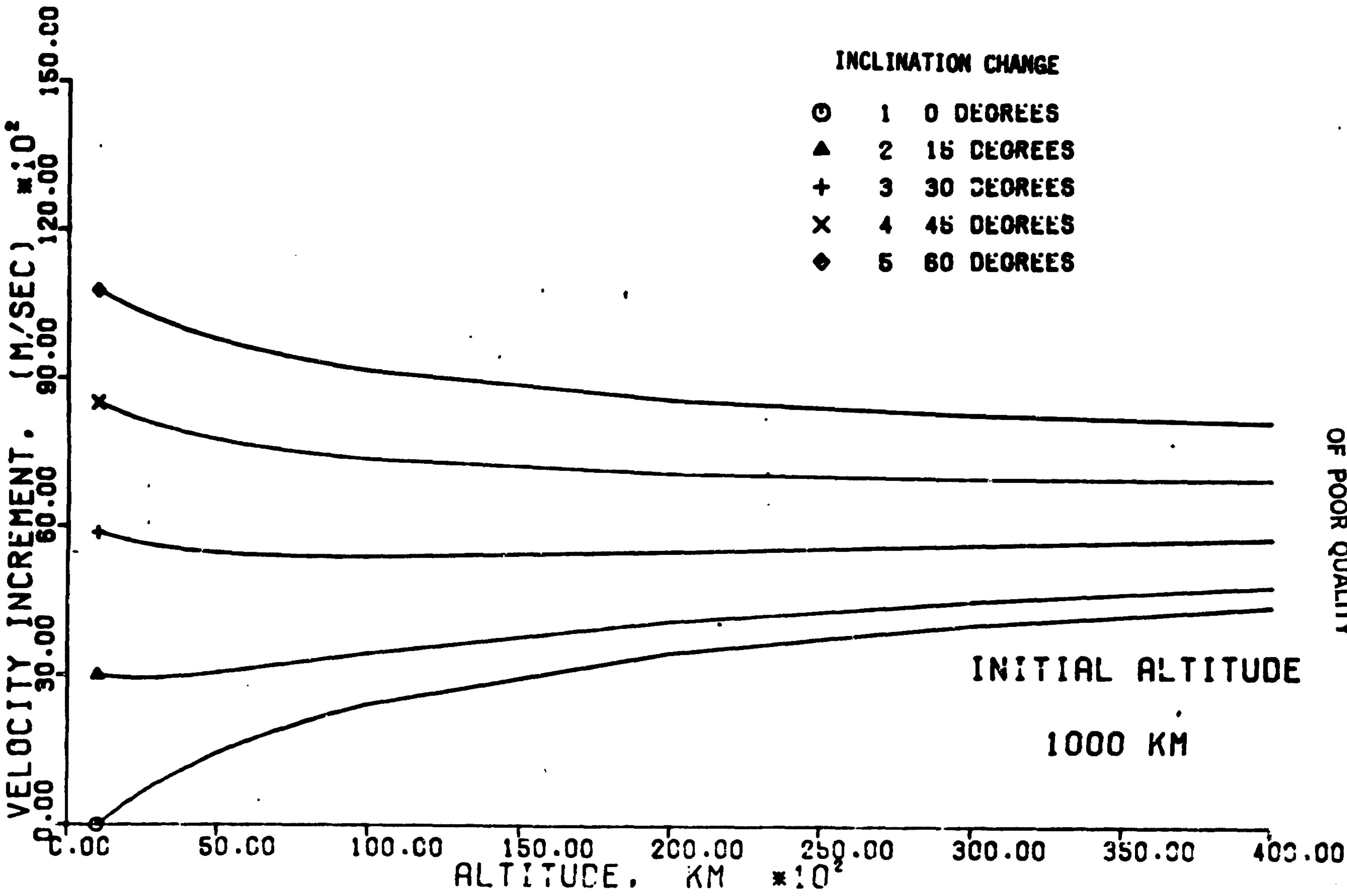

ORIGINAL PAGE IS OF POOR QUALITY

Figure B-6

VELOCITY INCREMENT FOR ORBIT TRANSFER FROM 200 km INITIAL ALTITUDE

ORIGINAL PAGE IS
OF POOR QUALITY

TABLE B-1 Velocity increments required to raise altitude from an initial altitude shown to geosynchronous orbit assuming a 28.5 degree inclination change is required.

Original Altitude (km)	Velocity Increment (ft/sec)	Velocity Increment (m/sec)
200	19709	6007.4
250	19619	5980.0
300	19530	5952.8
350	19442	5926.0
400	19355	5899.5
450	19269	5873.3
500	19184	5847.4
550	19101	5821.8
600	19018	5796.6
650	18936	5771.5
700	18854	5746.8
750	18774	5722.4
800	18695	5698.2
850	18616	5674.3
900	18539	5650.7
950	18462	5627.3
1000	18386	5604.2

The time required to lift a given mass from LEO to GEO is:

$$\Delta t = \frac{m}{T} (\Delta V)$$

where:

T - thrust (N)

m = mass (kg)

ΔV = velocity increment (m/sec)

ΔV = time required (sec)

Figure B-7 is a plot of the time required to travel from LEO to GEO as a function of available thrust. Also, plotted on the abcissa is the array output required to generate the given thrust.

The thrusters employed operate under the following parameters:

Type: Argon

Beam Voltage: ~800 volts

I_{SP}: 5600 seconds

Mass utilization efficiency: 90%

EPS efficiency: 80%

Thruster efficiency: 63%

Average sunlight %: 84%

Power required: ~55 KWe/N

The initial flight will start at point (1) of Figure B-7. Assuming all the degradation occurs at the end of the trip, the trip will take 132 days, and the array will degrade (Figure 2.2-3) by 25%. Assuming no annealing of the array, the return trip will start at point (2)(188 KW). The trips until the array has degraded to 58KW are shown in Table 2.

Table 2

IPOTV LEO to GEO Trips

Trip #	Begin S/A	End S/A	Days/Trip	Δ Degradation	Accum Degradation
1	250 KW	188 KW	132	25%	25%
1R	188 KW	168 KW	176	8%	33%
2	168 KW	150 KW	196	7%	40%
2R	150 KW	135 KW	220	6%	46%
3	135 KW	120 KW	244	6%	52%
3R	120 KW	105 KW	275	6%	58%
4	105 KW	93 KW	330	5%	63%
4R	93 KW	80 KW	390	5%	68%
5	80 KW	68 KW	440	5%	73%
5R	68 KW	58 KW	500	4%	77%

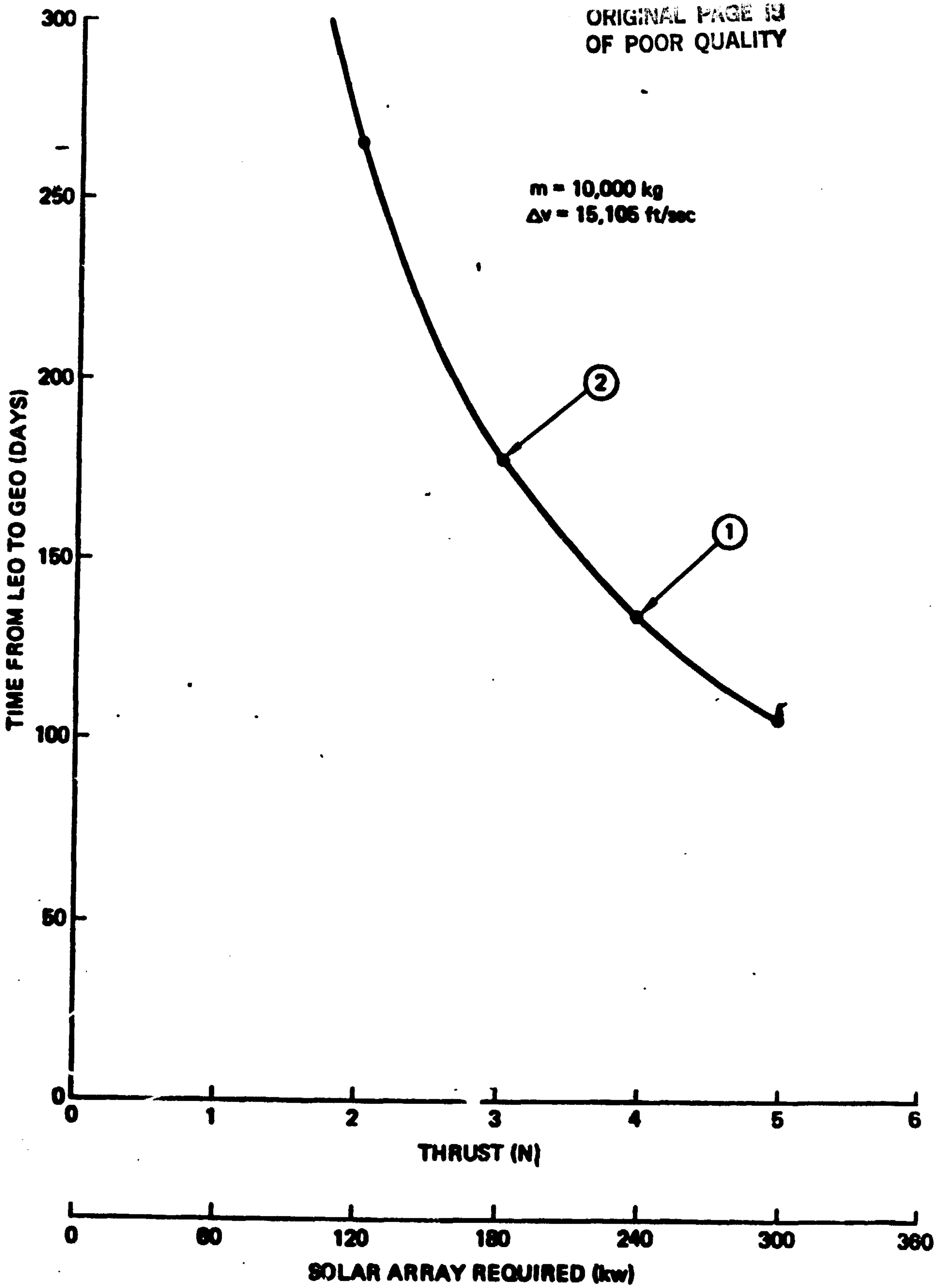

Figure B-7 Trip Duration for IPOTV Vehicle

Appendix C

ORIGINAL PAGE IS OF POOR QUALITY

Subsystem Specification
for
Electrical Power System
Manned Low Earth Orbiting Platform

1.0 SCOPE

1.1 Scope

This specification establishes the performance, design and development requirements for a Manned Low Earth Orbiting (LEO) Platform Electrical Power System. (EPS)

2.0 APPLICABLE DOCUMENTS

3.0 REQUIREMENTS

3.1 Item Definition

The EPS shall include the power generating system (solar array), the energy storage system (batteries), the power source controller system (array switching unit and control), the main power system controller, and output regulators for housekeeping and ion propulsion systems.

3.1.1 Item Diagrams

A simplified block diagram is depicted in Figure C-1.

3.1.1.1 Orbit

Low earth orbit (LEO): ~400 km, maximum eclipse period: 0.6 hrs, Minimum sunlight period: 0.9 hrs, Inclination: 0° to 57°.

3.1.2 Interface Definition

3.1.2.1 Electrical Interfaces

3.1.2.1.1 Undervoltage Signal

Relay contact closure indicates voltage less than 160 ± 1.0 volts, time delay variable 0.1 to 5.0 seconds.

3.1.2.1.2 Telemetry

For both the data system and PMS input.

3.1.2.1.2.1 Bilevel

Logic 0: $-0.6V \leq V_{oh} \leq +0.6V$ @ -1 ma max.

Logic 1: $+2.2V \leq V_{oh} \leq +6.0V$ @ 10 μa max.

3.1.2.1.2.2 Analog

0 to 5.12V, source impedance ≤ 2000 ohms, load input current of 0.5 μa dc during sampling interval, 0.1 μa dc otherwise, fault voltage ± 10V maximum.

3.1.2.1.2.3 Telemetry Sensor Characteristics

(a) Temperature: resistance, 220 ohms to 26.5K ohms

(b) Remote Power Controller:

Active: Switch closure, ≤ 2.0 ohms

(c) Current: Voltage of 0 to 6.5 Vdc, minimum impedance, 360K ohms.

(d) Voltage: 0 to 5.12 Vdc

3.1.2.1.3 Commands

(a) Relay state change: switch closure to ground, V_{ol} of + 30.0 Vdc maximum, I_{oh} of 300 μa @ + 30 Vdc.

3.2 Characteristics

3.2.1 Performance

3.2.1.1 Power

3.2.1.1.1 Solar Array

Output: Total Array

588 Kw @ BOL, ≥ 585 Kw @ EOL

Housekeeping and payloads

566 Kw @BOL, ≥ 566 Kw @ EOL

Ion Propulsion

22 Kw @ BOL, ≥ 19 Kw @ EOL

Voltage: Housekeeping and payload

≤ 250 V_{MPP} in sunlight, thermally stabilized (EOL)

≥ 575 V_{OC} in sunlight for 6 minutes exiting eclipse (BOL)

ORIGINAL PAGE IS
OF POOR QUALITY

Ion Propulsion

$\geq$ 765 V_{MPP} $\leq$ 850 V_{MPP} in sunlight, thermally stabilized (EOL)

$\leq$ 1950 V_{OC} in sunlight for 6 minutes exiting eclipse (BOL).

Temperature Range: - 80°C during eclipse to + 80°C during sunlight

Modularity: 11 channels, minimum switched section output step size, 1.5 amperes.

3.2.1.1.2 Battery

1 N_i-H_2, 250 AH, 160 cell battery for each of 11 channels.

Full charge current: 97 a ($C/_{2.6}$)

Trickle charge current: 3 a ($C/_{83}$)

Maximum DOD: 50%

3.2.1.1.3 Power Capability

	Payload	House-keeping	Ion Propulsion
Eclipse	250 Kw	25 Kw	0
Sunlight	250 Kw	25 Kw	23 Kw

3.2.1.1.4 Power Characteristics (Main Power Bus)

3.2.1.1.4.1 Voltage

Unregulated dc, steady state

Maximum voltage (battery trickle charge): 250 volts

Minimum voltage (battery discharging @ 50% DOD): 200 volts

3.2.1.1.4.2 Bus Impedance

$\leq$ 0.3 ohms, dc to 100 KHz

3.2.1.1.4.3 Power Quality

Conducted interference requirements of MIL-STD-1541 apply.

3.2.1.1.4.4 Ripple

Narrowband: $\leq$ 0.9V p-p, 30 H_z to KH_z, falling 10 db/decade to 0.28V p-p @ 70 KH_z, thereafter constant to 400 MH_z.

ORIGINAL PAGE IS
OF POOR QUALITY

Broadband: $\leq$ 1.6V p-p, 30 H_z to 7.KH_z, falling 10 db/decade to 0.5V p-p @ 70 KH_z, thereafter constant to 400 MH_z.

Resistive load: $\leq$ 0.8V p-p, dc to 50 MH_z.

3.2.1.1.4.5 Transients

Common mode dc: $\leq$ 300 x 10^{-6} v-sec above or below nominal (200 to 250V) bus voltage

Peak: $\leq$ 50V above nominal high (250) bus voltage
$\leq$ 30V on the return
Rise and fall time $\geq$ 1 usec.

3.2.1.1.5 Under/Overvoltage

No damage to components when operating from 0 to 200 volts, and 250 to 300 volts (batteries excepted).

Payload shall dump for voltages of $\leq$ 160 $\pm$ 1V for more than 5 sec on main power bus.

3.2.1.1.6 Shielding and Grounds

MIL-STD-1541 shall apply.

3.2.1.1.7 Radiated EMI

MIL-STD-461, Notice 3 shall apply.

3.2.1.2 Payload Power

3.2.1.2.1 Unregulated DC

250 Kw @ 200 Vdc to 250 Vdc to payload, continuously from main power bus.

25 Kw @ 200 - 250 Vdc to housekeeping loads continuously.

3.2.1.2.2 Regulated DC Power

23 Kw @ 860 $\pm$ 10% Vdc to ion propulsion in sunlight only.

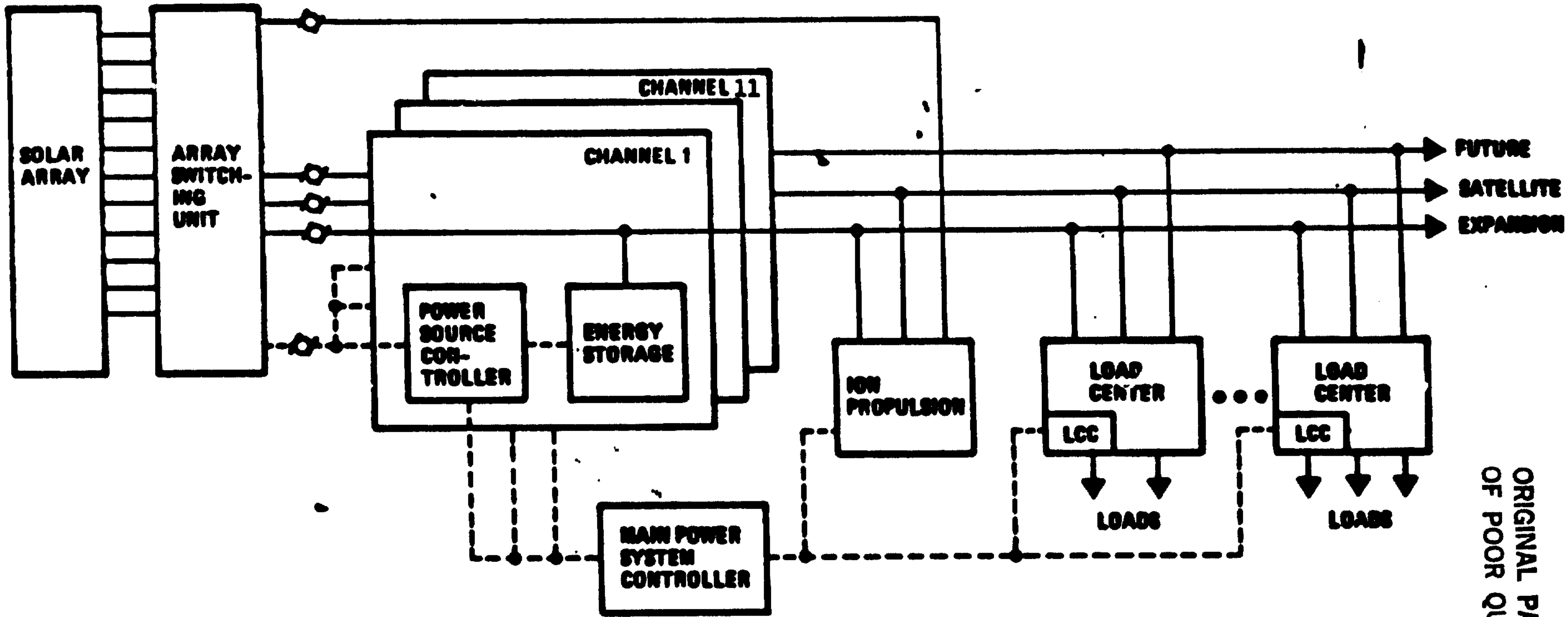

ORIGINAL PAGE IS
OF POOR QUALITY

GENERATION – CASSEGRANIAN CONCENTRATOR SOLAR ARRAY
ENERGY STORAGE – NICKEL-HYDROGEN BATTERY
BATTERY CHARGER – SOLAR ARRAY REGULATION
REGULATION – TBD
POWER TRANSMISSION – DIRECT CURRENT AT SOURCE VOLTAGE
POWER DISTRIBUTION – DIRECT CURRENT AT SOURCE VOLTAGE
POWER PROCESSING – AS NEEDED WITHIN EACH PAYLOAD OR LOAD CENTER
CHANNEL QUANTITY – DEFINED BY BATTERY CAPACITY (11)
RELIABILITY – FAIL OPERATIONAL, FAIL SAFE
GRACEFUL CAPACITY DEGRADATION WITH FAILURES
LIFE – INDEFINITE; REPLACE FAILED UNIT AT NEXT SERVICE OPPORTUNITY (30 YEAR GOAL)

LEO Baseline Electrical Power System Design

FIGURE C-1

Subsystem Specification for Electrical Power System Unmanned Geosynchronous Earth Orbiting Platform

1.0 SCOPE

1.1 Scope

This specification establishes the performance, design, and development requirements for an unmanned Geosynchronous Earth Orbiting (GEO) Electrical Power System (EPS).

2.0 APPLICABLE DOCUMENTS

3.0 REQUIREMENTS

3.1 Item Definition

The EPS shall include the power generating system (solar array), the energy storage system (batteries), the power source controller system (array switching unit and control), the main power system controller, and output regulators for housekeeping and ion propulsion systems.

3.1.1 Item Diagrams

A simplified block diagram is depicted in Figure C-2.

3.1.1.1 Orbit

Geosynchronous Earth Orbit (GEO): ∿ 36,000km, max eclipse period: 72 minutes (max)

3.1.2 Interface Definition

3.1.2.1 Electrical Interfaces

3.1.2.1.1 Undervoltage Signal

Relay contact closure indicates voltage less than 168 ± 1.0 volts, time delay variable 0.1 to 5.0 seconds.

3.1.2.1.2 Telemetry

For both the data system and PMS input.

3.1.2.1.2.1 Bilevel

Logic 0: $-0.6V \leq V_{oh} \leq 0.6V$ @ -1 ma max.

Logic 1: $+2.2V \leq V_{oh} \leq 0.6V$ @ 10 μa max.

3.1.2.1.2.2 Analog

0 to 5.12V, source impedance ≤ 2000 ohms, load input current of 0.5 μa dc during sampling interval, 0.1 μa dc otherwise, fault voltage ± 10V max.

3.1.2.1.2.3 Telemetry Sensor Characteristics

(a) Temperature: resistance, 220 ohms to 26.5K ohms

(b) Remote Power Controller:

Active: Switch closure, ≤ 2.0 ohms

(c) Current: Voltage of 0 to 6.5 Vdc, minimum input impedance, 360K ohms

(d) Voltage: 0 to 5.12 Vdc

3.1.2.1.3 Commands

(a) Relay state change: Switch closure to ground, V_{ol} of +30.0 Vdc max, I_{oh} of 300 μa @ +30 Vdc.

3.2 Characteristics

3.2.1 Performance

3.2.1.1 Power

3.2.1.1.1 Solar Array

Output: Total Array

96 KWe @ BOL

Ion Propulsion

64 KWe @ BOL, reconfigurable to supply payloads.

Payloads and housekeeping

96 KWe @ BOL

ORIGINAL PAGE IS
OF POOR QUALITY

Voltage: Payloads and housekeeping

$\leq$ 260 V_{MPP} in sunlight, thermally stabilized (EOL)

$\leq$ 585 V_{OC} in sunlight for six minutes exiting eclipse (BOL).

Ion Propulsion

$\geq$ 765 V_{MPP} $\leq$ 850 in sunlight, thermally stabilized.

Temperature Range: -180°C during eclipse to +60°C during sunlight.

Modularity: Four channels, minimum switched section output step size, 1.5 amperes.

3.2.1.1.2 Battery

One $Ag\text{-}H_2$, 150 AH, 168 cell battery for each of 4 channels.

Initial charge rate at 15 amperes, tapering to 2 amperes trickle charge.

Maximum DOD = 75%

3.2.1.1.3 Power Capability

	Payload	Housekeeping	Ion Propulsion
Eclipse	50 Kw	5 Kw	0
Sunlight	50 Kw	5 Kw	23 Kw

3.2.1.1.4 Power Characteristics (Main Power Bus)

3.2.1.1.4.1 Voltage

Unregulated DC steady state:

Housekeeping and payload busses

- Maximum voltage (battery trickle charge): 260 volts
- Minimum voltage (battery discharging @ 50% DOD): 200 volts

Ion Propulsion bus

800 $\pm$ 10% Vdc

3.2.1.1.4.2 Bus Impedance

$\leq$ 0.3 ohms, dc to 100 KH_z

3.2.1.1.4.3 Power Quality

Conducted interference requirements of MIL-STD-1541 apply.

ORIGINAL PAGE IS
OF POOR QUALITY

3.2.1.1.4.4 Ripple

Narrowband: $\leq$ 0.9V p-p 30 H_z to 7KH_z, falling 10 db/decade to 0.28V p-p @ 70 KH_z, thereafter constant to 400 MH_z.

Broadband: $\leq$ 1.6V p-p, 30 H_z to 7KH_z, falling 10 db/decade to 0.5V p-p @ 70 KH_z, thereafter constant to 400 MH_z.

Resistive load: $\leq$ 0.8V p-p, dc to 50 MH_z.

3.2.1.1.4.5 Transients

Common mode dc: $\leq 300 \times 10^{-6}$ v-sec above or below nominal (200 to 260V) bus voltage.

Peak: $\leq$ 50V above nominal high (260) bus voltage.

$\leq$ 30V on the return

Rise and fall time $\geq$ 1 usec.

3.2.1.1.5 Under/Overvoltage

No damage to components when operating from 0 to 300 volts (batteries excepted).

Payload shall dump for voltages of $\leq 168 \pm 1$V for more than 5 sec on main power bus.

3.2.1.1.6 Shielding & Ground

MIL-STD-1541 shall apply.

3.2.1.1.7 Radiated EMI

MIL-STD-461, Notice 3 shall apply.

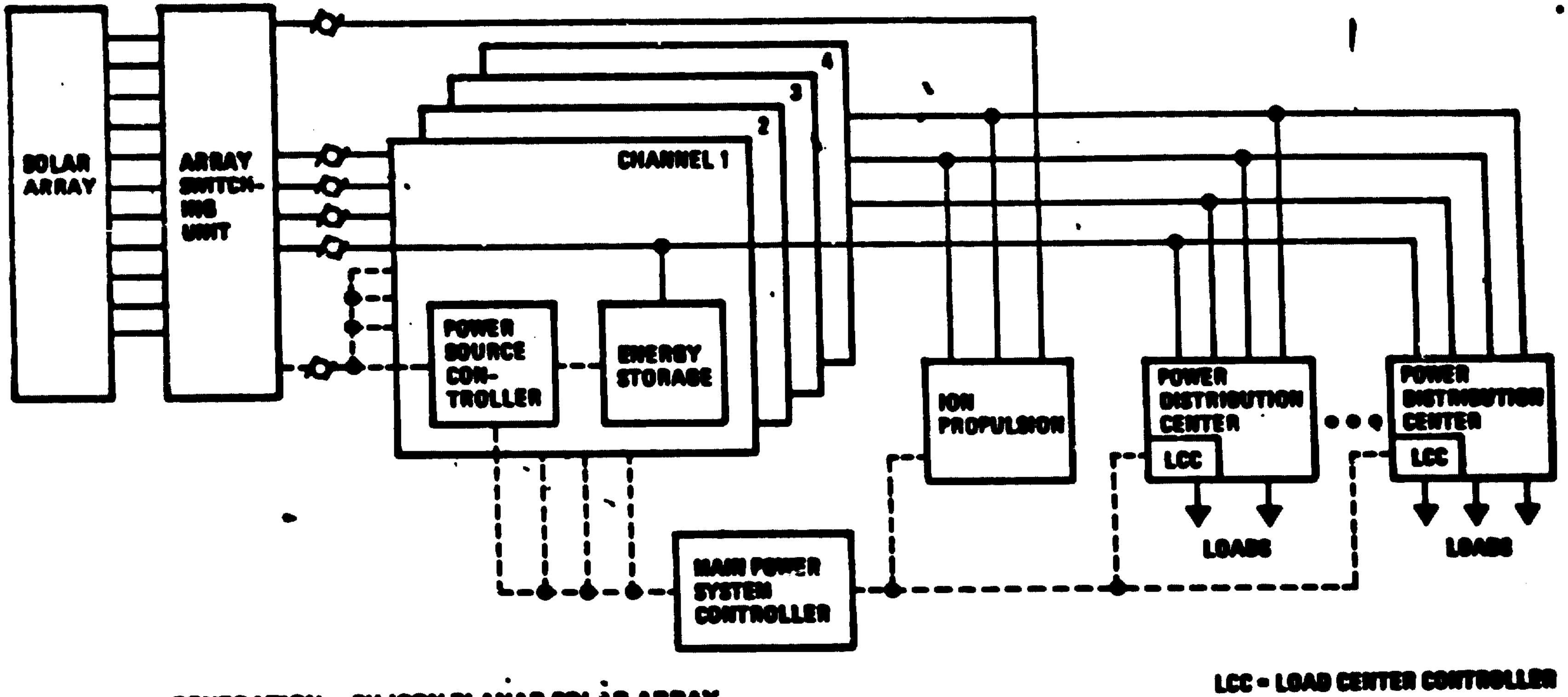

GENERATION – SILICON PLANAR SOLAR ARRAY
ENERGY STORAGE – SILVER-HYDROGEN BATTERY
BATTERY CHARGER – SOLAR ARRAY REGULATION
REGULATION – TBD
POWER TRANSMISSION – DIRECT CURRENT AT SOURCE VOLTAGE
POWER DISTRIBUTION – DIRECT CURRENT AT SOURCE VOLTAGE
POWER PROCESSING – AS NEEDED WITHIN EACH PAYLOAD OR LOAD CENTER
CHANNEL QUANTITY – DEFINED BY BATTERY CAPACITY (4)
RELIABILITY – FAIL OPERATIONAL, FAIL SAFE
LIFE – 8 - 10 YEARS

GEO Baseline Electrical Power System Design

FIGURE C-2

ORIGINAL PAGE IS
OF POOR QUALITY

Subsystem Specification for Electrical Power System Ion Propulsion Orbit Transfer Vehicle

1.0 SCOPE

1.1 Scope

This specification establishes the performance, design, and development requirements for an unmanned Ion Propulsion Orbit Transfer Vehicle (IPOTV) Electrical Power System (EPS).

2.0 APPLICABLE DOCUMENTS

3.0 REQUIREMENTS

3.1 Item Definition

The EPS shall include the power generating system (solar array), the energy storage system (batteries) the power source controller system (array switching unit and controls), the main power system controller, and output regulators for housekeeping and ion propulsion systems.

3.1.1 Item Diagrams

A simplified block diagram is depicted in Figure C-3.

3.1.1.1 Orbit

Transfer orbit from low earth orbit (LEO) to geosynchronous earth orbit (GEO) with dwell time in either or both orbits.

3.1.2 Interface Definition

3.1.2.1 Electrical Interface

3.1.2.1.1 Undervoltage Signal

Relay contact closure indicates voltage less than 100 $\pm$ 1.0 volts, time delay variable 0.1 to 5.0 seconds.

3.1.2.1.2 Telemetry

For both the data system and PMS input.

ORIGINAL PAGE IS
OF POOR QUALITY

3.1.2.1.2.1 Bilevel

Logic 0: $-0.6V \leq V_{oh} \leq 0.6V$ @ -1ma max

Logic 1: $+2.2V \leq V_{oh} \leq 0.6V$ @ 10 μa max

3.1.2.1.2.2 Analog

≈0 to 5.12V, source impedance ≤ 2000 ohms, load input current of 0.5 μa dc during sampling interval, 0.1 μa dc otherwise, fault voltage ± 10V max.

3.1.2.1.2.3 Telemetry Sensor Characteristics

(a) Temperature: resistance, 220 ohms to 26.5K ohms

(b) Remote Power Controller

Active: Switch closure, ≤ 2.0 ohms

(c) Current: Voltage of 0 to 6.5 Vdc,

minimum input impedance, 360K ohms

(d) Voltage: 0 to 5.12 Vdc

3.1.2.1.3 Commands

(a) Relay state change: switch closure to ground, V_{ol} of +30.0 Vdc max, I_{oh} of 300 μa @ +30 Vdc

3.2 Characteristics

3.2.1 Performance

3.2.1.1 Power

3.2.1.1.1 Solar Array

Output: Total Array

250 KWe @ BOL

Ion Propulsion

250 KWe @ BOL

Payloads and housekeeping

64 KWe @ BOL

Voltage: Housekeeping

$\leq$ 120 V_{MPP} in sunlight, thermally stabilized (EOL)

$\leq$ 270 V_{OC} in sunlight for six minutes exiting eclipse (BOL)

Ion Propulsion

$\geq$ 720 V_{MPP} $\leq$ 960 in sunlight, thermally stabilized.

Temperature Range -180°C during eclipse (GEO), to +80°C (LEO)

Modularity: Three channels, minimum switched section output step size, 1.0 amps.

3.2.1.1.2 Battery

One N_1-H_2, 50 AH, 80 cell battery for each of 3 channels.

Initial charge rate at 5 amperes, tapering to 1 ampere trickle charge.

Maximum DOD = 50% LEO, and 75% GEO

3.2.1.1.3 Power Capability

	Housekeeping	Ion Propulsion
Eclipse	5 Kw	0
Sunlight	10 Kw	240 Kw

3.2.1.1.4 Power Characteristics

3.2.1.1.4.1 Voltage

Unregulated dc steady state:

Housekeeping bus - Maximum voltage (battery trickle charge)

120 volts

Minimum voltage (battery discharging at 50% DOD):

100 volts

Ion Propulsion Bus: 360 $\pm$ 10% Vdc

3.2.1.1.4.2 Bus Impedance

$\leq$ 0.3 ohms, dc to 100 KHz

3.2.1.1.4.3 Power Quality

Conducted interference requirements of MIL-STD-1541 apply.

3.2.1.1.4.4 Ripple

Narrowband: ≤ 0.9V p-p, 30 H_z to $7KH_z$, falling 10 db/decade to 0.28V p-p @ 70 KH_z, thereafter constant to 400 MH_z

Broadband: ≤ 1.6V p-p, 30 H_z to $7KH_z$, falling 10 db/decade to 0.5V p-p @ 70 KH_z, thereafter constant to 400 MH_z.

Resistive Load: ≤ 0.8V p-p, dc to 50 MH_z.

3.2.1.1.4.5 Transients

Common mode dc: ≤ 300 x 10^{-6} v-sec above or below nominal (200 to 260V) bus voltage.

Peak: ≤ 50V above nominal high (260) bus voltage.

≤ 30V on the return

Rise and fall time ≥ 1 usec.

3.2.1.1.5 Under/Overvoltage

No damage to components when operating from 0 to 100 volts (batteries excepted).

Payload shall dump for voltages of ≤ 100 ± 1V for more than 5 sec on main power bus.

3.2.1.1.6 Shielding & Grounds

MIL-STD-1541 shall apply.

3.2.1.1.7 Radiated EMI

MIL-STD-461, Notice 3 shall apply.

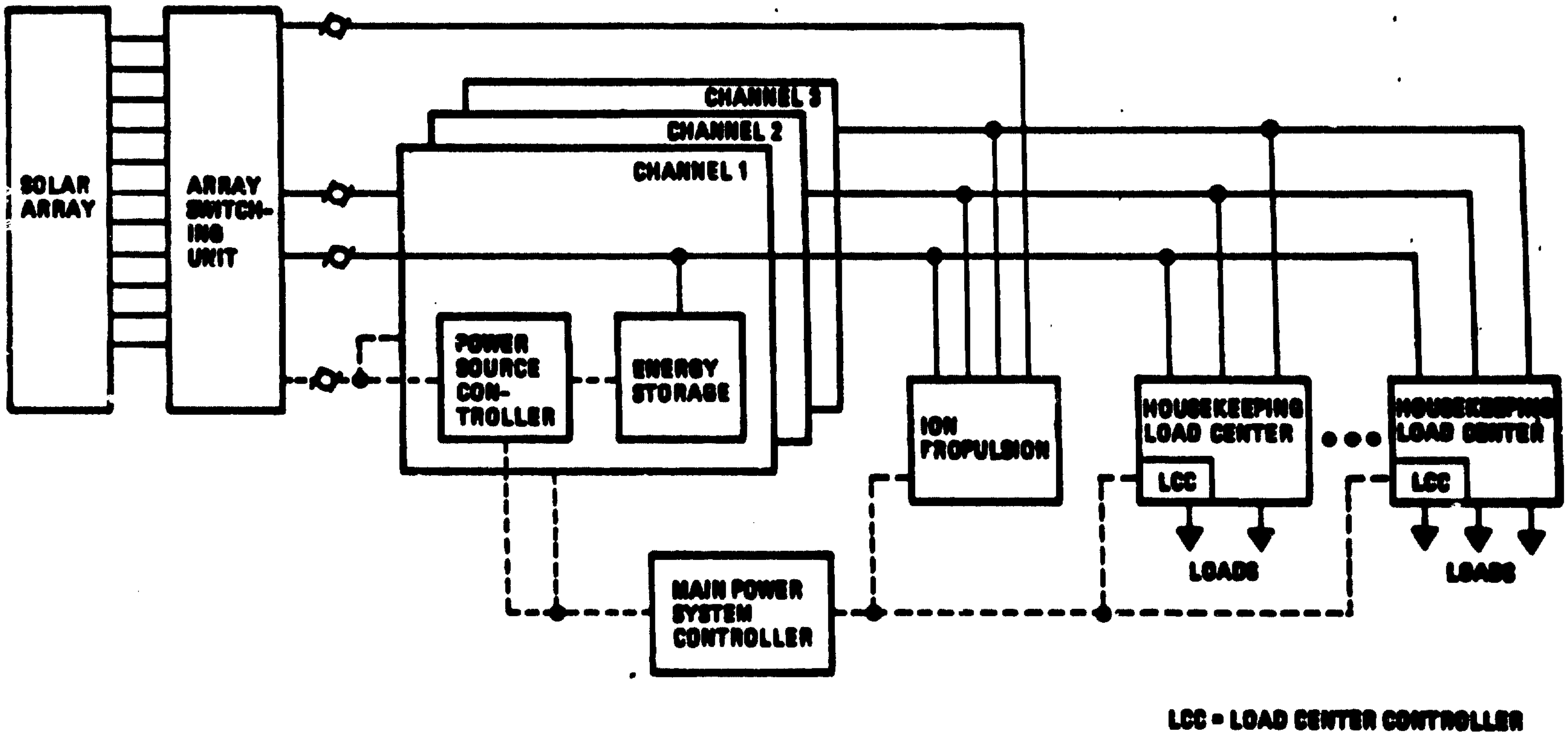

GENERATION – SILICON PLANAR SOLAR ARRAY
ENERGY STORAGE – NICKEL-HYDROGEN BATTERY
BATTERY CHARGER – SOLAR ARRAY REGULATION
POWER DISTRIBUTION – DIRECT CURRENT AT SOURCE VOLTAGE, 100 TO 120 VDC
POWER PROCESSING – AS NEEDED WITHIN EACH LOAD CENTER
CHANNEL QUANTITY – DEFINED BY BATTERY CAPACITY (3)
RELIABILITY – FAIL OPERATIONAL, FAIL SAFE
LIFE – FUNCTION OF USAGE, REPLACE FAILED UNIT AT NEXT SERVICE OPPORTUNITY

IPOTV Baseline Electrical Power System Design

FIGURE C-3

ORIGINAL PAGE IS
OF POOR QUALITY

APPENDIX D

STATEMENT OF WORK

Solar Array Switching Power Management (SASPM) is an approach to power management that uses switches to directly connect groups of solar cells in such a way as to provide system voltage regulation, electrical power distribution, and the ability to reconfigure the solar array input capability for changing load requirements or for maintenance operations.

The objective of this study is to identify SASPM concepts and technology advancements which, if developed, will have the capability of increasing power systems efficiency, and reducing overall cost. A comparison to conventional power management approaches will be made, demonstrating potential benefits of the SASPM in the areas of cost, weight, reliability, heat rejection, reconfiguration flexibility, and growth.

The study consists of the following:

a) <u>Task I. Mission Requirements and Definition</u>

Define a set of mission characteristics to the depth required to determine their power management requirements. Estimate the power management requirements and constraints. Task I is to be performed for three missions:

1) Manned Low Earth Orbit (LEO) Platform - 250 KWe average load

2) Unmanned Geosynchronous Equatorial Orbit (GEO) Platform - 50 KWe average load.

3) Ion Propulsion Orbit Transfer Vehicle (IPOTV) - 50-250 KWe

b) <u>Task II. Candidate Concepts Analysis and Selection</u>

Identify SASPM concepts that could satisfy the requirements defined in Task I. Compare the SASPM concepts according to cost, weight and volume, reliability, efficiency, and thermal control. Determine the concept impacts on mission characteristics and hardware. Establish conventional power processing baseline data.

c) <u>Task III. Concept(s) Definition and Impacts</u>

Provide further definition of the Task II concepts. Further define and quantify the SASPM concepts.

ORIGINAL PAGE IS
OF POOR QUALITY

d) Task IV. Comparisons

Compare the definition and impacts obtained in Task III with the use of conventional power processing techniques for each mission.

e) Task V. Technology Recommendations

Identify required technology advances necessary to implement SASPM for the three mission classes.

f) Task VI. Reporting Requirements

1) Monthly technical progress narratives

2) Monthly financial and schedular reporting

3) Mid Task II briefing

4) Mid Task III briefing

5) Final report.

APPENDIX E

Acronyms

ASU	Array switching unit
BOL	Beginning of life
DOD	Depth of discharge
EOL	End of life
EPS	Electrical power system
GEO	Geosynchronous equatorial orbit
IPOTV	Ion propulsion orbit transfer vehicle
I_{sp}	Specific impulse
LCC	Load center controller
LEO	Low earth orbit
LSI	Large scale integrated circuit
MEC	Materials Experiment Carrier
PEP	Power Extension Package
PMS	Power management system
RSSCB	Resettable solid state circuit breaker
SAS	Solar array switch
SASP	Science and applications space platform
SASPM	Solar array switching power management
SASU	Solar array switching unit
SEPS	Solar electric propulsion system
SP	Space platform
STS	Space transportation system
TCC	Transformer coupled converter
μP	Microprocessor